



**Politecnico
di Torino**

Politecnico di Torino

Master of Science Course in Electronic Engineering

Academic Year 2021/2022

Graduation Session July 2022

Channel Analysis of High Electron Mobility Transistors

A pathway from the Density Matrix to the
Quantum Drift-Diffusion approach

Supervisors

Prof. Simona Donati Guerrieri
Prof. Francesco Bertazzi
Dr. Alberto Tibaldi

Candidate

Simone Molinaro (S282577)

*It is nice to know that the computer understands the problem.
But I would like to understand it too.*

Eugene Wigner

Contents

| | | |
|----------|---|-----------|
| 1 | Introductory Concepts | 2 |
| 1.1 | Evolution of Physical Models | 2 |
| 1.2 | Objectives and Methodology | 4 |
| 1.3 | Schrödinger's Formalism | 5 |
| 1.4 | Dirac's Bra-Ket Notation | 7 |
| I | Wigner's Formalism | 9 |
| 2 | The Density Matrix | 10 |
| 2.1 | Pure States | 10 |
| 2.1.1 | Density Matrix (pure states) | 11 |
| 2.1.2 | Properties of the Density Matrix (pure states) | 11 |
| 2.2 | Mixed States | 12 |
| 2.2.1 | Density Matrix (mixed states) | 13 |
| 2.2.2 | Properties of the Density Matrix (mixed states) | 13 |
| 2.3 | Density Matrix and Expected Values | 14 |
| 2.4 | Time Evolution of the Density Matrix | 15 |
| 2.5 | Density Matrix Kernel | 17 |
| 2.6 | Time Evolution of the Density Matrix Kernel | 17 |
| 3 | The Weyl and Wigner Transforms | 19 |
| 3.1 | Quantization Schemes | 19 |
| 3.2 | Weyl Quantization of Polynomials (1-Dimensional Case) | 20 |
| 3.3 | Weyl Quantization of Polynomials (N-Dimensional Case) | 21 |
| 3.4 | Weyl Quantization of Generic Functions (N-Dimensional Case) | 21 |
| 3.5 | Inverse Weyl Quantization | 26 |
| 4 | The Wigner Function | 28 |
| 4.1 | Definition of the Wigner Function | 28 |
| 4.2 | Properties of the Wigner Function | 29 |
| 4.3 | Moments of the Wigner Function | 32 |
| 4.3.1 | 0 th moment | 33 |
| 4.3.2 | 1 st moment | 33 |
| 4.3.3 | 2 nd moment | 34 |
| 5 | The Wigner Equation | 35 |
| 5.1 | Steady-State Solution | 41 |
| 5.1.1 | Simplifying Assumptions | 41 |
| 5.1.2 | Solution Method | 44 |
| 6 | Moments of the Wigner Equation | 49 |
| 6.1 | 0 th Order Moment | 49 |
| 6.2 | 1 st Order Moment | 51 |
| 6.3 | Statistical Extension of the Moments | 56 |

| | | |
|------------|---|------------|
| II | Physical Models | 57 |
| 7 | The Density Gradient Model | 58 |
| 7.1 | Derivation | 58 |
| 7.2 | Density Gradient Model | 63 |
| 7.3 | More Practical Form | 63 |
| 8 | Generation/Recombination Mechanisms | 65 |
| 8.1 | Shockley Read Hall Generation/Recombination | 65 |
| 9 | Heterostructures and Boundary Conditions | 69 |
| 9.1 | Heterostructures | 69 |
| 9.1.1 | Modeling of Heterojunctions | 70 |
| 9.2 | Boundary Conditions | 71 |
| 9.2.1 | Heterojunctions and Homojunctions | 71 |
| 9.2.2 | Ohmic Contact | 73 |
| 9.2.3 | Schottky Contact | 75 |
| III | Discretization and Implementation | 77 |
| 10 | 1D Discretization Scheme | 78 |
| 10.1 | Poisson Equation Discretization | 78 |
| 10.1.1 | Boundary Conditions | 79 |
| 10.2 | Electron Continuity Equation Discretization | 80 |
| 10.2.1 | Boundary Conditions | 86 |
| 10.2.2 | Generation and Recombination | 88 |
| 10.3 | Hole Continuity Equation Discretization | 88 |
| 10.3.1 | Boundary Conditions | 93 |
| 10.3.2 | Generation and Recombination | 95 |
| 10.4 | Electron Density Gradient Equation Discretization | 95 |
| 10.4.1 | Boundary Conditions | 97 |
| 10.5 | Hole Density Gradient Equation Discretization | 99 |
| 10.5.1 | Boundary Conditions | 100 |
| 11 | Numerical Techniques | 103 |
| 11.1 | Introduction to Newton's method | 103 |
| 11.2 | Generalized Newton's method | 104 |
| 11.3 | Quantum Drift-Diffusion problem | 105 |
| 11.3.1 | Nonlinear Problem | 107 |
| 11.3.2 | Jacobian of the Nonlinear Problem | 108 |
| 11.4 | Initial guess | 130 |
| 11.5 | MATLAB [®] Implementation | 132 |
| 12 | Materials and Parameters | 133 |
| 12.1 | Materials | 133 |
| 12.2 | Material Parameters | 134 |
| 12.2.1 | Electromagnetic Parameters | 134 |
| 12.2.2 | Band Structure Parameters | 135 |
| 12.2.3 | Transport Parameters | 137 |
| 12.2.4 | SRH Recombination Parameters | 137 |
| IV | HEMT and QW-HEMT Simulations | 138 |
| 13 | Single Heterostructure HEMT | 139 |
| 13.1 | Device Structure | 139 |

| | | |
|-----------|---|------------|
| 13.2 | Operating Principle | 140 |
| 13.3 | Density Gradient Simulation | 142 |
| 13.3.1 | Comparison with Poisson-Boltzmann | 147 |
| 13.3.2 | Comparison with Poisson-Schrödinger | 148 |
| 13.3.3 | Modeling Issues: Classical vs Quantum | 149 |
| 14 | Double Heterostructure HEMT | 151 |
| 14.1 | Device Structure | 151 |
| 14.2 | Density Gradient Simulation | 152 |
| 14.2.1 | Comparison with Drift-Diffusion | 156 |
| 14.2.2 | Comparison with Poisson-Schrödinger | 157 |
| 15 | Conclusions | 159 |

Chapter 1

Introductory Concepts

1.1 Evolution of Physical Models

Device simulation is nowadays a fundamental step in the design of any new technological node. This is especially true since devices have recently started to become more and more geometrically complex, typically also exploiting the “third dimension” (i.e. the direction orthogonal to the wafer), hence making analytical models either impossible to derive or too complex to be useful for design purposes.

Any simulator for semiconductor devices needs to include equations modeling at least:

- the **states** of the quantum system (e.g. Schrödinger equation, approximate analytic densities of states for bulk semiconductors, etc.)
- the **statistics** with which the states are populated (e.g. Fermi-Dirac statistics, Boltzmann statistics, etc.)
- the **electromagnetic effects** (e.g. Maxwell’s equations, Poisson’s equation, etc.)

The best results in terms of accuracy would surely be obtained by considering Schrödinger’s equation for determining the states of the system, Fermi-Dirac statistics to populate them and Maxwell’s equations to relate the charge density and the electromagnetic fields. This approach would however be extremely complex for a number of reasons, among which:

- solving Schrödinger’s equation for the scattering states would lead to a nonlinear eigenvalue problem which cannot always be solved numerically
- the isolated Maxwell’s equations are already extremely complex to be solved, coupling them with other equations would make the solution of the problem almost impossible
- the complexity of the problem would be too high to tread 2-dimensional or 3-dimensional structures or even typical 1-dimensional structures

For this reason, ever since the introduction of semiconductor-based electronic devices, simpler models that can provide good enough results have been investigated. Such models should ideally allow to obtain rough estimates of the main properties of a device (mainly its IV characteristics and if possible its frequency behavior) within reasonable computational times (a few days at most, so as to allow multiple reiterations of the device design procedure). This reduction of computational time needed for the simulations is however typically only obtained by neglecting some physical effects which are assumed not to play any important role in the operation of the device.

The first model that has been found out to work reasonably well for the first generations of electronic devices (in particular for most bipolar transistors and for MOSFETs having channel length above 200 nm) was the drift-diffusion model. The main simplifying hypotheses under which such model is formulated are the following:

1. current is only related to either drift (due to electric fields) or diffusion of electrons
2. the materials are always characterized by a density of states which is the same as that of a bulk material

3. magnetic fields are neglected and electric fields are quasi-static

The drift-diffusion model is quite simple and has been successfully implemented in many commercial simulators such as Sentaurus TCAD and Comsol Multiphysics, but its many limitations are quickly becoming evident as device scaling progresses.

While assumptions 1. and 3. are quite reasonable and could also for deeply scaled devices (unless phenomena like ballistic transport, tunnelling and thermionic emission become particularly important, in which case assumption 1. could also fall apart), assumption 2. typically fails to hold true when **quantum confinement** becomes significant.

Quantum confinement is defined as the reduction in the degrees of freedom of the carrier particles implying a reduction in the allowed phase space (i.e. in the simultaneous values of position and momentum for the particles being confined) [1]. Because of the reduction in the allowed phase space not all energy values are possible for confined particles, hence the distribution of states with respect to energy is altered.

If the boundaries for the confinement are loose enough, which used to be the case for the first generations of electronic devices (in which dimensions were larger), the changes in the density of states will be negligible. This is however not the case anymore for deeply scaled devices, therefore making the drift-diffusion model not good enough for studying and designing many modern devices.

A new approach is therefore needed for studying the devices without neglecting the most important quantum effects.

Going back to its original derivation, the drift-diffusion model is obtained from the Boltzmann transport equation through a series of simplifications:

1. the Boltzmann transport equation is simplified into the hydrodynamic model (i.e. a model whose equations are extremely similar to the most common equations of fluid dynamics)
2. the hydrodynamic model is simplified into the energy-balance model
3. the energy-balance model is simplified into the drift-diffusion model

which are treated in detail in [2], [3].

The first idea might therefore be to use the Boltzmann transport equation instead of the drift-diffusion model. This model, besides requiring huge computational times, is still not well suited for taking quantum confinement effects into account. The reason for this is that the Boltzmann transport equation is a semiclassical model, while quantum models are required to treat quantum confinement effectively. While Schrödinger's equation is able to model well also semiclassical systems for which the Boltzmann transport equation works, the converse is often not true (especially when working at nanometer scale).

In order to derive a more effective model to include quantum effects it is therefore necessary to start back from Schrödinger's equation (more precisely, Schrödinger's equation is cast in a form that is more similar to the Boltzmann transport equation, which is known as the Wigner equation) and apply different simplifying hypotheses. If those hypotheses do not neglect any relevant quantum effect, then a **quantum hydrodynamic model** can be obtained (i.e. a model whose equations are extremely similar to the most common equations of fluid dynamics). Further simplification then allows to obtain a **quantum drift-diffusion model**, which is extremely similar in nature to the semiclassical drift-diffusion model but retains some first-order quantum corrections which were instead missing in it.

Figure 1.1 shows the hierarchy of models that are available for the simulation of electronic devices, with a particular focus on the chains of approximations that lead to the drift-diffusion model and to the quantum drift-diffusion model.

The quantum drift-diffusion model is neither the only nor the most accurate model for the simulation of semiconductor devices. non-equilibrium Green's functions can be introduced as a straightforward perturbative extension of Schrödinger's equation which is more suitable for a numerical solution.

Non-equilibrium Green's functions (typically known as NEGF) are however extremely computationally expensive to be computed and only suitable for 1-dimensional device simulations. The quantum drift-diffusion model, despite being less accurate, has much lower complexity and can be implemented in a 2 or

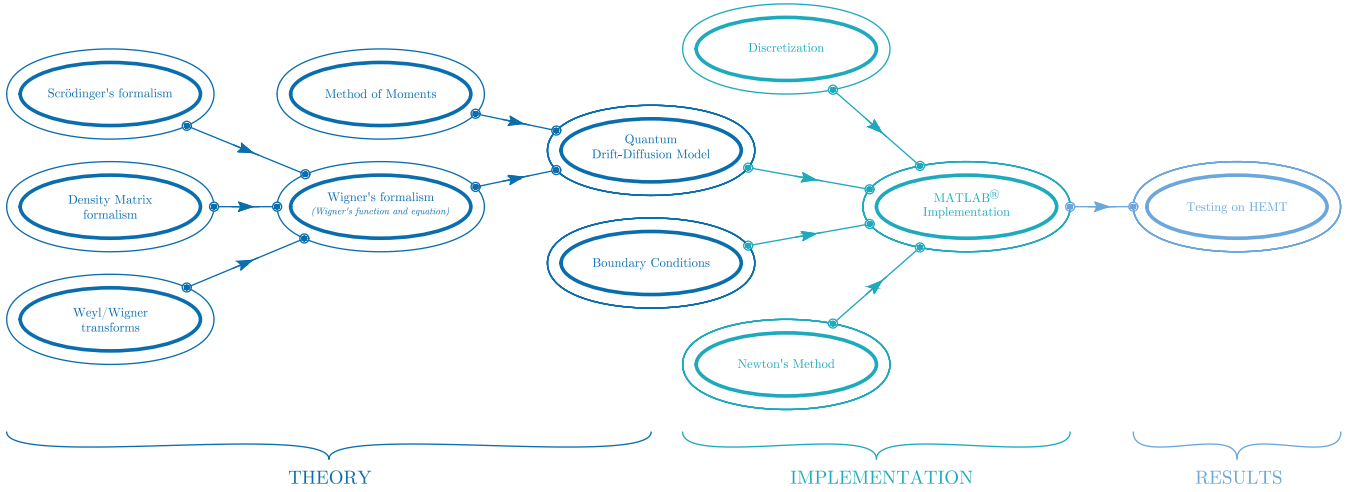


Figure 1.2: Workflow for this document

While several heuristic derivations exist for this model [4], a formal theoretical derivation of the model must touch several fields of theoretical physics and of mathematics. In particular, the logical flow for obtaining it is:

1. introducing the density matrix formalism to treat the system as a statistical ensemble of particles defined each by a single-particle wavefunction (according to Schrödinger's formalism)
2. applying Weyl/Wigner transforms to the density matrix operator with the goal of obtaining a semi-classical probability density function in phase space, which leads to the concept of Wigner function
3. deriving an evolution equation for the Wigner function, therefore effectively defining Wigner's formalism of quantum mechanics. Such an evolution equation is known as the Wigner equation
4. applying the method of moments to the Wigner equation to derive a drift-diffusion-like model

While the procedure is quite complex, the result is an extremely straightforward way of including quantum corrections in a drift-diffusion model.

The quantum drift-diffusion (QDD) model is then complemented with boundary conditions, which are necessary for the numerical solution of the problem.

The next focus of this work is then on discretizing the differential equations in the quantum drift-diffusion model and applying Newton's method for the solution of the resulting system of nonlinear equations.

Finally, the resulting simulator is tested on high electron mobility transistors (HEMT) made with III-V alloys (in particular AlGaAs) to determine whether the quantum drift-diffusion model is able to handle correctly quantum effects in these kinds of structures.

Figure 1.2 summarizes the logical flow that has been followed in this document for the derivation, implementation and testing of the quantum drift-diffusion (i.e. density gradient) model.

1.3 Schrödinger's Formalism

Since the quantum drift-diffusion model derives from Schrödinger's formalism and equation, it is useful to review some of its main aspects and to define the notation that will be used throughout this treatment.

Schrödinger's formalism for quantum mechanics is founded on 6 postulates: [5]

1. The state of a quantum mechanical system is completely specified by the wavefunction $\Psi(\mathbf{r}, t)$ that depends on the coordinates of the particle(s) and on time.

This function, called the wave function or state function, has the important property that $\Psi^*(\mathbf{r}, t)\Psi(\mathbf{r}, t)d\mathbf{r}$ is the probability that the particle lies within the volume element $d\mathbf{r}$ located at \mathbf{r} at time t .

In order for this probabilistic interpretation to hold true the wavefunction must be normalized, i.e. it must satisfy the condition:

$$\int_{\Omega} \Psi^*(\mathbf{r}, t) \Psi(\mathbf{r}, t) d\mathbf{r} = 1$$

where Ω is the domain for the quantum-mechanical problem (in practical cases $\Omega \equiv \mathbb{R}^n$ but in simulations this space is often restricted to a region in which the probability of finding the particle is almost unitary).

2. To every observable in classical mechanics there corresponds a linear, Hermitian operator in quantum mechanics.

The hermiticity condition is necessary in order for the operator to have real eigenvalues.

Some operators that commonly occur in quantum mechanics are reported in Table 1.1.

| Observable | | Operator | |
|------------------|------------------|-----------------------|--|
| Name | Classical Symbol | Operator Symbol | Operation |
| Position | \mathbf{r} | $\hat{\mathbf{R}}$ | Multiply by \mathbf{r} |
| Momentum | \mathbf{p} | $\hat{\mathbf{P}}$ | $-i\hbar \left(\hat{\mathbf{x}} \frac{\partial}{\partial \mathbf{x}} \right)$ |
| Kinetic Energy | T | \hat{T} | $-\frac{\hbar^2}{2m} \left(\frac{\partial^2}{\partial x^2} + \frac{\partial^2}{\partial y^2} + \frac{\partial^2}{\partial z^2} \right)$ |
| Potential Energy | $U(\mathbf{r})$ | $\hat{U}(\mathbf{r})$ | Under proper regularity assumptions (a power series for $V(\mathbf{r})$ must exist) Multiply by $V(\mathbf{r})$ |
| Total Energy | E | \hat{H} | $-\frac{\hbar^2}{2m} \left(\frac{\partial^2}{\partial x^2} + \frac{\partial^2}{\partial y^2} + \frac{\partial^2}{\partial z^2} + V(\mathbf{r}) \right)$ |
| Angular Momentum | l_x | \hat{L}_x | $-i\hbar \left(y \frac{\partial}{\partial z} - z \frac{\partial}{\partial y} \right)$ |
| | l_y | \hat{L}_y | $-i\hbar \left(z \frac{\partial}{\partial x} - x \frac{\partial}{\partial z} \right)$ |
| | l_z | \hat{L}_z | $-i\hbar \left(x \frac{\partial}{\partial y} - y \frac{\partial}{\partial x} \right)$ |

Table 1.1: quantum-mechanical operators

3. In any measurement of the observable associated with an operator \hat{A} , the only values that will ever be observed are the eigenvalues a , which satisfy the eigenvalue equation:

$$\hat{A} \{ \varphi(\mathbf{r}, t) \} = a \varphi(\mathbf{r}, t)$$

where φ is an eigenfunction corresponding to the eigenstate a .

If the system is in an eigenstate of the operator \hat{A} for the observable A with eigenvalue a , then any measurement of the quantity A will yield a .

Even though measurements must always yield an eigenvalue of the operator associated to the observable, the state of the system does not have to be an eigenstate of \hat{A} . An arbitrary state can be expanded in the complete set of eigenvectors of \hat{A} ($\hat{A} \{ \varphi_i \} = a_i \varphi_i$) as:

$$\Psi = \sum_i c_i \psi_i$$

The result of a measurement of the quantity A on a system in this state will always be one of the eigenvalues a_i of the operator \hat{A} . The probability of obtaining a specific eigenvalue a_i from the measurement is given by $|c_i|^2$.

4. If a system is in a state described by a normalized wavefunction Ψ , then the expected value of the observable corresponding to \hat{A} is given by:

$$\langle A \rangle = \int_{-\infty}^{+\infty} \Psi^*(\mathbf{r}, t) \hat{A} \{ \Psi(\mathbf{r}, t) \} d\mathbf{r} = \sum_i |c_i|^2 a_i$$

where c_i are the coefficients for the expansion of the eigenfunction Ψ in terms of the eigenfunctions of the operator \hat{A} .

5. The wavefunction or state function of a system evolves in time according to the time-dependent Schrödinger equation:

$$\hat{H} \{ \Psi(\mathbf{r}, t) \} = i\hbar \frac{\partial \Psi}{\partial t}(\mathbf{r}, t)$$

where \hat{H} is the Hamiltonian operator as described in Table 1.1.

6. The total wavefunction must be antisymmetric with respect to the interchange of all coordinates of one fermion with those of another. Electronic spin must be included in this set of coordinates.

The Pauli exclusion principle is a direct result of this antisymmetry principle.

1.4 Dirac's Bra-Ket Notation

Typical operations of quantum mechanics are:

- applying an operator \hat{A} to the wavefunction Ψ representing a state:

$$\hat{A} \{ \Psi(\mathbf{r}, t) \}$$

- computing the inner product of two wavefunctions Ψ_1 and Ψ_2 representing two states:

$$\int_{\Omega} \Psi_1^*(\mathbf{r}, t) \Psi_2(\mathbf{r}, t) d\mathbf{r}$$

- computing the inner product between a wavefunction φ belonging to a complete orthonormal set and the result of applying an operator \hat{A} to a wavefunction Ψ :

$$\int_{\Omega} \varphi^*(\mathbf{r}, t) \hat{A} \{ \Psi(\mathbf{r}, t) \} d\mathbf{r}$$

- computing the expected value of the observable associated to \hat{A} on a system in a state represented by Ψ

Since the integral notation involved in these operations is quite heavy, Paul Dirac suggested the use of the more compact **Bra-Ket notation**, in which:

- the state corresponding to the wavefunction $\Psi(\mathbf{r}, t)$ is represented by $|\Psi\rangle$
- the inner product between two wavefunctions Ψ_1 and Ψ_2 is represented as:

$$\langle \Psi_1 | \Psi_2 \rangle \triangleq \int_{\Omega} \Psi_1^*(\mathbf{r}, t) \Psi_2(\mathbf{r}, t) d\mathbf{r}$$

- the result of applying an operator \hat{A} to the state having wavefunction Ψ is represented as:

$$|\hat{A}|\Psi\rangle \triangleq \hat{A} \{ \Psi(\mathbf{r}, t) \}$$

- the inner product between a wavefunction φ and the result of applying an operator \hat{A} to the state having wavefunction Ψ is represented as:

$$\langle \varphi | \hat{A} | \Psi \rangle \triangleq \int_{\Omega} \varphi^*(\mathbf{r}, t) \hat{A} \{ \Psi(\mathbf{r}, t) \} d\mathbf{r}$$

- the operator that takes the inner product of its argument with a reference wavefunction φ is:

$$\langle \varphi | \{ \Psi \} \triangleq \int_{\Omega} \varphi^*(\mathbf{r}, t) \Psi(\mathbf{r}, t) d\mathbf{r}$$

This notation then offers the advantage that combining the operator $\langle \varphi |$ and the wavefunction $| \Psi \rangle$ yields the inner product $\langle \varphi | \Psi \rangle$ exactly as defined by the notation.

Operators of the kind $\langle a |$ are known as **bra**, while wavefunctions of the kind $| b \rangle$ are known as **ket**, from which the name of this notation.

This notation will be particularly convenient in chapter 2 when introducing the concept of density matrix and its properties. This is however not always the most clear notation (and, moreover, in order to get any kind of results it is anyway necessary to compute the values of the integrals), so the integral notation will be adopted instead for all the remaining part of this treatment.

Moreover, due to the sheer size of the equations involved in this treatment the spatial and time dependencies of the wavefunctions will be often dropped. Every wavefunction is anyway to be intended as being dependent on both space and time.

Part I

Wigner's Formalism

Chapter 2

The Density Matrix

In solid state physics states are generally derived using quantum mechanics and filled according to principles deriving from Statistical Physics.

This concept of weighting pure states (whose definition will be given in the next section) by their probability of being filled by one electron is one of the main foundations of modern analysis of devices and is at the basis of the introduction of density matrices.

The simplest way to introduce this class of operators is to start from pure states and then expand the resulting definition to mixed states.

2.1 Pure States

Consider a set of given objects; if all the objects within the set are described by the same wavefunction Ψ then the ensemble is said to be represented by a **pure state** $|\Psi\rangle$.

Pure states are the most simple kind of ensemble, as treating them is basically equivalent to treating each particle individually.

The typical goal in solid state physics is to obtain the expected value for a given observable A . It is therefore reasonable to consider a Hermitian operator \hat{A} representing such observable.

Moreover, as the operator being considered is hermitian there exists at least a basis $\{\varphi_i\}$ consisting of its eigenfunctions that is orthonormal. [6]

This translates into the conditions:

$$\hat{A} \{\varphi_i\} = a_i \varphi_i \quad \langle \varphi_i | \varphi_j \rangle = \delta_{ij}$$

where δ_{ij} represents Kronecker's delta and a_i is the eigenvalue corresponding to the eigenvector φ_i under the operator A .

The wavefunction Ψ representing the ensemble can then be expanded in terms of such basis as:

$$\Psi = \sum_i c_i \varphi_i$$

This decomposition in terms of an orthonormal basis of eigenvectors is the starting point for deriving most of the properties of a pure state and will be heavily used in the following.

Under these assumptions, quantum mechanics postulates [7] that the expected value $\langle A \rangle_\Psi$ of an observable A represented by the operator \hat{A} is given for a pure state $|\Psi\rangle$ by:

$$\langle A \rangle_\Psi = \sum_n |c_n|^2 a_n$$

From this last relationship it is therefore clear that $|c_n|^2$ can be interpreted as the probability of obtaining a result a_n when measuring the observable represented by the operator \hat{A} over the pure ensemble whose state is represented by the wavefunction Ψ .

2.1.1 Density Matrix (pure states)

Let Ψ be the wavefunction describing the pure state, then the density matrix ρ for it is defined as:

$$\rho_{\Psi} \triangleq |\Psi\rangle \langle\Psi|$$

i.e. as the operator ρ_{Ψ} that applied to a wavefunction α yields as a result:

$$\rho_{\Psi}\{\alpha\} = \Psi \int_{\Omega} \Psi^*(\mathbf{r}) \alpha(\mathbf{r}) d\mathbf{r}$$

where Ω is the domain of definition of the quantum mechanical problem and \mathbf{r} is the spatial coordinate that spans it.

The density matrix ρ_{Ψ} for a pure state Ψ can be geometrically interpreted as the projection operator along the direction defined in the Hilbert space of wavefunctions by Ψ .

2.1.2 Properties of the Density Matrix (pure states)

The density matrix operator ρ_{Ψ} has the following properties:

- **Projector property:**

$$\rho_{\Psi}^2 = \rho_{\Psi}$$

Proof:

$$\begin{aligned} \rho_{\Psi}^2 \{\alpha\} &\triangleq \rho_{\Psi} \{\rho_{\Psi} \{\alpha\}\} \\ &= |\Psi\rangle \langle\Psi| \{|\Psi\rangle \langle\Psi|\alpha\rangle\} \\ &= |\Psi\rangle \langle\Psi|\alpha\rangle \langle\Psi|\Psi\rangle && \text{(sesquilinearity of } \langle | \rangle) \\ &= |\Psi\rangle \langle\Psi|\alpha\rangle && \text{(orthonormality of } \Psi) \\ &\triangleq \rho_{\Psi} \{\alpha\} \end{aligned}$$

- **Hermiticity property:**

$$\rho_{\Psi}^{\dagger} = \rho_{\Psi}$$

where ρ_{Ψ}^{\dagger} is the Hermitian adjoint operator to ρ_{Ψ} and is defined as the operator such that:

$$\langle\alpha|\rho_{\Psi}|\beta\rangle = \langle\rho_{\Psi}^{\dagger}(\alpha)|\beta\rangle$$

(with α and β two arbitrary wavefunctions)

Proof:

$$\begin{aligned} \langle\alpha|\rho_{\Psi}|\beta\rangle &\triangleq \langle\alpha|(|\Psi\rangle \langle\Psi|)|\beta\rangle \\ &= \langle\Psi|\beta\rangle \langle\alpha|\Psi\rangle \\ &= \int_{\Omega} \Psi^*(\mathbf{r}) \beta(\mathbf{r}) d\mathbf{r} \int_{\Omega} \alpha^*(\mathbf{r}') \Psi(\mathbf{r}') d\mathbf{r}' \\ &= \int_{\Omega} \int_{\Omega} \alpha^*(\mathbf{r}') \Psi(\mathbf{r}') d\mathbf{r}' \Psi^*(\mathbf{r}) \beta(\mathbf{r}) d\mathbf{r} \\ &= \int_{\Omega} \left[\int_{\Omega} \alpha(\mathbf{r}') \Psi^*(\mathbf{r}') d\mathbf{r}' \Psi(\mathbf{r}) \right]^* \beta(\mathbf{r}) d\mathbf{r} \\ &= \int_{\Omega} [|\Psi\rangle \langle\Psi|\alpha\rangle]^* \beta(\mathbf{r}) d\mathbf{r} \end{aligned}$$

$$\begin{aligned} &\triangleq \int_{\Omega} [\rho_{\Psi} \{ \alpha \}]^* \beta(\mathbf{r}) d\mathbf{r} \\ &= \langle \rho_{\Psi} \{ \alpha \} | \beta \rangle \end{aligned}$$

- **Normalization property:**

$$\text{Tr}(\rho_{\Psi}) = 1$$

where $\text{Tr}(\rho_{\Psi})$ is the trace of an operator A and can be defined in terms of its eigenvector basis $\{\varphi_i\}$ as:

$$\text{Tr}(\rho_{\Psi}) = \sum_i \langle \varphi_i | A | \varphi_i \rangle$$

Proof:

$$\begin{aligned} \text{Tr}(\rho_{\Psi}) &\triangleq \sum_i \langle \varphi_i | \rho_{\Psi} | \varphi_i \rangle \\ &= \sum_i \langle \varphi_i | (|\Psi\rangle \langle \Psi|) | \varphi_i \rangle \\ &= \sum_i \langle \phi_i | \Psi \rangle \langle \Psi | \phi_i \rangle \\ &= \sum_i c_i c_i^* && \text{(projection onto eigenfunctions)} \\ &= 1 && \text{(completeness of the eigenfunction basis)} \end{aligned}$$

- **Positivity property:**

$$\langle \alpha | \rho_{\Psi} | \alpha \rangle \geq 0$$

(with α an arbitrary wavefunction)

Proof:

$$\begin{aligned} \langle \alpha | \rho_{\Psi} | \alpha \rangle &\triangleq \langle \alpha | \Psi \rangle \langle \Psi | \alpha \rangle \\ &\triangleq (\langle \Psi | \alpha \rangle)^* \langle \Psi | \alpha \rangle \\ &\triangleq |\langle \Psi | \alpha \rangle|^2 \\ &\geq 0 \end{aligned}$$

These properties will be useful in the following to discuss the properties of the more complex density matrix definition for mixed states.

2.2 Mixed States

Consider a set of given objects; if it is possible to define more than one subset that are represented by different pure states (i.e. different wavefunctions) the ensemble is said to be represented by a **mixed state**. In the following, the case of a mixed state with a discrete number of pure substates will be treated for the sake of simplicity and since it is best suited for simulations.

Since the different pure substates may have different probability of occurring it is useful to define as p_i the probability of an object in the ensemble (which is described by the mixed state) to be in the i -th pure state. A complete statistical quantum mechanical characterization of the system can be then given by providing:

- the set Ψ_i of *unique* wavefunctions of the particles that make up the ensemble
- the set p_i of probabilities of a particle being in a pure state described by the wavefunctions Ψ_i

under the assumption that the particles are not interacting with each other.

Since the pure substates must add up to the mixed state, the constraint:

$$\sum_i p_i = 1$$

must hold true on the probabilities of occurrence of the pure states.

2.2.1 Density Matrix (mixed states)

With the notation for mixed states of section 2.2 the density matrix operator can be defined for a mixed state as:

$$\rho^{\text{mix}} \triangleq \sum_i p_i \rho_{\Psi_i}^{\text{pure}} = \sum_i p_i |\Psi_i\rangle \langle \Psi_i|$$

i.e. by simply averaging the density matrices for pure states by their probabilities of occurring.

2.2.2 Properties of the Density Matrix (mixed states)

The density matrix operator ρ^{mix} for mixed states has the same properties of the density matrix for pure states except for the projector property, which does not hold anymore:

- **Hermiticity property:**

$$(\rho^{\text{mix}})^\dagger = \rho^{\text{mix}}$$

Proof:

$$\begin{aligned} \langle \alpha | \rho^{\text{mix}} | \beta \rangle &\triangleq \langle \alpha | \left(\sum_i p_i \rho_{\Psi_i}^{\text{pure}} \right) | \beta \rangle \\ &= \sum_i p_i \langle \alpha | \rho_{\Psi_i}^{\text{pure}} | \beta \rangle \\ &= \sum_i p_i \langle \rho_{\Psi_i}^{\text{pure}}(\alpha) | \beta \rangle \\ &= \left\langle \sum_i p_i \rho_{\Psi_i}^{\text{pure}}(\alpha) | \beta \right\rangle \\ &\triangleq \langle \rho^{\text{mix}}(\alpha) | \beta \rangle \end{aligned}$$

- **Normalization property:**

$$\text{Tr}(\rho^{\text{mix}}) = 1$$

Proof:

$$\begin{aligned} \text{Tr}(\rho^{\text{mix}}) &\triangleq \sum_i \langle \varphi_i | \rho^{\text{mix}} | \varphi_i \rangle \\ &\triangleq \sum_i \langle \varphi_i | \sum_j p_j \rho_{\Psi_j}^{\text{pure}} | \varphi_i \rangle \\ &= \sum_j p_j \sum_i \langle \varphi_i | \rho_{\Psi_j}^{\text{pure}} | \varphi_i \rangle \\ &= \sum_j p_j \quad \quad \quad (\text{normalization property of } \rho^{\text{pure}}) \\ &= 1 \end{aligned}$$

- **Positivity property:**

$$\langle \alpha | \rho^{\text{mix}} | \alpha \rangle \geq 0$$

Proof:

$$\begin{aligned} \langle \alpha | \rho^{\text{mix}} | \alpha \rangle &\triangleq \sum_i p_i \langle \alpha | \Psi_i \rangle \langle \Psi_i | \alpha \rangle \\ &\triangleq \sum_i p_i |\langle \Psi_i | \alpha \rangle|^2 && \text{(probabilities are positive)} \\ &\geq 0 \end{aligned}$$

(the notation is the same that was already defined in subsection 2.1.2).

2.3 Density Matrix and Expected Values

Density matrix operators are extremely useful in treating mixed states.

Their usefulness is mainly related to the existence of a theorem that allows to quite easily compute the expected value of the operator representing an observable.

Let:

- ρ^{mix} be the density matrix for the mixed state
- \hat{A} be the operator for an observable

then the following relationship holds true for the expected value $\langle A \rangle_{\rho^{\text{mix}}}$ of the operator \hat{A} applied to the mixed state:

$$\langle A \rangle_{\rho^{\text{mix}}} = \text{Tr}(\rho^{\text{mix}} \hat{A})$$

where $\rho^{\text{mix}} \hat{A}$ is the composition (i.e. subsequent application) of the observable operator and of the density matrix operator.

Proof:

$$\begin{aligned} \langle A \rangle_{\rho^{\text{mix}}} &\triangleq \sum_i p_i \langle \Psi_i | \hat{A} | \Psi_i \rangle \\ &= \sum_i p_i \langle \Psi_i | \hat{A} \left[\sum_j |\varphi_j\rangle \langle \varphi_j | \Psi_i \rangle \right] \rangle && \left(\sum_j |\varphi_j\rangle \langle \varphi_j | = \mathbb{I} \right) \\ &= \sum_j \sum_i p_i \langle \Psi_i | \hat{A} | [\varphi_j] \rangle \langle \varphi_j | \Psi_i \rangle \\ &= \sum_j \sum_i p_i \langle \Psi_i | \hat{A} | [\varphi_j] \rangle \langle \varphi_j | \Psi_i \rangle \\ &= \sum_j \sum_i p_i \langle \varphi_j | \Psi_i \rangle \langle \Psi_i | \hat{A} | \varphi_j \rangle \\ &= \sum_j \sum_i p_i \langle \varphi_j | \Psi_i \rangle \langle \Psi_i | \hat{A} \{ |\varphi_j\rangle \} \\ &= \sum_j \langle \varphi_j | \left[\sum_i p_i |\Psi_i\rangle \langle \Psi_i | \right] \hat{A} \{ |\varphi_j\rangle \} \\ &= \sum_j \langle \varphi_j | \rho^{\text{mix}} \hat{A} | \varphi_j \rangle \end{aligned}$$

with \mathbb{I} the identity operator and $\{|\varphi_j\rangle\}$ an orthonormal basis of eigenvectors of the operator \hat{A} .

This property is particularly important since many physical interpretations of the density matrix follow directly from it, as it is giving a simple relationship between the density matrix of a mixed state and the statistical expected value of any observable operator.

Moreover, this relationship shows how the density matrix contains *sufficient* information to predict the result of *any* measurement that can be performed on an ensemble in a mixed state.

2.4 Time Evolution of the Density Matrix

As was shown before, the density matrix is simply a statistical extension (i.e. accounting statistically for the presence of multiple pure substates) of the quantum-mechanical projection operator along the pure states.

In a way, it could be seen as a statistical extension of the concept of probability density $|\Psi|^2$ to an ensemble in a mixed state since this operator has kernel (section 2.5):

$$\kappa_\rho(\mathbf{r}, \mathbf{r}') = \sum_i p_i \Psi_i^*(\mathbf{r}') \Psi_i(\mathbf{r})$$

whose "diagonal" is given by:

$$\kappa_\rho(\mathbf{r}, \mathbf{r}) = \sum_i p_i |\Psi_i(\mathbf{r}')|^2$$

i.e. the combination of the probability densities for the pure states appearing in the ensemble weighted by their relative probability of occurrence.

Clearly, the density matrix is more complex than a simple weighted average of the probability densities of the pure states in the ensemble, since it also includes "off-diagonal" terms $\kappa_\rho(\mathbf{r}, \mathbf{r}')$ (with $\mathbf{r} \neq \mathbf{r}'$) that could be interpreted as cross-correlation terms.

Similarly to what is done with the wavefunction Ψ and with the probability density $|\Psi|^2$ it is possible to introduce the time evolution of the density matrix ρ^{mix} for a mixed state (for which a single wavefunction cannot be easily defined without the dimensionality of the problem becoming quickly untreatable).

The counterpart of the time evolution equation for a mixed state is known as the **von Neumann Equation**:

$$i\hbar \frac{\partial}{\partial t} \rho^{\text{mix}} = [\hat{H}, \rho^{\text{mix}}]$$

where \hat{H} is the Hamiltonian of the problem and $[\alpha, \beta]$ is the commutator of two operators and is defined as the operator:

$$[\hat{A}, \hat{B}] = \hat{A}\hat{B} - \hat{B}\hat{A}$$

Proof:

Starting from the Schrödinger equation for a single particle:

$$i\hbar \frac{\partial}{\partial t} |\Psi\rangle = \hat{H} |\Psi\rangle \tag{2.1}$$

it is possible to derive the evolution equation for the covector $\langle\Psi|$ (defined from the wavefunction Ψ by means of the inner product $\langle|\rangle$).

In order to do this, consider to apply the covector $\langle\Psi|\hat{H}$ to the wavefunction describing the state α , i.e.:

$$\langle\Psi|\hat{H}|\alpha\rangle$$

Introducing the adjoint H^\dagger of the Hamiltonian (the concept of adjoint operator was introduced in subsection 2.1.2) this last expression can be rewritten as:

$$\langle\Psi|\hat{H}|\alpha\rangle = \langle\hat{H}^\dagger(\Psi)|\alpha\rangle$$

Moreover, since the Hamiltonian is self-adjoint $\hat{H}^\dagger = \hat{H}$ and:

$$\langle\Psi|\hat{H}|\alpha\rangle = \langle\hat{H}(\Psi)|\alpha\rangle$$

Substituting Schrödinger's equation (Equation 2.1) into this result the following equation is obtained:

$$\langle \Psi | \hat{H} | \alpha \rangle = \langle i\hbar \frac{\partial}{\partial t} | \Psi \rangle | \alpha \rangle$$

Extracting the derivative and the constants from the inner product (the constants in the Bra get conjugated due to the sesquilinearity of the inner product) the evolution equation for the covector $\langle \Psi |$ is obtained:

$$\langle \Psi | \hat{H} | \alpha \rangle = -i\hbar \frac{\partial}{\partial t} \langle \Psi | \alpha \rangle$$

Dropping the vector α to which the covector is applied and writing it in *operator equation* form leads to the more compact form:

$$-i\hbar \frac{\partial}{\partial t} \langle \Psi | = \langle \Psi | \hat{H} \quad (2.2)$$

Starting from the definition of the density matrix operator ρ^{mix} for a mixed state:

$$\rho^{\text{mix}} \triangleq \sum_i p_i \rho_{\Psi_i}^{\text{pure}} = \sum_i p_i |\Psi_i\rangle \langle \Psi_i|$$

through the application of the operator $i\hbar \frac{\partial}{\partial t}$ to both sides of the equation the following result is obtained:

$$i\hbar \frac{\partial}{\partial t} \rho^{\text{mix}} = \sum_i p_i i\hbar \frac{\partial}{\partial t} \{ |\Psi_i\rangle \langle \Psi_i| \} \quad (2.3)$$

The derivative of the product between a vector α and a *continuous* operator \hat{A} satisfies the identity:

$$\frac{\partial}{\partial t} \{ \alpha(t) \hat{A}(t) \} = \alpha(t) \frac{\partial}{\partial t} \{ \hat{A}(t) \} + \frac{\partial}{\partial t} \{ \alpha(t) \} \hat{A}(t)$$

which when applied to Equation 2.3 yields the expression:

$$i\hbar \frac{\partial}{\partial t} \rho^{\text{mix}} = \sum_i p_i i\hbar \left[|\Psi_i\rangle \frac{\partial}{\partial t} \{ \langle \Psi_i| \} + \frac{\partial}{\partial t} \{ |\Psi_i\rangle \} \langle \Psi_i| \right]$$

Substituting Equation 2.1 and Equation 2.2 into it and simplifying leads to the final form of the evolution equation for the density matrix operator:

$$\begin{aligned} i\hbar \frac{\partial}{\partial t} \rho^{\text{mix}} &= \sum_i p_i i\hbar \left[|\Psi_i\rangle \frac{i}{\hbar} \{ \langle \Psi_i| \hat{H} \} - \frac{i}{\hbar} \{ \hat{H} | \Psi_i \rangle \} \langle \Psi_i| \right] \\ i\hbar \frac{\partial}{\partial t} \rho^{\text{mix}} &= \sum_i p_i \left[\{ \hat{H} | \Psi_i \rangle \} \langle \Psi_i| - |\Psi_i\rangle \{ \langle \Psi_i| \hat{H} \} \right] \\ i\hbar \frac{\partial}{\partial t} \rho^{\text{mix}} &= \sum_i p_i \left[\hat{H} | \Psi_i \rangle \langle \Psi_i| - |\Psi_i\rangle \langle \Psi_i| \hat{H} \right] \\ i\hbar \frac{\partial}{\partial t} \rho^{\text{mix}} &= \left(\hat{H} \left(\sum_i p_i |\Psi_i\rangle \langle \Psi_i| \right) - \left(\sum_i p_i |\Psi_i\rangle \langle \Psi_i| \right) \hat{H} \right) \\ i\hbar \frac{\partial}{\partial t} \rho^{\text{mix}} &= \left(\hat{H} \rho^{\text{mix}} - \rho^{\text{mix}} \hat{H} \right) \end{aligned}$$

Introducing the quantum-mechanical commutator of two operators \hat{A} and \hat{B} as defined above then the evolution equation for the density matrix operator can be rewritten in the more compact form:

$$i\hbar \frac{\partial}{\partial t} \rho^{\text{mix}} = \left[\hat{H}, \rho^{\text{mix}} \right]$$

which is the most common form of the **von Neumann Equation**.

The von Neumann Equation is also commonly called the **quantum Liouville equation**, as it is the quantum counterpart of the statistical-mechanical Liouville equation [8]:

$$\frac{\partial \rho}{\partial t} = - \{ \rho, H \}$$

where:

- $\rho(p, q)$ is the probability distribution in phase space
- \hat{H} is the Hamiltonian for the system

2.5 Density Matrix Kernel

A concept that is fundamental for the development of the concept of Wigner function and for the density gradient model is the kernel of the density matrix operator.

The integral kernel of an operator \hat{A} is the function κ_A that satisfies the following requirement:

$$\hat{A}\{\alpha\}(\mathbf{r}) = \int_{\Omega} \kappa_A(\mathbf{r}, \mathbf{r}'') \alpha(\mathbf{r}'') d\mathbf{r}''$$

In order to determine the kernel $\kappa_A(\mathbf{r}, \mathbf{r}')$ it is sufficient to apply the operator \hat{A} to a delta function $\delta_{\mathbf{r}'}$ centered in \mathbf{r}' since:

$$\hat{A}\{\delta_{\mathbf{r}'}\}(\mathbf{r}, \mathbf{r}') = \int_{\Omega} \kappa_A(\mathbf{r}, \mathbf{r}'') \delta_{\mathbf{r}'}(\mathbf{r}'') d\mathbf{r}'' = \kappa_A(\mathbf{r}, \mathbf{r}')$$

Applying this procedure to the density matrix operator leads to:

$$\kappa_{\rho}(\mathbf{r}, \mathbf{r}') = \rho^{\text{mix}}\{\delta_{\mathbf{r}'}\} = \sum_i p_i |\Psi_i(\mathbf{r})\rangle \langle \Psi_i | \delta_{\mathbf{r}'} \rangle = \sum_i p_i \Psi_i^*(\mathbf{r}') \Psi_i(\mathbf{r}) \quad (2.4)$$

2.6 Time Evolution of the Density Matrix Kernel

Similarly to what was done in section 2.4 an evolution equation can be written also for the kernel of the density matrix operator.

The time evolution equation for the kernel of the density matrix operator takes the form:

$$i\hbar \frac{\partial}{\partial t} \kappa_{\rho}(\mathbf{r}, \mathbf{r}') = \left(\hat{H}_r \{\rho^{\text{mix}}(\mathbf{r}, \mathbf{r}')\} - \hat{H}_{r'} \{\rho^{\text{mix}}(\mathbf{r}, \mathbf{r}')\} \right) \quad (2.5)$$

where \hat{H}_r and $\hat{H}_{r'}$ are the hamiltonians with respect to the coordinate systems \mathbf{r} and \mathbf{r}' respectively.

It is important to notice that while Von Neumann's equation is an operator equation, this is instead a standard equation on functions.

Proof:

Starting from the Schrödinger equation for a single particle:

$$i\hbar \frac{\partial}{\partial t} |\Psi\rangle = \hat{H} |\Psi\rangle \quad (2.6)$$

by conjugating it the following equation is obtained:

$$-i\hbar \frac{\partial}{\partial t} |\Psi^*\rangle = \hat{H} |\Psi^*\rangle \quad (2.7)$$

(by linearity the of the Hamiltonian the conjugation can be brought inside the argument of the operator).

Applying the operator $i\hbar \frac{\partial}{\partial t}$ to both sides of Equation 2.4 leads to:

$$i\hbar \frac{\partial}{\partial t} \kappa_{\rho}(\mathbf{r}, \mathbf{r}') = i\hbar \frac{\partial}{\partial t} \left(\sum_i p_i \Psi_i^*(\mathbf{r}') \Psi_i(\mathbf{r}) \right)$$

$$i\hbar \frac{\partial}{\partial t} \kappa_{\rho}(\mathbf{r}, \mathbf{r}') = i\hbar \sum_i p_i \frac{\partial}{\partial t} (\Psi_i^*(\mathbf{r}') \Psi_i(\mathbf{r}))$$

Expanding the derivative of the product through the product rule for the derivative the following result is obtained:

$$i\hbar \frac{\partial}{\partial t} \kappa_{\rho}(\mathbf{r}, \mathbf{r}') = i\hbar \sum_i p_i \left(\Psi_i(\mathbf{r}) \frac{\partial}{\partial t} \Psi_i^*(\mathbf{r}') + \Psi_i^*(\mathbf{r}') \frac{\partial}{\partial t} \Psi_i(\mathbf{r}) \right)$$

Substituting Equation 2.6 and Equation 2.7 into this last result leads to:

$$i\hbar \frac{\partial}{\partial t} \kappa_\rho(\mathbf{r}, \mathbf{r}') = \sum_i p_i \left(\Psi_i^*(\mathbf{r}') \hat{H}_r \{ \Psi_i(\mathbf{r}) \} - \Psi_i(\mathbf{r}) \hat{H}_{r'} \{ \Psi_i^*(\mathbf{r}') \} \right)$$

where the variable at the subscript of the Hamiltonians \hat{H}_r and $\hat{H}_{r'}$ represents the variable in which the hamiltonian is taken (i.e. the variable with respect to which differentiations are taken and to which the potentials are referred).

Simplification of this last equation leads to the evolution equation for the kernel of the density matrix:

$$i\hbar \frac{\partial}{\partial t} \kappa_\rho(\mathbf{r}, \mathbf{r}') = \left(\hat{H}_r \left\{ \sum_i p_i \Psi_i^*(\mathbf{r}') \Psi_i(\mathbf{r}) \right\} - \hat{H}_{r'} \left\{ \sum_i p_i \Psi_i(\mathbf{r}) \Psi_i^*(\mathbf{r}') \right\} \right)$$

$$i\hbar \frac{\partial}{\partial t} \kappa_\rho(\mathbf{r}, \mathbf{r}') = \left(\hat{H}_r \{ \rho^{\text{mix}}(\mathbf{r}, \mathbf{r}') \} - \hat{H}_{r'} \{ \rho^{\text{mix}}(\mathbf{r}, \mathbf{r}') \} \right)$$

Chapter 3

The Weyl and Wigner Transforms

The concept of Weyl quantization and Wigner inverse quantization used to be of extreme importance in the first quantum-mechanical theories, particularly before the introduction of Feynman's formulation of quantization and quantum mechanics.

While less important in the development of the modern quantum theories, quantization schemes were at the basis of the definition of the Wigner function (which was introduced for the first time in 1932 by Eugene Wigner) and of the density gradient theory and it is therefore important to at least qualitatively justify them.

3.1 Quantization Schemes

In classical mechanics, observables (i.e. measurable physical quantities) are expressed by functions:

$$f(\mathbf{r}_1, \mathbf{r}_2, \dots, \mathbf{p}_1, \mathbf{p}_2, \dots)$$

of the momenta and positions (which are deterministic vectors, or, in the limit case of statistical mechanics, probability density functions) of all the particles/objects in the system.

In quantum mechanics observables are instead expressed by operators that act on the wavefunction of the state.

If the observable being considered is expressed by an operator \hat{A} and a pure state is identified by a wavefunction Ψ accepting decomposition in terms of a basis $\{\varphi_i\}$ of eigenvectors of the operator \hat{A} :

$$\Psi = \sum_i c_i \varphi_i$$

and if a_i denotes the eigenvalue of \hat{A} corresponding to the eigenvector φ_i then quantum mechanics postulates the expected value for the observable over the state to be:

$$\langle \hat{A} \rangle_{\Psi} = \sum_i |c_i|^2 a_i$$

If a mixed state is being considered, the expected values of the pure states Ψ_i within the mixed state (which can be represented by means of a density matrix formalism) should be weighted by the probability of occurrence p_i of their respective pure states and averaged to obtain the expected value of the observable:

$$\langle \hat{A} \rangle_{\rho} = \sum_i p_i \langle \hat{A} \rangle_{\Psi_i}$$

It is then clear that, while in classical mechanics defining mathematically an observable is quite simple and can be done experimentally or theoretically (starting from basic experimental laws), defining quantum-mechanical observables is extremely complex as it requires the design of operators instead of functions.

An intuitive way of obtaining some possible operators on which further experimental refinements can be performed is then to try and extend the classical function for the observable into an operator by "substitution" of the position and momentum variables within the functions with position and momentum *operators*:

$$f(\mathbf{r}, \mathbf{p}) \quad \longrightarrow \quad f(\hat{\mathbf{R}}, \hat{\mathbf{P}})$$

where \mathbf{r} and \mathbf{p} are the position and momentum variables respectively and $\hat{\mathbf{R}}$ and $\hat{\mathbf{P}}$ are the position and momentum operators respectively.

It is important to notice that in the above equation, while the expression on the left is a function, the expression on the right is an operator that acts on a function from a Hilbert space, returning another function from the same Hilbert space [9].

These kinds of ways of constructing quantum-mechanical observable from classical observables are known as **quantization schemes**.

While this method appears to be simple, there are complications related to the non-commutativity of the position and momenta operators in quantum mechanics. Since this is not present in classical mechanics, the result is a clear wedge between the two theories that leads to considerable ambiguity in the definition of a valid quantization scheme.

To understand the origin of this ambiguity and the possible choices that can be made it is useful to first study the case of quantization of polynomial classical functions of momentum and position, then extending it to the case of general functions by means of infinite series.

3.2 Weyl Quantization of Polynomials (1-Dimensional Case)

In order to more intuitively deal with the case of the quantization of classical observables defined by polynomial functions of position and momentum, whose general form in one dimension is of the kind:

$$f(r, p) = \sum_i \sum_j k_{i,j} x^i p^j$$

it is useful to consider the simple example:

$$f(r, p) = x^2 p^2$$

When quantizing it the product of two position operators \hat{X} and two momentum operators \hat{P} must be considered. Multiple possible orderings of these operators are however possible that all correspond to the same classical function (as the product of variables is commutative, while the product of operators is not):

$$\hat{X}^2 \hat{P}^2 \quad \hat{X} \hat{P} \hat{X} \hat{P} \quad \hat{X} \hat{P}^2 \hat{X} \quad \hat{P} \hat{X}^2 \hat{P} \quad \hat{P} \hat{X} \hat{P} \hat{X} \quad \hat{P}^2 \hat{X}^2$$

When quantizing a classical function to obtain a quantum-mechanical operator it is therefore of fundamental importance to decide which ordering of the position and momentum operators to take.

A less decisive choice might also be to take weighted averages of different possible combinations in order to account for multiple possibilities.

The most impartial way of defining an operator is then to take the average of all the possible permutations of $\hat{P} \hat{P} \hat{X} \hat{X}$ assuming equal probability for each one:

$$f(\hat{X}, \hat{P}) = \frac{1}{6} \left[\hat{X}^2 \hat{P}^2 + \hat{X} \hat{P} \hat{X} \hat{P} + \hat{X} \hat{P}^2 \hat{X} + \hat{P} \hat{X}^2 \hat{P} + \hat{P} \hat{X} \hat{P} \hat{X} + \hat{P}^2 \hat{X}^2 \right]$$

which is known as Weyl quantization.

In the most general case of a polynomial this quantization scheme can be expressed as:

$$f(x, p) = \sum_i \sum_j k_{i,j} x^i p^j \quad \longrightarrow \quad f(X, P) = \sum_i \sum_j k_{i,j} (\hat{X}^i \hat{P}^j)_W$$

where $(\hat{X}^i \hat{P}^j)_W$ is the Weyl quantization of the polynomial term $x^i p^j$ and is given by: [10]

$$(\hat{X}^i \hat{P}^j)_W = \binom{i+j}{i}^{-1} \sum_{(\hat{C}_1, \dots, \hat{C}_{i+j}) \in \sigma(\hat{X}^i \hat{P}^j)} \hat{C}_1 \cdots \hat{C}_{i+j}$$

with $\sigma(\hat{X}^i \hat{P}^j)$ representing the set of unique permutations of $\hat{X}^i \hat{P}^j$ (permutations which result in identical literal expressions are represented only once in the set).

A fundamental property of the Weyl quantization which will be exploited to allow the extension of its definition to multidimensional vector spaces is:

$$(ax + bp)^n \longrightarrow (a\hat{X} + b\hat{P})^n$$

Proof:

$$\begin{aligned} (ax + bp)^n &= \sum_{k=0}^n \binom{n}{k} (ax)^k (bp)^{n-k} \\ &= \sum_{k=0}^n \binom{n}{k} a^k b^{n-k} x^k p^{n-k} \end{aligned}$$

Applying Weyl's quantization scheme:

$$\begin{aligned} &\rightarrow \sum_{k=0}^n \binom{n}{k} a^k b^{n-k} (\hat{X}^k \hat{P}^{n-k})_W \\ &= \sum_{k=0}^n \binom{n}{k} a^k b^{n-k} \binom{k+n-k}{k}^{-1} \sum_{(\hat{C}_1, \dots, \hat{C}_{k+n-k}) \in \sigma(\hat{X}^k \hat{P}^{n-k})} \hat{C}_1 \cdots \hat{C}_{k+n-k} \\ &= \sum_{k=0}^n \binom{n}{k} a^k b^{n-k} \binom{n}{k}^{-1} \sum_{(\hat{C}_1, \dots, \hat{C}_n) \in \sigma(\hat{X}^k \hat{P}^{n-k})} \hat{C}_1 \cdots \hat{C}_n \\ &= \sum_{k=0}^n a^k b^{n-k} \sum_{(\hat{C}_1, \dots, \hat{C}_n) \in \sigma(\hat{X}^k \hat{P}^{n-k})} \hat{C}_1 \cdots \hat{C}_n \\ &= (a\hat{X} + b\hat{P})^n \end{aligned}$$

3.3 Weyl Quantization of Polynomials (N-Dimensional Case)

The N-dimensional case of the Weyl quantization can be obtained by extending the property of the 1D Weyl quantization scheme:

$$(ax + bp)^n \longrightarrow (a\hat{X} + b\hat{P})^n$$

into the N-dimensional version: [9]

$$(\mathbf{a} \cdot \mathbf{r} + \mathbf{b} \cdot \mathbf{p})^n \longrightarrow (\mathbf{a} \cdot \hat{\mathbf{R}} + \mathbf{b} \cdot \hat{\mathbf{P}})^n$$

3.4 Weyl Quantization of Generic Functions (N-Dimensional Case)

The goal of this introductory work is to determine a way of inverting the quantization of operators which do not represent observables (which is the case for the density matrix operator) and therefore do not have a straightforward classical counterpart. In this regard, it is important to understand how a general function (which is more complex than a polynomial involving position and momentum) might be quantized.

The first useful step to determine how to quantize a generic function is to determine how to quantize exponentials, as they constitute an infinite basis for any regular enough function.

Consider the exponential function of momentum and position $\exp\{\mathbf{a} \cdot \mathbf{r} + \mathbf{b} \cdot \mathbf{p}\}$. By rewriting it through its *formal* infinite series expansion:

$$\exp\{\mathbf{a} \cdot \mathbf{r} + \mathbf{b} \cdot \mathbf{p}\} = \sum_{i=0}^{\infty} \frac{(\mathbf{a} \cdot \mathbf{r} + \mathbf{b} \cdot \mathbf{p})^i}{i!}$$

Applying then the property of the Weyl quantization that was mentioned in section 3.3 to the terms of this infinite series leads to the *quantized* expression:

$$(\exp\{\mathbf{a} \cdot \mathbf{r} + \mathbf{b} \cdot \mathbf{p}\})_W = \sum_{i=0}^{\infty} \frac{(\mathbf{a} \cdot \hat{\mathbf{R}} + \mathbf{b} \cdot \hat{\mathbf{P}})^i}{i!}$$

where the infinite series on the right can be formally seen as the exponential of an operator, therefore obtaining:

$$(\exp \{ \mathbf{a} \cdot \mathbf{r} + \mathbf{b} \cdot \mathbf{p} \})_{\text{W}} = \exp \{ \mathbf{a} \cdot \hat{\mathbf{R}} + \mathbf{b} \cdot \hat{\mathbf{P}} \}$$

Since exponentials are transforming so easily under Weyl quantization it is then reasonable when treating the case of a generic function $\mathbf{f}(\mathbf{r}, \mathbf{p})$ of position and momentum to expand it by means of a double n-dimensional Fourier transform as:

$$\mathbf{f}(\mathbf{r}, \mathbf{p}) = \frac{1}{(2\pi)^{2n}} \int_{\Omega} \int_{\Omega} \hat{\mathbf{f}}(\mathbf{a}, \mathbf{b}) \exp \{ i (\mathbf{a} \cdot \mathbf{r} + \mathbf{b} \cdot \mathbf{p}) \} d\mathbf{a} d\mathbf{b} \quad (3.1)$$

where the **double n-dimensional Fourier Transform** $\hat{\mathbf{f}}(\mathbf{r}, \mathbf{p})$ of the function $\mathbf{f}(\mathbf{r}, \mathbf{p})$ is defined as the function:

$$\hat{\mathbf{f}}(\mathbf{r}, \mathbf{p}) = \int_{\Omega} \int_{\Omega} \mathbf{f}(\mathbf{a}, \mathbf{b}) \exp \{ -i (\mathbf{a} \cdot \mathbf{r} + \mathbf{b} \cdot \mathbf{p}) \} d\mathbf{a} d\mathbf{b} \quad (3.2)$$

The next step is to consider the Baker-Campbell-Hausdorff formula: [11]

$$\exp \{ \hat{X} \} \exp \{ \hat{Y} \} = \exp \left\{ \hat{X} + \hat{Y} + \frac{1}{2} [\hat{X}, \hat{Y}] + \frac{1}{12} [\hat{X}, [\hat{X}, \hat{Y}]] - \frac{1}{12} [\hat{Y}, [\hat{X}, \hat{Y}]] + \dots \right\} \quad (3.3)$$

where the terms that are omitted are higher-order stacks of commutators.

It is then possible to notice that the operators $\mathbf{a} \cdot \hat{\mathbf{R}}$ and $\mathbf{b} \cdot \hat{\mathbf{P}}$ commute with their commutator, i.e.:

$$[\mathbf{a} \cdot \hat{\mathbf{R}}, [\mathbf{a} \cdot \hat{\mathbf{R}}, \mathbf{b} \cdot \hat{\mathbf{P}}]] = 0 \quad [\mathbf{b} \cdot \hat{\mathbf{P}}, [\mathbf{a} \cdot \hat{\mathbf{R}}, \mathbf{b} \cdot \hat{\mathbf{P}}]] = 0$$

Proof:

A simple proof can be given for the first identity (the second one is similar) by expanding the dot products as sums:

$$[\mathbf{a} \cdot \hat{\mathbf{R}}, [\mathbf{a} \cdot \hat{\mathbf{R}}, \mathbf{b} \cdot \hat{\mathbf{P}}]] = \left[\sum_{\mathbf{k}} a_{\mathbf{k}} \hat{R}_{\mathbf{k}}, \left[\sum_{\mathbf{i}} a_{\mathbf{i}} \hat{R}_{\mathbf{i}}, \sum_{\mathbf{j}} b_{\mathbf{j}} \hat{P}_{\mathbf{j}} \right] \right]$$

and then extracting the linear combinations from the commutator:

$$[\mathbf{a} \cdot \hat{\mathbf{R}}, [\mathbf{a} \cdot \hat{\mathbf{R}}, \mathbf{b} \cdot \hat{\mathbf{P}}]] = \left[\sum_{\mathbf{k}} a_{\mathbf{k}} \hat{R}_{\mathbf{k}}, \sum_{\mathbf{i}} \sum_{\mathbf{j}} a_{\mathbf{i}} b_{\mathbf{j}} [\hat{R}_{\mathbf{i}}, \hat{P}_{\mathbf{j}}] \right]$$

By the commutation relation: [12]

$$[\hat{R}_{\mathbf{i}}, \hat{P}_{\mathbf{j}}] = i\hbar \delta_{\mathbf{ij}} \mathbb{I}$$

the last expression can then be rewritten as:

$$\begin{aligned} [\mathbf{a} \cdot \hat{\mathbf{R}}, [\mathbf{a} \cdot \hat{\mathbf{R}}, \mathbf{b} \cdot \hat{\mathbf{P}}]] &= \left[\sum_{\mathbf{k}} a_{\mathbf{k}} \hat{R}_{\mathbf{k}}, \sum_{\mathbf{i}} \sum_{\mathbf{j}} a_{\mathbf{i}} b_{\mathbf{j}} i\hbar \delta_{\mathbf{ij}} \mathbb{I} \right] \\ &= \left[\sum_{\mathbf{k}} a_{\mathbf{k}} \hat{R}_{\mathbf{k}}, \sum_{\mathbf{i}} a_{\mathbf{i}} b_{\mathbf{i}} i\hbar \mathbb{I} \right] \\ &= \sum_{\mathbf{i}} a_{\mathbf{i}} b_{\mathbf{i}} \left[\sum_{\mathbf{k}} a_{\mathbf{k}} \hat{R}_{\mathbf{k}}, i\hbar \mathbb{I} \right] \end{aligned}$$

Since the identity operator commutes with every operator the last expression is then identically zero:

$$[\mathbf{a} \cdot \hat{\mathbf{R}}, [\mathbf{a} \cdot \hat{\mathbf{R}}, \mathbf{b} \cdot \hat{\mathbf{P}}]] = \sum_{\mathbf{i}} a_{\mathbf{i}} b_{\mathbf{i}} \left[\sum_{\mathbf{k}} a_{\mathbf{k}} \hat{R}_{\mathbf{k}}, i\hbar \mathbb{I} \right] = 0$$

Then, the Baker-Campbell-Hausdorff formula simplifies since all the terms involving more than one commutator are identically zero:

$$\exp\{\hat{X}\}\exp\{\hat{Y}\} = \exp\left\{\hat{X} + \hat{Y} + \frac{1}{2}[\hat{X}, \hat{Y}]\right\} \quad (3.4)$$

Another equation that is needed to justify the final form of the Weyl quantization scheme (or Weyl transform) for a general function is the relationship:

$$\exp\{i\mathbf{b} \cdot \hat{\mathbf{P}}\}\Psi(\mathbf{x}) = \Psi(\mathbf{x} + \hbar\mathbf{b}) \quad (3.5)$$

Proof:

The first step of the proof is to rewrite the exponential of the operator by means of its *formal* infinite power series:

$$\exp\{i\mathbf{b} \cdot \hat{\mathbf{P}}\}\Psi(\mathbf{x}) = \sum_{j=0}^{\infty} \frac{1}{j!} (i\mathbf{b} \cdot \hat{\mathbf{P}})^j \Psi(\mathbf{x})$$

Then, the definition of the momentum operator $\hat{\mathbf{P}} = -i\hbar\nabla$ can be substituted, yielding

$$\exp\{i\mathbf{b} \cdot \hat{\mathbf{P}}\}\Psi(\mathbf{x}) = \sum_{j=0}^{\infty} \frac{1}{j!} (\hbar\mathbf{b} \cdot \nabla)^j \Psi(\mathbf{x})$$

Expanding $\Psi(\mathbf{x})$ in terms of the momentum eigenstates (free waves) $\left(\frac{1}{\sqrt{2\pi\hbar}}\right)^n \exp\left\{\frac{i}{\hbar}\mathbf{p} \cdot \mathbf{x}\right\}$:

$$\Psi(\mathbf{x}) = \int_{\Omega_p} \tilde{\Psi}(\mathbf{p}) \left(\frac{1}{\sqrt{2\pi\hbar}}\right)^n \exp\left\{\frac{i}{\hbar}\mathbf{p} \cdot \mathbf{x}\right\} d\mathbf{p}$$

and substituting into the formal infinite series for the exponential of the operator the following equation is obtained:

$$\exp\{i\mathbf{b} \cdot \hat{\mathbf{P}}\}\Psi(\mathbf{x}) = \sum_{j=0}^{\infty} \frac{1}{j!} (\hbar\mathbf{b} \cdot \nabla)^j \int_{\Omega_p} \tilde{\Psi}(\mathbf{p}) \left(\frac{1}{\sqrt{2\pi\hbar}}\right)^n \exp\left\{\frac{i}{\hbar}\mathbf{p} \cdot \mathbf{x}\right\} d\mathbf{p}$$

Which can be simplified as follows:

$$\begin{aligned} \exp\{i\mathbf{b} \cdot \hat{\mathbf{P}}\}\Psi(\mathbf{x}) &= \int_{\Omega_p} \sum_{j=0}^{\infty} \frac{1}{j!} (\hbar\mathbf{b} \cdot \nabla)^j \left\{ \tilde{\Psi}(\mathbf{p}) \left(\frac{1}{\sqrt{2\pi\hbar}}\right)^n \exp\left\{\frac{i}{\hbar}\mathbf{p} \cdot \mathbf{x}\right\} \right\} d\mathbf{p} \\ &= \int_{\Omega_p} \tilde{\Psi}(\mathbf{p}) \left(\frac{1}{\sqrt{2\pi\hbar}}\right)^n \exp\left\{\frac{i}{\hbar}\mathbf{p} \cdot \mathbf{x}\right\} \sum_{j=0}^{\infty} \frac{1}{j!} \hbar^j \left(\frac{i}{\hbar}\mathbf{b} \cdot \nabla\right)^j d\mathbf{p} \\ &= \int_{\Omega_p} \tilde{\Psi}(\mathbf{p}) \left(\frac{1}{\sqrt{2\pi\hbar}}\right)^n \exp\left\{\frac{i}{\hbar}\mathbf{p} \cdot \mathbf{x}\right\} \sum_{j=0}^{\infty} \frac{1}{j!} (i\mathbf{b} \cdot \nabla)^j d\mathbf{p} \\ &= \int_{\Omega_p} \tilde{\Psi}(\mathbf{p}) \left(\frac{1}{\sqrt{2\pi\hbar}}\right)^n \exp\left\{\frac{i}{\hbar}\mathbf{p} \cdot \mathbf{x}\right\} \exp\{i\mathbf{b} \cdot \nabla\} d\mathbf{p} \\ &= \int_{\Omega_p} \tilde{\Psi}(\mathbf{p}) \left(\frac{1}{\sqrt{2\pi\hbar}}\right)^n \exp\left\{\frac{i}{\hbar}\mathbf{p} \cdot \mathbf{x} + i\mathbf{b} \cdot \nabla\right\} d\mathbf{p} \\ &= \int_{\Omega_p} \tilde{\Psi}(\mathbf{p}) \left(\frac{1}{\sqrt{2\pi\hbar}}\right)^n \exp\left\{\frac{i}{\hbar}\mathbf{p} \cdot (\mathbf{x} + \hbar\mathbf{b})\right\} d\mathbf{p} \end{aligned}$$

Then, inverting the decomposition in terms of eigenfunctions of the momentum operator yields the expected result:

$$\exp\{i\mathbf{b} \cdot \hat{\mathbf{P}}\}\Psi(\mathbf{x}) = \Psi(\mathbf{x} + \hbar\mathbf{b})$$

Then, applying Equation 3.4 with $\hat{A} = i\mathbf{a} \cdot \hat{\mathbf{R}}$ and $\hat{B} = i\mathbf{b} \cdot \hat{\mathbf{P}}$ to a wavefunction $\Psi(\mathbf{r})$ the following equation is obtained:

$$\exp\{i\mathbf{a} \cdot \hat{\mathbf{R}}\} \exp\{i\mathbf{b} \cdot \hat{\mathbf{P}}\} \Psi(\mathbf{r}) = \exp\left\{i\mathbf{a} \cdot \hat{\mathbf{R}} + i\mathbf{b} \cdot \hat{\mathbf{P}} + \frac{1}{2}[i\mathbf{a} \cdot \hat{\mathbf{R}}, i\mathbf{b} \cdot \hat{\mathbf{P}}]\right\} \Psi(\mathbf{r})$$

The modified Campbell-Baker-Hausdorff equation derived in Equation 3.4 can then be applied again by considering:

$$\hat{X} = i\mathbf{a} \cdot \hat{\mathbf{R}} + i\mathbf{b} \cdot \hat{\mathbf{P}} \quad \hat{Y} = \frac{1}{2}[i\mathbf{a} \cdot \hat{\mathbf{R}}, i\mathbf{b} \cdot \hat{\mathbf{P}}]$$

which clearly satisfy the commutativity requirements $[\hat{X}, [\hat{X}, \hat{Y}]] = 0$ and $[\hat{Y}, [\hat{X}, \hat{Y}]] = 0$, obtaining:

$$\exp\{i\mathbf{a} \cdot \hat{\mathbf{R}}\} \exp\{i\mathbf{b} \cdot \hat{\mathbf{P}}\} \Psi(\mathbf{r}) = \exp\left\{i\mathbf{a} \cdot \hat{\mathbf{R}} + i\mathbf{b} \cdot \hat{\mathbf{P}}\right\} \exp\left\{\frac{1}{2}[i\mathbf{a} \cdot \hat{\mathbf{R}}, i\mathbf{b} \cdot \hat{\mathbf{P}}]\right\} \Psi(\mathbf{r}) \quad (3.6)$$

The commutation relations [12]

$$[\hat{R}_i, \hat{P}_j] = i\hbar\delta_{ij}\mathbb{I}$$

(where \mathbb{I} is the scalar identity operator) can then be used to derive the value of the exponential of the commutator:

$$\begin{aligned} \exp\left\{\frac{1}{2}[i\mathbf{a} \cdot \hat{\mathbf{R}}, i\mathbf{b} \cdot \hat{\mathbf{P}}]\right\} &= \exp\left\{\frac{1}{2}\left[\sum_i i a_i \hat{R}_i, \sum_j i b_j \hat{P}_j\right]\right\} \\ &= \exp\left\{\frac{1}{2}\sum_i i a_i \sum_j i b_j [\hat{R}_i, \hat{P}_j]\right\} \\ &= \exp\left\{\frac{1}{2}\sum_i i a_i \sum_j i b_j i\hbar\delta_{ij}\mathbb{I}\right\} \\ &= \exp\left\{\frac{1}{2}i\hbar\mathbb{I}\sum_i i a_i i b_i\right\} \\ &= \exp\left\{-\frac{1}{2}i\hbar\mathbf{a} \cdot \mathbf{b}\right\} \end{aligned}$$

which substituted into Equation 3.6 to obtain:

$$\exp\{i\mathbf{a} \cdot \hat{\mathbf{R}}\} \exp\{i\mathbf{b} \cdot \hat{\mathbf{P}}\} \Psi(\mathbf{r}) = \exp\left\{i\mathbf{a} \cdot \hat{\mathbf{R}} + i\mathbf{b} \cdot \hat{\mathbf{P}}\right\} \exp\left\{-\frac{1}{2}i\hbar\mathbf{a} \cdot \mathbf{b}\right\} \Psi(\mathbf{r})$$

Applying then Equation 3.5 yields:

$$\exp\{i\mathbf{a} \cdot \hat{\mathbf{R}}\} \Psi(\mathbf{r} + \hbar\mathbf{b}) = \exp\left\{i\mathbf{a} \cdot \hat{\mathbf{R}} + i\mathbf{b} \cdot \hat{\mathbf{P}}\right\} \exp\left\{-\frac{1}{2}i\hbar\mathbf{a} \cdot \mathbf{b}\right\} \Psi(\mathbf{r})$$

The term $\exp\left\{-\frac{1}{2}i\hbar\mathbf{a} \cdot \mathbf{b}\right\}$ is a scalar term only and can therefore be moved to the other side of the equation, yielding:

$$\exp\left\{\frac{1}{2}i\hbar\mathbf{a} \cdot \mathbf{b}\right\} \exp\{i\mathbf{a} \cdot \hat{\mathbf{R}}\} \Psi(\mathbf{r} + \hbar\mathbf{b}) = \exp\left\{i\mathbf{a} \cdot \hat{\mathbf{R}} + i\mathbf{b} \cdot \hat{\mathbf{P}}\right\} \Psi(\mathbf{r})$$

Moreover, since by definition the position operator is $\hat{\mathbf{R}} \triangleq \mathbf{r}$ the equation can be cast into the form:

$$\exp\left\{\frac{1}{2}i\hbar\mathbf{a} \cdot \mathbf{b}\right\} \exp\{i\mathbf{a} \cdot \mathbf{r}\} \Psi(\mathbf{r} + \hbar\mathbf{b}) = \exp\left\{i\mathbf{a} \cdot \hat{\mathbf{R}} + i\mathbf{b} \cdot \hat{\mathbf{P}}\right\} \Psi(\mathbf{r})$$

Rewriting the translation by means of an integration and a delta function yields:

$$\int_{\Omega} \exp \left\{ \frac{1}{2} i \hbar \mathbf{a} \cdot \mathbf{b} \right\} \exp \{ i \mathbf{a} \cdot \mathbf{r} \} \Psi(\mathbf{r} + \hbar \mathbf{b}) \delta(\mathbf{y} - \mathbf{r} - \hbar \mathbf{b}) \Psi(\mathbf{y}) d\mathbf{y} = \exp \left\{ i \mathbf{a} \cdot \hat{\mathbf{R}} + i \mathbf{b} \cdot \hat{\mathbf{P}} \right\} \Psi(\mathbf{r}) \quad (3.7)$$

Assuming now linearity of the Weyl quantization, the expansion of the function through the Fourier transform that was presented in Equation 3.1:

$$\mathbf{f}(\mathbf{r}, \mathbf{p}) = \frac{1}{(2\pi)^{2n}} \int_{\Omega} \int_{\Omega} \hat{\mathbf{f}}(\mathbf{a}, \mathbf{b}) \exp \{ i(\mathbf{a} \cdot \mathbf{r} + \mathbf{b} \cdot \mathbf{p}) \} d\mathbf{a} d\mathbf{b}$$

gets quantized as:

$$\mathbf{F}(\hat{\mathbf{R}}, \hat{\mathbf{P}})\{\Psi\}(\mathbf{r}) = (\mathbf{f}(\mathbf{r}, \mathbf{p}))_{\text{W}} = \frac{1}{(2\pi)^{2n}} \int_{\Omega} \int_{\Omega} \hat{\mathbf{f}}(\mathbf{a}, \mathbf{b}) \exp \left\{ i \mathbf{a} \cdot \hat{\mathbf{R}} + i \mathbf{b} \cdot \hat{\mathbf{P}} \right\} d\mathbf{a} d\mathbf{b}$$

Substituting the expression of Equation 3.7 a simpler expression not involving operators is found for the quantization of a generic function:

$$\mathbf{F}(\hat{\mathbf{R}}, \hat{\mathbf{P}})\{\Psi\}(\mathbf{r}) = \frac{1}{(2\pi)^{2n}} \int_{\Omega} \int_{\Omega} \hat{\mathbf{f}}(\mathbf{a}, \mathbf{b}) \int_{\Omega} \exp \left\{ \frac{1}{2} i \hbar \mathbf{a} \cdot \mathbf{b} \right\} \exp \{ i \mathbf{a} \cdot \mathbf{r} \} \delta(\mathbf{y} - \mathbf{r} - \hbar \mathbf{b}) \Psi(\mathbf{y}) d\mathbf{y} d\mathbf{a} d\mathbf{b}$$

Changing the order of integration allows to make explicit the kernel for the operator:

$$\mathbf{F}(\hat{\mathbf{R}}, \hat{\mathbf{P}})\{\Psi\}(\mathbf{r}) = \frac{1}{(2\pi)^{2n}} \int_{\Omega} \int_{\Omega} \int_{\Omega} \hat{\mathbf{f}}(\mathbf{a}, \mathbf{b}) \exp \left\{ \frac{1}{2} i \hbar \mathbf{a} \cdot \mathbf{b} \right\} \exp \{ i \mathbf{a} \cdot \mathbf{r} \} \delta(\mathbf{y} - \mathbf{r} - \hbar \mathbf{b}) d\mathbf{a} d\mathbf{b} \Psi(\mathbf{y}) d\mathbf{y}$$

which is given by:

$$\kappa_{\text{F}}(\mathbf{r}, \mathbf{y}) = \frac{1}{(2\pi)^{2n}} \int_{\Omega} \int_{\Omega} \hat{\mathbf{f}}(\mathbf{a}, \mathbf{b}) \exp \left\{ \frac{1}{2} i \hbar \mathbf{a} \cdot \mathbf{b} \right\} \exp \{ i \mathbf{a} \cdot \mathbf{r} \} \delta(\mathbf{y} - \mathbf{r} - \hbar \mathbf{b}) d\mathbf{a} d\mathbf{b}$$

Applying a change of variable $\mathbf{c} = \hbar \mathbf{b}$ leads to the equivalent expression:

$$\kappa_{\text{F}}(\mathbf{r}, \mathbf{y}) = \frac{1}{(2\pi)^{2n} \hbar^n} \int_{\Omega} \int_{\Omega} \hat{\mathbf{f}}\left(\mathbf{a}, \frac{\mathbf{c}}{\hbar}\right) \exp \left\{ \frac{1}{2} i \mathbf{a} \cdot \mathbf{c} \right\} \exp \{ i \mathbf{a} \cdot \mathbf{r} \} \delta(\mathbf{y} - \mathbf{r} - \mathbf{c}) d\mathbf{a} d\mathbf{c}$$

Changing the order of integration and exploiting the evenness of the delta function then gives:

$$\kappa_{\text{F}}(\mathbf{r}, \mathbf{y}) = \frac{1}{(2\pi)^{2n} \hbar^n} \int_{\Omega} \int_{\Omega} \hat{\mathbf{f}}\left(\mathbf{a}, \frac{\mathbf{c}}{\hbar}\right) \exp \left\{ \frac{1}{2} i \mathbf{a} \cdot \mathbf{c} \right\} \exp \{ i \mathbf{a} \cdot \mathbf{r} \} \delta(\mathbf{c} - [\mathbf{y} - \mathbf{r}]) d\mathbf{c} d\mathbf{a}$$

which upon integration with respect to \mathbf{c} simplifies to:

$$\kappa_{\text{F}}(\mathbf{r}, \mathbf{y}) = \frac{1}{(2\pi)^{2n} \hbar^n} \int_{\Omega} \hat{\mathbf{f}}\left(\mathbf{a}, \frac{\mathbf{y} - \mathbf{r}}{\hbar}\right) \exp \left\{ \frac{1}{2} i \mathbf{a} \cdot [\mathbf{y} - \mathbf{r}] \right\} \exp \{ i \mathbf{a} \cdot \mathbf{r} \} d\mathbf{a}$$

which can be rewritten in the form:

$$\kappa_{\text{F}}(\mathbf{r}, \mathbf{y}) = \frac{1}{(2\pi)^{2n} \hbar^n} \int_{\Omega} \hat{\mathbf{f}}\left(\mathbf{a}, \frac{\mathbf{y} - \mathbf{r}}{\hbar}\right) \exp \left\{ \frac{1}{2} i \mathbf{a} \cdot [\mathbf{y} + \mathbf{r}] \right\} d\mathbf{a}$$

$$\kappa_{\text{F}}(\mathbf{r}, \mathbf{y}) = \frac{1}{(2\pi \hbar)^n} \frac{1}{(2\pi)^n} \int_{\Omega} \hat{\mathbf{f}}\left(\mathbf{a}, \frac{\mathbf{y} - \mathbf{r}}{\hbar}\right) \exp \left\{ i \mathbf{a} \cdot \frac{\mathbf{y} + \mathbf{r}}{2} \right\} d\mathbf{a}$$

Observing then the definition of the double n-dimensional Fourier transform $\hat{\mathbf{f}}\left(\mathbf{a}, \frac{\mathbf{y} - \mathbf{r}}{\hbar}\right)$ given in Equation 3.2:

$$\hat{\mathbf{f}}\left(\mathbf{a}, \frac{\mathbf{y}-\mathbf{r}}{\hbar}\right) = \int_{\Omega} \int_{\Omega} \mathbf{f}(\mathbf{w}, \mathbf{z}) \exp\left\{-i\mathbf{z} \cdot \frac{\mathbf{y}-\mathbf{r}}{\hbar}\right\} d\mathbf{z} \exp\{-i\mathbf{w} \cdot \mathbf{a}\} d\mathbf{w}$$

leads to noticing that the symbols highlighting in blue coincide with a Fourier transform and an inverse Fourier transform with a modified spatial coordinate.

Therefore, putting together the two equations and simplifying the blue terms introducing a different expression at the first argument of \mathbf{f} leads to:

$$\kappa_{\mathbf{F}}(\mathbf{r}, \mathbf{y}) = \frac{1}{(2\pi\hbar)^n} \int_{\Omega} \mathbf{f}\left(\frac{\mathbf{y}+\mathbf{r}}{2}, \mathbf{z}\right) \exp\left\{-i\mathbf{z} \cdot \frac{\mathbf{y}-\mathbf{r}}{\hbar}\right\} d\mathbf{z}$$

Giving to the variable \mathbf{z} its correct interpretation of a classical momentum \mathbf{p} then the final form for the kernel of the Weyl-quantized operator \mathbf{F} is obtained:

$$\kappa_{\mathbf{F}}(\mathbf{r}, \mathbf{y}) = \frac{1}{(2\pi\hbar)^n} \int_{\Omega} \mathbf{f}\left(\frac{\mathbf{y}+\mathbf{r}}{2}, \mathbf{p}\right) \exp\left\{-i\mathbf{p} \cdot \frac{\mathbf{y}-\mathbf{r}}{\hbar}\right\} d\mathbf{p} \quad (3.8)$$

The full Weyl-quantized operator \mathbf{F} derived from the classical function $\mathbf{f}(\mathbf{r}, \mathbf{p})$ then reads:

$$\mathbf{F}\{\Psi\}(\mathbf{r}) = \int_{\Omega} \kappa_{\mathbf{F}}(\mathbf{r}, \mathbf{y}) \Psi(\mathbf{y}) d\mathbf{y} \quad (3.9)$$

$$\mathbf{F}\{\Psi\}(\mathbf{r}) = \frac{1}{(2\pi\hbar)^n} \int_{\Omega} \int_{\Omega} \mathbf{f}\left(\frac{\mathbf{y}+\mathbf{r}}{2}, \mathbf{p}\right) \exp\left\{-i\mathbf{p} \cdot \frac{\mathbf{y}-\mathbf{r}}{\hbar}\right\} d\mathbf{p} \Psi(\mathbf{y}) d\mathbf{y} \quad (3.10)$$

The **Weyl transform** is the operator that takes the classical function \mathbf{f} and yields the integral kernel $\kappa_{\mathbf{F}}$ of the corresponding quantum-mechanical operator \mathbf{F} ; its analytical formulation is given by Equation 3.8.

3.5 Inverse Weyl Quantization

Not all operators derive from applying a quantization scheme to a classical function. There is a class of operators that have been originally defined in a quantum-mechanical framework and do not have any classical function from which they derive; among this class of operators the most important one is probably the density matrix.

In this case it may then be of practical interest to do the inverse of the quantization procedure, i.e. trying to derive a classical or statistical function from a quantum-mechanical operator \mathbf{F} .

The **inverse Weyl quantization** is born with the goal of being an inverse quantization scheme corresponding to the Weyl quantization scheme.

Consider now the integral kernel of the Weyl quantization that is shown in Equation 3.8; it is clear that recovering the classical function \mathbf{f} from it requires:

- performing a change of variable
- undoing the Fourier transformation

The first step is to try and obtain a function $\mathbf{f}(\mathbf{r}, \mathbf{p})$ within the integral kernel $\kappa_{\mathbf{F}}$; this can be done by evaluating $\kappa_{\mathbf{F}}$ at the following coordinates:

$$\kappa_{\mathbf{F}}\left(\mathbf{r} - \hbar\frac{\mathbf{b}}{2}, \mathbf{r} + \hbar\frac{\mathbf{b}}{2}\right) = \frac{1}{(2\pi\hbar)^n} \int_{\Omega} \mathbf{f}\left(\frac{\mathbf{r} - \hbar\frac{\mathbf{b}}{2} + \mathbf{r} + \hbar\frac{\mathbf{b}}{2}}{2}, \mathbf{p}\right) \exp\left\{-i\mathbf{p} \cdot \frac{\mathbf{r} + \hbar\frac{\mathbf{b}}{2} - \mathbf{r} + \hbar\frac{\mathbf{b}}{2}}{\hbar}\right\} d\mathbf{p}$$

$$\kappa_{\mathbf{F}}\left(\mathbf{r} - \hbar\frac{\mathbf{b}}{2}, \mathbf{r} + \hbar\frac{\mathbf{b}}{2}\right) = \frac{1}{(2\pi\hbar)^n} \int_{\Omega} \mathbf{f}(\mathbf{r}, \mathbf{p}) \exp\{-i\mathbf{p} \cdot \mathbf{b}\} d\mathbf{p}$$

This also has the clearly beneficial effect of making the Fourier transformation explicit (it is hereby highlighted in blue).

The next logical step to obtain \mathbf{f} back is to undo the Fourier transformation. Since the $(2\pi)^{-n}$ factor is already present all that needs to be done is to introduce a factor of \hbar^n to remove the \hbar^{-n} and to add an exponential factor and an integration to form the inverse Fourier transform:

$$\hbar^n \int_{\Omega} \kappa_{\mathbf{F}} \left(\mathbf{r} - \hbar \frac{\mathbf{b}}{2}, \mathbf{r} + \hbar \frac{\mathbf{b}}{2} \right) \exp\{+i\mathbf{p}' \cdot \mathbf{b}\} d\mathbf{b} = \int_{\Omega} \frac{1}{(2\pi)^n} \int_{\Omega} \mathbf{f}(\mathbf{r}, \mathbf{p}) \exp\{-i\mathbf{p} \cdot \mathbf{b}\} d\mathbf{p} \exp\{+i\mathbf{p}' \cdot \mathbf{b}\} d\mathbf{b}$$

Clearly, the **inverse Fourier transform** and the **Fourier transform** cancel out yielding back the function \mathbf{f} :

$$\hbar^n \int_{\Omega} \kappa_{\mathbf{F}} \left(\mathbf{r} - \hbar \frac{\mathbf{b}}{2}, \mathbf{r} + \hbar \frac{\mathbf{b}}{2} \right) \exp\{+i\mathbf{p}' \cdot \mathbf{b}\} d\mathbf{b} = \mathbf{f}(\mathbf{r}, \mathbf{p}')$$

Therefore, the **inverse Weyl quantization** can be expressed as:

$$\boxed{\mathbf{f}(\mathbf{r}, \mathbf{p}) = \hbar^n \int_{\Omega} \kappa_{\mathbf{F}} \left(\mathbf{r} - \hbar \frac{\mathbf{b}}{2}, \mathbf{r} + \hbar \frac{\mathbf{b}}{2} \right) \exp\{+i\mathbf{p} \cdot \mathbf{b}\} d\mathbf{b}} \quad (3.11)$$

The **Wigner transform** is the operator that from the kernel of \mathbf{F} produces the original classical function \mathbf{f} that yields the operator under Weyl quantization.

Moreover, since the kernel of an operator can be retrieved by applying that operator to a delta function the kernel of the operator \mathbf{F} can be replaced by:

$$\kappa_{\mathbf{F}}(\mathbf{r}, \mathbf{r}') = \mathbf{F} \{ \delta_{\mathbf{r}'}(\mathbf{r}) \}$$

obtaining the final expression with the explicit operator \mathbf{F} :

$$\boxed{\mathbf{f}(\mathbf{r}, \mathbf{p}) = \hbar^n \int_{\Omega} \mathbf{F} \left\{ \delta_{\mathbf{r} + \hbar \frac{\mathbf{b}}{2}} \left(\mathbf{r} - \hbar \frac{\mathbf{b}}{2} \right) \right\} \exp\{+i\mathbf{p} \cdot \mathbf{b}\} d\mathbf{b}} \quad (3.12)$$

Now that a possible scheme for inverse quantization has been defined the next step is to apply it to operators which do not have classical counterparts (such as the density matrix) in order to obtain something as close as possible to that.

Chapter 4

The Wigner Function

The Wigner function aims at replacing the concept of the wavefunction within Wigner's formalism of quantum mechanics. Moreover, it is an attempt at obtaining a "more classical" alternative to the wavefunction, i.e. a quantity that can be characterized as a probability density function in phase space (which leads to encouraging results that are however not exactly a probability density function).

Since the density matrix operator was shown in chapter 2 to hold all the statistical information necessary to evaluate the expected value of an operator A representing an observable, the natural starting point to obtain a probability density function (i.e. a classical function of statistical physics) is to try and apply the inverse Weyl quantization to the density matrix operator ρ^{mix} for a mixed state.

4.1 Definition of the Wigner Function

The Wigner function is the Wigner transform (i.e. the inverse Weyl transform) of the kernel of the density matrix operator κ_ρ for a given mixed state. [13]

According to the definition of the Wigner transform that was given in Equation 3.11 the Wigner function f_W could then be mathematically defined as:

$$f_W(\mathbf{r}, \mathbf{p}) = \hbar^n \int_{\Omega} \kappa_{\rho^{\text{mix}}} \left(\mathbf{r} - \hbar \frac{\mathbf{b}}{2}, \mathbf{r} + \hbar \frac{\mathbf{b}}{2} \right) \exp\{+i\mathbf{p} \cdot \mathbf{b}\} d\mathbf{b} \quad (4.1)$$

Substituting then the expression for the kernel $\kappa_{\rho^{\text{mix}}}$ of the density matrix operator for the mixed state that was given in Equation 2.4 the following equivalent definition is obtained:

$$f_W(\mathbf{r}, \mathbf{p}) = \hbar^n \int_{\Omega} \sum_i p_i \Psi_i^* \left(\mathbf{r} + \hbar \frac{\mathbf{b}}{2} \right) \Psi_i \left(\mathbf{r} - \hbar \frac{\mathbf{b}}{2} \right) \exp\{+i\mathbf{p} \cdot \mathbf{b}\} d\mathbf{b}$$
$$f_W(\mathbf{r}, \mathbf{p}) = \sum_i p_i \hbar^n \int_{\Omega} \Psi_i^* \left(\mathbf{r} + \hbar \frac{\mathbf{b}}{2} \right) \Psi_i \left(\mathbf{r} - \hbar \frac{\mathbf{b}}{2} \right) \exp\{+i\mathbf{p} \cdot \mathbf{b}\} d\mathbf{b}$$

The Wigner function for the mixed state can then be seen as the average of the Wigner functions for the pure states in the ensemble, weighted by their relative probabilities of occurrence:

$$f_W(\mathbf{r}, \mathbf{p}) = \sum_i p_i f_{W,i} \quad (4.2)$$

where the Wigner functions $f_{W,i}$ for the i -th pure state in the ensemble could then be defined as:

$$f_{W,i} = \hbar^n \int_{\Omega} \Psi_i^* \left(\mathbf{r} + \hbar \frac{\mathbf{b}}{2} \right) \Psi_i \left(\mathbf{r} - \hbar \frac{\mathbf{b}}{2} \right) \exp\{+i\mathbf{p} \cdot \mathbf{b}\} d\mathbf{b} \quad (4.3)$$

The definition of Equations 4.2 and 4.3 must however be refined; since the goal of this procedure is to obtain a function that acts as a probability density function in phase space a normalization must be applied.

It is therefore necessary to evaluate the result of the integration of this function over phase space:

$$\int_{\Omega} \int_{\Omega_{\mathbf{p}}} f_{\text{W}}(\mathbf{r}, \mathbf{p}) \, d\mathbf{p} \, d\mathbf{r} = \int_{\Omega} \int_{\Omega_{\mathbf{p}}} \sum_i p_i \hbar^n \int_{\Omega} \Psi_i^* \left(\mathbf{r} + \hbar \frac{\mathbf{b}}{2} \right) \Psi_i \left(\mathbf{r} - \hbar \frac{\mathbf{b}}{2} \right) \exp\{+i\mathbf{p} \cdot \mathbf{b}\} \, d\mathbf{b} \, d\mathbf{p} \, d\mathbf{r}$$

By linearity of the integration and by swapping the order of integration the equation can be cast into the form:

$$\int_{\Omega} \int_{\Omega_{\mathbf{p}}} f_{\text{W}}(\mathbf{r}, \mathbf{p}) \, d\mathbf{p} \, d\mathbf{r} = \sum_i p_i \hbar^n \int_{\Omega} \int_{\Omega} \Psi_i^* \left(\mathbf{r} + \hbar \frac{\mathbf{b}}{2} \right) \Psi_i \left(\mathbf{r} - \hbar \frac{\mathbf{b}}{2} \right) \int_{\Omega_{\mathbf{p}}} \exp\{+i\mathbf{p} \cdot \mathbf{b}\} \, d\mathbf{p} \, d\mathbf{r} \, d\mathbf{b}$$

Applying then the identity for the n-dimensional Dirac delta function:

$$\int_{\Omega} \int_{\Omega_{\mathbf{y}}} \exp\{+i\mathbf{y} \cdot \mathbf{r}\} \, d\mathbf{y} = (2\pi)^n \delta(\mathbf{r})$$

(where n is the dimension of the vector space being considered) leads to the result:

$$\begin{aligned} \int_{\Omega} \int_{\Omega_{\mathbf{p}}} f_{\text{W}}(\mathbf{r}, \mathbf{p}) \, d\mathbf{p} \, d\mathbf{r} &= \sum_i p_i \hbar^n \int_{\Omega} \int_{\Omega} \Psi_i^* \left(\mathbf{r} + \hbar \frac{\mathbf{b}}{2} \right) \Psi_i \left(\mathbf{r} - \hbar \frac{\mathbf{b}}{2} \right) \int_{\Omega_{\mathbf{p}}} \exp\{+i\mathbf{p} \cdot \mathbf{b}\} \, d\mathbf{p} \, d\mathbf{r} \, d\mathbf{b} \\ &= \sum_i p_i \hbar^n \int_{\Omega} \int_{\Omega} \Psi_i^* \left(\mathbf{r} + \hbar \frac{\mathbf{b}}{2} \right) \Psi_i \left(\mathbf{r} - \hbar \frac{\mathbf{b}}{2} \right) (2\pi)^n \delta(\mathbf{b}) \, d\mathbf{r} \, d\mathbf{b} \\ &= \sum_i p_i \hbar^n \int_{\Omega} \int_{\Omega} \Psi_i^* \left(\mathbf{r} + \hbar \frac{\mathbf{b}}{2} \right) \Psi_i \left(\mathbf{r} - \hbar \frac{\mathbf{b}}{2} \right) (2\pi)^n \delta(\mathbf{b}) \, d\mathbf{b} \, d\mathbf{r} \\ &= \sum_i p_i \hbar^n \int_{\Omega} \Psi_i^*(\mathbf{r}) \Psi_i(\mathbf{r}) (2\pi)^n \, d\mathbf{r} \\ &= (2\pi\hbar)^n \sum_i p_i \int_{\Omega} \Psi_i^*(\mathbf{r}) \Psi_i(\mathbf{r}) \, d\mathbf{r} \\ &= (2\pi\hbar)^n \sum_i p_i \\ &= (2\pi\hbar)^n \end{aligned}$$

A normalized version of the Wigner function that integrates to 1 is then usually preferred since it can be attributed the interpretation of a probability density function:

$$f_{\text{W}}(\mathbf{r}, \mathbf{p}) \triangleq \sum_i p_i f_{\text{W},i} \quad f_{\text{W},i} \triangleq \frac{1}{(2\pi)^n} \int_{\Omega} \Psi_i^* \left(\mathbf{r} + \hbar \frac{\mathbf{b}}{2} \right) \Psi_i \left(\mathbf{r} - \hbar \frac{\mathbf{b}}{2} \right) \exp\{+i\mathbf{p} \cdot \mathbf{b}\} \, d\mathbf{b} \quad (4.4)$$

Moreover, a change of variable $\mathbf{a} = \hbar \frac{\mathbf{b}}{2}$ can be applied to the integral, casting it into the simpler form:

$$\boxed{f_{\text{W}}(\mathbf{r}, \mathbf{p}) \triangleq \sum_i p_i f_{\text{W},i} \quad f_{\text{W},i} \triangleq \frac{1}{(\hbar\pi)^n} \int_{\Omega} \Psi_i^*(\mathbf{r} + \mathbf{a}) \Psi_i(\mathbf{r} - \mathbf{a}) \exp\left\{+\frac{2i}{\hbar} \mathbf{p} \cdot \mathbf{a}\right\} \, d\mathbf{a}} \quad (4.5)$$

This will be taken as the reference definition for the **Wigner function** for further work.

4.2 Properties of the Wigner Function

Because of the normalization performed in order to define it in section 4.1, the Wigner function is **unitary** under integration over phase space:

$$\int_{\Omega} \int_{\Omega_{\mathbf{p}}} f_{\text{W}}(\mathbf{r}, \mathbf{p}) \, d\mathbf{r} \, d\mathbf{p} = 1$$

Also the marginals of the Wigner function interpreted as a probability density function can be checked to determine whether it can fulfill the role for which it is designed.

Integration of the Wigner function (as defined in Equation 4.5) in momentum space yields (the equivalent version of Equation 4.4 to the definition is used as it makes easier to explicitate the Dirac delta):

$$\begin{aligned}
\int_{\Omega_{\mathbf{p}}} f_{\text{W}}(\mathbf{r}, \mathbf{p}) \, d\mathbf{p} &= \int_{\Omega_{\mathbf{p}}} \sum_i p_i \frac{1}{(2\pi)^n} \int_{\Omega} \Psi_i^* \left(\mathbf{r} + \hbar \frac{\mathbf{b}}{2} \right) \Psi_i \left(\mathbf{r} - \hbar \frac{\mathbf{b}}{2} \right) \exp\{+i \mathbf{p} \cdot \mathbf{b}\} \, d\mathbf{b} \, d\mathbf{p} \\
&= \sum_i p_i \frac{1}{(2\pi)^n} \int_{\Omega} \Psi_i^* \left(\mathbf{r} + \hbar \frac{\mathbf{b}}{2} \right) \Psi_i \left(\mathbf{r} - \hbar \frac{\mathbf{b}}{2} \right) \int_{\Omega_{\mathbf{p}}} \exp\{+i \mathbf{p} \cdot \mathbf{b}\} \, d\mathbf{p} \, d\mathbf{b} \\
&= \sum_i p_i \frac{1}{(2\pi)^n} \int_{\Omega} \Psi_i^* \left(\mathbf{r} + \hbar \frac{\mathbf{b}}{2} \right) \Psi_i \left(\mathbf{r} - \hbar \frac{\mathbf{b}}{2} \right) (2\pi)^n \delta(\mathbf{b}) \, d\mathbf{b} \\
&= \sum_i p_i \Psi_i^*(\mathbf{r}) \Psi_i(\mathbf{r}) \\
&= \sum_i p_i |\Psi_i(\mathbf{r})|^2
\end{aligned}$$

which has the correct meaning of a probability density marginal in position space.

Integration of the Wigner function (as defined in Equation 4.5) in position space yields:

$$\begin{aligned}
\int_{\Omega} f_{\text{W}}(\mathbf{r}, \mathbf{p}) \, d\mathbf{r} &= \int_{\Omega} \sum_i p_i \frac{1}{(\hbar\pi)^n} \int_{\Omega} \Psi_i^*(\mathbf{r} + \mathbf{a}) \Psi_i(\mathbf{r} - \mathbf{a}) \exp\left\{+\frac{2i}{\hbar} \mathbf{p} \cdot \mathbf{a}\right\} \, d\mathbf{a} \, d\mathbf{r} \\
&= \sum_i p_i \frac{1}{(\hbar\pi)^n} \int_{\Omega} \int_{\Omega} \Psi_i^*(\mathbf{r} + \mathbf{a}) \Psi_i(\mathbf{r} - \mathbf{a}) \exp\left\{+\frac{2i}{\hbar} \mathbf{p} \cdot \mathbf{a}\right\} \, d\mathbf{a} \, d\mathbf{r}
\end{aligned}$$

Introducing a change of variable $\mathbf{w} = \mathbf{r} + \mathbf{a}$ yields:

$$\begin{aligned}
&= \sum_i p_i \frac{1}{(\hbar\pi)^n} \int_{\Omega} \int_{\Omega} \Psi_i^*(\mathbf{w}) \Psi_i(2\mathbf{r} - \mathbf{w}) \exp\left\{+\frac{2i}{\hbar} \mathbf{p} \cdot (\mathbf{w} - \mathbf{r})\right\} \, d\mathbf{w} \, d\mathbf{r} \\
&= \sum_i p_i \frac{1}{(\hbar\pi)^n} \int_{\Omega} \int_{\Omega} \Psi_i^*(\mathbf{w}) \Psi_i(2\mathbf{r} - \mathbf{w}) \exp\left\{+\frac{i}{\hbar} \mathbf{p} \cdot (\mathbf{w} - 2\mathbf{r})\right\} \, d\mathbf{w} \exp\left\{+\frac{i}{\hbar} \mathbf{p} \cdot \mathbf{w}\right\} \, d\mathbf{r}
\end{aligned}$$

Introducing another change of variable $\mathbf{v} = 2\mathbf{r} - \mathbf{w}$ leads to:

$$\begin{aligned}
&= \sum_i p_i \frac{1}{(2\hbar\pi)^n} \int_{\Omega} \int_{\Omega} \Psi_i^*(\mathbf{w}) \Psi_i(\mathbf{v}) \exp\left\{-\frac{i}{\hbar} \mathbf{p} \cdot \mathbf{v}\right\} \, d\mathbf{w} \exp\left\{+\frac{i}{\hbar} \mathbf{p} \cdot \mathbf{w}\right\} \, d\mathbf{v} \\
&= \sum_i p_i \frac{1}{(2\hbar\pi)^n} \int_{\Omega} \Psi_i^*(\mathbf{w}) \exp\left\{+\frac{i}{\hbar} \mathbf{p} \cdot \mathbf{w}\right\} \, d\mathbf{w} \cdot \int_{\Omega} \Psi_i(\mathbf{v}) \exp\left\{-\frac{i}{\hbar} \mathbf{p} \cdot \mathbf{v}\right\} \, d\mathbf{v} \\
&= \sum_i p_i \frac{1}{(2\hbar\pi)^n} \left[\int_{\Omega} \Psi_i(\mathbf{w}) \exp\left\{-\frac{i}{\hbar} \mathbf{p} \cdot \mathbf{w}\right\} \, d\mathbf{w} \right]^* \cdot \int_{\Omega} \Psi_i(\mathbf{v}) \exp\left\{-\frac{i}{\hbar} \mathbf{p} \cdot \mathbf{v}\right\} \, d\mathbf{v} \\
&= \sum_i p_i \langle \tilde{\mathbf{p}} | \Psi_i \rangle^* \langle \tilde{\mathbf{p}} | \Psi_i \rangle
\end{aligned}$$

where $\tilde{\mathbf{p}} = \sqrt{\frac{1}{(2\pi\hbar)^n}} \exp\left\{-\frac{i}{\hbar} \mathbf{p} \cdot \mathbf{w}\right\}$ is the eigenstate of the momentum operator having momentum \mathbf{p} and $\langle \tilde{\mathbf{p}} | \Psi_i \rangle$ represents the projection of the wavefunction Ψ_i over the momentum eigenstate.

This last expression can then be interpreted as a probability density marginal in momentum space.

The last and most important property of the Wigner function that will be analyzed here is its capability of yielding expected values for the classical version of an operator that are the same as the quantum ones

(assuming the operators to have been quantized through a Weyl scheme):

$$\langle A \rangle_{\rho^{\text{mix}}} = \int_{\Omega_{\mathbf{p}}} \int_{\Omega} f_{\text{W}}(\mathbf{r}, \mathbf{p}) a(\mathbf{r}, \mathbf{p}) d\mathbf{r} d\mathbf{p}$$

where $a(\mathbf{r}, \mathbf{p})$ yields the operator A under Weyl quantization.

Proof:

$$\int_{\Omega_{\mathbf{p}}} \int_{\Omega} f_{\text{W}}(\mathbf{r}, \mathbf{p}) a(\mathbf{r}, \mathbf{p}) d\mathbf{r} d\mathbf{p} = \int_{\Omega_{\mathbf{p}}} \int_{\Omega} \sum_i p_i \frac{1}{(\hbar\pi)^n} \int_{\Omega} \Psi_i^*(\mathbf{r} + \mathbf{a}) \Psi_i(\mathbf{r} - \mathbf{a}) \exp\left\{+\frac{2i}{\hbar} \mathbf{p} \cdot \mathbf{a}\right\} d\mathbf{a} a(\mathbf{r}, \mathbf{p}) d\mathbf{r} d\mathbf{p}$$

Changing the order of integration and summation yields:

$$\int_{\Omega_{\mathbf{p}}} \int_{\Omega} f_{\text{W}}(\mathbf{r}, \mathbf{p}) a(\mathbf{r}, \mathbf{p}) d\mathbf{r} d\mathbf{p} = \sum_i p_i \int_{\Omega_{\mathbf{p}}} \int_{\Omega} \Psi_i^*(\mathbf{r} + \mathbf{a}) \Psi_i(\mathbf{r} - \mathbf{a}) \frac{1}{(\hbar\pi)^n} \int_{\Omega} \exp\left\{+\frac{2i}{\hbar} \mathbf{p} \cdot \mathbf{a}\right\} a(\mathbf{r}, \mathbf{p}) d\mathbf{p} d\mathbf{a} d\mathbf{r}$$

The goal is now to apply the change of variable:

$$\mathbf{r} = \frac{\mathbf{r} + \mathbf{b}}{2} \quad \mathbf{a} = \frac{\mathbf{b} - \mathbf{r}}{2}$$

in order to reconstruct the Weyl transform of the operator.

In order to understand the Jacobian of the change of variable it is useful to rewrite the volume differentials as:

$$d\mathbf{a} d\mathbf{r} = da_1 \cdots da_n dr_1 \cdots dr_n$$

The Jacobian J for the change of variable can then be written as: from which follows that:

$$J = \begin{bmatrix} \frac{\partial r_1}{\partial x_1} & \cdots & \frac{\partial r_1}{\partial x_n} & \frac{\partial r_1}{\partial b_1} & \cdots & \frac{\partial r_1}{\partial b_n} \\ \vdots & \ddots & \vdots & \vdots & \ddots & \vdots \\ \frac{\partial r_n}{\partial x_1} & \cdots & \frac{\partial x_n}{\partial x_n} & \frac{\partial r_n}{\partial b_1} & \cdots & \frac{\partial r_n}{\partial b_n} \\ \frac{\partial a_1}{\partial x_1} & \cdots & \frac{\partial a_1}{\partial x_n} & \frac{\partial a_1}{\partial b_1} & \cdots & \frac{\partial a_1}{\partial b_n} \\ \vdots & \ddots & \vdots & \vdots & \ddots & \vdots \\ \frac{\partial a_n}{\partial x_1} & \cdots & \frac{\partial a_n}{\partial x_n} & \frac{\partial a_n}{\partial b_1} & \cdots & \frac{\partial a_n}{\partial b_n} \end{bmatrix} = \begin{bmatrix} \frac{1}{2} \mathbb{I}_{n,n} & \frac{1}{2} \mathbb{I}_{n,n} \\ -\frac{1}{2} \mathbb{I}_{n,n} & \frac{1}{2} \mathbb{I}_{n,n} \end{bmatrix}$$

where $\mathbb{I}_{n,n}$ represents the $n \times n$ identity matrix.

Applying then the following result for the determinant of a block matrix: [14]

$$M = \begin{bmatrix} A & B \\ C & D \end{bmatrix} \quad \Rightarrow \quad \det(M) = \det(A - BD^{-1}C) \cdot \det(D)$$

leads to the result:

$$\det(J) = \det(\mathbb{I}_{n,n}) \cdot \det\left(\frac{1}{2} \mathbb{I}_{n,n}\right) = \frac{1}{2^n}$$

Applying then the change of variables results in:

$$\int_{\Omega_{\mathbf{p}}} \int_{\Omega} f_{\text{W}}(\mathbf{r}, \mathbf{p}) a(\mathbf{r}, \mathbf{p}) d\mathbf{r} d\mathbf{p} = \sum_i p_i \int_{\Omega_{\mathbf{p}}} \Psi_i^*(\mathbf{b}) \int_{\Omega} \Psi_i(\mathbf{r}) \frac{1}{(2\hbar\pi)^n} \int_{\Omega} \exp\left\{+\frac{i}{\hbar} \mathbf{p} \cdot (\mathbf{b} - \mathbf{r})\right\} a\left(\frac{\mathbf{r} + \mathbf{b}}{2}, \mathbf{p}\right) d\mathbf{p} d\mathbf{r} d\mathbf{b}$$

Recognizing then the Weyl transform of the operator a (as defined in Equation 3.10) and substituting it with the corresponding operator A yields:

$$\int_{\Omega_{\mathbf{p}}} \int_{\Omega} f_{\mathbf{W}}(\mathbf{r}, \mathbf{p}) a(\mathbf{r}, \mathbf{p}) d\mathbf{r} d\mathbf{p} = \sum_i p_i \int_{\Omega_{\mathbf{p}}} \Psi_i^*(\mathbf{b}) A \{\Psi_i\}(\mathbf{b}) d\mathbf{b}$$

which can be rewritten as an inner product and, consequently, as an expected value (according to the postulates of quantum mechanics):

$$\int_{\Omega_{\mathbf{p}}} \int_{\Omega} f_{\mathbf{W}}(\mathbf{r}, \mathbf{p}) a(\mathbf{r}, \mathbf{p}) d\mathbf{r} d\mathbf{p} = \sum_i p_i \langle \Psi_i | A | \Psi_i \rangle = \langle A \rangle_{\rho_{\text{mix}}}$$

Another property of the Wigner function is that $f_{\mathbf{W}}$ is **always real**.

Proof:

In order to prove this property for a mixed state it is sufficient to prove it for pure states, as the Wigner function for a mixed state is simply a weighted average (with real weights) of Wigner functions for pure states.

Considering the conjugate of the Wigner function for a pure state:

$$f_{\mathbf{W},i}^*(\mathbf{r}, \mathbf{p}) = \frac{1}{(\hbar\pi)^n} \int_{\Omega} \Psi_i(\mathbf{r} + \mathbf{a}) \Psi_i^*(\mathbf{r} - \mathbf{a}) \exp\left\{-\frac{2i}{\hbar} \mathbf{p} \cdot \mathbf{a}\right\} d\mathbf{a}$$

then a change of variables of the kind:

$$\mathbf{a}' = -\mathbf{a}$$

which has determinant of the Jacobian $\det(J) = -1$ gives as a result:

$$f_{\mathbf{W},i}^*(\mathbf{r}, \mathbf{p}) = -\frac{1}{(\hbar\pi)^n} \int_{\Omega} \Psi_i(\mathbf{r} - \mathbf{a}') \Psi_i^*(\mathbf{r} + \mathbf{a}') \exp\left\{+\frac{2i}{\hbar} \mathbf{p} \cdot \mathbf{a}'\right\} d\mathbf{a}'$$

which from the definition of the Wigner function can be seen to be:

$$f_{\mathbf{W},i}^*(\mathbf{r}, \mathbf{p}) = -f_{\mathbf{W},i}(\mathbf{r}, \mathbf{p})$$

This last condition corresponds to stating that $\text{Im}\{f_{\mathbf{W},i}^*(\mathbf{r}, \mathbf{p})\} = 0$, i.e. that the Wigner function be always real.

While the Wigner function satisfies most of the requirements of a probability density function it is however **not always everywhere positive**; several examples exist of quantum-mechanical problems for which the Wigner function is negative.

For this reason, it is not a proper probability density function but it is typically classified as a **quasi-probability density function** in phase space.

4.3 Moments of the Wigner Function

When working with probability density functions on phase space, the quantity that is of relevance is generally not the probability density function itself (which is however often quite complicated to be obtained) but its moments.

The k^{th} moment of the Wigner function is defined as:

$$\int_{\Omega_{\mathbf{p}}} \mathbf{p}^k f_{\mathbf{W}}(\mathbf{r}, \mathbf{p}) d\mathbf{p}$$

where \mathbf{p}^k is the result of the tensor product of k identical momentum vectors \mathbf{p}

$$\mathbf{p}^k = \underbrace{\mathbf{p} \otimes \mathbf{p} \otimes \cdots \otimes \mathbf{p} \otimes \mathbf{p}}_{k \text{ times}}$$

(it is understood that $\mathbf{p}^0 = 1$ and $\mathbf{p}^1 = \mathbf{p}$)

It is important to give the moments of the Wigner function a physical meaning, as they will also appear when taking the moments of the Wigner equation (chapter 6).

4.3.1 0th moment

The 0th moment of the Wigner function is defined as:

$$\int_{\Omega_{\mathbf{p}}} f_{\text{W}}(\mathbf{r}, \mathbf{p}) \, d\mathbf{p}$$

i.e. as the marginal of the probability density function for a particle in phase space.

From statistical physics, the marginal (integrated with respect to momentum) of a phase-space probability density function tells the probability of finding a particle with any value of momentum at a certain point in space.

Therefore, the 0th order moment of the Wigner function can be interpreted as the *single-electron* electron density $\bar{n}(\mathbf{r})$:

$$\bar{n}(\mathbf{r}) \triangleq \int_{\Omega_{\mathbf{p}}} f_{\text{W}}(\mathbf{r}, \mathbf{p}) \, d\mathbf{p} \quad (4.6)$$

4.3.2 1st moment

The 1st order moment of the Wigner function is defined as:

$$\int_{\Omega_{\mathbf{p}}} \mathbf{p} f_{\text{W}}(\mathbf{r}, \mathbf{p}) \, d\mathbf{p}$$

In order to give this moment a physical meaning it is first necessary to understand the concept of *single-electron* momentum $\bar{\mathbf{p}}(\mathbf{r})$.

This quantity is simply the statistical average of the momentum \mathbf{p} taken at a *fixed* point in space \mathbf{r} . The average momentum is then defined as the "conditional average" in momentum space given that the position in space of the particle is \mathbf{r} :

$$\bar{\mathbf{p}}(\mathbf{r}) = \int_{\Omega_{\mathbf{p}}} \mathbf{p} f_{\text{W},\text{P}|\text{R}}(\mathbf{p}|\mathbf{r}) \, d\mathbf{p}$$

A conditional probability density function $f_{\text{W},\text{P}|\text{R}}(\mathbf{p}|\mathbf{r})$ can then be defined using the result from probability:

$$f_{\text{Y}|\text{X}}(y|x) = \frac{f_{\text{X},\text{Y}}(x, y)}{f_{\text{X}}(x)}$$

where:

- $f_{\text{Y}|\text{X}}(x|y)$ is the conditional probability density function for the random variable Y given that the random variable X has taken a *fixed* value x
- $f_{\text{X}}(x) = \int_{-\infty}^{+\infty} f_{\text{X},\text{Y}}(x, y) \, dy$ is the marginal of the probability density function (integrated with respect to y)
- $f_{\text{X},\text{Y}}(x, y)$ is the joint probability density function for the two random variables X and Y

Then, substituting this result in the definition of the average momentum considering f_{W} as the joint probability density for the position and momentum of the particle gives:

$$\bar{\mathbf{p}}(\mathbf{r}) = \int_{\Omega_{\mathbf{p}}} \mathbf{p} \frac{f_{\text{W}}(\mathbf{r}, \mathbf{p})}{\int_{\Omega_{\mathbf{p}}} f_{\text{W}}(\mathbf{r}, \mathbf{p}) \, d\mathbf{p}} \, d\mathbf{p}$$

As the denominator of the fraction is independent from the momentum, it can be extracted from the integral and both sides of the equation can be multiplied by it to obtain:

$$\bar{\mathbf{p}}(\mathbf{r}) \int_{\Omega_{\mathbf{p}}} f_{\text{W}}(\mathbf{r}, \mathbf{p}) \, d\mathbf{p} = \int_{\Omega_{\mathbf{p}}} \mathbf{p} f_{\text{W}}(\mathbf{r}, \mathbf{p}) \, d\mathbf{p}$$

Recognizing the 0th moment of the Wigner function and substituting it leads to the final expression for the 1st moment of the Wigner function:

$$\bar{\mathbf{p}}(\mathbf{r}) \bar{n}(\mathbf{r}) = \int_{\Omega_{\mathbf{p}}} \mathbf{p} f_{\text{W}}(\mathbf{r}, \mathbf{p}) d\mathbf{p}$$

Since the single-electron current density $\bar{\mathbf{J}}_n(\mathbf{r})$ can be expressed as:

$$\bar{\mathbf{J}}_n(\mathbf{r}) = -q \bar{\mathbf{v}}(\mathbf{r}) = -\frac{q}{m^*} \bar{\mathbf{p}}(\mathbf{r})$$

(where $\bar{\mathbf{v}}$ is the average electron velocity, m^* is the effective mass of the electron and q is the elementary positive charge) then the previous momentum can also be rewritten as:

$$-\frac{m^*}{q} \bar{\mathbf{J}}_n(\mathbf{r}) \bar{n}(\mathbf{r}) = \int_{\Omega_{\mathbf{p}}} \mathbf{p} f_{\text{W}}(\mathbf{r}, \mathbf{p}) d\mathbf{p} \quad (4.7)$$

4.3.3 2nd moment

The 2nd moment of the Wigner function is defined as:

$$\int_{\Omega_{\mathbf{p}}} \mathbf{p}\mathbf{p} f_{\text{W}}(\mathbf{r}, \mathbf{p}) d\mathbf{p}$$

where $\mathbf{p}\mathbf{p}$ is a dyadic (i.e. a 2nd order tensor obtained from the tensor product of identical vectors).

If an orthonormal basis is defined for the vector space, the dyadic can be seen with respect to it as a square matrix having components:

$$\mathbf{p}\mathbf{p} = \begin{bmatrix} p_1 p_1 & p_1 p_2 & p_1 p_3 \\ p_2 p_1 & p_2 p_2 & p_2 p_3 \\ p_3 p_1 & p_3 p_2 & p_3 p_3 \end{bmatrix}$$

Following a reasoning involving conditional probabilities that is entirely similar to the one that was considered for the 1st moment the following result is obtained for the (i, j) th component of the 2nd moment:

$$\overline{p_i p_j}(\mathbf{r}) \bar{n}(\mathbf{r}) = \int_{\Omega_{\mathbf{p}}} p_i p_j f_{\text{W}}(\mathbf{r}, \mathbf{p}) d\mathbf{p}$$

where the tensor $\overline{p_i p_j}(\mathbf{r})$ is often known as the stress-energy tensor

Since the average kinetic energy in the j -th direction is given by the statistical average of $\frac{p_j^2}{2m^*}$ (using the conditional probability density function described for the previous moment) then it follows that the diagonal entries $\overline{p_j p_j}$ of the dyadic are proportional the kinetic energies in the different directions as:

$$\overline{p_j p_j} = 2 m^* E_k^{(j)}$$

($E_k^{(j)}$ is the kinetic energy due to the velocity in the k -th direction; the kinetic energies in all directions must add up to the total kinetic energy)

Chapter 5

The Wigner Equation

As in every other formalism of quantum mechanics, an evolution equation must be derived also for the Wigner function.

The starting point is the definition of the Wigner function:

$$f_W(\mathbf{r}, \mathbf{p}) \triangleq \sum_i p_i \frac{1}{(\hbar\pi)^n} \int_{\Omega} \Psi_i^*(\mathbf{r} + \mathbf{a}) \Psi_i(\mathbf{r} - \mathbf{a}) \exp\left\{+\frac{2i}{\hbar} \mathbf{p} \cdot \mathbf{a}\right\} d\mathbf{a}$$

which can then be differentiated with respect to time, getting:

$$\begin{aligned} \frac{\partial}{\partial t} f_W(\mathbf{r}, \mathbf{p}) &= \frac{\partial}{\partial t} \left\{ \sum_i p_i \frac{1}{(\hbar\pi)^n} \int_{\Omega} \Psi_i^*(\mathbf{r} + \mathbf{a}) \Psi_i(\mathbf{r} - \mathbf{a}) \exp\left\{+\frac{2i}{\hbar} \mathbf{p} \cdot \mathbf{a}\right\} d\mathbf{a} \right\} \\ \frac{\partial}{\partial t} f_W(\mathbf{r}, \mathbf{p}) &\triangleq \sum_i p_i \frac{1}{(\hbar\pi)^n} \int_{\Omega} \frac{\partial}{\partial t} \left\{ \Psi_i^*(\mathbf{r} + \mathbf{a}) \Psi_i(\mathbf{r} - \mathbf{a}) \right\} \exp\left\{+\frac{2i}{\hbar} \mathbf{p} \cdot \mathbf{a}\right\} d\mathbf{a} \end{aligned}$$

Expanding the derivative of the product of wavefunctions with the product rule yields:

$$\frac{\partial}{\partial t} f_W(\mathbf{r}, \mathbf{p}) \triangleq \sum_i p_i \frac{1}{(\hbar\pi)^n} \int_{\Omega} \left[\Psi_i(\mathbf{r} - \mathbf{a}) \frac{\partial \Psi_i^*}{\partial t}(\mathbf{r} + \mathbf{a}) + \Psi_i^*(\mathbf{r} + \mathbf{a}) \frac{\partial \Psi_i}{\partial t}(\mathbf{r} - \mathbf{a}) \right] \exp\left\{+\frac{2i}{\hbar} \mathbf{p} \cdot \mathbf{a}\right\} d\mathbf{a}$$

Substituting Schrödinger's equation (Equation 2.6) and its conjugated version (Equation 2.7) gives:

$$\begin{aligned} \frac{\partial}{\partial t} f_W(\mathbf{r}, \mathbf{p}) &\triangleq \sum_i p_i \frac{1}{(\hbar\pi)^n} \int_{\Omega} \left[\Psi_i(\mathbf{r} - \mathbf{a}) \frac{i}{\hbar} H\{\Psi_i^*\}|_{\mathbf{r}+\mathbf{a}} - \Psi_i^*(\mathbf{r} + \mathbf{a}) \frac{i}{\hbar} H\{\Psi_i\}|_{\mathbf{r}-\mathbf{a}} \right] \exp\left\{+\frac{2i}{\hbar} \mathbf{p} \cdot \mathbf{a}\right\} d\mathbf{a} \\ \frac{\partial}{\partial t} f_W(\mathbf{r}, \mathbf{p}) &\triangleq \sum_i p_i \frac{1}{(\hbar\pi)^n} \int_{\Omega} \left[\Psi_i(\mathbf{r} - \mathbf{a}) \frac{i}{\hbar} [H\{\Psi_i^*\}]_{\mathbf{r}+\mathbf{a}} - \Psi_i^*(\mathbf{r} + \mathbf{a}) \frac{i}{\hbar} [H\{\Psi_i\}]_{\mathbf{r}-\mathbf{a}} \right] \exp\left\{+\frac{2i}{\hbar} \mathbf{p} \cdot \mathbf{a}\right\} d\mathbf{a} \end{aligned}$$

Substituting the Hamiltonian for the simplified case of a parabolic dispersion relationship (i.e. under an effective mass approximation) leads to:

$$\begin{aligned} \frac{\partial}{\partial t} f_W(\mathbf{r}, \mathbf{p}) &\triangleq \sum_i p_i \frac{1}{(\hbar\pi)^n} \int_{\Omega} \left[\Psi_i(\mathbf{r} - \mathbf{a}) \frac{i}{\hbar} \left[-\frac{\hbar^2}{2m^*} \nabla^2 \{\Psi_i^*\} + U \Psi_i^* \right]_{\mathbf{r}+\mathbf{a}} + \right. \\ &\quad \left. - \Psi_i^*(\mathbf{r} + \mathbf{a}) \frac{i}{\hbar} \left[-\frac{\hbar^2}{2m^*} \nabla^2 \{\Psi_i\} + U \Psi_i \right]_{\mathbf{r}-\mathbf{a}} \right] \exp\left\{+\frac{2i}{\hbar} \mathbf{p} \cdot \mathbf{a}\right\} d\mathbf{a} \\ \frac{\partial}{\partial t} f_W(\mathbf{r}, \mathbf{p}) &= \sum_i p_i \frac{1}{(\hbar\pi)^n} \int_{\Omega} \left[\Psi_i(\mathbf{r} - \mathbf{a}) \frac{i}{\hbar} U(\mathbf{r} + \mathbf{a}) \Psi_i^*(\mathbf{r} + \mathbf{a}) \right. \\ &\quad \left. - \Psi_i^*(\mathbf{r} + \mathbf{a}) \frac{i}{\hbar} U(\mathbf{r} - \mathbf{a}) \Psi_i(\mathbf{r} - \mathbf{a}) \right] \exp\left\{+\frac{2i}{\hbar} \mathbf{p} \cdot \mathbf{a}\right\} d\mathbf{a} \end{aligned}$$

$$\begin{aligned}
& + \sum_i p_i \frac{1}{(\hbar\pi)^n} \int_{\Omega} \left[-\Psi_i(\mathbf{r} - \mathbf{a}) \frac{\hbar i}{2m^*} [\nabla^2 \Psi_i^*]_{\mathbf{r}+\mathbf{a}} \right. \\
& \left. + \Psi_i^*(\mathbf{r} + \mathbf{a}) \frac{\hbar i}{2m^*} [\nabla^2 \Psi_i]_{\mathbf{r}-\mathbf{a}} \right] \exp \left\{ + \frac{2i}{\hbar} \mathbf{p} \cdot \mathbf{a} \right\} d\mathbf{a}
\end{aligned}$$

Collecting the terms multiplying the potential energy gives:

$$\begin{aligned}
\frac{\partial}{\partial t} f_W(\mathbf{r}, \mathbf{p}) & = \sum_i p_i \frac{1}{(\hbar\pi)^n} \int_{\Omega} \left[\Psi_i(\mathbf{r} - \mathbf{a}) \frac{i}{\hbar} [U(\mathbf{r} + \mathbf{a}) - U(\mathbf{r} - \mathbf{a})] \Psi_i^*(\mathbf{r} + \mathbf{a}) \right] \exp \left\{ + \frac{2i}{\hbar} \mathbf{p} \cdot \mathbf{a} \right\} d\mathbf{a} \\
& + \sum_i p_i \frac{1}{(\hbar\pi)^n} \int_{\Omega} \left[-\Psi_i(\mathbf{r} - \mathbf{a}) \frac{\hbar i}{2m^*} [\nabla^2 \Psi_i^*]_{\mathbf{r}+\mathbf{a}} + \Psi_i^*(\mathbf{r} + \mathbf{a}) \frac{\hbar i}{2m^*} [\nabla^2 \Psi_i]_{\mathbf{r}-\mathbf{a}} \right] \exp \left\{ + \frac{2i}{\hbar} \mathbf{p} \cdot \mathbf{a} \right\} d\mathbf{a}
\end{aligned}$$

The goal is now to apply the vector calculus identity:

$$[\alpha \nabla^2 \beta]_x = [\nabla \cdot (\alpha \nabla \beta)]_x - [\nabla \alpha \cdot \nabla \beta]_x \quad (5.1)$$

In order to apply it, all the terms must be written as being functions of the same variable (which appears as \mathbf{x} in the general relationship above).

This is possible by treating \mathbf{r} as a shift and adopting the notation for the shifted version of a function:

$$\overset{\rightarrow{\mathbf{r}}}{f}(\boldsymbol{\eta}) = f(\boldsymbol{\eta} + \mathbf{r})$$

Moreover, in order to explicitly write function transformations like mirrorings $f(-\boldsymbol{\eta})$ when writing a function its argument will be symbolically denoted as $\boldsymbol{\eta}$. All the expressions of the kind $f(\boldsymbol{\eta})$ are however to be understood as being functions yet to be evaluated at a specific point (and not as values).

Then the above differential equation becomes:

$$\begin{aligned}
\frac{\partial}{\partial t} f_W(\mathbf{r}, \mathbf{p}) & = \sum_i p_i \frac{1}{(\hbar\pi)^n} \int_{\Omega} \left[\Psi_i(\mathbf{r} - \mathbf{a}) \frac{i}{\hbar} [U(\mathbf{r} + \mathbf{a}) - U(\mathbf{r} - \mathbf{a})] \Psi_i^*(\mathbf{r} + \mathbf{a}) \right] \exp \left\{ + \frac{2i}{\hbar} \mathbf{p} \cdot \mathbf{a} \right\} d\mathbf{a} \\
& - \sum_i p_i \frac{1}{(\hbar\pi)^n} \int_{\Omega} \left(\left[\overset{\rightarrow{\mathbf{r}}}{\Psi}_i(-\boldsymbol{\eta}) \frac{\hbar i}{2m^*} [\nabla_{\boldsymbol{\eta}}^2 \overset{\rightarrow{\mathbf{r}}}{\Psi}_i^*(\boldsymbol{\eta})] \right] \exp \left\{ + \frac{2i}{\hbar} \mathbf{p} \cdot \boldsymbol{\eta} \right\} \right)_{\boldsymbol{\eta}=\mathbf{a}} d\mathbf{a} \\
& + \sum_i p_i \frac{1}{(\hbar\pi)^n} \int_{\Omega} \left(\left[\overset{\rightarrow{\mathbf{r}}}{\Psi}_i^*(\boldsymbol{\eta}) \frac{\hbar i}{2m^*} [\nabla_{\boldsymbol{\eta}}^2 \overset{\rightarrow{\mathbf{r}}}{\Psi}_i(-\boldsymbol{\eta})] \right] \exp \left\{ + \frac{2i}{\hbar} \mathbf{p} \cdot \boldsymbol{\eta} \right\} \right)_{\boldsymbol{\eta}=\mathbf{a}} d\mathbf{a}
\end{aligned}$$

(the notation $\nabla_{\boldsymbol{\eta}}^2$ is used to clearly distinguish between the function and its argument when transformed or composed functions like $f(-\boldsymbol{\eta})$ are being considered, in which case the variable with respect to which the differentiation is carried out might not be clear enough; $\boldsymbol{\eta}$ should however be considered only as a placeholder to denote which is the argument of a function and nothing more since the concept of function or laplacian of a function mathematically exist without the need of specifying their arguments)

Then, applying the vector identity of Equation 5.1 leads to the result:

$$\begin{aligned}
\frac{\partial}{\partial t} f_W(\mathbf{r}, \mathbf{p}) & = \sum_i p_i \frac{1}{(\hbar\pi)^n} \int_{\Omega} \left[\Psi_i(\mathbf{r} - \mathbf{a}) \frac{i}{\hbar} [U(\mathbf{r} + \mathbf{a}) - U(\mathbf{r} - \mathbf{a})] \Psi_i^*(\mathbf{r} + \mathbf{a}) \right] \exp \left\{ + \frac{2i}{\hbar} \mathbf{p} \cdot \mathbf{a} \right\} d\mathbf{a} \\
& - \sum_i p_i \frac{\hbar i}{2m^*} \frac{1}{(\hbar\pi)^n} \int_{\Omega} \left(\nabla_{\boldsymbol{\eta}} \cdot \left[\overset{\rightarrow{\mathbf{r}}}{\Psi}_i(-\boldsymbol{\eta}) \exp \left\{ + \frac{2i}{\hbar} \mathbf{p} \cdot \boldsymbol{\eta} \right\} \nabla_{\boldsymbol{\eta}} \left\{ \overset{\rightarrow{\mathbf{r}}}{\Psi}_i^*(\boldsymbol{\eta}) \right\} \right] \right)_{\boldsymbol{\eta}=\mathbf{a}} d\mathbf{a} \\
& + \sum_i p_i \frac{\hbar i}{2m^*} \frac{1}{(\hbar\pi)^n} \int_{\Omega} \left(\nabla_{\boldsymbol{\eta}} \cdot \left[\overset{\rightarrow{\mathbf{r}}}{\Psi}_i^*(\boldsymbol{\eta}) \exp \left\{ + \frac{2i}{\hbar} \mathbf{p} \cdot \boldsymbol{\eta} \right\} \cdot \nabla_{\boldsymbol{\eta}} \left\{ \overset{\rightarrow{\mathbf{r}}}{\Psi}_i(-\boldsymbol{\eta}) \right\} \right] \right)_{\boldsymbol{\eta}=\mathbf{a}} d\mathbf{a} \\
& + \sum_i p_i \frac{\hbar i}{2m^*} \frac{1}{(\hbar\pi)^n} \int_{\Omega} \left(\nabla_{\boldsymbol{\eta}} \left[\overset{\rightarrow{\mathbf{r}}}{\Psi}_i(-\boldsymbol{\eta}) \exp \left\{ + \frac{2i}{\hbar} \mathbf{p} \cdot \boldsymbol{\eta} \right\} \right] \cdot \nabla_{\boldsymbol{\eta}} \left[\overset{\rightarrow{\mathbf{r}}}{\Psi}_i^*(\boldsymbol{\eta}) \right] \right)_{\boldsymbol{\eta}=\mathbf{a}} d\mathbf{a}
\end{aligned}$$

$$- \sum_i p_i \frac{\hbar i}{2m^*} \frac{1}{(\hbar\pi)^n} \int_{\Omega} \left(\nabla_{\boldsymbol{\eta}} \left[\Psi_i^*(\boldsymbol{\eta}) \exp \left\{ + \frac{2i}{\hbar} \mathbf{p} \cdot \boldsymbol{\eta} \right\} \right] \cdot \nabla_{\boldsymbol{\eta}} \left[\Psi_i(-\boldsymbol{\eta}) \right] \right)_{\boldsymbol{\eta}=\mathbf{a}} d\mathbf{a}$$

The terms highlighted in blue can be treated applying Stoke's theorem in n dimensions:

$$\int_{\Omega} \nabla \cdot \mathbf{F} d\mathbf{V} = \int_{\partial\Omega} \mathbf{F} \cdot \hat{\mathbf{n}} d\mathbf{S}$$

where $\partial\Omega$ is the boundary of the spatial domain for the problem.

The first of the blue terms then becomes:

$$\begin{aligned} \sum_i p_i \frac{\hbar i}{2m^*} \frac{1}{(\hbar\pi)^n} \int_{\Omega} \left(\nabla_{\boldsymbol{\eta}} \cdot \left[\Psi_i^*(-\boldsymbol{\eta}) \exp \left\{ + \frac{2i}{\hbar} \mathbf{p} \cdot \boldsymbol{\eta} \right\} \nabla_{\boldsymbol{\eta}} \left\{ \Psi_i^*(\boldsymbol{\eta}) \right\} \right] \right)_{\boldsymbol{\eta}=\mathbf{a}} d\mathbf{a} = \\ = \sum_i p_i \frac{\hbar i}{2m^*} \frac{1}{(\hbar\pi)^n} \int_{\Omega} \left[\Psi_i^*(-\boldsymbol{\eta}) \exp \left\{ + \frac{2i}{\hbar} \mathbf{p} \cdot \boldsymbol{\eta} \right\} \nabla_{\boldsymbol{\eta}} \left\{ \Psi_i^*(\boldsymbol{\eta}) \right\} \right]_{\boldsymbol{\eta}=\mathbf{a}} \cdot \hat{\mathbf{n}} d\mathbf{S}_{\mathbf{a}} \approx 0 \end{aligned}$$

under the assumption that the wavefunction Ψ_i decays close to zero at the boundary of the domain that is considered for the problem.

Similarly, also the second blue term can be neglected; hence the evolution equation simplifies to:

$$\begin{aligned} \frac{\partial}{\partial t} f_{\mathbf{W}}(\mathbf{r}, \mathbf{p}) = \sum_i p_i \frac{1}{(\hbar\pi)^n} \int_{\Omega} \left[\Psi_i(\mathbf{r} - \mathbf{a}) \frac{i}{\hbar} [U(\mathbf{r} + \mathbf{a}) - U(\mathbf{r} - \mathbf{a})] \Psi_i^*(\mathbf{r} + \mathbf{a}) \right] \exp \left\{ + \frac{2i}{\hbar} \mathbf{p} \cdot \mathbf{a} \right\} d\mathbf{a} \\ + \sum_i p_i \frac{\hbar i}{2m^*} \frac{1}{(\hbar\pi)^n} \int_{\Omega} \left(\nabla_{\boldsymbol{\eta}} \left[\Psi_i^*(-\boldsymbol{\eta}) \exp \left\{ + \frac{2i}{\hbar} \mathbf{p} \cdot \boldsymbol{\eta} \right\} \right] \cdot \nabla_{\boldsymbol{\eta}} \left[\Psi_i^*(\boldsymbol{\eta}) \right] \right)_{\boldsymbol{\eta}=\mathbf{a}} d\mathbf{a} \\ - \sum_i p_i \frac{\hbar i}{2m^*} \frac{1}{(\hbar\pi)^n} \int_{\Omega} \left(\nabla_{\boldsymbol{\eta}} \left[\Psi_i^*(\boldsymbol{\eta}) \exp \left\{ + \frac{2i}{\hbar} \mathbf{p} \cdot \boldsymbol{\eta} \right\} \right] \cdot \nabla_{\boldsymbol{\eta}} \left[\Psi_i(-\boldsymbol{\eta}) \right] \right)_{\boldsymbol{\eta}=\mathbf{a}} d\mathbf{a} \end{aligned}$$

The gradient of the product of a function and an exponential in the same variable obeys the following rule for its components:

$$\begin{aligned} \left[\nabla_{\boldsymbol{\eta}} \left\{ \exp \left\{ \frac{2i}{\hbar} \mathbf{p} \cdot \boldsymbol{\eta} \right\} \alpha(\boldsymbol{\eta}) \right\} \right]_j = \frac{\partial}{\partial \eta_j} \left\{ \exp \left\{ \frac{2i}{\hbar} \sum_k p_k \eta_k \right\} \alpha(\boldsymbol{\eta}) \right\} \\ = \frac{2i}{\hbar} p_j \exp \left\{ \frac{2i}{\hbar} \sum_k p_k \eta_k \right\} \alpha(\boldsymbol{\eta}) + \exp \left\{ \frac{2i}{\hbar} \sum_k p_k \eta_k \right\} \frac{\partial}{\partial \eta_j} \{ \alpha(\boldsymbol{\eta}) \} \\ = \frac{2i}{\hbar} p_j \exp \left\{ \frac{2i}{\hbar} \mathbf{p} \cdot \boldsymbol{\eta} \right\} \alpha(\boldsymbol{\eta}) + \exp \left\{ \frac{2i}{\hbar} \mathbf{p} \cdot \boldsymbol{\eta} \right\} \frac{\partial}{\partial \eta_j} \{ \alpha(\boldsymbol{\eta}) \} \end{aligned}$$

which corresponds to the vector relationship:

$$\left[\nabla_{\boldsymbol{\eta}} \left\{ \exp \left\{ \frac{2i}{\hbar} \mathbf{p} \cdot \boldsymbol{\eta} \right\} \alpha(\boldsymbol{\eta}) \right\} \right]_j = \frac{2i}{\hbar} \mathbf{p} \exp \left\{ \frac{2i}{\hbar} \mathbf{p} \cdot \boldsymbol{\eta} \right\} \alpha(\boldsymbol{\eta}) + \exp \left\{ \frac{2i}{\hbar} \mathbf{p} \cdot \boldsymbol{\eta} \right\} \nabla_{\boldsymbol{\eta}} \{ \alpha(\boldsymbol{\eta}) \}$$

Applying this last result to the above evolution equation gives:

$$\begin{aligned} \frac{\partial}{\partial t} f_{\mathbf{W}}(\mathbf{r}, \mathbf{p}) = \sum_i p_i \frac{1}{(\hbar\pi)^n} \int_{\Omega} \left[\Psi_i(\mathbf{r} - \mathbf{a}) \frac{i}{\hbar} [U(\mathbf{r} + \mathbf{a}) - U(\mathbf{r} - \mathbf{a})] \Psi_i^*(\mathbf{r} + \mathbf{a}) \right] \exp \left\{ + \frac{2i}{\hbar} \mathbf{p} \cdot \mathbf{a} \right\} d\mathbf{a} \\ + \sum_i p_i \frac{\hbar i}{2m^*} \frac{1}{(\hbar\pi)^n} \int_{\Omega} \left(\frac{2i}{\hbar} \Psi_i^*(-\boldsymbol{\eta}) \exp \left\{ + \frac{2i}{\hbar} \mathbf{p} \cdot \boldsymbol{\eta} \right\} \mathbf{p} \cdot \nabla_{\boldsymbol{\eta}} \left[\Psi_i^*(\boldsymbol{\eta}) \right] \right)_{\boldsymbol{\eta}=\mathbf{a}} d\mathbf{a} \\ + \sum_i p_i \frac{\hbar i}{2m^*} \frac{1}{(\hbar\pi)^n} \int_{\Omega} \left(\exp \left\{ + \frac{2i}{\hbar} \mathbf{p} \cdot \boldsymbol{\eta} \right\} \nabla_{\boldsymbol{\eta}} \left[\Psi_i^*(-\boldsymbol{\eta}) \right] \cdot \nabla_{\boldsymbol{\eta}} \left[\Psi_i^*(\boldsymbol{\eta}) \right] \right)_{\boldsymbol{\eta}=\mathbf{a}} d\mathbf{a} \end{aligned}$$

$$\begin{aligned}
& - \sum_i p_i \frac{\hbar i}{2m^*} \frac{1}{(\hbar\pi)^n} \int_{\Omega} \left(\frac{2i}{\hbar} \vec{\Psi}_i^*(\boldsymbol{\eta}) \exp \left\{ + \frac{2i}{\hbar} \mathbf{p} \cdot \boldsymbol{\eta} \right\} \mathbf{p} \cdot \nabla_{\boldsymbol{\eta}} \left[\vec{\Psi}_i(-\boldsymbol{\eta}) \right] \right)_{\boldsymbol{\eta}=\mathbf{a}} d\mathbf{a} \\
& - \sum_i p_i \frac{\hbar i}{2m^*} \frac{1}{(\hbar\pi)^n} \int_{\Omega} \left(\exp \left\{ + \frac{2i}{\hbar} \mathbf{p} \cdot \boldsymbol{\eta} \right\} \nabla_{\boldsymbol{\eta}} \left[\vec{\Psi}_i^*(\boldsymbol{\eta}) \right] \cdot \nabla_{\boldsymbol{\eta}} \left[\vec{\Psi}_i(-\boldsymbol{\eta}) \right] \right)_{\boldsymbol{\eta}=\mathbf{a}} d\mathbf{a}
\end{aligned}$$

The terms highlighted in red cancel out and the equation simplifies to:

$$\begin{aligned}
\frac{\partial}{\partial t} f_W(\mathbf{r}, \mathbf{p}) &= \sum_i p_i \frac{1}{(\hbar\pi)^n} \int_{\Omega} \left[\Psi_i(\mathbf{r} - \mathbf{a}) \frac{i}{\hbar} [U(\mathbf{r} + \mathbf{a}) - U(\mathbf{r} - \mathbf{a})] \Psi_i^*(\mathbf{r} + \mathbf{a}) \right] \exp \left\{ + \frac{2i}{\hbar} \mathbf{p} \cdot \mathbf{a} \right\} d\mathbf{a} \\
&+ \sum_i p_i \frac{\hbar i}{2m^*} \frac{1}{(\hbar\pi)^n} \int_{\Omega} \left(\frac{2i}{\hbar} \vec{\Psi}_i(-\boldsymbol{\eta}) \exp \left\{ + \frac{2i}{\hbar} \mathbf{p} \cdot \boldsymbol{\eta} \right\} \mathbf{p} \cdot \nabla_{\boldsymbol{\eta}} \left[\vec{\Psi}_i^*(\boldsymbol{\eta}) \right] \right)_{\boldsymbol{\eta}=\mathbf{a}} d\mathbf{a} \\
&- \sum_i p_i \frac{\hbar i}{2m^*} \frac{1}{(\hbar\pi)^n} \int_{\Omega} \left(\frac{2i}{\hbar} \vec{\Psi}_i^*(\boldsymbol{\eta}) \exp \left\{ + \frac{2i}{\hbar} \mathbf{p} \cdot \boldsymbol{\eta} \right\} \mathbf{p} \cdot \nabla_{\boldsymbol{\eta}} \left[\vec{\Psi}_i(-\boldsymbol{\eta}) \right] \right)_{\boldsymbol{\eta}=\mathbf{a}} d\mathbf{a}
\end{aligned}$$

Canceling out the constants in front of the right-hand-side terms yields a further simplification of the expression to:

$$\begin{aligned}
\frac{\partial}{\partial t} f_W(\mathbf{r}, \mathbf{p}) &= \sum_i p_i \frac{1}{(\hbar\pi)^n} \int_{\Omega} \left[\Psi_i(\mathbf{r} - \mathbf{a}) \frac{i}{\hbar} [U(\mathbf{r} + \mathbf{a}) - U(\mathbf{r} - \mathbf{a})] \Psi_i^*(\mathbf{r} + \mathbf{a}) \right] \exp \left\{ + \frac{2i}{\hbar} \mathbf{p} \cdot \mathbf{a} \right\} d\mathbf{a} \\
&- \sum_i p_i \frac{1}{(\hbar\pi)^n} \int_{\Omega} \left(\vec{\Psi}_i(-\boldsymbol{\eta}) \exp \left\{ + \frac{2i}{\hbar} \mathbf{p} \cdot \boldsymbol{\eta} \right\} \frac{\mathbf{p}}{m^*} \cdot \nabla_{\boldsymbol{\eta}} \left[\vec{\Psi}_i^*(\boldsymbol{\eta}) \right] \right)_{\boldsymbol{\eta}=\mathbf{a}} d\mathbf{a} \\
&+ \sum_i p_i \frac{1}{(\hbar\pi)^n} \int_{\Omega} \left(\vec{\Psi}_i^*(\boldsymbol{\eta}) \exp \left\{ + \frac{2i}{\hbar} \mathbf{p} \cdot \boldsymbol{\eta} \right\} \frac{\mathbf{p}}{m^*} \cdot \nabla_{\boldsymbol{\eta}} \left[\vec{\Psi}_i(-\boldsymbol{\eta}) \right] \right)_{\boldsymbol{\eta}=\mathbf{a}} d\mathbf{a}
\end{aligned}$$

By the chain rule $\nabla_{\boldsymbol{\eta}} [\alpha(-\boldsymbol{\eta})]_{\boldsymbol{\eta}=\mathbf{a}} = -[\nabla_{\boldsymbol{\eta}} [\alpha(\boldsymbol{\eta})]]_{\boldsymbol{\eta}=-\mathbf{a}}$, therefore the above differential equation simplifies to:

$$\begin{aligned}
\frac{\partial}{\partial t} f_W(\mathbf{r}, \mathbf{p}) &= \sum_i p_i \frac{1}{(\hbar\pi)^n} \int_{\Omega} \left[\Psi_i(\mathbf{r} - \mathbf{a}) \frac{i}{\hbar} [U(\mathbf{r} + \mathbf{a}) - U(\mathbf{r} - \mathbf{a})] \Psi_i^*(\mathbf{r} + \mathbf{a}) \right] \exp \left\{ + \frac{2i}{\hbar} \mathbf{p} \cdot \mathbf{a} \right\} d\mathbf{a} \\
&- \sum_i p_i \frac{1}{(\hbar\pi)^n} \int_{\Omega} \vec{\Psi}_i(-\mathbf{a}) \exp \left\{ + \frac{2i}{\hbar} \mathbf{p} \cdot \mathbf{a} \right\} \frac{\mathbf{p}}{m^*} \cdot \left[\nabla \vec{\Psi}_i^* \right]_{\mathbf{a}} d\mathbf{a} \\
&- \sum_i p_i \frac{1}{(\hbar\pi)^n} \int_{\Omega} \vec{\Psi}_i^*(\mathbf{a}) \exp \left\{ + \frac{2i}{\hbar} \mathbf{p} \cdot \mathbf{a} \right\} \frac{\mathbf{p}}{m^*} \cdot \left[\nabla \vec{\Psi}_i \right]_{-\mathbf{a}} d\mathbf{a}
\end{aligned}$$

The derivative of a shifted function is the shifted derivative of the function then the equation can be rewritten in the form:

$$\begin{aligned}
\frac{\partial}{\partial t} f_W(\mathbf{r}, \mathbf{p}) &= \sum_i p_i \frac{1}{(\hbar\pi)^n} \int_{\Omega} \left[\Psi_i(\mathbf{r} - \mathbf{a}) \frac{i}{\hbar} [U(\mathbf{r} + \mathbf{a}) - U(\mathbf{r} - \mathbf{a})] \Psi_i^*(\mathbf{r} + \mathbf{a}) \right] \exp \left\{ + \frac{2i}{\hbar} \mathbf{p} \cdot \mathbf{a} \right\} d\mathbf{a} \\
&- \sum_i p_i \frac{1}{(\hbar\pi)^n} \int_{\Omega} \Psi_i(\mathbf{r} - \mathbf{a}) \exp \left\{ + \frac{2i}{\hbar} \mathbf{p} \cdot \mathbf{a} \right\} \frac{\mathbf{p}}{m^*} \cdot [\nabla \Psi_i^*](\mathbf{r} + \mathbf{a}) d\mathbf{a} \\
&- \sum_i p_i \frac{1}{(\hbar\pi)^n} \int_{\Omega} \Psi_i^*(\mathbf{r} + \mathbf{a}) \exp \left\{ + \frac{2i}{\hbar} \mathbf{p} \cdot \mathbf{a} \right\} \frac{\mathbf{p}}{m^*} \cdot [\nabla \Psi_i](\mathbf{r} - \mathbf{a}) d\mathbf{a}
\end{aligned}$$

Then, since by the rule for the differentiation of a product of functions $\nabla[\vec{\Psi}_i^* \Psi_i] = \vec{\Psi}_i^* \nabla[\Psi_i] + \nabla[\vec{\Psi}_i^*] \Psi_i$, the previous equation is easily rewritten (also leveraging again on the shift operator) as:

$$\frac{\partial}{\partial t} f_W(\mathbf{r}, \mathbf{p}) = \sum_i p_i \frac{1}{(\hbar\pi)^n} \int_{\Omega} \left[\Psi_i(\mathbf{r} - \mathbf{a}) \frac{i}{\hbar} [U(\mathbf{r} + \mathbf{a}) - U(\mathbf{r} - \mathbf{a})] \Psi_i^*(\mathbf{r} + \mathbf{a}) \right] \exp \left\{ + \frac{2i}{\hbar} \mathbf{p} \cdot \mathbf{a} \right\} d\mathbf{a}$$

$$- \sum_i p_i \frac{1}{(\hbar\pi)^n} \int_{\Omega} \exp \left\{ + \frac{2i}{\hbar} \mathbf{p} \cdot \mathbf{a} \right\} \frac{\mathbf{p}}{m^*} \cdot \left[\nabla (\overset{\rightarrow}{\Psi}_i^* \overset{\rightarrow}{\Psi}_i) \right] (\mathbf{r}) d\mathbf{a}$$

which, showing explicitly the variable $\boldsymbol{\eta}$ for the differentiation of $\overset{\rightarrow}{\Psi}_i^* \overset{\rightarrow}{\Psi}_i$, is equivalent to:

$$\begin{aligned} \frac{\partial}{\partial t} f_W(\mathbf{r}, \mathbf{p}) &= \sum_i p_i \frac{1}{(\hbar\pi)^n} \int_{\Omega} \left[\Psi_i(\mathbf{r} - \mathbf{a}) \frac{i}{\hbar} [U(\mathbf{r} + \mathbf{a}) - U(\mathbf{r} - \mathbf{a})] \Psi_i^*(\mathbf{r} + \mathbf{a}) \right] \exp \left\{ + \frac{2i}{\hbar} \mathbf{p} \cdot \mathbf{a} \right\} d\mathbf{a} \\ &\quad - \sum_i p_i \frac{1}{(\hbar\pi)^n} \int_{\Omega} \exp \left\{ + \frac{2i}{\hbar} \mathbf{p} \cdot \mathbf{a} \right\} \frac{\mathbf{p}}{m^*} \cdot [\nabla_{\boldsymbol{\eta}} \{ \Psi_i^*(\boldsymbol{\eta} + \mathbf{a}) \Psi_i(\boldsymbol{\eta} - \mathbf{a}) \}]_{\boldsymbol{\eta}=\mathbf{r}} d\mathbf{a} \end{aligned}$$

Swapping then the integral and the gradient gives:

$$\begin{aligned} \frac{\partial}{\partial t} f_W(\mathbf{r}, \mathbf{p}) &= \sum_i p_i \frac{1}{(\hbar\pi)^n} \int_{\Omega} \left[\Psi_i(\mathbf{r} - \mathbf{a}) \frac{i}{\hbar} [U(\mathbf{r} + \mathbf{a}) - U(\mathbf{r} - \mathbf{a})] \Psi_i^*(\mathbf{r} + \mathbf{a}) \right] \exp \left\{ + \frac{2i}{\hbar} \mathbf{p} \cdot \mathbf{a} \right\} d\mathbf{a} \\ &\quad - \frac{\mathbf{p}}{m^*} \cdot \left[\nabla_{\boldsymbol{\eta}} \left\{ \sum_i p_i \frac{1}{(\hbar\pi)^n} \int_{\Omega} \exp \left\{ + \frac{2i}{\hbar} \mathbf{p} \cdot \mathbf{a} \right\} \Psi_i^*(\boldsymbol{\eta} + \mathbf{a}) \Psi_i(\boldsymbol{\eta} - \mathbf{a}) d\mathbf{a} \right\} \right]_{\boldsymbol{\eta}=\mathbf{r}} \end{aligned}$$

The blue term can be seen to be the definition of the Wigner function as given in Equation 4.5.

Substituting it then the time evolution equation becomes:

$$\begin{aligned} \frac{\partial}{\partial t} f_W(\mathbf{r}, \mathbf{p}) &= \sum_i p_i \frac{1}{(\hbar\pi)^n} \int_{\Omega} \left[\Psi_i(\mathbf{r} - \mathbf{a}) \frac{i}{\hbar} [U(\mathbf{r} + \mathbf{a}) - U(\mathbf{r} - \mathbf{a})] \Psi_i^*(\mathbf{r} + \mathbf{a}) \right] \exp \left\{ + \frac{2i}{\hbar} \mathbf{p} \cdot \mathbf{a} \right\} d\mathbf{a} \\ &\quad - \frac{\mathbf{p}}{m^*} \cdot [\nabla_{\boldsymbol{\eta}} f_W(\boldsymbol{\eta}, \mathbf{p})]_{\boldsymbol{\eta}=\mathbf{r}} \end{aligned}$$

Adopting the more compact notation $[\nabla_{\mathbf{r}} f_W(\mathbf{r}, \mathbf{p})] \triangleq [\nabla_{\boldsymbol{\eta}} f_W(\boldsymbol{\eta}, \mathbf{p})]_{\boldsymbol{\eta}=\mathbf{r}}$ for the gradient of the Wigner function with respect to its position argument evaluated at a position \mathbf{r} then the equation can be rewritten as:

$$\begin{aligned} \frac{\partial}{\partial t} f_W(\mathbf{r}, \mathbf{p}) &= \sum_i p_i \frac{1}{(\hbar\pi)^n} \int_{\Omega} \left[\Psi_i(\mathbf{r} - \mathbf{a}) \frac{i}{\hbar} [U(\mathbf{r} + \mathbf{a}) - U(\mathbf{r} - \mathbf{a})] \Psi_i^*(\mathbf{r} + \mathbf{a}) \right] \exp \left\{ + \frac{2i}{\hbar} \mathbf{p} \cdot \mathbf{a} \right\} d\mathbf{a} \\ &\quad - \frac{\mathbf{p}}{m^*} \cdot [\nabla_{\mathbf{r}} f_W(\mathbf{r}, \mathbf{p})] \end{aligned}$$

Bringing the gradient of the Wigner function on the other side of the equation gives:

$$\begin{aligned} \frac{\partial}{\partial t} f_W(\mathbf{r}, \mathbf{p}) + \frac{\mathbf{p}}{m^*} \cdot [\nabla_{\mathbf{r}} f_W(\mathbf{r}, \mathbf{p})] \\ = \sum_i p_i \frac{1}{(\hbar\pi)^n} \int_{\Omega} \left[\Psi_i(\mathbf{r} - \mathbf{a}) \frac{i}{\hbar} [U(\mathbf{r} + \mathbf{a}) - U(\mathbf{r} - \mathbf{a})] \Psi_i^*(\mathbf{r} + \mathbf{a}) \right] \exp \left\{ + \frac{2i}{\hbar} \mathbf{p} \cdot \mathbf{a} \right\} d\mathbf{a} \end{aligned}$$

To obtain the final form of this equation the term of the kind $U(\mathbf{r} + \mathbf{b})$ (where \mathbf{b} can be either \mathbf{a} or $-\mathbf{a}$) must then be expanded into Taylor series, treating \mathbf{b} as the displacement:

$$U(\mathbf{r} + \mathbf{b}) = \sum_{\lambda_1, \dots, \lambda_n \geq 0} [\partial_1^{\lambda_1} \partial_2^{\lambda_2} \dots \partial_n^{\lambda_n} U](\mathbf{r}) \frac{b_1^{\lambda_1} b_2^{\lambda_2} \dots b_n^{\lambda_n}}{\lambda_1! \lambda_2! \dots \lambda_n!}$$

Applying then this Taylor series to the cases of $U(\mathbf{r} + \mathbf{a})$ and $U(\mathbf{r} - \mathbf{a})$ gives:

$$U(\mathbf{r} + \mathbf{a}) = \sum_{\lambda_1, \dots, \lambda_n \geq 0} [\partial_1^{\lambda_1} \partial_2^{\lambda_2} \dots \partial_n^{\lambda_n} U](\mathbf{r}) \frac{a_1^{\lambda_1} a_2^{\lambda_2} \dots a_n^{\lambda_n}}{\lambda_1! \lambda_2! \dots \lambda_n!}$$

$$U(\mathbf{r} - \mathbf{a}) = \sum_{\lambda_1, \dots, \lambda_n \geq 0} [\partial_1^{\lambda_1} \partial_2^{\lambda_2} \dots \partial_n^{\lambda_n} U](\mathbf{r}) \frac{(-a_1)^{\lambda_1} (-a_2)^{\lambda_2} \dots (-a_n)^{\lambda_n}}{\lambda_1! \lambda_2! \dots \lambda_n!}$$

When subtracted the two expressions give:

$$U(\mathbf{r} + \mathbf{a}) - U(\mathbf{r} - \mathbf{a}) = \sum_{\lambda_1, \dots, \lambda_n \geq 0} [\partial_1^{\lambda_1} \partial_2^{\lambda_2} \dots \partial_n^{\lambda_n} U](\mathbf{r}) \frac{[a_1^{\lambda_1} a_2^{\lambda_2} \dots a_n^{\lambda_n}] - [(-a_1)^{\lambda_1} (-a_2)^{\lambda_2} \dots (-a_n)^{\lambda_n}]}{\lambda_1! \lambda_2! \dots \lambda_n!}$$

The terms of the sum are then clearly zero if $\lambda_1 + \lambda_2 + \dots + \lambda_n$ is even and twice the terms of the series for $U(\mathbf{r} + \mathbf{a})$ if $\lambda_1 + \lambda_2 + \dots + \lambda_n$ is odd.

The series can then be more compactly rewritten as:

$$U(\mathbf{r} + \mathbf{a}) - U(\mathbf{r} - \mathbf{a}) = 2 \sum_{\substack{\lambda_1, \dots, \lambda_n \geq 0 \\ \lambda_1 + \dots + \lambda_n \text{ odd}}} [\partial_1^{\lambda_1} \partial_2^{\lambda_2} \dots \partial_n^{\lambda_n} U](\mathbf{r}) \frac{[a_1^{\lambda_1} a_2^{\lambda_2} \dots a_n^{\lambda_n}]}{\lambda_1! \lambda_2! \dots \lambda_n!}$$

Substituting it into the time evolution equation results in:

$$\begin{aligned} \frac{\partial}{\partial t} f_W(\mathbf{r}, \mathbf{p}) + \frac{\mathbf{p}}{m^*} \cdot [\nabla_{\mathbf{r}} f_W(\mathbf{r}, \mathbf{p})] &= \\ &= \sum_i p_i \frac{1}{(\hbar\pi)^n} \int_{\Omega} \frac{2i}{\hbar} \left[\sum_{\substack{\lambda_1, \dots, \lambda_n \geq 0 \\ \lambda_1 + \dots + \lambda_n \text{ odd}}} [\partial_1^{\lambda_1} \partial_2^{\lambda_2} \dots \partial_n^{\lambda_n} U](\mathbf{r}) \frac{[a_1^{\lambda_1} a_2^{\lambda_2} \dots a_n^{\lambda_n}]}{\lambda_1! \lambda_2! \dots \lambda_n!} \right] \\ &\quad \Psi_i^*(\mathbf{r} + \mathbf{a}) \Psi_i(\mathbf{r} - \mathbf{a}) \exp \left\{ + \frac{2i}{\hbar} \mathbf{p} \cdot \mathbf{a} \right\} d\mathbf{a} \end{aligned}$$

It is now possible to observe that the powers of the components of \mathbf{a} can be rewritten by exploiting the relationship:

$$\partial_{p_j}^{\lambda_j} \left\{ \exp \left\{ + \frac{2i}{\hbar} \mathbf{p} \cdot \mathbf{a} \right\} \right\} = \left(\frac{2i}{\hbar} a_j \right)^{\lambda_j} \exp \left\{ + \frac{2i}{\hbar} \mathbf{p} \cdot \mathbf{a} \right\}$$

which can be rewritten as:

$$a_j^{\lambda_j} \exp \left\{ + \frac{2i}{\hbar} \mathbf{p} \cdot \mathbf{a} \right\} = \left(\frac{\hbar}{2i} \right)^{\lambda_j} \partial_{p_j}^{\lambda_j} \left\{ \exp \left\{ + \frac{2i}{\hbar} \mathbf{p} \cdot \mathbf{a} \right\} \right\}$$

Substituting this result in the evolution equation for all the variables of the power series gives:

$$\begin{aligned} \frac{\partial}{\partial t} f_W(\mathbf{r}, \mathbf{p}) + \frac{\mathbf{p}}{m^*} \cdot [\nabla_{\mathbf{r}} f_W(\mathbf{r}, \mathbf{p})] &= \\ &= \sum_i p_i \frac{1}{(\hbar\pi)^n} \int_{\Omega} \frac{2i}{\hbar} \left[\sum_{\substack{\lambda_1, \dots, \lambda_n \geq 0 \\ \lambda_1 + \dots + \lambda_n \text{ odd}}} [\partial_1^{\lambda_1} \partial_2^{\lambda_2} \dots \partial_n^{\lambda_n} U](\mathbf{r}) \frac{1}{\lambda_1! \lambda_2! \dots \lambda_n!} \left(\frac{\hbar}{2i} \right)^{\lambda_1 + \dots + \lambda_n} \right. \\ &\quad \left. [\partial_{p_1}^{\lambda_1} \partial_{p_2}^{\lambda_2} \dots \partial_{p_n}^{\lambda_n}] \left\{ \exp \left\{ + \frac{2i}{\hbar} \mathbf{p} \cdot \mathbf{a} \right\} \right\} \right] \Psi_i^*(\mathbf{r} + \mathbf{a}) \Psi_i(\mathbf{r} - \mathbf{a}) d\mathbf{a} \end{aligned}$$

Extracting all the terms that are not in the variable \mathbf{a} and the derivatives from the integral gives:

$$\begin{aligned} \frac{\partial}{\partial t} f_W(\mathbf{r}, \mathbf{p}) + \frac{\mathbf{p}}{m^*} \cdot [\nabla_{\mathbf{r}} f_W(\mathbf{r}, \mathbf{p})] &= \\ &= \sum_{\substack{\lambda_1, \dots, \lambda_n \geq 0 \\ \lambda_1 + \dots + \lambda_n \text{ odd}}} [\partial_1^{\lambda_1} \partial_2^{\lambda_2} \dots \partial_n^{\lambda_n} U](\mathbf{r}) \frac{1}{\lambda_1! \lambda_2! \dots \lambda_n!} \left(\frac{\hbar}{2i} \right)^{\lambda_1 + \dots + \lambda_n - 1} \partial_{p_1}^{\lambda_1} \partial_{p_2}^{\lambda_2} \dots \partial_{p_n}^{\lambda_n} \left[\sum_i p_i \frac{1}{(\hbar\pi)^n} \right. \\ &\quad \left. \int_{\Omega} \Psi_i^*(\mathbf{r} + \mathbf{a}) \Psi_i(\mathbf{r} - \mathbf{a}) \exp \left\{ + \frac{2i}{\hbar} \mathbf{p} \cdot \mathbf{a} \right\} d\mathbf{a} \right] \end{aligned}$$

Noticing that the blue term is the Wigner function and substituting it in the equation yields the final form of the evolution equation:

$$\boxed{\begin{aligned} \frac{\partial}{\partial t} f_W(\mathbf{r}, \mathbf{p}) + \frac{\mathbf{p}}{m^*} \cdot [\nabla_{\mathbf{r}} f_W(\mathbf{r}, \mathbf{p})] = \\ = \sum_{\substack{\lambda_1, \dots, \lambda_n \geq 0 \\ \lambda_1 + \dots + \lambda_n \text{ odd}}} \frac{1}{\lambda_1! \lambda_2! \dots \lambda_n!} \left(\frac{\hbar}{2i} \right)^{\lambda_1 + \dots + \lambda_n - 1} [\partial_1^{\lambda_1} \partial_2^{\lambda_2} \dots \partial_n^{\lambda_n} U(\mathbf{r})] [\partial_{p_1}^{\lambda_1} \partial_{p_2}^{\lambda_2} \dots \partial_{p_n}^{\lambda_n} f_W(\mathbf{r}, \mathbf{p})] \end{aligned}} \quad (5.2)$$

which is known as the **Wigner equation**.

5.1 Steady-State Solution

Before proceeding with the application of the method of moments to the Wigner equation to derive a simple model, it is useful to try and solve it at equilibrium and at steady state.

The usefulness of this will be evident later on when describing the density gradient model.

Under the steady-state assumption ($\partial/\partial t = 0$) the Wigner equation (Equation 5.2) becomes:

$$\frac{\mathbf{p}}{m^*} \cdot [\nabla_{\mathbf{r}} f_W(\mathbf{r}, \mathbf{p})] = \sum_{\substack{\lambda_1, \dots, \lambda_n \geq 0 \\ \lambda_1 + \dots + \lambda_n \text{ odd}}} \frac{1}{\lambda_1! \lambda_2! \dots \lambda_n!} \left(\frac{\hbar}{2i} \right)^{\lambda_1 + \dots + \lambda_n - 1} [\partial_1^{\lambda_1} \partial_2^{\lambda_2} \dots \partial_n^{\lambda_n} U(\mathbf{r})] [\partial_{p_1}^{\lambda_1} \partial_{p_2}^{\lambda_2} \dots \partial_{p_n}^{\lambda_n} f_W(\mathbf{r}, \mathbf{p})] \quad (5.3)$$

5.1.1 Simplifying Assumptions

Since the framework is that of quantum mechanics the solution to the problem is assumed to exhibit a dependency on \hbar .

It is therefore reasonable to assume a Taylor expansion of the solution f_W with respect to \hbar :

$$f_W(\mathbf{r}, \mathbf{p}) = \sum_{m=0}^{\infty} f_W^{(m)}(\mathbf{r}, \mathbf{p}) \hbar^m$$

This allows to give the solution a resemblance to the right-hand side of Equation 5.3, which is also expressed as a power series with respect to \hbar .

The terms of the solution can then be more easily determined by considering of the terms of the power series.

Since the goal is to get a first order approximation for the quantum corrections, only terms up to \hbar^2 are retained in the ansatz for the solution, therefore considering a function of the kind:

$$f_W(\mathbf{r}, \mathbf{p}) = f^{(0)}(\mathbf{r}, \mathbf{p}) + f^{(1)}(\mathbf{r}, \mathbf{p}) \hbar + f^{(2)}(\mathbf{r}, \mathbf{p}) \hbar^2$$

In the classical limit, i.e. for $\hbar \rightarrow 0$, the Wigner function must become a probability density function in phase space.

This means that $f^{(0)}(\mathbf{r}, \mathbf{p})$ has to be a classical probability density function in phase space; neglecting quantum effects on the statistics of the particles the statistics can be approximated with a Boltzmann probability density function of the kind $\exp\{-\beta E\}$ (it is not normalized, a final renormalization of the solution will therefore be necessary to obtain a unitary integral over phase space), hence:

$$f^{(0)} = \exp\{-\beta E\}$$

with $E = \frac{\mathbf{p} \cdot \mathbf{p}}{2m^*} + U$ the classical definition of energy.

The trial solution will therefore have to be of the kind:

$$f_W(\mathbf{r}, \mathbf{p}) = \exp\{-\beta E\} + f^{(1)}(\mathbf{r}, \mathbf{p}) \hbar + f^{(2)}(\mathbf{r}, \mathbf{p}) \hbar^2$$

In order to determine the remaining functions $f^{(1)}$ and $f^{(2)}$, this trial solution is then replaced within the Wigner equation at steady state (Equation 5.3), giving:

$$\begin{aligned} & \frac{\mathbf{p}}{m^*} \cdot \nabla_{\mathbf{r}} \left[\exp\{-\beta E\} + f^{(1)}(\mathbf{r}, \mathbf{p}) \hbar + f^{(2)}(\mathbf{r}, \mathbf{p}) \hbar^2 \right] \\ &= \sum_{\substack{\lambda_1, \dots, \lambda_n \geq 0 \\ \lambda_1 + \dots + \lambda_n \text{ odd}}} \frac{1}{\lambda_1! \lambda_2! \dots \lambda_n!} \left(\frac{\hbar}{2i} \right)^{\lambda_1 + \dots + \lambda_n - 1} \left[\partial_1^{\lambda_1} \partial_2^{\lambda_2} \dots \partial_n^{\lambda_n} U(\mathbf{r}) \right] \left[\partial_{p_1}^{\lambda_1} \partial_{p_2}^{\lambda_2} \dots \partial_{p_n}^{\lambda_n} f_W(\mathbf{r}, \mathbf{p}) \right] \end{aligned} \quad (5.4)$$

As all terms featuring powers of \hbar with degree higher than \hbar^2 have been neglected in the trial solution and cannot therefore appear at the left-hand side of the equation, they must be neglected also in the infinite sum on the right.

Since the exponent of \hbar is $\lambda_1 + \lambda_2 + \lambda_3 - 1$ then this means that all the terms with $\lambda_1 + \lambda_2 + \lambda_3 - 1 > 2$ must be neglected.

Hence, only terms with $\lambda_1 + \lambda_2 + \lambda_3 = 1$ and $\lambda_1 + \lambda_2 + \lambda_3 = 3$ remain (only odd values of the sum of the λ 's are allowed).

For $\lambda_1 + \lambda_2 + \lambda_3 = 1$ the possible combinations are:

- $\lambda_1 = 0 \quad \lambda_2 = 0 \quad \lambda_3 = 1$ and its permutations (3 possibilities)

For $\lambda_1 + \lambda_2 + \lambda_3 = 3$ the possible combinations are:

- $\lambda_1 = 1 \quad \lambda_2 = 1 \quad \lambda_3 = 1$ (no other permutations)
- $\lambda_1 = 0 \quad \lambda_2 = 1 \quad \lambda_3 = 2$ and its permutations (6 possibilities)
- $\lambda_1 = 0 \quad \lambda_2 = 0 \quad \lambda_3 = 3$ and its permutations (3 possibilities)

The case of $\lambda_1 = 0, \lambda_2 = 0, \lambda_3 = 1$ and permutations therefore results in the following terms of the series at the right-hand side of 5.4:

$$\sum_{k \in \{1,2,3\}} \frac{\partial U}{\partial r_k}(\mathbf{r}) \frac{\partial}{\partial p_k} \left\{ \exp\{-\beta E\} + f^{(1)}(\mathbf{r}, \mathbf{p}) \hbar + f^{(2)}(\mathbf{r}, \mathbf{p}) \hbar^2 \right\}$$

The case of $\lambda_1 = 1, \lambda_2 = 1, \lambda_3 = 1$ results in a single term:

$$\frac{\partial^3 U}{\partial r_1 \partial r_2 \partial r_3}(\mathbf{r}) \frac{\partial^3}{\partial p_1 \partial p_2 \partial p_3} \left\{ \exp\{-\beta E\} + f^{(1)}(\mathbf{r}, \mathbf{p}) \hbar + f^{(2)}(\mathbf{r}, \mathbf{p}) \hbar^2 \right\} \left(\frac{\hbar}{2i} \right)^2$$

The case of $\lambda_1 = 0, \lambda_2 = 1, \lambda_3 = 2$ and permutations yields instead the terms:

$$\sum_{\substack{k \in \{1,2,3\} \\ l \neq k}} \frac{\partial^3 U}{\partial r_k^2 \partial r_l}(\mathbf{r}) \frac{\partial^3}{\partial p_k^2 \partial p_l} \left\{ \exp\{-\beta E\} + f^{(1)}(\mathbf{r}, \mathbf{p}) \hbar + f^{(2)}(\mathbf{r}, \mathbf{p}) \hbar^2 \right\} \frac{1}{2!} \left(\frac{\hbar}{2i} \right)^2$$

(a double index is needed since first the variable for the double partial differentiation must be chosen and then, among the other two, the variable for the single differentiation must be chosen)

Finally, the case of $\lambda_1 = 0, \lambda_2 = 0, \lambda_3 = 3$ results in the terms:

$$\sum_{k \in \{1,2,3\}} \frac{\partial^3 U}{\partial r_k^3}(\mathbf{r}) \frac{\partial^3}{\partial p_k^3} \left\{ \exp\{-\beta E\} + f^{(1)}(\mathbf{r}, \mathbf{p}) \hbar + f^{(2)}(\mathbf{r}, \mathbf{p}) \hbar^2 \right\} \frac{1}{3!} \left(\frac{\hbar}{2i} \right)^2$$

Substituting the series with all of its non-negligible terms that have been introduced up to now yields:

$$\begin{aligned} & \frac{\mathbf{p}}{m^*} \cdot \nabla_{\mathbf{r}} \left[\exp\{-\beta E\} + f^{(1)}(\mathbf{r}, \mathbf{p}) \hbar + f^{(2)}(\mathbf{r}, \mathbf{p}) \hbar^2 \right] \\ &= \sum_{k \in \{1,2,3\}} \frac{\partial U}{\partial r_k}(\mathbf{r}) \frac{\partial}{\partial p_k} \left\{ \exp\{-\beta E\} + f^{(1)}(\mathbf{r}, \mathbf{p}) \hbar + f^{(2)}(\mathbf{r}, \mathbf{p}) \hbar^2 \right\} \end{aligned}$$

$$\begin{aligned}
& + \frac{\partial^3 U}{\partial r_1 \partial r_2 \partial r_3}(\mathbf{r}) \frac{\partial^3}{\partial p_1 \partial p_2 \partial p_3} \left\{ \exp\{-\beta E\} + f^{(1)}(\mathbf{r}, \mathbf{p}) \hbar + f^{(2)}(\mathbf{r}, \mathbf{p}) \hbar^2 \right\} \left(\frac{\hbar}{2i} \right)^2 \\
& + \sum_{\substack{k \in \{1,2,3\} \\ l \neq k}} \frac{\partial^3 U}{\partial r_k^2 \partial r_l}(\mathbf{r}) \frac{\partial^3}{\partial p_k^2 \partial p_l} \left\{ \exp\{-\beta E\} + f^{(1)}(\mathbf{r}, \mathbf{p}) \hbar + f^{(2)}(\mathbf{r}, \mathbf{p}) \hbar^2 \right\} \frac{1}{2!} \left(\frac{\hbar}{2i} \right)^2 \\
& + \sum_{k \in \{1,2,3\}} \frac{\partial^3 U}{\partial r_k^3}(\mathbf{r}) \frac{\partial^3}{\partial p_k^3} \left\{ \exp\{-\beta E\} + f^{(1)}(\mathbf{r}, \mathbf{p}) \hbar + f^{(2)}(\mathbf{r}, \mathbf{p}) \hbar^2 \right\} \frac{1}{3!} \left(\frac{\hbar}{2i} \right)^2
\end{aligned}$$

Splitting all the terms by linearity of the derivative operator gives:

$$\begin{aligned}
& \sum_{k \in \{1,2,3\}} \frac{p_k}{m^*} \frac{\partial}{\partial r_k} \left\{ \exp\{-\beta E\} \right\} + \sum_{k \in \{1,2,3\}} \frac{p_k}{m^*} \frac{\partial}{\partial r_k} \left\{ f^{(1)} \hbar \right\} + \sum_{k \in \{1,2,3\}} \frac{p_k}{m^*} \frac{\partial}{\partial r_k} \left\{ f^{(2)} \hbar^2 \right\} \\
= & \sum_{k \in \{1,2,3\}} \frac{\partial U}{\partial r_k} \frac{\partial}{\partial p_k} \left\{ \exp\{-\beta E\} \right\} + \sum_{k \in \{1,2,3\}} \frac{\partial U}{\partial r_k} \frac{\partial}{\partial p_k} \left\{ f^{(1)} \hbar \right\} + \sum_{k \in \{1,2,3\}} \frac{\partial U}{\partial r_k} \frac{\partial}{\partial p_k} \left\{ f^{(2)} \hbar^2 \right\} \\
& + \frac{\partial^3 U}{\partial r_1 \partial r_2 \partial r_3} \frac{\partial^3}{\partial p_1 \partial p_2 \partial p_3} \left\{ \exp\{-\beta E\} \right\} \left(\frac{\hbar}{2i} \right)^2 + \frac{\partial^3 U}{\partial r_1 \partial r_2 \partial r_3} \frac{\partial^3}{\partial p_1 \partial p_2 \partial p_3} \left\{ f^{(1)} \hbar \right\} \left(\frac{\hbar}{2i} \right)^2 \\
& + \frac{\partial^3 U}{\partial r_1 \partial r_2 \partial r_3} \frac{\partial^3}{\partial p_1 \partial p_2 \partial p_3} \left\{ f^{(2)} \hbar^2 \right\} \left(\frac{\hbar}{2i} \right)^2 + \sum_{\substack{k \in \{1,2,3\} \\ l \neq k}} \frac{\partial^3 U}{\partial r_k^2 \partial r_l} \frac{\partial^3}{\partial p_k^2 \partial p_l} \left\{ \exp\{-\beta E\} \right\} \frac{1}{2!} \left(\frac{\hbar}{2i} \right)^2 \\
& + \sum_{\substack{k \in \{1,2,3\} \\ l \neq k}} \frac{\partial^3 U}{\partial r_k^2 \partial r_l} \frac{\partial^3}{\partial p_k^2 \partial p_l} \left\{ f^{(1)} \hbar \right\} \frac{1}{2!} \left(\frac{\hbar}{2i} \right)^2 + \sum_{\substack{k \in \{1,2,3\} \\ l \neq k}} \frac{\partial^3 U}{\partial r_k^2 \partial r_l} \frac{\partial^3}{\partial p_k^2 \partial p_l} \left\{ \hbar + f^{(2)} \hbar^2 \right\} \frac{1}{2!} \left(\frac{\hbar}{2i} \right)^2 \\
& + \sum_{k \in \{1,2,3\}} \frac{\partial^3 U}{\partial r_k^3} \frac{\partial^3}{\partial p_k^3} \left\{ \exp\{-\beta E\} \right\} \frac{1}{3!} \left(\frac{\hbar}{2i} \right)^2 + \sum_{k \in \{1,2,3\}} \frac{\partial^3 U}{\partial r_k^3} \frac{\partial^3}{\partial p_k^3} \left\{ f^{(1)} \hbar \right\} \frac{1}{3!} \left(\frac{\hbar}{2i} \right)^2 \\
& + \sum_{k \in \{1,2,3\}} \frac{\partial^3 U}{\partial r_k^3} \frac{\partial^3}{\partial p_k^3} \left\{ f^{(2)} \hbar^2 \right\} \frac{1}{3!} \left(\frac{\hbar}{2i} \right)^2
\end{aligned}$$

Under the approximation of neglecting all the terms involving powers of \hbar higher than \hbar^2 , only the terms that are highlighted in the previous equation remain, giving:

$$\begin{aligned}
& \sum_{k \in \{1,2,3\}} \frac{p_k}{m^*} \frac{\partial}{\partial r_k} \left\{ \exp\{-\beta E\} \right\} + \sum_{k \in \{1,2,3\}} \frac{p_k}{m^*} \frac{\partial}{\partial r_k} \left\{ f^{(1)} \hbar \right\} + \sum_{k \in \{1,2,3\}} \frac{p_k}{m^*} \frac{\partial}{\partial r_k} \left\{ f^{(2)} \hbar^2 \right\} \\
= & \sum_{k \in \{1,2,3\}} \frac{\partial U}{\partial r_k} \frac{\partial}{\partial p_k} \left\{ \exp\{-\beta E\} \right\} + \sum_{k \in \{1,2,3\}} \frac{\partial U}{\partial r_k} \frac{\partial}{\partial p_k} \left\{ f^{(1)} \hbar \right\} + \sum_{k \in \{1,2,3\}} \frac{\partial U}{\partial r_k} \frac{\partial}{\partial p_k} \left\{ f^{(2)} \hbar^2 \right\} \\
& + \frac{\partial^3 U}{\partial r_1 \partial r_2 \partial r_3} \frac{\partial^3}{\partial p_1 \partial p_2 \partial p_3} \left\{ \exp\{-\beta E\} \right\} \left(\frac{\hbar}{2i} \right)^2 + \sum_{\substack{k \in \{1,2,3\} \\ l \neq k}} \frac{\partial^3 U}{\partial r_k^2 \partial r_l} \frac{\partial^3}{\partial p_k^2 \partial p_l} \left\{ \exp\{-\beta E\} \right\} \frac{1}{2!} \left(\frac{\hbar}{2i} \right)^2 \\
& + \sum_{k \in \{1,2,3\}} \frac{\partial^3 U}{\partial r_k^3} \frac{\partial^3}{\partial p_k^3} \left\{ \exp\{-\beta E\} \right\} \frac{1}{3!} \left(\frac{\hbar}{2i} \right)^2
\end{aligned}$$

The next step is then to compare the coefficients of all the powers of \hbar . Doing this results in a set of three partial differential equations:

- comparing terms of order zero in \hbar yields:

$$\sum_{k \in \{1,2,3\}} \frac{p_k}{m^*} \frac{\partial}{\partial r_k} \left\{ \exp\{-\beta E\} \right\} = \sum_{k \in \{1,2,3\}} \frac{\partial U}{\partial r_k} \frac{\partial}{\partial p_k} \left\{ \exp\{-\beta E\} \right\}$$

- comparing terms of order one in \hbar yields:

$$\sum_{k \in \{1,2,3\}} \frac{p_k}{m^*} \frac{\partial}{\partial r_k} \left\{ f^{(1)} \right\} = \sum_{k \in \{1,2,3\}} \frac{\partial U}{\partial r_k} \frac{\partial}{\partial p_k} \left\{ f^{(1)} \right\}$$

- comparing terms of order two in \hbar yields:

$$\begin{aligned}
& \sum_{k \in \{1,2,3\}} \frac{p_k}{m^*} \frac{\partial}{\partial r_k} \left\{ f^{(2)} \right\} = \\
& = \sum_{k \in \{1,2,3\}} \frac{\partial U}{\partial r_k} \frac{\partial}{\partial p_k} \left\{ f^{(2)} \right\} + \frac{\partial^3 U}{\partial r_1 \partial r_2 \partial r_3} \frac{\partial^3}{\partial p_1 \partial p_2 \partial p_3} \left\{ \exp\{-\beta E\} \right\} \left(\frac{1}{2i} \right)^2 \\
& + \sum_{\substack{k \in \{1,2,3\} \\ l \neq k}} \frac{\partial^3 U}{\partial r_k^2 \partial r_l} \frac{\partial^3}{\partial p_k^2 \partial p_l} \left\{ \exp\{-\beta E\} \right\} \frac{1}{2!} \left(\frac{1}{2i} \right)^2 + \sum_{k \in \{1,2,3\}} \frac{\partial^3 U}{\partial r_k^3} \frac{\partial^3}{\partial p_k^3} \left\{ \exp\{-\beta E\} \right\} \frac{1}{3!} \left(\frac{1}{2i} \right)^2
\end{aligned}$$

5.1.2 Solution Method

The solution method that will be proposed here is inspired to the work of Eugene Wigner. [15]

The 1st equation, deriving from the comparison of the terms without \hbar , becomes an identity when substituting the classical definition $E = \frac{\mathbf{p} \cdot \mathbf{p}}{2m^*} + U$ of the energy:

$$\sum_{k \in \{1,2,3\}} \frac{p_k}{m^*} \frac{\partial U}{\partial r_k} \exp\{-\beta E\} \equiv \sum_{k \in \{1,2,3\}} \frac{\partial U}{\partial r_k} \frac{p_k}{m^*} \exp\{-\beta E\}$$

This simply confirms that $\exp\{-\beta E\}$ is the classical limit of the Wigner function.

As the 2nd equation accepts the trivial solution (due to the absence of any forcing term in the equation).

Therefore, the function $f^{(1)}$ is taken to be:

$$f^{(1)} = 0$$

For the 3rd equation the first step is instead to evaluate the derivatives of the exponentials and the numeric constants, obtaining:

$$\sum_{k \in \{1,2,3\}} \frac{p_k}{m^*} \frac{\partial f^{(2)}}{\partial r_k} = \tag{5.5}$$

$$= \sum_{k \in \{1,2,3\}} \frac{\partial U}{\partial r_k} \frac{\partial f^{(2)}}{\partial p_k} + \frac{1}{4} \frac{\partial^3 U}{\partial r_1 \partial r_2 \partial r_3} \frac{\beta^3}{(m^*)^3} p_1 p_2 p_3 \exp\{-\beta E\} \tag{5.6}$$

$$+ \frac{1}{8} \sum_{\substack{k \in \{1,2,3\} \\ l \neq k}} \frac{\partial^3 U}{\partial r_k^2 \partial r_l} \left(\frac{\beta^3}{(m^*)^3} p_k^2 p_l - \frac{\beta^2}{(m^*)^2} p_l \right) \exp\{-\beta E\} \tag{5.7}$$

$$+ \frac{1}{24} \sum_{k \in \{1,2,3\}} \frac{\partial^3 U}{\partial r_k^3} \left(-\frac{\beta^2}{(m^*)^2} 3 p_k + \frac{\beta^3}{(m^*)^3} p_k^3 \right) \exp\{-\beta E\} \tag{5.8}$$

Recalling that E is quadratic in $|p|$ multiple derivatives of the exponential in the same variable must be treated using the product rule, hence:

$$\begin{aligned}
\frac{\partial^2}{\partial p_k^2} \left\{ \exp\{-\beta E\} \right\} &= -\beta \frac{1}{m^*} \exp\{-\beta E\} + \beta^2 \frac{p_k^2}{(m^*)^2} \exp\{-\beta E\} \\
\frac{\partial^3}{\partial p_k^3} \left\{ \exp\{-\beta E\} \right\} &= 3\beta^2 \frac{p_k}{(m^*)^2} \exp\{-\beta E\} - \beta^3 \frac{p_k^3}{(m^*)^3} \exp\{-\beta E\}
\end{aligned}$$

Since the first part of equation Equation 5.8:

$$\sum_{k \in \{1,2,3\}} \frac{p_k}{m^*} \frac{\partial f^{(2)}}{\partial r_k} = \sum_{k \in \{1,2,3\}} \frac{\partial U}{\partial r_k} \frac{\partial f^{(2)}}{\partial p_k} + (\dots) \exp\{-\beta E\}$$

is exactly the same as the 1st equation and all of the additional terms are multiplied by $\exp\{-\beta E\}$, it is reasonable to look for a solution of the kind:

$$f^{(2)} = \exp\{-\beta E\} g^{(2)}$$

In fact, when differentiated by the product rule it will yield both the terms of the 1st equation (which will cancel out) and additional terms involving $\exp\{-\beta E\}$:

$$\begin{aligned} g^{(2)} \sum_{k \in \{1,2,3\}} \frac{p_k}{m^*} \frac{\partial}{\partial r_k} \{\exp\{-\beta E\}\} + \exp\{-\beta E\} \sum_{k \in \{1,2,3\}} \frac{p_k}{m^*} \frac{\partial g^{(2)}}{\partial r_k} = \\ = g^{(2)} \sum_{k \in \{1,2,3\}} \frac{\partial U}{\partial r_k} \frac{\partial}{\partial p_k} \{\exp\{-\beta E\}\} + \sum_{k \in \{1,2,3\}} \frac{\partial U}{\partial r_k} \frac{\partial g^{(2)}}{\partial p_k} \exp\{-\beta E\} \\ + \frac{1}{4} \frac{\partial^3 U}{\partial r_1 \partial r_2 \partial r_3} \frac{\beta^3}{(m^*)^3} p_1 p_2 p_3 \exp\{-\beta E\} \\ + \frac{1}{8} \sum_{\substack{k \in \{1,2,3\} \\ l \neq k}} \frac{\partial^3 U}{\partial r_k^2 \partial r_l} \left(\frac{\beta^3}{(m^*)^3} p_k^2 p_l - \frac{\beta^2}{(m^*)^2} p_l \right) \exp\{-\beta E\} \\ + \frac{1}{24} \sum_{k \in \{1,2,3\}} \frac{\partial^3 U}{\partial r_k^3} \left(-\frac{\beta^2}{(m^*)^2} 3 p_k + \frac{\beta^3}{(m^*)^3} p_k^3 \right) \exp\{-\beta E\} \end{aligned}$$

After cancelling out the terms similar to those of the 1st equation the remaining equation is:

$$\begin{aligned} \exp\{-\beta E\} \sum_{k \in \{1,2,3\}} \frac{p_k}{m^*} \frac{\partial g^{(2)}}{\partial r_k} = \exp\{-\beta E\} \sum_{k \in \{1,2,3\}} \frac{\partial U}{\partial r_k} \frac{\partial g^{(2)}}{\partial p_k} + \underbrace{\frac{1}{4} \frac{\partial^3 U}{\partial r_1 \partial r_2 \partial r_3} \frac{\beta^3}{(m^*)^3} p_1 p_2 p_3 \exp\{-\beta E\}}_{(a)} \\ + \underbrace{\frac{1}{8} \sum_{\substack{k \in \{1,2,3\} \\ l \neq k}} \frac{\partial^3 U}{\partial r_k^2 \partial r_l} \frac{\beta^3}{(m^*)^3} p_k^2 p_l \exp\{-\beta E\}}_{(b)} + \underbrace{\frac{1}{24} \sum_{k \in \{1,2,3\}} \frac{\partial^3 U}{\partial r_k^3} \frac{\beta^3}{(m^*)^3} p_k^3 \exp\{-\beta E\}}_{(c)} \\ - \underbrace{\frac{1}{8} \sum_{\substack{k \in \{1,2,3\} \\ l \neq k}} \frac{\partial^3 U}{\partial r_k^2 \partial r_l} \frac{\beta^2}{(m^*)^2} p_l \exp\{-\beta E\}}_{(d)} - \underbrace{\frac{1}{8} \sum_{k \in \{1,2,3\}} \frac{\partial^3 U}{\partial r_k^3} \frac{\beta^2}{(m^*)^2} p_k \exp\{-\beta E\}}_{(e)} \end{aligned}$$

The blue term is the only one that can generate the spatial derivatives of the potential that are present in the forcing terms. Therefore, such derivatives must be built by tailoring the solution so that it spawns them when inserted in this term.

A possible solution method is to start from terms (a), (b) and (c) and try to build them one step at a time, then refining the solution to make it work.

In order for the blue term to yield triple derivatives of the potential with respect to the position, $g^{(2)}$ must include two additional differentiations in two possible spatial coordinates r_q and r_z so that:

- when $z = q = k$ a derivative of the kind of that in term (c) is generated
- when $z \neq q = k$ or $k \neq z = q$ or $q \neq z = k$ then a derivative of the kind of those in term (b) is generated
- when $z \neq q \neq k$ then a derivative of the kind of those in term (a) is generated

The coefficient in front must be the smallest one to be able to reproduce also the terms with a 1/24 coefficient. Then the first term of the solution must be:

$$g^{(2)} = \frac{1}{24} \sum_{\substack{q \in \{1,2,3\} \\ m \in \{1,2,3\}}} \frac{\partial^2 U}{\partial r_q \partial r_m} \frac{\beta^3}{(m^*)^3} p_q p_m + \dots$$

A brief combinatorial analysis immediately shows that plugging this first part of $g^{(2)}$ into the blue term:

$$\exp\{-\beta E\} \sum_{k \in \{1,2,3\}} \frac{p_k}{m^*} \frac{\partial}{\partial r_k} \left\{ \frac{1}{24} \sum_{\substack{q \in \{1,2,3\} \\ m \in \{1,2,3\}}} \frac{\partial^2 U}{\partial r_q \partial r_m} \frac{\beta^3}{(m^*)^2} p_q p_m \right\}$$

is able to generate:

- term (a) for a total of 6 times
- each term of (b) for a total of 4 times
- each term of (c) only once

therefore giving the wanted terms as:

$$\begin{aligned} & \exp\{-\beta E\} \sum_{k \in \{1,2,3\}} \frac{p_k}{m^*} \frac{\partial}{\partial r_k} \left\{ \frac{1}{24} \sum_{\substack{q \in \{1,2,3\} \\ m \in \{1,2,3\}}} \frac{\partial^2 U}{\partial r_q \partial r_m} \frac{\beta^3}{(m^*)^3} p_q p_m \right\} \\ &= \underbrace{\frac{1}{4} \frac{\partial^3 U}{\partial r_1 \partial r_2 \partial r_3} \frac{\beta^3}{(m^*)^3} p_1 p_2 p_3 \exp\{-\beta E\}}_{(a)} \\ & \quad + \underbrace{\frac{1}{8} \sum_{\substack{k \in \{1,2,3\} \\ l \neq k}} \frac{\partial^3 U}{\partial r_k^2 \partial r_l} \frac{\beta^3}{(m^*)^3} p_k^2 p_l \exp\{-\beta E\}}_{(b)} + \underbrace{\frac{1}{24} \sum_{k \in \{1,2,3\}} \frac{\partial^3 U}{\partial r_k^3} \frac{\beta^3}{(m^*)^2} p_k^3 \exp\{-\beta E\}}_{(c)} \end{aligned}$$

However, when plugging this first guess into the red term, also unwanted terms appear in the equation, as:

$$\begin{aligned} & \exp\{-\beta E\} \sum_{k \in \{1,2,3\}} \frac{\partial U}{\partial r_k} \frac{\partial}{\partial p_k} \left\{ \frac{1}{24} \sum_{\substack{q \in \{1,2,3\} \\ m \in \{1,2,3\}}} \frac{\partial^2 U}{\partial r_q \partial r_m} \frac{\beta^3}{(m^*)^2} p_q p_m \right\} \\ &= \frac{1}{24} \exp\{-\beta E\} \sum_{\substack{q \in \{1,2,3\} \\ m \in \{1,2,3\} \\ k \in \{1,2,3\}}} \frac{\partial U}{\partial r_k} \frac{\partial^2 U}{\partial r_q \partial r_m} \frac{\beta^3}{(m^*)^2} \frac{\partial}{\partial p_k} \{p_q p_m\} \end{aligned}$$

In order for this term not to be zero, either $m = k$ or $q = k$ or $q = k = m$ must be true. Splitting then the case of $q \neq m$ from the case of $q = m$ the expression becomes:

$$\begin{aligned} &= \frac{1}{24} \exp\{-\beta E\} \sum_{m \in \{1,2,3\}} \frac{\partial U}{\partial r_m} \frac{\partial^2 U}{\partial r_m^2} \frac{\beta^3}{(m^*)^2} \frac{\partial}{\partial p_m} \{p_m^2\} \\ & \quad + \frac{1}{24} \exp\{-\beta E\} 2 \sum_{\substack{m \in \{1,2,3\} \\ k \in \{1,2,3\} \\ m \neq k}} \frac{\partial U}{\partial r_k} \frac{\partial^2 U}{\partial r_k \partial r_m} \frac{\beta^3}{(m^*)^2} \frac{\partial}{\partial p_k} \{p_m p_k\} \end{aligned}$$

where the factor 2 has been added in the second term to account for the two possible ways in which k can be equal to either m or q .

Solving the derivatives yields:

$$= \frac{1}{24} \exp\{-\beta E\} \sum_{m \in \{1,2,3\}} \frac{\partial U}{\partial r_k} \frac{\partial^2 U}{\partial r_m^2} \frac{\beta^3}{(m^*)^2} \cdot 2 p_m$$

$$+ \frac{1}{24} \exp\{-\beta E\} \sum_{\substack{m \in \{1,2,3\} \\ k \in \{1,2,3\} \\ m \neq k}} \frac{\partial U}{\partial r_k} \frac{\partial^2 U}{\partial r_k \partial r_m} \frac{\beta^3}{(m^*)^2} 2 p_m$$

Then, the two terms can be collected by merging the case of $m = k$ with the case of $m \neq k$ as:

$$= \frac{1}{24} \exp\{-\beta E\} \sum_{\substack{m \in \{1,2,3\} \\ k \in \{1,2,3\}}} \frac{\partial U}{\partial r_k} \frac{\partial^2 U}{\partial r_k \partial r_m} \frac{\beta^3}{(m^*)^2} 2 p_m$$

This term can be rewritten by exploiting the chain rule as:

$$= \frac{1}{24} \exp\{-\beta E\} \sum_{\substack{m \in \{1,2,3\} \\ k \in \{1,2,3\}}} \frac{\beta^3}{(m^*)^2} p_m \frac{\partial}{\partial r_k} \left\{ \left(\frac{\partial U}{\partial r_m} \right)^2 \right\}$$

This term is unwanted and must therefore be compensated through the addition of a further term to the solution that is being built.

The **blue term** can again be exploited for this, as it is quite similar to the term that must be introduced to compensate it; then the solution becomes:

$$g^{(2)} = \frac{1}{24} \sum_{\substack{q \in \{1,2,3\} \\ m \in \{1,2,3\}}} \frac{\partial^2 U}{\partial r_q \partial r_m} \frac{\beta^3}{(m^*)^2} p_q p_m + \underbrace{\frac{1}{24} \sum_{q \in \{1,2,3\}} \left(\frac{\partial U}{\partial r_q} \right)^2 \frac{\beta^3}{m^*}}_{\text{added term}} + \dots$$

It is clear that, being the term that was added independent from the momentum, it will not generate any additional terms when plugged in the **red term**. Therefore, it behaves exactly as the compensation term that was needed.

Now that terms (a), (b) and (c) have successfully been compensated, terms (d) and (e) must be compensated as well. Also for this terms, the compensation is more conveniently performed by exploiting the **blue term**.

The first step consists in rewriting **terms (d) and (e)** into a unique double sum:

$$\begin{aligned} & - \frac{1}{8} \underbrace{\sum_{\substack{k \in \{1,2,3\} \\ l \neq k}} \frac{\partial^3 U}{\partial r_k^2 \partial r_l} \frac{\beta^2}{(m^*)^2} p_l \exp\{-\beta E\}}_{\text{(d)}} - \frac{1}{8} \underbrace{\sum_{k \in \{1,2,3\}} \frac{\partial^3 U}{\partial r_k^3} \frac{\beta^2}{(m^*)^2} p_k \exp\{-\beta E\}}_{\text{(e)}} \\ & = - \frac{1}{8} \sum_{\substack{k \in \{1,2,3\} \\ l \in \{1,2,3\}}} \frac{\partial^3 U}{\partial r_k^2 \partial r_l} \frac{\beta^2}{(m^*)^2} p_l \exp\{-\beta E\} \end{aligned}$$

Swapping the names of the indexes and renaming l with q gives:

$$= - \frac{1}{8} \sum_{\substack{k \in \{1,2,3\} \\ q \in \{1,2,3\}}} \frac{\partial^3 U}{\partial r_q^2 \partial r_k} \frac{\beta^2}{(m^*)^2} p_k \exp\{-\beta E\}$$

This term can be generated by the **blue term** by including in the solution that is being built a term:

$$g^{(2)} = \frac{1}{24} \sum_{\substack{q \in \{1,2,3\} \\ m \in \{1,2,3\}}} \frac{\partial^2 U}{\partial r_q \partial r_m} \frac{\beta^3}{(m^*)^2} p_q p_m + \frac{1}{24} \sum_{q \in \{1,2,3\}} \left(\frac{\partial U}{\partial r_q} \right)^2 \frac{\beta^3}{m^*} - \underbrace{\frac{1}{8} \sum_{q \in \{1,2,3\}} \left(\frac{\partial^2 U}{\partial r_q^2} \right) \frac{\beta^2}{m^*}}_{\text{added term}}$$

The added term does not introduce any spurious term when plugged into the **red term** since it does not depend on the momentum.

Since this solution is able to yield all the forcing terms (a), (b), (c), (d), (e) without any spurious components it can be considered as definitive and be substituted into the expression for $f^{(2)}$, giving:

$$f^{(2)} = \exp\{-\beta E\} \left[\frac{1}{24} \sum_{\substack{q \in \{1,2,3\} \\ m \in \{1,2,3\}}} \frac{\partial^2 U}{\partial r_q \partial r_m} \frac{\beta^3}{(m^*)^2} p_q p_m + \frac{1}{24} \sum_{q \in \{1,2,3\}} \left(\frac{\partial U}{\partial r_q} \right)^2 \frac{\beta^3}{m^*} - \frac{1}{8} \sum_{q \in \{1,2,3\}} \left(\frac{\partial^2 U}{\partial r_q^2} \right) \frac{\beta^2}{m^*} \right] \quad (5.9)$$

Substituting it into the initial second order power series in \hbar ansatz for the Wigner function leads to:

$$f_W = \exp\{-\beta E\} \left[1 + \frac{\hbar^2}{24} \sum_{\substack{q \in \{1,2,3\} \\ m \in \{1,2,3\}}} \frac{\partial^2 U}{\partial r_q \partial r_m} \frac{\beta^3}{(m^*)^2} p_q p_m + \frac{\hbar^2}{24} \sum_{q \in \{1,2,3\}} \left(\frac{\partial U}{\partial r_q} \right)^2 \frac{\beta^3}{m^*} - \frac{\hbar^2}{8} \sum_{q \in \{1,2,3\}} \left(\frac{\partial^2 U}{\partial r_q^2} \right) \frac{\beta^2}{m^*} \right] \quad (5.10)$$

Equation 5.10 is the steady state (/equilibrium) solution to the Wigner equation, as can be verified by substituting it into the Wigner function and neglecting all the powers of \hbar of degree higher than 2.

Chapter 6

Moments of the Wigner Equation

The Wigner equation (Equation 5.2) is quite a challenging equation to be solved, either analytically or numerically.

Simpler models (hydrodynamic models) can however be derived from the Wigner equation by taking its statistical moments.

Taking the k^{th} order statistical moment of an equation means:

1. multiplying both sides of the equation by the tensor \mathbf{p}^k , where \mathbf{p} is the momentum vector and its "power" is defined as the tensor product:

$$\mathbf{p}^k = \underbrace{\mathbf{p} \otimes \mathbf{p} \otimes \cdots \otimes \mathbf{p}}_{k \text{ times}}$$

where it is understood that $\mathbf{p}^0 = 1$ and $\mathbf{p}^1 = \mathbf{p}$

2. integrating $\int_{\Omega_{\mathbf{p}}} \bullet d\mathbf{p}$ over the momentum space both sides of the equation

This procedure will be applied here to obtain the moments of order 0 and 1 of the Wigner equation.

As the Wigner equation is similar to the semiclassical Boltzmann transport equation, the treatment will be carried out in analogy with [2] [16]

6.1 0th Order Moment

In a 3-dimensional vector space the Wigner equation takes the form:

$$\begin{aligned} \frac{\partial}{\partial t} f_W(\mathbf{r}, \mathbf{p}) + \frac{\mathbf{p}}{m^*} \cdot [\nabla_{\mathbf{r}} f_W(\mathbf{r}, \mathbf{p})] &= \\ &= \sum_{\substack{\lambda_1, \dots, \lambda_n \geq 0 \\ \lambda_1 + \dots + \lambda_n \text{ odd}}} \frac{1}{\lambda_1! \lambda_2! \lambda_3!} \left(\frac{\hbar}{2i} \right)^{\lambda_1 + \lambda_2 + \lambda_3 - 1} [\partial_1^{\lambda_1} \partial_2^{\lambda_2} \partial_3^{\lambda_3} U(\mathbf{r})] [\partial_{p_1}^{\lambda_1} \partial_{p_2}^{\lambda_2} \partial_{p_3}^{\lambda_3} f_W(\mathbf{r}, \mathbf{p})] \end{aligned}$$

Integrating it over the momentum space yields:

$$\begin{aligned} \int_{\Omega_{\mathbf{p}}} \frac{\partial}{\partial t} f_W(\mathbf{r}, \mathbf{p}) d\mathbf{p} + \int_{\Omega_{\mathbf{p}}} \frac{\mathbf{p}}{m^*} \cdot [\nabla_{\mathbf{r}} f_W(\mathbf{r}, \mathbf{p})] d\mathbf{p} &= \\ &= \int_{\Omega_{\mathbf{p}}} \sum_{\substack{\lambda_1, \dots, \lambda_n \geq 0 \\ \lambda_1 + \dots + \lambda_n \text{ odd}}} \frac{1}{\lambda_1! \lambda_2! \lambda_3!} \left(\frac{\hbar}{2i} \right)^{\lambda_1 + \lambda_2 + \lambda_3 - 1} [\partial_1^{\lambda_1} \partial_2^{\lambda_2} \partial_3^{\lambda_3} U(\mathbf{r})] [\partial_{p_1}^{\lambda_1} \partial_{p_2}^{\lambda_2} \partial_{p_3}^{\lambda_3} f_W(\mathbf{r}, \mathbf{p})] d\mathbf{p} \end{aligned}$$

Considering the 3rd term first, assuming at least one derivative $\partial_{p_m}^{\lambda_m}$ with respect to a component of the momentum to have order $\lambda_m \geq 1$ then:

$$\int_{\Omega_{\mathbf{p}}} \sum_{\substack{\lambda_1, \dots, \lambda_n \geq 0 \\ \lambda_1 + \dots + \lambda_n \text{ odd}}} \frac{1}{\lambda_1! \lambda_2! \lambda_3!} \left(\frac{\hbar}{2i} \right)^{\lambda_1 + \lambda_2 + \lambda_3 - 1} [\partial_1^{\lambda_1} \partial_2^{\lambda_2} \partial_3^{\lambda_3} U(\mathbf{r})] [\partial_{p_1}^{\lambda_1} \partial_{p_2}^{\lambda_2} \partial_{p_3}^{\lambda_3} f_W(\mathbf{r}, \mathbf{p})] d\mathbf{p}$$

$$= [\partial_1^{\lambda_1} \partial_2^{\lambda_2} \partial_3^{\lambda_3} U(\mathbf{r})] \sum_{\substack{\lambda_1, \dots, \lambda_n \geq 0 \\ \lambda_1 + \dots + \lambda_n \text{ odd}}} \frac{1}{\lambda_1! \lambda_2! \lambda_3!} \left(\frac{\hbar}{2i} \right)^{\lambda_1 + \lambda_2 + \lambda_3 - 1} \\ \int_{-\infty}^{+\infty} \partial_{p_k}^{\lambda_k} \int_{-\infty}^{+\infty} \partial_{p_l}^{\lambda_l} \int_{-\infty}^{+\infty} \partial_{p_m}^{\lambda_m} f_W(\mathbf{r}, \mathbf{p}) dp_m dp_l dp_k$$

(with $l \neq k \neq m$) which results in the differentiation and integration of the Wigner function or one of its derivatives evaluated as $[\bullet]_{p_m \rightarrow -\infty}^{p_m \rightarrow +\infty}$ as :

$$= [\partial_1^{\lambda_1} \partial_2^{\lambda_2} \partial_3^{\lambda_3} U(\mathbf{r})] \sum_{\substack{\lambda_1, \dots, \lambda_n \geq 0 \\ \lambda_1 + \dots + \lambda_n \text{ odd}}} \frac{1}{\lambda_1! \lambda_2! \lambda_3!} \left(\frac{\hbar}{2i} \right)^{\lambda_1 + \lambda_2 + \lambda_3 - 1} \\ \int_{-\infty}^{+\infty} \partial_{p_k}^{\lambda_k} \int_{-\infty}^{+\infty} \partial_{p_l}^{\lambda_l} \left[\partial_{p_m}^{\lambda_m - 1} f_W(\mathbf{r}, \mathbf{p}) \right]_{p_m \rightarrow -\infty}^{p_m \rightarrow +\infty} dp_l dp_k$$

Assuming the quasi-probability density function to go to zero for infinite values of either momentum yields that the overall result must be zero.

The remaining case of all derivatives having order zero does not need to be taken into account because the sum $\lambda_1 + \lambda_2 + \lambda_3$ would be even, giving a term that is not part of the infinite series.

Therefore:

$$\int_{\Omega_{\mathbf{p}}} \sum_{\substack{\lambda_1, \dots, \lambda_n \geq 0 \\ \lambda_1 + \dots + \lambda_n \text{ odd}}} \frac{1}{\lambda_1! \lambda_2! \lambda_3!} \left(\frac{\hbar}{2i} \right)^{\lambda_1 + \lambda_2 + \lambda_3 - 1} [\partial_1^{\lambda_1} \partial_2^{\lambda_2} \partial_3^{\lambda_3} U(\mathbf{r})] [\partial_{p_1}^{\lambda_1} \partial_{p_2}^{\lambda_2} \partial_{p_3}^{\lambda_3} f_W(\mathbf{r}, \mathbf{p})] d\mathbf{p} = 0$$

The **2nd** term can instead be rewritten as:

$$\int_{\Omega_{\mathbf{p}}} \frac{\mathbf{p}}{m^*} \cdot [\nabla_{\mathbf{r}} f_W(\mathbf{r}, \mathbf{p})] d\mathbf{p} = \int_{\Omega_{\mathbf{p}}} \left[\frac{p_1}{m^*} \frac{\partial f_W}{\partial r_1}(\mathbf{r}, \mathbf{p}) + \frac{p_2}{m^*} \frac{\partial f_W}{\partial r_2}(\mathbf{r}, \mathbf{p}) + \frac{p_3}{m^*} \frac{\partial f_W}{\partial r_3}(\mathbf{r}, \mathbf{p}) \right] d\mathbf{p} \\ = \int_{\Omega_{\mathbf{p}}} \frac{p_1}{m^*} \frac{\partial f_W}{\partial r_1}(\mathbf{r}, \mathbf{p}) d\mathbf{p} + \int_{\Omega_{\mathbf{p}}} \frac{p_2}{m^*} \frac{\partial f_W}{\partial r_2}(\mathbf{r}, \mathbf{p}) d\mathbf{p} + \int_{\Omega_{\mathbf{p}}} \frac{p_3}{m^*} \frac{\partial f_W}{\partial r_3}(\mathbf{r}, \mathbf{p}) d\mathbf{p} \\ = \frac{\partial}{\partial r_1} \int_{\Omega_{\mathbf{p}}} \frac{p_1}{m^*} f_W(\mathbf{r}, \mathbf{p}) d\mathbf{p} + \frac{\partial}{\partial r_2} \int_{\Omega_{\mathbf{p}}} \frac{p_2}{m^*} f_W(\mathbf{r}, \mathbf{p}) d\mathbf{p} + \frac{\partial}{\partial r_3} \int_{\Omega_{\mathbf{p}}} \frac{p_3}{m^*} f_W(\mathbf{r}, \mathbf{p}) d\mathbf{p} \\ = \nabla_{\mathbf{r}} \cdot \int_{\Omega_{\mathbf{p}}} \frac{\mathbf{p}}{m^*} f_W(\mathbf{r}, \mathbf{p}) d\mathbf{p}$$

which recognizing the expression of $\bar{n}(\mathbf{r}) \bar{\mathbf{p}}(\mathbf{r})$ of the Wigner function can be rewritten as:

$$= \frac{1}{m^*} \nabla_{\mathbf{r}} \cdot \{ \bar{n}(\mathbf{r}) \bar{\mathbf{p}}(\mathbf{r}) \}$$

Finally, the **1st** term can be rewritten as:

$$\int_{\Omega_{\mathbf{p}}} \frac{\partial}{\partial t} f_W(\mathbf{r}, \mathbf{p}) d\mathbf{p} = \frac{\partial}{\partial t} \int_{\Omega_{\mathbf{p}}} f_W(\mathbf{r}, \mathbf{p}) d\mathbf{p} \\ = \frac{\partial}{\partial t} \{ \bar{n}(\mathbf{r}) \}$$

Substituting these three terms into the integrated Wigner function yields:

$$\frac{\partial}{\partial t} \{ \bar{n}(\mathbf{r}) \} + \frac{1}{m^*} \nabla_{\mathbf{r}} \cdot \{ \bar{n}(\mathbf{r}) \bar{\mathbf{p}}(\mathbf{r}) \} = 0 \quad (6.1)$$

Introducing the average velocity $\bar{\mathbf{v}}(\mathbf{r})$ so that $\bar{\mathbf{p}}(\mathbf{r}) = m^* \bar{\mathbf{v}}(\mathbf{r})$ then:

$$\frac{\partial}{\partial t} \{\bar{n}(\mathbf{r})\} + \nabla_{\mathbf{r}} \cdot \{\bar{n}(\mathbf{r}) \bar{\mathbf{v}}(\mathbf{r})\} = 0 \quad (6.2)$$

Since the probability current density is given by:

$$\bar{\mathbf{J}}(\mathbf{r}) = z q \bar{n}(\mathbf{r}) \bar{\mathbf{v}}(\mathbf{r})$$

(where $\bar{\mathbf{v}}(\mathbf{r}) = \frac{\bar{\mathbf{p}}(\mathbf{r})}{m^*}$ is the velocity moment as defined in subsection 4.3.2 and z is the charge of the particle in atomic units, i.e. expressed as an integer multiple of the proton charge) the 0th order moment of the Wigner equation can be rewritten (multiplying it by $z q$ and substituting) as:

$$z q \frac{\partial}{\partial t} \{\bar{n}(\mathbf{r})\} + \nabla_{\mathbf{r}} \cdot \{\bar{\mathbf{J}}(\mathbf{r})\} = 0 \quad (6.3)$$

Introducing $\bar{\rho}(\mathbf{r}) = z q \bar{n}(\mathbf{r})$ as the probability charge density (the definition is straightforward once the density \bar{n} of charged particles is defined as in subsection 4.3.1) then the moment further simplifies to:

$$\boxed{\frac{\partial}{\partial t} \{\bar{\rho}(\mathbf{r})\} + \nabla_{\mathbf{r}} \cdot \{\bar{\mathbf{J}}(\mathbf{r})\} = 0} \quad (6.4)$$

The resulting equation is nothing more than a **continuity equation on the charge**, exactly like the semiclassical one.

In the presence of scattering, a net recombination term $z q R$ (which accounts also negatively for generation processes) should be added to take into account the different kinds of recombination that are possible in the semiconductor. The final form of the continuity equation is then:

$$\boxed{\frac{\partial}{\partial t} \{\bar{\rho}(\mathbf{r})\} + \nabla_{\mathbf{r}} \cdot \{\bar{\mathbf{J}}(\mathbf{r})\} + z q R = 0} \quad (6.5)$$

6.2 1st Order Moment

In a 3-dimensional vector space the Wigner equation takes the form:

$$\begin{aligned} & \frac{\partial}{\partial t} f_{\text{W}}(\mathbf{r}, \mathbf{p}) + \frac{\mathbf{p}}{m^*} \cdot [\nabla_{\mathbf{r}} f_{\text{W}}(\mathbf{r}, \mathbf{p})] = \\ & = \sum_{\substack{\lambda_1, \dots, \lambda_n \geq 0 \\ \lambda_1 + \dots + \lambda_n \text{ odd}}} \frac{1}{\lambda_1! \lambda_2! \lambda_3!} \left(\frac{\hbar}{2i} \right)^{\lambda_1 + \lambda_2 + \lambda_3 - 1} [\partial_1^{\lambda_1} \partial_2^{\lambda_2} \partial_3^{\lambda_3} U(\mathbf{r})] [\partial_{p_1}^{\lambda_1} \partial_{p_2}^{\lambda_2} \partial_{p_3}^{\lambda_3} f_{\text{W}}(\mathbf{r}, \mathbf{p})] \end{aligned}$$

Multiplying it by the momentum \mathbf{p} and integrating over the momentum space yields:

$$\begin{aligned} & \int_{\Omega_{\mathbf{p}}} \mathbf{p} \frac{\partial}{\partial t} f_{\text{W}}(\mathbf{r}, \mathbf{p}) \, d\mathbf{p} + \int_{\Omega_{\mathbf{p}}} \mathbf{p} \frac{\mathbf{p}}{m^*} \cdot [\nabla_{\mathbf{r}} f_{\text{W}}(\mathbf{r}, \mathbf{p})] \, d\mathbf{p} = \\ & = \int_{\Omega_{\mathbf{p}}} \mathbf{p} \sum_{\substack{\lambda_1, \dots, \lambda_n \geq 0 \\ \lambda_1 + \dots + \lambda_n \text{ odd}}} \frac{1}{\lambda_1! \lambda_2! \lambda_3!} \left(\frac{\hbar}{2i} \right)^{\lambda_1 + \lambda_2 + \lambda_3 - 1} [\partial_1^{\lambda_1} \partial_2^{\lambda_2} \partial_3^{\lambda_3} U(\mathbf{r})] [\partial_{p_1}^{\lambda_1} \partial_{p_2}^{\lambda_2} \partial_{p_3}^{\lambda_3} f_{\text{W}}(\mathbf{r}, \mathbf{p})] \, d\mathbf{p} \end{aligned}$$

Being a vector equation it must be treated one component at a time; therefore the j^{th} component of the equation will be considered:

$$\begin{aligned} & \int_{\Omega_{\mathbf{p}}} p_j \frac{\partial}{\partial t} f_{\text{W}}(\mathbf{r}, \mathbf{p}) \, d\mathbf{p} + \int_{\Omega_{\mathbf{p}}} p_j \frac{\mathbf{p}}{m^*} \cdot [\nabla_{\mathbf{r}} f_{\text{W}}(\mathbf{r}, \mathbf{p})] \, d\mathbf{p} = \\ & = \int_{\Omega_{\mathbf{p}}} p_j \sum_{\substack{\lambda_1, \dots, \lambda_n \geq 0 \\ \lambda_1 + \dots + \lambda_n \text{ odd}}} \frac{1}{\lambda_1! \lambda_2! \lambda_3!} \left(\frac{\hbar}{2i} \right)^{\lambda_1 + \lambda_2 + \lambda_3 - 1} [\partial_1^{\lambda_1} \partial_2^{\lambda_2} \partial_3^{\lambda_3} U(\mathbf{r})] [\partial_{p_1}^{\lambda_1} \partial_{p_2}^{\lambda_2} \partial_{p_3}^{\lambda_3} f_{\text{W}}(\mathbf{r}, \mathbf{p})] \, d\mathbf{p} \end{aligned}$$

Considering the 3rd term first, reordering the derivatives to get $\partial_{p_j}^{\lambda_j}$ after the other derivatives of the Wigner function (which is possible under proper regularity assumptions on the Wigner function) and taking out of the integral all the quantities that do not depend on the j^{th} component of the momentum yields:

$$\begin{aligned} & \int_{\Omega_{\mathbf{p}}} p_j \sum_{\substack{\lambda_1, \dots, \lambda_n \geq 0 \\ \lambda_1 + \dots + \lambda_n \text{ odd}}} \frac{1}{\lambda_1! \lambda_2! \lambda_3!} \left(\frac{\hbar}{2i} \right)^{\lambda_1 + \lambda_2 + \lambda_3 - 1} [\partial_1^{\lambda_1} \partial_2^{\lambda_2} \partial_3^{\lambda_3} U(\mathbf{r})] [\partial_{p_1}^{\lambda_1} \partial_{p_2}^{\lambda_2} \partial_{p_3}^{\lambda_3} f_W(\mathbf{r}, \mathbf{p})] d\mathbf{p} \\ &= \sum_{\substack{\lambda_1, \dots, \lambda_n \geq 0 \\ \lambda_1 + \dots + \lambda_n \text{ odd}}} \frac{1}{\lambda_1! \lambda_2! \lambda_3!} \left(\frac{\hbar}{2i} \right)^{\lambda_1 + \lambda_2 + \lambda_3 - 1} [\partial_1^{\lambda_1} \partial_2^{\lambda_2} \partial_3^{\lambda_3} U(\mathbf{r})] \int_{\Omega_{\mathbf{p}}} \partial_{p_k}^{\lambda_k} \partial_{p_l}^{\lambda_l} \left\{ p_j [\partial_{p_j}^{\lambda_j} f_W(\mathbf{r}, \mathbf{p})] \right\} dp_j dp_k dp_l \end{aligned}$$

with $l \neq k \neq j$.

Then, if $\lambda_j \geq 1$ integrating by parts (using Green's theorem for integration by parts in multiple dimensions) with respect to the variable p_j yields:

$$\begin{aligned} &= \sum_{\substack{\lambda_1, \dots, \lambda_n \geq 0 \\ \lambda_1 + \dots + \lambda_n \text{ odd}}} \left(\frac{\hbar}{2i} \right)^{\lambda_1 + \lambda_2 + \lambda_3 - 1} \frac{[\partial_1^{\lambda_1} \partial_2^{\lambda_2} \partial_3^{\lambda_3} U(\mathbf{r})]}{\lambda_1! \lambda_2! \lambda_3!} \int_{-\infty}^{+\infty} \int_{-\infty}^{+\infty} \int_{-\infty}^{+\infty} \partial_{p_k}^{\lambda_k} \partial_{p_l}^{\lambda_l} \left\{ p_j [\partial_{p_j}^{\lambda_j} f_W(\mathbf{r}, \mathbf{p})] \right\} dp_j dp_k dp_l \\ &= \sum_{\substack{\lambda_1, \dots, \lambda_n \geq 0 \\ \lambda_1 + \dots + \lambda_n \text{ odd}}} \left(\frac{\hbar}{2i} \right)^{\lambda_1 + \lambda_2 + \lambda_3 - 1} \frac{[\partial_1^{\lambda_1} \partial_2^{\lambda_2} \partial_3^{\lambda_3} U(\mathbf{r})]}{\lambda_1! \lambda_2! \lambda_3!} \int_{-\infty}^{+\infty} \partial_{p_l}^{\lambda_l} \int_{-\infty}^{+\infty} \partial_{p_k}^{\lambda_k} \int_{-\infty}^{+\infty} p_j [\partial_{p_j}^{\lambda_j} f_W(\mathbf{r}, \mathbf{p})] dp_j dp_k dp_l \\ &= \sum_{\substack{\lambda_1, \dots, \lambda_n \geq 0 \\ \lambda_1 + \dots + \lambda_n \text{ odd}}} \left(\frac{\hbar}{2i} \right)^{\lambda_1 + \lambda_2 + \lambda_3 - 1} \frac{[\partial_1^{\lambda_1} \partial_2^{\lambda_2} \partial_3^{\lambda_3} U(\mathbf{r})]}{\lambda_1! \lambda_2! \lambda_3!} \\ & \quad \int_{-\infty}^{+\infty} \partial_{p_l}^{\lambda_l} \int_{-\infty}^{+\infty} \partial_{p_k}^{\lambda_k} \left(\left[p_j \partial_{p_j}^{\lambda_j - 1} f_W(\mathbf{r}, \mathbf{p}) \right]_{p_j \rightarrow -\infty}^{p_j \rightarrow +\infty} - \int_{-\infty}^{+\infty} \partial_{p_j}^{\lambda_j - 1} f_W(\mathbf{r}, \mathbf{p}) dp_j \right) dp_k dp_l \end{aligned}$$

Assuming the Wigner function and its derivatives to tend to zero for infinite values of momentum, which is reasonable because of its interpretation as a quasi-probability density function in phase space, then:

$$= \sum_{\substack{\lambda_1, \dots, \lambda_n \geq 0 \\ \lambda_1 + \dots + \lambda_n \text{ odd}}} \left(\frac{\hbar}{2i} \right)^{\lambda_1 + \lambda_2 + \lambda_3 - 1} \frac{[\partial_1^{\lambda_1} \partial_2^{\lambda_2} \partial_3^{\lambda_3} U(\mathbf{r})]}{\lambda_1! \lambda_2! \lambda_3!} \int_{-\infty}^{+\infty} \partial_{p_l}^{\lambda_l} \int_{-\infty}^{+\infty} \partial_{p_k}^{\lambda_k} \left(- \int_{-\infty}^{+\infty} \partial_{p_j}^{\lambda_j - 1} f_W(\mathbf{r}, \mathbf{p}) dp_j \right) dp_k dp_l$$

Then, if the order of any of the remaining derivatives is higher than zero, when integration by parts is performed in the same variable p_m it results in the evaluation $[\bullet]_{p_m \rightarrow -\infty}^{p_m \rightarrow +\infty}$ of the Wigner function or one of its marginals or a derivative of either of them; these are however zero since the probability density for infinite values of momentum must drop to zero, as do all of its derivatives.

Instead, if $\lambda_j = 0$ integrating by parts with respect to the variable p_j yields:

$$\begin{aligned} & \int_{\Omega_{\mathbf{p}}} p_j \sum_{\substack{\lambda_1, \dots, \lambda_n \geq 0 \\ \lambda_1 + \dots + \lambda_n \text{ odd}}} \frac{1}{\lambda_1! \lambda_2! \lambda_3!} \left(\frac{\hbar}{2i} \right)^{\lambda_1 + \lambda_2 + \lambda_3 - 1} [\partial_1^{\lambda_1} \partial_2^{\lambda_2} \partial_3^{\lambda_3} U(\mathbf{r})] [\partial_{p_1}^{\lambda_1} \partial_{p_2}^{\lambda_2} \partial_{p_3}^{\lambda_3} f_W(\mathbf{r}, \mathbf{p})] d\mathbf{p} \\ &= \sum_{\substack{\lambda_1, \dots, \lambda_n \geq 0 \\ \lambda_1 + \dots + \lambda_n \text{ odd}}} \frac{1}{\lambda_1! \lambda_2! \lambda_3!} \left(\frac{\hbar}{2i} \right)^{\lambda_1 + \lambda_2 + \lambda_3 - 1} [\partial_1^{\lambda_1} \partial_2^{\lambda_2} \partial_3^{\lambda_3} U(\mathbf{r})] \\ & \quad \int_{-\infty}^{+\infty} p_j \int_{-\infty}^{+\infty} \partial_{p_l}^{\lambda_l} \int_{-\infty}^{+\infty} \partial_{p_k}^{\lambda_k} [f_W(\mathbf{r}, \mathbf{p})] dp_k dp_l dp_j \end{aligned}$$

Also in this case, if any of the orders of the remaining derivatives is higher than zero it results in the evaluation of the surface integral $[\bullet]_{p_m \rightarrow -\infty}^{p_m \rightarrow +\infty}$ (with p_m the momentum with respect to which the remaining derivative is carried out) of the probability density function, one of its derivatives or one of its marginals. Since all of these quantities must drop to zero for infinite momentum values then if $\lambda_j = 0$ only terms with $\lambda_k = \lambda_l = 0$ could in principle not be negligible; since these values of λ however add up to an even number, they shall *not be part of the series*. Hence, all there terms may be dropped.

Hence, only terms with $\lambda_j = 1$, $\lambda_k = 0$, $\lambda_l = 0$ are nonzero in the series, giving a contribution to the 1st order moment:

$$\begin{aligned} & \int_{\Omega_{\mathbf{p}}} p_j \sum_{\substack{\lambda_1, \dots, \lambda_n \geq 0 \\ \lambda_1 + \dots + \lambda_n \text{ odd}}} \frac{1}{\lambda_1! \lambda_2! \lambda_3!} \left(\frac{\hbar}{2i} \right)^{\lambda_1 + \lambda_2 + \lambda_3 - 1} [\partial_{\lambda_1}^{\lambda_1} \partial_{\lambda_2}^{\lambda_2} \partial_{\lambda_3}^{\lambda_3} U(\mathbf{r})] [\partial_{p_1}^{\lambda_1} \partial_{p_2}^{\lambda_2} \partial_{p_3}^{\lambda_3} f_W(\mathbf{r}, \mathbf{p})] d\mathbf{p} \\ &= - [\partial_{r_j} U(\mathbf{r})] \int_{\Omega_{\mathbf{p}}} f_W(\mathbf{r}, \mathbf{p}) d\mathbf{p} \\ &= -n(\mathbf{r}) [\partial_{r_j} U(\mathbf{r})] \end{aligned}$$

where the result of the previous integration by parts has been used along to the conclusions of the previous reasoning on the null terms of the series to derive this final form of the term.

Considering now the 2nd term and extracting the gradient with respect to position (which makes it become a divergence):

$$\begin{aligned} & \int_{\Omega_{\mathbf{p}}} p_j \frac{\mathbf{p}}{m^*} \cdot [\nabla_{\mathbf{r}} f_W(\mathbf{r}, \mathbf{p})] d\mathbf{p} \\ &= \int_{\Omega_{\mathbf{p}}} \frac{1}{m^*} p_j p_1 \frac{\partial f_W}{\partial r_1}(\mathbf{r}, \mathbf{p}) d\mathbf{p} + \int_{\Omega_{\mathbf{p}}} \frac{1}{m^*} p_j p_2 \frac{\partial f_W}{\partial r_2}(\mathbf{r}, \mathbf{p}) d\mathbf{p} + \int_{\Omega_{\mathbf{p}}} \frac{1}{m^*} p_j p_3 \frac{\partial f_W}{\partial r_3}(\mathbf{r}, \mathbf{p}) d\mathbf{p} \\ &= \frac{\partial}{\partial r_1} \int_{\Omega_{\mathbf{p}}} \frac{1}{m^*} p_j p_1 f_W(\mathbf{r}, \mathbf{p}) d\mathbf{p} + \frac{\partial}{\partial r_2} \int_{\Omega_{\mathbf{p}}} \frac{1}{m^*} p_j p_2 f_W(\mathbf{r}, \mathbf{p}) d\mathbf{p} + \frac{\partial}{\partial r_3} \int_{\Omega_{\mathbf{p}}} \frac{1}{m^*} p_j p_3 f_W(\mathbf{r}, \mathbf{p}) d\mathbf{p} \\ &= \nabla_{\mathbf{r}} \cdot \int_{\Omega_{\mathbf{p}}} \left[\frac{p_j p_1}{m^*} \hat{\mathbf{i}} + \frac{p_j p_2}{m^*} \hat{\mathbf{j}} + \frac{p_j p_3}{m^*} \hat{\mathbf{k}} \right] f_W(\mathbf{r}, \mathbf{p}) d\mathbf{p} \\ &= \nabla_{\mathbf{r}} \cdot \int_{\Omega_{\mathbf{p}}} p_j \frac{\mathbf{p}}{m^*} f_W(\mathbf{r}, \mathbf{p}) d\mathbf{p} \end{aligned}$$

Observing the intermediate form:

$$\int_{\Omega_{\mathbf{p}}} p_j \frac{\mathbf{p}}{m^*} \cdot [\nabla_{\mathbf{r}} f_W(\mathbf{r}, \mathbf{p})] d\mathbf{p} = \nabla_{\mathbf{r}} \cdot \int_{\Omega_{\mathbf{p}}} \left[\frac{p_j p_1}{m^*} \hat{\mathbf{i}} + \frac{p_j p_2}{m^*} \hat{\mathbf{j}} + \frac{p_j p_3}{m^*} \hat{\mathbf{k}} \right] f_W(\mathbf{r}, \mathbf{p}) d\mathbf{p}$$

and rewriting each component of the momentum as its average \bar{p}_j (considering the Wigner function as the quasi-probability density function for the average) plus an additional random component \tilde{p}_j the following result is obtained:

$$\begin{aligned} & \int_{\Omega_{\mathbf{p}}} p_j \frac{\mathbf{p}}{m^*} \cdot [\nabla_{\mathbf{r}} f_W(\mathbf{r}, \mathbf{p})] d\mathbf{p} \\ &= \nabla_{\mathbf{r}} \cdot \int_{\Omega_{\mathbf{p}}} \left[\frac{(\bar{p}_j + \tilde{p}_j)(\bar{p}_1 + \tilde{p}_1)}{m^*} \hat{\mathbf{i}} + \frac{(\bar{p}_j + \tilde{p}_j)(\bar{p}_2 + \tilde{p}_2)}{m^*} \hat{\mathbf{j}} + \frac{(\bar{p}_j + \tilde{p}_j)(\bar{p}_3 + \tilde{p}_3)}{m^*} \hat{\mathbf{k}} \right] f_W(\mathbf{r}, \mathbf{p}) d\mathbf{p} \end{aligned}$$

Developing the products of binomials and *assuming the covariance of the random components of different component of the momentum to be zero* (i.e. assuming the momentum oscillations in orthogonal directions to be uncorrelated) leads to:

$$= \nabla_{\mathbf{r}} \cdot \int_{\Omega_{\mathbf{p}}} \left[\frac{\bar{p}_j \bar{p}_1}{m^*} \hat{\mathbf{i}} + \frac{\bar{p}_j \bar{p}_2}{m^*} \hat{\mathbf{j}} + \frac{\bar{p}_j \bar{p}_3}{m^*} \hat{\mathbf{k}} \right] f_W(\mathbf{r}, \mathbf{p}) d\mathbf{p} + \nabla_{\mathbf{r}} \cdot \int_{\Omega_{\mathbf{p}}} \left[\frac{\tilde{p}_j \tilde{p}_1}{m^*} \hat{\mathbf{r}}_j \right] f_W(\mathbf{r}, \mathbf{p}) d\mathbf{p}$$

where $\hat{\mathbf{r}}_j$ is the unit versor in the j -th direction.

It is then useful to define in analogy with subsection 4.3.3 the average kinetic energy $\bar{E}_{k,j}^{(R)}$ due to random motion in the j -th direction as $2 m^* \bar{E}_{k,j}^{(R)} \triangleq \bar{p}_j \bar{p}_j$.

Recognizing then the expression for the product $\bar{n}(\mathbf{r}) \bar{E}_{k,j}^{(R)}(\mathbf{r})$ between the probability density and the component of the kinetic energy due to the j^{th} random component of the momentum these terms can be substituted with:

$$\begin{aligned} &= \nabla_{\mathbf{r}} \cdot \left[2 \bar{n}(\mathbf{r}) \bar{E}_{k,j}^{(R)}(\mathbf{r}) \hat{\mathbf{r}}_j \right] + \nabla_{\mathbf{r}} \cdot \left\{ \left[\frac{\bar{p}_j \bar{p}_1}{m^*} \hat{\mathbf{i}} + \frac{\bar{p}_j \bar{p}_2}{m^*} \hat{\mathbf{j}} + \frac{\bar{p}_j \bar{p}_3}{m^*} \hat{\mathbf{k}} \right] \int_{\Omega_{\mathbf{p}}} f_{\mathbf{W}}(\mathbf{r}, \mathbf{p}) d\mathbf{p} \right\} \\ &= \frac{\partial}{\partial r_j} \left[2 \bar{n}(\mathbf{r}) \bar{E}_{k,j}^{(R)}(\mathbf{r}) \right] + \nabla_{\mathbf{r}} \cdot \left\{ \left[\frac{\bar{p}_j \bar{p}_1}{m^*} \hat{\mathbf{i}} + \frac{\bar{p}_j \bar{p}_2}{m^*} \hat{\mathbf{j}} + \frac{\bar{p}_j \bar{p}_3}{m^*} \hat{\mathbf{k}} \right] n(\mathbf{r}) \right\} \end{aligned}$$

which can be rewritten through the vector calculus identity $\nabla \cdot (\alpha \mathbf{A}) = \alpha \nabla \cdot \mathbf{A} + \mathbf{A} \cdot \nabla \alpha$ as: (the first term then simplifies due to \bar{p}_i being an average over the whole phase space, i.e. both momentum and space, and therefore nothing more than a constant)

$$= \frac{\partial}{\partial r_j} \left[2 \bar{n}(\mathbf{r}) \bar{E}_{k,j}^{(R)}(\mathbf{r}) \right] + \left[\frac{\bar{p}_j \bar{p}_1}{m^*} \hat{\mathbf{i}} + \frac{\bar{p}_j \bar{p}_2}{m^*} \hat{\mathbf{j}} + \frac{\bar{p}_j \bar{p}_3}{m^*} \hat{\mathbf{k}} \right] \cdot \nabla_{\mathbf{r}} [n(\mathbf{r})]$$

Considering now the **1st term**, swapping the order of integral and derivative gives:

$$\begin{aligned} \int_{\Omega_{\mathbf{p}}} p_j \frac{\partial}{\partial t} f_{\mathbf{W}}(\mathbf{r}, \mathbf{p}) d\mathbf{p} &= \frac{\partial}{\partial t} \int_{\Omega_{\mathbf{p}}} p_j f_{\mathbf{W}}(\mathbf{r}, \mathbf{p}) d\mathbf{p} \\ &= \frac{\partial}{\partial t} \{ \bar{n}(\mathbf{r}) \bar{p}_j(\mathbf{r}) \} \end{aligned}$$

where the expression of the moment $\bar{n}(\mathbf{r}) \bar{p}_j(\mathbf{r})$ has been recognized and substituted.

Notice the different meaning of $\bar{p}_j(\mathbf{r})$ and \bar{p}_j :

- $\bar{p}_j(\mathbf{r})$ is a moment of the Wigner function obtained by integrating the momentum in momentum space only
- \bar{p}_j is the expected value of the momentum operator over the whole region, obtained by integrating the momentum against the Wigner function in both space and momentum (\bar{p}_j is an entirely deterministic quantity)

Substituting then the final expressions for the three terms leads to:

$$\frac{\partial}{\partial t} \{ \bar{n}(\mathbf{r}) \bar{p}_j(\mathbf{r}) \} + \frac{\partial}{\partial r_j} \left[2 \bar{n}(\mathbf{r}) \bar{E}_{k,j}^{(R)}(\mathbf{r}) \right] + \left[\frac{\bar{p}_j \bar{p}_1}{m^*} \hat{\mathbf{i}} + \frac{\bar{p}_j \bar{p}_2}{m^*} \hat{\mathbf{j}} + \frac{\bar{p}_j \bar{p}_3}{m^*} \hat{\mathbf{k}} \right] \cdot \nabla_{\mathbf{r}} [n(\mathbf{r})] + \bar{n}(\mathbf{r}) [\partial_{r_j} U(\mathbf{r})] = 0 \quad (6.6)$$

Assuming the random fluctuations in the momentum to be thermal then the kinetic energy for each degree of freedom is $E_{k,j} = \frac{1}{2} k_B T$ and therefore the equation becomes:

$$\frac{\partial}{\partial t} \{ \bar{n}(\mathbf{r}) \bar{p}_j(\mathbf{r}) \} + \frac{\partial}{\partial r_j} [k_B T \bar{n}(\mathbf{r})] + \left[\frac{\bar{p}_j \bar{p}_1}{m^*} \hat{\mathbf{i}} + \frac{\bar{p}_j \bar{p}_2}{m^*} \hat{\mathbf{j}} + \frac{\bar{p}_j \bar{p}_3}{m^*} \hat{\mathbf{k}} \right] \cdot \nabla_{\mathbf{r}} [\bar{n}(\mathbf{r})] + \bar{n}(\mathbf{r}) [\partial_{r_j} U(\mathbf{r})] = 0 \quad (6.7)$$

which can be rewritten in more compact vector form as:

$$\frac{\partial}{\partial t} \{ \bar{n}(\mathbf{r}) \bar{\mathbf{p}}(\mathbf{r}) \} + k_B T \nabla_{\mathbf{r}} [\bar{n}(\mathbf{r})] + \bar{\mathbf{p}} \bar{\mathbf{p}} \cdot \nabla_{\mathbf{r}} [\bar{n}(\mathbf{r})] + \bar{n}(\mathbf{r}) \nabla_{\mathbf{r}} [U(\mathbf{r})] = 0 \quad (6.8)$$

Scattering events (i.e. collisions) can then be taken into account under the momentum relaxation time approximation as an additional term:

$$\frac{\partial}{\partial t} \{ \bar{n}(\mathbf{r}) \bar{\mathbf{p}}(\mathbf{r}) \} \Big|_{\text{coll.}} = - \frac{\bar{n}(\mathbf{r}) \bar{\mathbf{p}}(\mathbf{r})}{\tau_{\text{pn}}} \quad (6.9)$$

where τ_{pn} is the momentum relaxation time. [2]

When included in Equation 6.10 it gives:

$$\boxed{\frac{\partial}{\partial t} \{\bar{n}(\mathbf{r}) \bar{\mathbf{p}}(\mathbf{r})\} + k_{\text{B}}T \nabla_{\mathbf{r}} [\bar{n}(\mathbf{r})] + \bar{\mathbf{p}} \bar{\mathbf{p}} \cdot \nabla_{\mathbf{r}} [\bar{n}(\mathbf{r})] + \bar{n}(\mathbf{r}) \nabla_{\mathbf{r}} [U(\mathbf{r})] = -\frac{\bar{n}(\mathbf{r}) \bar{\mathbf{p}}(\mathbf{r})}{\tau_{\text{pn}}}} \quad (6.10)$$

Under steady state conditions ($\partial/\partial t = 0$) it simplifies to:

$$k_{\text{B}}T \nabla_{\mathbf{r}} [\bar{n}(\mathbf{r})] + \bar{\mathbf{p}} \bar{\mathbf{p}} \cdot \nabla_{\mathbf{r}} [\bar{n}(\mathbf{r})] + \bar{n}(\mathbf{r}) \nabla_{\mathbf{r}} [U(\mathbf{r})] = -\frac{\bar{n}(\mathbf{r}) \bar{\mathbf{p}}(\mathbf{r})}{\tau_{\text{pn}}}$$

Multiplying by the momentum relaxation time and moving the collision term to the left-hand-side gives:

$$\tau_{\text{pn}} k_{\text{B}}T \nabla_{\mathbf{r}} [\bar{n}(\mathbf{r})] + \tau_{\text{pn}} \bar{\mathbf{p}} \bar{\mathbf{p}} \cdot \nabla_{\mathbf{r}} [\bar{n}(\mathbf{r})] + \tau_{\text{pn}} \bar{n}(\mathbf{r}) \nabla_{\mathbf{r}} [U(\mathbf{r})] + \bar{n}(\mathbf{r}) \bar{\mathbf{p}}(\mathbf{r}) = 0$$

The convection term $\tau_{\text{pn}} \bar{\mathbf{p}} \bar{\mathbf{p}} \cdot \nabla_{\mathbf{r}} [\bar{n}(\mathbf{r})]$ is typically small when compared to the collision term:

$$\tau_{\text{pn}} \bar{\mathbf{p}} \bar{\mathbf{p}} \cdot \nabla_{\mathbf{r}} [\bar{n}(\mathbf{r})] \ll \bar{n}(\mathbf{r}) \bar{\mathbf{p}}$$

(since the momentum relaxation time τ_{pn} is typically small) and it can therefore be neglected, giving:

$$\tau_{\text{pn}} k_{\text{B}}T \nabla_{\mathbf{r}} [\bar{n}(\mathbf{r})] + \tau_{\text{pn}} \bar{n}(\mathbf{r}) \nabla_{\mathbf{r}} [U(\mathbf{r})] + \bar{n}(\mathbf{r}) \bar{\mathbf{p}}(\mathbf{r}) = 0$$

Since the probability current density is given by:

$$\bar{\mathbf{J}}(\mathbf{r}) = z q \bar{n}(\mathbf{r}) \bar{\mathbf{v}}(\mathbf{r})$$

(where $\bar{\mathbf{v}}(\mathbf{r}) = \frac{\bar{\mathbf{p}}(\mathbf{r})}{m^*}$ is the velocity moment as defined in subsection 4.3.2 and z is the charge of the particle in atomic units, i.e. expressed as a multiple of the proton charge) the 1st order moment of the Wigner equation can be rewritten as:

$$\tau_{\text{pn}} k_{\text{B}}T \nabla_{\mathbf{r}} [\bar{n}(\mathbf{r})] + \tau_{\text{pn}} \bar{n}(\mathbf{r}) \nabla_{\mathbf{r}} [U(\mathbf{r})] + z \frac{m^*}{q} \bar{\mathbf{J}}(\mathbf{r}) = 0$$

which is equivalent to:

$$\bar{\mathbf{J}}(\mathbf{r}) = -\frac{z q \tau_{\text{pn}}}{m^*} k_{\text{B}}T \nabla_{\mathbf{r}} [\bar{n}(\mathbf{r})] - \frac{z q \tau_{\text{pn}}}{m^*} \bar{n}(\mathbf{r}) \nabla_{\mathbf{r}} [U(\mathbf{r})]$$

Defining the low-field mobility for the particle as $\mu \frac{q \tau_{\text{pn}}}{m^*}$ the equation takes the form:

$$\bar{\mathbf{J}}(\mathbf{r}) = -z \mu k_{\text{B}}T \nabla_{\mathbf{r}} [\bar{n}(\mathbf{r})] - z \mu \bar{n}(\mathbf{r}) \nabla_{\mathbf{r}} [U(\mathbf{r})]$$

which can be rewritten for the separate case of electrons and holes (with $z = -1$ and $z = +1$ respectively) as:

$$\begin{aligned} \bar{\mathbf{J}}_{\mathbf{n}}(\mathbf{r}) &= \mu_{\text{n}} k_{\text{B}}T \nabla_{\mathbf{r}} [\bar{n}(\mathbf{r})] + \mu_{\text{n}} \bar{n}(\mathbf{r}) \nabla_{\mathbf{r}} [U_{\text{n}}(\mathbf{r})] \\ \bar{\mathbf{J}}_{\mathbf{p}}(\mathbf{r}) &= -\mu_{\text{p}} k_{\text{B}}T \nabla_{\mathbf{r}} [\bar{p}(\mathbf{r})] - \mu_{\text{p}} \bar{p}(\mathbf{r}) \nabla_{\mathbf{r}} [U_{\text{p}}(\mathbf{r})] \end{aligned}$$

where the subscript n refers to electrons and the subscript p refers to holes.

Substituting then the relationship between potential energy and electrostatic potential $U = z \phi$ in an homogeneous material yields:

$$\begin{aligned} \bar{\mathbf{J}}_{\mathbf{n}}(\mathbf{r}) &= \mu_{\text{n}} k_{\text{B}}T \nabla_{\mathbf{r}} [\bar{n}(\mathbf{r})] - q \mu_{\text{n}} \bar{n}(\mathbf{r}) \nabla_{\mathbf{r}} [\phi(\mathbf{r})] \\ \bar{\mathbf{J}}_{\mathbf{p}}(\mathbf{r}) &= -\mu_{\text{p}} k_{\text{B}}T \nabla_{\mathbf{r}} [\bar{p}(\mathbf{r})] - q \mu_{\text{p}} \bar{p}(\mathbf{r}) \nabla_{\mathbf{r}} [\phi(\mathbf{r})] \end{aligned}$$

Introducing the diffusivity as $D = \frac{\mu k_{\text{B}}T}{q}$ into the above equations finally puts them in the standard form for the electron and hole continuity equations:

$$\boxed{\bar{\mathbf{J}}_{\mathbf{n}}(\mathbf{r}) = q D_{\text{n}} \nabla_{\mathbf{r}} [\bar{n}(\mathbf{r})] - q \mu_{\text{n}} \bar{n}(\mathbf{r}) \nabla_{\mathbf{r}} [\phi(\mathbf{r})]} \quad (6.11)$$

$$\boxed{\bar{\mathbf{J}}_{\mathbf{p}}(\mathbf{r}) = -q D_{\text{p}} \nabla_{\mathbf{r}} [\bar{p}(\mathbf{r})] - q \mu_{\text{p}} \bar{p}(\mathbf{r}) \nabla_{\mathbf{r}} [\phi(\mathbf{r})]} \quad (6.12)$$

The resulting equations are the **drift-diffusion equations** for the probability current density.

6.3 Statistical Extension of the Moments

All the moments of the Wigner equation that have been derived up to now, and in particular the **drift-diffusion equations** for the probability current density (Equation 6.11,6.12):

$$\begin{aligned}\bar{\mathbf{J}}_{\mathbf{n}}(\mathbf{r}) &= q D_{\mathbf{n}} \nabla_{\mathbf{r}} [\bar{n}(\mathbf{r})] - q\mu_{\mathbf{n}} n(\mathbf{r}) \nabla_{\mathbf{r}} [\phi(\mathbf{r})] \\ \bar{\mathbf{J}}_{\mathbf{p}}(\mathbf{r}) &= -q D_{\mathbf{p}} \nabla_{\mathbf{r}} [\bar{n}(\mathbf{r})] - q\mu_{\mathbf{p}} p(\mathbf{r}) \nabla_{\mathbf{r}} [\phi(\mathbf{r})]\end{aligned}$$

involve *single-particle* current densities ($\bar{\mathbf{J}}(\mathbf{r})$), electron densities ($\bar{n}(\mathbf{r})$) and charges ($\bar{\rho}(\mathbf{r})$).

This is however usually not the case when studying a device, in which N charges are present.

The extension of the previously defined *single-particle* quantities to their more common *multi-particle* counterparts (hereby represented without the $\bar{\quad}$ on top) can be done by the law of large numbers, simply multiplying them by N :

$$n(\mathbf{r}) = N \bar{n}(\mathbf{r}) \qquad \bar{\mathbf{J}}(\mathbf{r}) = N \mathbf{J}(\mathbf{r}) \qquad \rho(\mathbf{r}) = N \bar{\rho}(\mathbf{r})$$

Multiplying the single-particle drift-diffusion equations by N and substituting these identities leads to the classical drift-diffusion equations:

$$\boxed{\begin{aligned}\mathbf{J}_{\mathbf{n}}(\mathbf{r}) &= q D_{\mathbf{n}} \nabla_{\mathbf{r}} [n(\mathbf{r})] - q\mu_{\mathbf{n}} n(\mathbf{r}) \nabla_{\mathbf{r}} [\phi(\mathbf{r})] \\ \mathbf{J}_{\mathbf{p}}(\mathbf{r}) &= -q D_{\mathbf{p}} \nabla_{\mathbf{r}} [n(\mathbf{r})] - q\mu_{\mathbf{p}} p(\mathbf{r}) \nabla_{\mathbf{r}} [\phi(\mathbf{r})]\end{aligned}}$$

Since these equations are *identical to the semiclassical continuity equations for electrons and holes* the density gradient model does not appear to change in any way the fundamental equations describing the physics of the device. The main difference between the density gradient model and the traditional drift-diffusion model will later be shown to be in the statistics that is adopted for the particles.

Part II

Physical Models

Chapter 7

The Density Gradient Model

As the continuity equations and the Poisson equation are the same as in a traditional drift-diffusion model, the main difference due to quantum corrections must be included within the expression for the carrier densities (i.e. within the carrier statistics).

The density gradient model aims at introducing the quantum corrections into the expressions for the carrier densities n and p .

7.1 Derivation

The density gradient model is derived here with an approach inspired to works of M. G. Ancona, G. J. Iafrate and A. Jünger. [3][17]

The starting point for the derivation of the density gradient model is the steady state (/equilibrium) solution to the Wigner equation presented in Equation 5.10:

$$f_W = \exp\{-\beta E\} \left[1 + \frac{\hbar^2}{24} \sum_{\substack{q \in \{1,2,3\} \\ m \in \{1,2,3\}}} \frac{\partial^2 U}{\partial r_q \partial r_m} \frac{\beta^3}{(m^*)^2} p_q p_m + \frac{\hbar^2}{24} \sum_{q \in \{1,2,3\}} \left(\frac{\partial U}{\partial r_q} \right)^2 \frac{\beta^3}{m^*} - \frac{\hbar^2}{8} \sum_{q \in \{1,2,3\}} \left(\frac{\partial^2 U}{\partial r_q^2} \right) \frac{\beta^2}{m^*} \right] \quad (7.1)$$

which can be more compactly rewritten as:

$$f_W = \exp\{-\beta E\} \left[1 + \frac{\hbar^2}{24} \sum_{\substack{q \in \{1,2,3\} \\ m \in \{1,2,3\}}} \frac{\partial^2 U}{\partial r_q \partial r_m} \frac{\beta^3}{(m^*)^2} p_q p_m + \frac{\hbar^2 \beta^3}{24 m^*} \nabla U \cdot \nabla U - \frac{\hbar^2 \beta^2}{8 m^*} \nabla^2 U \right] \quad (7.2)$$

Notice that a normalization factor is still missing from this expression of f_W . However, this is of no practical importance for the derivations that will follow as long as they result in equations such that a scalar factor in front of f_W simplify out (which is the case for the equations that will be obtained).

The first step is then to integrate it over the momentum space to obtain the single-electron density $\bar{n}(\mathbf{r})$ as:

$$\begin{aligned} \bar{n} &= \int_{\Omega_{\mathbf{p}}} f_W d\mathbf{p} \\ &= \int_{\Omega_{\mathbf{p}}} \exp\{-\beta E\} d\mathbf{p} + \frac{\hbar^2 \beta^3}{24 (m^*)^2} \int_{\Omega_{\mathbf{p}}} \sum_{\substack{q \in \{1,2,3\} \\ m \in \{1,2,3\}}} \frac{\partial^2 U}{\partial r_q \partial r_m} p_q p_m \exp\{-\beta E\} d\mathbf{p} \\ &\quad + \frac{\hbar^2 \beta^3}{24 m^*} \nabla U \cdot \nabla U \int_{\Omega_{\mathbf{p}}} \exp\{-\beta E\} d\mathbf{p} - \frac{\hbar^2 \beta^2}{8 m^*} \nabla^2 U \int_{\Omega_{\mathbf{p}}} \exp\{-\beta E\} d\mathbf{p} \end{aligned}$$

In order to be able to more effectively handle this expression it is useful to first consider some basic integrals involving gaussians.

The first useful identity is:

$$\int_{\Omega_{\mathbf{p}}} \exp \{-\beta E\} d\mathbf{p} = \left(\frac{2\pi m^*}{\beta} \right)^{3/2} \exp \{-\beta E\} \quad (7.3)$$

Proof:

Substituting the classical definition $E = \frac{\mathbf{p} \cdot \mathbf{p}}{2m^*} + U$ of energy into the left-hand side gives:

$$\begin{aligned} & \int_{\Omega_{\mathbf{p}}} \exp \left\{ -\beta \frac{\mathbf{p} \cdot \mathbf{p}}{2m^*} - \beta U \right\} d\mathbf{p} \\ &= \int_{-\infty}^{+\infty} \int_{-\infty}^{+\infty} \int_{-\infty}^{+\infty} \exp \left\{ -\beta \frac{p_1^2 + p_2^2 + p_3^2}{2m^*} - \beta U \right\} dp_1 dp_2 dp_3 \\ &= \exp \{-\beta U\} \int_{-\infty}^{+\infty} \exp \left\{ -\beta \frac{p_3^2}{2m^*} \right\} \int_{-\infty}^{+\infty} \exp \left\{ -\beta \frac{p_2^2}{2m^*} \right\} \int_{-\infty}^{+\infty} \exp \left\{ -\beta \frac{p_1^2}{2m^*} \right\} dp_1 dp_2 dp_3 \\ &= \exp \{-\beta U\} \int_{-\infty}^{+\infty} \exp \left\{ -\beta \frac{p_3^2}{2m^*} \right\} dp_3 \int_{-\infty}^{+\infty} \exp \left\{ -\beta \frac{p_2^2}{2m^*} \right\} dp_2 \int_{-\infty}^{+\infty} \exp \left\{ -\beta \frac{p_1^2}{2m^*} \right\} dp_1 \end{aligned}$$

Applying then the identity $\int_{-\infty}^{+\infty} \exp \{-a x^2\} dx = \left(\frac{\pi}{a} \right)^{1/2}$ (from the table of integrals [18]) to all three gaussian integrals results in:

$$= \left(\frac{2\pi m^*}{\beta} \right)^{3/2} \exp \{-\beta U\}$$

The second useful identity is instead:

$$\int_{\Omega_{\mathbf{p}}} p_j p_l \exp \{-\beta E\} d\mathbf{p} = \frac{m^*}{\beta} \left(\frac{2\pi m^*}{\beta} \right)^{3/2} \delta_{j,l} \exp \{-\beta E\} \quad (7.4)$$

Proof:

Substituting the classical definition $E = \frac{\mathbf{p} \cdot \mathbf{p}}{2m^*} + U$ of energy into the left-hand side gives:

$$\begin{aligned} & \int_{\Omega_{\mathbf{p}}} p_j p_l \exp \left\{ -\beta \frac{\mathbf{p} \cdot \mathbf{p}}{2m^*} - \beta U \right\} d\mathbf{p} \\ &= \int_{-\infty}^{+\infty} \int_{-\infty}^{+\infty} \int_{-\infty}^{+\infty} p_j p_l \exp \left\{ -\beta \frac{p_1^2 + p_2^2 + p_3^2}{2m^*} - \beta U \right\} dp_1 dp_2 dp_3 \end{aligned}$$

Two cases are then possible: $l = j$ and $l \neq j$.

If $l \neq j$ then, calling z the index of the momentum that is neither p_j nor p_l results in:

$$\begin{aligned} &= \exp \{-\beta U\} \int_{-\infty}^{+\infty} \exp \left\{ -\beta \frac{p_z^2}{2m^*} \right\} \int_{-\infty}^{+\infty} p_l \exp \left\{ -\beta \frac{p_l^2}{2m^*} \right\} \int_{-\infty}^{+\infty} p_j \exp \left\{ -\beta \frac{p_j^2}{2m^*} \right\} dp_j dp_l dp_z \\ &= 0 \end{aligned}$$

since the functions under the integrals are odd with respect to the variable of integration and since the interval of integration is symmetric around zero

If $l = j$ then, calling z and q the indexes of the momenta that are different from p_j results in:

$$\begin{aligned} &= \exp\{-\beta U\} \int_{-\infty}^{+\infty} \exp\left\{-\beta \frac{p_z^2}{2m^*}\right\} \int_{-\infty}^{+\infty} \exp\left\{-\beta \frac{p_q^2}{2m^*}\right\} \int_{-\infty}^{+\infty} p_j^2 \exp\left\{-\beta \frac{p_j^2}{2m^*}\right\} dp_j dp_q dp_z \\ &= \exp\{-\beta U\} \int_{-\infty}^{+\infty} \exp\left\{-\beta \frac{p_z^2}{2m^*}\right\} dp_z \int_{-\infty}^{+\infty} \exp\left\{-\beta \frac{p_q^2}{2m^*}\right\} dp_q \int_{-\infty}^{+\infty} p_j^2 \exp\left\{-\beta \frac{p_j^2}{2m^*}\right\} dp_j \end{aligned}$$

Applying then the identities $\int_{-\infty}^{+\infty} \exp\{-a x^2\} dx = \left(\frac{\pi}{a}\right)^{1/2}$ and $\int_{-\infty}^{+\infty} x^2 \exp\{-a x^2\} dx = \frac{1}{2a} \left(\frac{\pi}{a}\right)^{1/2}$ (from the table of integrals [18]) to all three gaussian integrals results in:

$$= \frac{m^*}{\beta} \left(\frac{2\pi m^*}{\beta}\right)^{3/2} \exp\{-\beta U\}$$

The two cases can then be merged under the unique expression involving Kronecker's delta:

$$\int_{\Omega_{\mathbf{p}}} p_j p_l \exp\{-\beta E\} d\mathbf{p} = \frac{m^*}{\beta} \left(\frac{2\pi m^*}{\beta}\right)^{3/2} \delta_{j,l} \exp\{-\beta E\}$$

Substituting these integrals into the expression for $\bar{n}(\mathbf{r})$ yields:

$$\begin{aligned} \bar{n} &= \left(\frac{2\pi m^*}{\beta}\right)^{3/2} \exp\{-\beta U\} + \frac{\hbar^2 \beta^3}{24 (m^*)^2} \frac{m^*}{\beta} \left(\frac{2\pi m^*}{\beta}\right)^{3/2} \exp\{-\beta U\} \sum_{\substack{q \in \{1,2,3\} \\ m \in \{1,2,3\}}} \frac{\partial^2 U}{\partial r_q \partial r_m} \delta_{q,m} \\ &+ \frac{\hbar^2 \beta^3}{24 m^*} \left(\frac{2\pi m^*}{\beta}\right)^{3/2} \exp\{-\beta U\} \nabla U \cdot \nabla U - \frac{\hbar^2 \beta^2}{8 m^*} \left(\frac{2\pi m^*}{\beta}\right)^{3/2} \exp\{-\beta U\} \nabla^2 U \end{aligned}$$

which, because of the presence of Kronecker's delta, simplifies to:

$$\begin{aligned} &= \left(\frac{2\pi m^*}{\beta}\right)^{3/2} \exp\{-\beta U\} + \frac{\hbar^2 \beta^2}{24 m^*} \left(\frac{2\pi m^*}{\beta}\right)^{3/2} \exp\{-\beta U\} \nabla^2 U \\ &+ \frac{\hbar^2 \beta^3}{24 m^*} \left(\frac{2\pi m^*}{\beta}\right)^{3/2} \exp\{-\beta U\} \nabla U \cdot \nabla U - \frac{\hbar^2 \beta^2}{8 m^*} \left(\frac{2\pi m^*}{\beta}\right)^{3/2} \exp\{-\beta U\} \nabla^2 U \end{aligned}$$

Combining the [blue terms](#) and collecting the coefficients in the resulting expression finally gives:

$$= \left(\frac{2\pi m^*}{\beta}\right)^{3/2} \exp\{-\beta U\} \left[1 + \frac{\hbar^2 \beta}{12 m^*} \left(\frac{\beta^2}{2} \nabla U \cdot \nabla U - \beta \nabla^2 U\right)\right] \quad (7.5)$$

While this expression is already more compact than the starting one, it can be further simplified by writing the electron density as the deterministic one plus an additional term of the order of \hbar^2 :

$$\bar{n} = \left(\frac{2\pi m^*}{\beta}\right)^{3/2} \exp\{-\beta U\} + O(\hbar^2)$$

Taking the gradient of this expression yields:

$$\nabla \bar{n} = -\beta (\nabla U) \left(\frac{2\pi m^*}{\beta}\right)^{3/2} \exp\{-\beta U\} + O(\hbar^2)$$

Recognizing the [electron density](#) in the equation and substituting it gives:

$$\nabla \bar{n} = -\beta (\nabla U) \bar{n} + O(\hbar^2) \quad (7.6)$$

Taking the divergence of Equation 7.6 results in the equation:

$$\nabla \cdot (\nabla \bar{n}) = -\beta \nabla \cdot (\bar{n} \nabla U) + O(\hbar^2)$$

Applying the vector calculus identity: [19]

$$\nabla \cdot (\alpha \mathbf{A}) = \alpha \nabla \cdot \mathbf{A} + \mathbf{A} \cdot \nabla \alpha$$

and recognizing the laplacian ($\nabla^2 = \nabla \cdot \nabla$) then gives:

$$\nabla^2 \bar{n} = -\beta \bar{n} \nabla^2 U + \beta^2 \nabla U \cdot \nabla U \bar{n} + O(\hbar^2) \quad (7.7)$$

An expression for $\nabla U \cdot \nabla U$ can be found by taking the dot product of Equation 7.6 with itself, obtaining:

$$\nabla \bar{n} \cdot \nabla \bar{n} = \beta^2 \bar{n}^2 \nabla U \cdot \nabla U \quad (7.8)$$

Substituting Equation 7.8 into Equation 7.7 then yields an expression for the term $-\beta \nabla^2 U$ in the original equation as:

$$\begin{aligned} \nabla^2 \bar{n} &= -\beta \bar{n} \nabla^2 U + \frac{\nabla \bar{n} \cdot \nabla \bar{n}}{\bar{n}} + O(\hbar^2) \\ -\beta \nabla^2 U &= \frac{\nabla^2 \bar{n}}{\bar{n}} - \frac{\nabla \bar{n} \cdot \nabla \bar{n}}{\bar{n}^2} + O(\hbar^2) \end{aligned} \quad (7.9)$$

Equation 7.8 gives instead an expression for $\beta^2 \nabla U \cdot \nabla U$ as:

$$\beta^2 \nabla U \cdot \nabla U = \frac{\nabla \bar{n} \cdot \nabla \bar{n}}{\bar{n}^2} \quad (7.10)$$

Substituting Equation 7.10 and Equation 7.9 in Equation 7.5 then gives:

$$\bar{n} = \left(\frac{2\pi m^*}{\beta} \right)^{3/2} \exp\{-\beta U\} \left[1 + \frac{\hbar^2 \beta}{12 m^*} \left(\frac{1}{2} \frac{\nabla \bar{n} \cdot \nabla \bar{n}}{\bar{n}^2} + \frac{\nabla^2 \bar{n}}{\bar{n}} - \frac{\nabla \bar{n} \cdot \nabla \bar{n}}{\bar{n}^2} + O(\hbar^2) \right) \right]$$

Being the term $\hbar^2 O(\hbar^2)$ of order $O(\hbar^4)$ it is then neglected (in this model only quantum corrections of order up to \hbar^2 are retained):

$$\bar{n} = \left(\frac{2\pi m^*}{\beta} \right)^{3/2} \exp\{-\beta U\} \left[1 + \frac{\hbar^2 \beta}{12 m^*} \left(\frac{\nabla^2 \bar{n}}{\bar{n}} - \frac{1}{2} \frac{\nabla \bar{n} \cdot \nabla \bar{n}}{\bar{n}^2} \right) \right] \quad (7.11)$$

Consider now the vector identities: [19]

$$\begin{aligned} \nabla^2 (\phi \psi) &= \phi \nabla^2 \psi + 2 (\nabla \phi) \cdot (\nabla \psi) + \psi \nabla^2 \phi \\ \nabla (\psi \phi) &= \phi \nabla \psi + \psi \nabla \phi \end{aligned}$$

and apply them to identical functions ϕ ; the result is then:

$$\nabla^2 (\phi^2) = 2 \phi \nabla^2 \phi + 2 (\nabla \phi) \cdot (\nabla \phi) \quad (7.12)$$

$$\nabla (\phi^2) = 2 \phi \nabla \phi \quad (7.13)$$

Then multiply Equation 7.12 by $2 \phi^2$ and take the dot product of with itself, obtaining:

$$2 \phi^2 \nabla^2 (\phi^2) = 4 \phi^3 \nabla^2 \phi + 4 \phi^2 \nabla \phi \cdot \nabla \phi \quad (7.14)$$

$$\nabla (\phi^2) \cdot \nabla (\phi^2) = 4 \phi^2 \nabla \phi \cdot \nabla \phi \quad (7.15)$$

Subtracting Equation 7.15 from Equation 7.14 results in:

$$2 \phi^2 \nabla^2 (\phi^2) - \nabla \phi^2 \cdot \nabla \phi^2 = 4 \phi^3 \nabla^2 \phi \quad (7.16)$$

Applying this relationship to $\phi = \sqrt{\bar{n}}$ then gives:

$$2 \bar{n} \nabla^2 \bar{n} - \nabla \bar{n} \cdot \nabla \bar{n} = 4 \bar{n} \sqrt{\bar{n}} \nabla^2 \sqrt{\bar{n}}$$

Dividing both sides by $2\bar{n}^2$ the following relationship is obtained:

$$\frac{\nabla^2 \bar{n}}{\bar{n}} - \frac{1}{2} \frac{\nabla \bar{n} \cdot \nabla \bar{n}}{\bar{n}^2} = 2 \frac{\nabla^2 \sqrt{\bar{n}}}{\sqrt{\bar{n}}}$$

Applying this relationship to Equation 7.11 reduces it to:

$$\bar{n} = \left(\frac{2\pi m^*}{\beta} \right)^{3/2} \exp\{-\beta U\} \left[1 + \frac{\hbar^2 \beta}{6 m^*} \frac{\nabla^2 \sqrt{\bar{n}}}{\sqrt{\bar{n}}} \right] \quad (7.17)$$

Since this must be a *single-electron* electron density it must be normalized to have unitary integral in space:

$$\bar{n} = \frac{\exp\{-\beta U\} \left[1 + \frac{\hbar^2 \beta}{6 m^*} \frac{\nabla^2 \sqrt{\bar{n}}}{\sqrt{\bar{n}}} \right]}{\int_{\Omega} \exp\{-\beta U\} \left[1 + \frac{\hbar^2 \beta}{6 m^*} \frac{\nabla^2 \sqrt{\bar{n}}}{\sqrt{\bar{n}}} \right] d\mathbf{r}}$$

Multiplying both sides by $\exp\left\{-\beta \frac{\mathbf{p} \cdot \mathbf{p}}{2 m^*}\right\}$ and neglecting the quantum correction at the denominator (with the underlying assumption that the domain is much larger than the quantum confinement region) gives:

$$\bar{n} = \frac{\exp\{-\beta E\} \left[1 + \frac{\hbar^2 \beta}{6 m^*} \frac{\nabla^2 \sqrt{\bar{n}}}{\sqrt{\bar{n}}} \right]}{\int_{\Omega} \exp\{-\beta E\} d\mathbf{r}}$$

The density of electrons is then found by the law of large numbers by multiplying this single-particle density by the number N of particles within the system:

$$n = N \frac{\exp\{-\beta E\} \left[1 + \frac{\hbar^2 \beta}{6 m^*} \frac{\nabla^2 \sqrt{\bar{n}}}{\sqrt{\bar{n}}} \right]}{\int_{\Omega} \exp\{-\beta E\} d\mathbf{r}}$$

It is now useful to recall that in Boltzmann statistics the expected number $\langle N_i \rangle$ of particles with energy between E is given for electrons by:

$$n \underset{\hbar \rightarrow 0}{=} N_c \exp\left\{ \frac{-E + \mu_n}{k_B T} \right\}$$

where:

- N_c is the effective density of states in conduction band
- μ_n is the quasi-Fermi energy for the electrons
- k_B is the Boltzmann constant
- T is the temperature

As in the classical limit $\hbar \rightarrow 0$ the quantum-corrected distribution must become the Boltzmann distribution then it follows that:

$$n = N_c \exp\left\{ \frac{-E + \mu_n}{k_B T} \right\} \left[1 + \frac{1}{k_B T} \frac{\hbar^2}{6 m^*} \frac{\nabla^2 \sqrt{\bar{n}}}{\sqrt{\bar{n}}} \right] \quad (7.18)$$

If the quantum correction term $\frac{1}{k_B T} \frac{\hbar^2}{6 m^*} \frac{\nabla^2 \sqrt{\bar{n}}}{\sqrt{\bar{n}}}$ is not excessively large (i.e. for moderate quantum effects) the term:

$$\left[1 + \frac{1}{k_B T} \frac{\hbar^2}{6 m^*} \frac{\nabla^2 \sqrt{\bar{n}}}{\sqrt{\bar{n}}} \right]$$

can be interpreted as the 1st order expansion of an exponential and can therefore be rewritten as:

$$\left[1 + \frac{1}{k_B T} \frac{\hbar^2}{6 m^*} \frac{\nabla^2 \sqrt{n}}{\sqrt{n}} \right] \approx \exp \left\{ \frac{1}{k_B T} \frac{\hbar^2}{6 m^*} \frac{\nabla^2 \sqrt{n}}{\sqrt{n}} \right\}$$

Introducing this approximation in the expression for the electron density (Equation 7.18) casts it into the final form:

$$n = N_c \exp \left\{ \frac{-E_c + \mu_n + q \Lambda_n}{k_B T} \right\} \quad \Lambda_n = \frac{\hbar^2}{6 m_n^* q} \frac{\nabla^2 \sqrt{n}}{\sqrt{n}} \quad (7.19)$$

Equation 7.19 is the final formulation of the **density gradient model**.

From this equation it is clear that the main effect of taking quantum corrections of the order of \hbar^2 into account introduces a correction to the potential energy when computing the carrier densities. This correction Λ is typically known as **quantum potential**.

The name of this model derives from the fact that the quantum potential depends on the derivative of the charge density.

A similar expression can be introduced also for holes by following the same procedure as above:

$$p = N_v \exp \left\{ \frac{E_v - \mu_p + q \Lambda_p}{k_B T} \right\} \quad \Lambda_p = \frac{\hbar^2}{6 m_p^* q} \frac{\nabla^2 \sqrt{p}}{\sqrt{p}} \quad (7.20)$$

7.2 Density Gradient Model

Considering the effective masses to be dependent on the position, the expressions derived above take the forms: [20]

$$n = N_c \exp \left\{ \frac{-E_c + E_{f,n} + q \Lambda_n}{k_B T} \right\} \quad \Lambda_n = \frac{\hbar^2}{6 q} \frac{\nabla \cdot [(m_n^*)^{-1} \nabla \sqrt{n}]}{\sqrt{n}} \quad (7.21)$$

$$p = N_v \exp \left\{ \frac{E_v - E_{f,p} + q \Lambda_p}{k_B T} \right\} \quad \Lambda_p = \frac{\hbar^2}{6 q} \frac{\nabla \cdot [(m_p^*)^{-1} \nabla \sqrt{p}]}{\sqrt{p}} \quad (7.22)$$

and completing the density gradient model for the carrier concentrations with:

- the Poisson equation (relating the charge density ρ to the electrostatic potential ϕ) [21]

$$\nabla \cdot [\epsilon \nabla \phi] = -\rho \quad \rho = q (N_D^+ - N_A^- + p - n) \quad (7.23)$$

- the electron and hole continuity equations derived in section 6.3

$$-q \frac{\partial}{\partial t} \{n(\mathbf{r})\} + \nabla_r \cdot \{\mathbf{J}_n(\mathbf{r})\} - q R_n = 0 \quad \mathbf{J}_n(\mathbf{r}) = q D_n \nabla \{n(\mathbf{r})\} - q \mu_n n(\mathbf{r}) \nabla [\phi(\mathbf{r})] \quad (7.24)$$

$$q \frac{\partial}{\partial t} \{p(\mathbf{r})\} + \nabla \cdot \{\mathbf{J}_p(\mathbf{r})\} + q R_p = 0 \quad \mathbf{J}_p(\mathbf{r}) = -q D_p \nabla_r \{p(\mathbf{r})\} - q \mu_p p(\mathbf{r}) \nabla [\phi(\mathbf{r})] \quad (7.25)$$

then the **quantum drift-diffusion** model is obtained.

7.3 More Practical Form

The continuity equations as they are reported in Equation 7.24 and 7.25 are extremely common in the literature but are not the most convenient form for the implementation in a numerical solver.

Since by the chain rule the following identity holds:

$$\nabla n(\mathbf{r}) = n(\mathbf{r}) \nabla \{\ln n\}(\mathbf{r})$$

then the expression for the current due to an electron flow can be rewritten as:

$$\mathbf{J}_n(\mathbf{r}) = q D_n n(\mathbf{r}) \nabla \{\ln n\}(\mathbf{r}) - q\mu_n n(\mathbf{r}) \nabla [\phi(\mathbf{r})]$$

Assuming then the value of the effective density of states in conduction band $N_c(\mathbf{r})$ to be piecewise-constant in all the regions of the device, the addition of its gradient does not alter the validity of the equation, which becomes:

$$\mathbf{J}_n(\mathbf{r}) = q D_n n(\mathbf{r}) \nabla \{\ln(n) - \ln(N_c)\}(\mathbf{r}) - q\mu_n n(\mathbf{r}) \nabla [\phi(\mathbf{r})]$$

$$\mathbf{J}_n(\mathbf{r}) = q D_n n(\mathbf{r}) \nabla \left\{ \ln \left(\frac{n}{N_c} \right) \right\}(\mathbf{r}) - q\mu_n n(\mathbf{r}) \nabla [\phi(\mathbf{r})]$$

Assuming the quantum-corrected distribution to be close to a Boltzmann distribution (i.e. the quantum correction to be small) then the expression for the electron current can be rewritten neglecting the correction terms as:

$$\mathbf{J}_n(\mathbf{r}) = q D_n n(\mathbf{r}) \nabla \left\{ \frac{-E_c(\mathbf{r}) + E_{f,n}(\mathbf{r})}{k_B T} \right\}(\mathbf{r}) - q\mu_n n(\mathbf{r}) \nabla [\phi(\mathbf{r})]$$

Since $-q\phi$ and E_c are piecewise parallel in each region of the device, then the following substitution is allowed:

$$\mathbf{J}_n(\mathbf{r}) = q D_n n(\mathbf{r}) \nabla \left\{ \frac{q\phi + E_{f,n}(\mathbf{r})}{k_B T} \right\}(\mathbf{r}) - q\mu_n n(\mathbf{r}) \nabla [\phi(\mathbf{r})]$$

Recalling Einstein's relationships for the diffusivity:

$$D_n = \frac{k_B T}{q} \mu_n$$

the terms involving $\nabla\phi$ cancel out and the expression simplifies to:

$$\mathbf{J}_n(\mathbf{r}) = \mu_n n(\mathbf{r}) \nabla E_{f,n}(\mathbf{r}) \tag{7.26}$$

Similarly, the following expression can be derived for holes:

$$\mathbf{J}_p(\mathbf{r}) = \mu_p p(\mathbf{r}) \nabla E_{f,p}(\mathbf{r}) \tag{7.27}$$

These expressions for the current densities are not entirely identical to the ones that were reported in Equation 7.24 and 7.25, since there is the underlying assumption that the statistics be close to a *classical Boltzmann* one. This should be an acceptable approximation in the case of either Fermi statistics without excessive degeneracy or small quantum corrections.

This expression can also be obtained in the semiclassical case from the method of moments applied to the Boltzmann transport equation by applying slightly different assumptions and approximations from the ones that have been treated in section 6.2. [22] These kinds of derivations however also rely on the similar assumption that the statistics be close to an equilibrium Boltzmann statistics (therefore being equivalent to the derivation presented here, in several points of which the quantum correction is assumed to be small).

This kind of formulation is typically preferred when treating modifications to the Boltzmann statistics (both quantum and semiclassical). Indeed, adopting the formulation of Equation 7.24 and 7.25 would lead to the equation for the quantum potential being completely decoupled from the other differential equations, which is of course not physical (it would mean that it would be possible to compute the quantum correction but it would not be then applied in any way to the resulting system of equations; this will however be more evident when discussing the discretization of this model).

Chapter 8

Generation/Recombination Mechanisms

8.1 Shockley Read Hall Generation/Recombination

In absence of relevant optical generation/recombination phenomena, which is the case for most high-speed electronic devices, the most important generation and recombination phenomena are of thermal nature. This means that both the energy and momentum required for the transition are supplied by lattice vibrations, i.e. phonons.

A well-known trend in solid-state physics is that any thermal generation or recombination process involving carriers at two energy levels becomes exponentially less likely as the spacing between the levels increases.

The presence of additional trap levels within the gap (typically ascribed to defects in the crystal lattice) allows for two-step generation and recombination phenomena in which the energy difference is much smaller at each step, therefore potentially increasing exponentially the probability of transition.

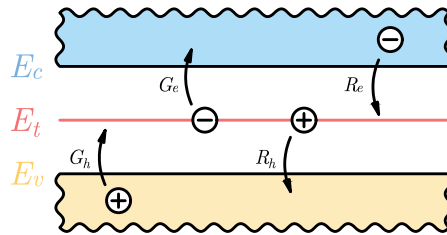


Figure 8.1: Shockley Read Hall processes

In a semiconductor with a single trap level, such as the one shown in Figure 8.1 four possible processes can take place:

- an electron can be emitted from the trap level E_t into the conduction band E_c ; it is an electron generation phenomenon (denoted by G_e in Figure 8.1).

If the trap level accounts for N_t states and the state probability of occupation for electrons in it is $f(E_t)$ (with f the probability of occupation being considered) then the generation rate for electrons can be quantified as:

$$G_n^{SRH} = r_{e,n}^{SRH} N_t f(E_t)$$

where $r_{e,n}^{SRH}$ is the emission probability for an electron from the trap level into the conduction band. The conduction band has been assumed here to have enough empty electron states not to limit the probability for these transitions.

- a hole can be emitted from the trap level E_t into the valence band E_v ; it is a hole generation phenomenon (denoted by G_h in Figure 8.1).

If the trap level accounts for N_t states and the state probability of occupation for holes in it is $1 - f(E_t)$ then the generation rate for holes can be quantified as:

$$G_p^{SRH} = r_{e,p}^{SRH} N_t (1 - f(E_t))$$

where $r_{e,p}^{SRH}$ is the emission probability for a hole from the trap level into the valence band. The valence band has been assumed here to have enough empty hole states not to limit the probability for these transitions.

- an electron can be captured by the trap level E_t from the conduction band E_c ; it is an electron recombination phenomenon (denoted by R_e in Figure 8.1).

If the trap level accounts for N_t states and the state probability of non-occupation for electrons in it is $1 - f(E_t)$ then the recombination rate for electrons can be quantified as:

$$R_n^{SRH} = r_{c,n}^{SRH} n N_t (1 - f(E_t))$$

where $r_{c,n}^{SRH}$ is the capture probability for an electron from the conduction band by the trap level. The density of electrons n in the conduction band includes both the density of states and the probability of occupation for electrons (in this case both destination and source probabilities of occupation must be taken into account since there are few electrons in valence band).

- a hole can be captured by the trap level E_t from the valence band E_v ; it is a hole recombination phenomenon (denoted by R_h in Figure 8.1).

If the trap level accounts for N_t states and the state probability of non-occupation for holes in it is $f(E_t)$ then the recombination rate for holes can be quantified as:

$$R_p^{SRH} = r_{c,p}^{SRH} p N_t f(E_t)$$

where $r_{c,p}^{SRH}$ is the capture probability for a hole from the valence band by the trap level. The density of holes p in the valence band includes both the density of states and the probability of occupation of holes (in this case both destination and source probabilities of occupation must be taken into account since there are few holes in valence band).

At thermodynamic equilibrium the electron population should not vary, hence the condition $R_n^{SRH} = G_n^{SRH}$ must be satisfied. Then the following relationship must hold true:

$$\begin{aligned} r_{e,n}^{SRH} N_t f_{eq}(E_t) &= r_{c,n}^{SRH} n_{eq} N_t (1 - f_{eq}(E_t)) \\ r_{e,n}^{SRH} &= r_{c,n}^{SRH} n_{eq} \frac{1 - f_{eq}(E_t)}{f_{eq}(E_t)} \end{aligned} \quad (8.1)$$

where f_{eq} is the equilibrium probability density function.

Similarly, at thermodynamic equilibrium the hole population should not vary, hence the condition $R_p^{SRH} = G_p^{SRH}$ must be satisfied. Then the following relationship must hold true:

$$\begin{aligned} r_{e,p}^{SRH} N_t (1 - f_{eq}(E_t)) &= r_{c,p}^{SRH} p_{eq} N_t f_{eq}(E_t) \\ r_{e,p}^{SRH} &= r_{c,p}^{SRH} p_{eq} \frac{f_{eq}(E_t)}{1 - f_{eq}(E_t)} \end{aligned} \quad (8.2)$$

Defining then the trap hole and electron densities at equilibrium n_t and p_t as:

$$n_t \triangleq n_{eq} \frac{1 - f_{eq}(E_t)}{f_{eq}(E_t)} \quad p_t \triangleq p_{eq} \frac{f_{eq}(E_t)}{1 - f_{eq}(E_t)} \quad (8.3)$$

then the previous relationships reduce to:

$$r_{e,n}^{SRH} = r_{c,n}^{SRH} n_t \quad r_{e,p}^{SRH} = r_{c,p}^{SRH} p_t \quad (8.4)$$

Writing then the net recombination rates for electrons and holes and substituting these relationships then yields:

$$U_n^{SRH} = R_n^{SRH} - G_n^{SRH} = r_{c,n}^{SRH} N_t [n (1 - f(E_t)) - n_t f(E_t)] \quad (8.5)$$

$$U_p^{SRH} = R_p^{SRH} - G_p^{SRH} = r_{c,p}^{SRH} N_t [p f(E_t) - p_t (1 - f(E_t))] \quad (8.6)$$

Since generation processes always lead to the formation of a free electron-free hole pair and since recombination processes always lead to the mutual annihilation of a free electron and a free hole then the two net recombination rates must be equal:

$$U_n^{SRH} = U_p^{SRH} \triangleq U^{SRH}$$

Equating then Equation 8.5 and 8.6 the following result is obtained:

$$\begin{aligned} r_{c,n}^{SRH} N_t [n (1 - f(E_t)) - n_t f(E_t)] &= r_{c,p}^{SRH} N_t [p f(E_t) - p_t (1 - f(E_t))] \\ r_{c,n}^{SRH} N_t n - r_{c,n}^{SRH} N_t (n + n_t) f(E_t) &= -r_{c,p}^{SRH} N_t p_t + r_{c,p}^{SRH} N_t (p + p_t) f(E_t) \\ r_{c,n}^{SRH} n - r_{c,n}^{SRH} (n + n_t) f(E_t) &= -r_{c,p}^{SRH} p_t + r_{c,p}^{SRH} (p + p_t) f(E_t) \\ r_{c,p}^{SRH} (p + p_t) f(E_t) + r_{c,n}^{SRH} (n + n_t) f(E_t) &= r_{c,n}^{SRH} n + r_{c,p}^{SRH} p_t \\ f(E_t) &= \frac{r_{c,n}^{SRH} n + r_{c,p}^{SRH} p_t}{r_{c,p}^{SRH} (p + p_t) + r_{c,n}^{SRH} (n + n_t)} \end{aligned} \quad (8.7)$$

Substituting Equation 8.7 into Equation 8.5 leads to:

$$U^{SRH} = r_{c,n}^{SRH} N_t \left[n \left(1 - \frac{r_{c,n}^{SRH} n + r_{c,p}^{SRH} p_t}{r_{c,p}^{SRH} (p + p_t) + r_{c,n}^{SRH} (n + n_t)} \right) - n_t \frac{r_{c,n}^{SRH} n + r_{c,p}^{SRH} p_t}{r_{c,p}^{SRH} (p + p_t) + r_{c,n}^{SRH} (n + n_t)} \right]$$

which can be rearranged as:

$$U^{SRH} = r_{c,n}^{SRH} N_t \left[n \left(\frac{r_{c,p}^{SRH} (p + p_t) + r_{c,n}^{SRH} (n + n_t) - r_{c,n}^{SRH} n - r_{c,p}^{SRH} p_t}{r_{c,p}^{SRH} (p + p_t) + r_{c,n}^{SRH} (n + n_t)} \right) + \right. \\ \left. - n_t \frac{r_{c,n}^{SRH} n + r_{c,p}^{SRH} p_t}{r_{c,p}^{SRH} (p + p_t) + r_{c,n}^{SRH} (n + n_t)} \right]$$

$$U^{SRH} = r_{c,n}^{SRH} N_t \left[\frac{r_{c,p}^{SRH} np + r_{c,p}^{SRH} np_t + r_{c,n}^{SRH} n^2 + r_{c,n}^{SRH} nn_t - r_{c,n}^{SRH} n^2 - r_{c,p}^{SRH} np_t}{r_{c,p}^{SRH} (p + p_t) + r_{c,n}^{SRH} (n + n_t)} + \right. \\ \left. + \frac{-n_t r_{c,n}^{SRH} n - n_t r_{c,p}^{SRH} p_t}{r_{c,p}^{SRH} (p + p_t) + r_{c,n}^{SRH} (n + n_t)} \right]$$

$$U^{SRH} = r_{cn}^{SRH} r_{cp}^{SRH} N_t \left[\frac{np - n_t p_t}{r_{cn}^{SRH} (n + n_t) + r_{cp}^{SRH} (p + p_t)} \right]$$

$$U^{SRH} = \frac{np - n_t p_t}{\frac{r_{cn}^{SRH}}{r_{cn}^{SRH} r_{cp}^{SRH} N_t} (n + n_t) + \frac{r_{cp}^{SRH}}{r_{cn}^{SRH} r_{cp}^{SRH} N_t} (p + p_t)}$$

$$U^{SRH} = \frac{np - n_t p_t}{\frac{1}{r_{cp}^{SRH} N_t} (n + n_t) + \frac{1}{r_{cn}^{SRH} N_t} (p + p_t)} \quad (8.8)$$

The term $n_t p_t$ can be rewritten by substituting the definition of the trap level densities n_t and p_t given in Equation 8.3:

$$n_t p_t = n_{eq} \frac{f_{eq}(E_t)}{1 - f_{eq}(E_t)} p_{eq} \frac{1 - f_{eq}(E_t)}{f_{eq}(E_t)} = n_{eq} p_{eq}$$

Assuming the degeneracy of the material to be negligible and quasi-Boltzmann statistics to apply, the mass-action law $n_{eq} p_{eq} \approx n_i^2$ approximately holds and:

$$n_t p_t = n_{eq} p_{eq} \approx n_i^2 \quad (8.9)$$

Substituting this result in Equation 8.10 leads to the final equation:

$$U^{SRH} \approx \frac{np - n_i^2}{\frac{1}{r_{cp}^{SRH} N_t} (n + n_t) + \frac{1}{r_{cn}^{SRH} N_t} (p + p_t)} \quad (8.10)$$

Defining then the non-radiative Shockley-Read-Hall lifetimes:

$$\tau_p \triangleq \frac{1}{r_{cp}^{SRH} N_t} \quad \tau_n \triangleq \frac{1}{r_{cn}^{SRH} N_t}$$

the equation for the Shockley-Read-Hall recombination rate becomes:

$$\boxed{U^{SRH} \approx \frac{np - n_i^2}{\tau_p(n + n_t) + \tau_n(p + p_t)}} \quad (8.11)$$

Considering Fermi statistics with no degenerate levels, i.e. with a probability of occupation:

$$f_{eq}(E) = \frac{1}{1 + \exp\{E - E_f\}}$$

then the expressions of Equation 8.3 for n_t and p_t of can be rewritten as:

$$n_t \triangleq n_{eq} \frac{1 - \frac{1}{1 + \exp\{E_t - E_f\}}}{1 + \exp\{E_t - E_f\}} = n_{eq} \exp\left\{\frac{E_t - E_f}{k_B T}\right\}$$

$$p_t \triangleq p_{eq} \frac{\frac{1}{1 + \exp\{E_t - E_f\}}}{1 - \frac{1}{1 + \exp\{E_t - E_f\}}} = p_{eq} \exp\left\{\frac{E_f - E_t}{k_B T}\right\}$$

Assuming also in this case the degeneracy of the material to be negligible and quasi-Boltzmann statistics to apply, the Shockley equations:

$$n_{eq} \approx n_i \exp\left\{\frac{E_f - E_{fi}}{k_B T}\right\} \quad p_{eq} \approx n_i \exp\left\{\frac{E_{fi} - E_f}{k_B T}\right\}$$

can be applied, rewriting the previous expressions for n_t and p_t as:

$$\boxed{n_t = n_i \exp\left\{\frac{E_t - E_{fi}}{k_B T}\right\} \quad p_t = n_i \exp\left\{\frac{E_{fi} - E_t}{k_B T}\right\}} \quad (8.12)$$

Chapter 9

Heterostructures and Boundary Conditions

9.1 Heterostructures

A **heterojunction** is an interface between two layers or regions of different semiconductors.

At a heterojunction many properties of the material can therefore change, ideally also in an abrupt way; among these the bandgap, the electron affinity, the effective masses of electrons and holes, the conduction and valence band effective densities of states, the mobilities and the generation/recombination lifetimes.

The combination of one or more heterojunctions within a device yields a **heterostructure**.

Heterostructures are of utmost importance in electronics and optoelectronics as they allow to obtain effective carrier confinement. This is possible because at heterojunctions the conduction and valence band edges (E_c and E_v) can be discontinuous, as is shown in the example of Figure 9.1.

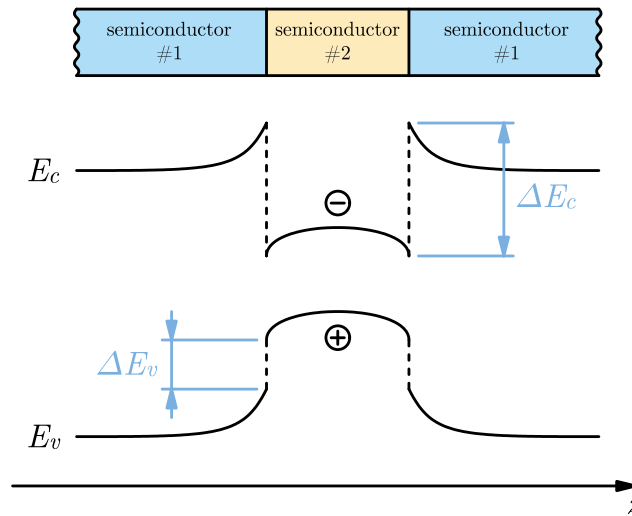


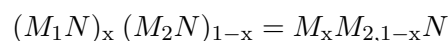
Figure 9.1: Confinement with heterostructures

The simplest way to obtain tunable heterostructures (in which the discontinuities in the parameters and in the band structure can be finely tuned) is to use **semiconductor alloys**.

Semiconductor alloys are intimately united (in a uniform way) mixtures of two or more components that together exhibit semiconductive behavior. By controlling the molar fractions (usually known as x and y) of the components of the alloy it is possible to tune the parameters of the resulting semiconductor.

Two most common types of semiconductor alloys exist:

- **ternary alloys**, they are obtained by combining two different compound semiconductors which share either the same metal or the same nonmetal:



$$(MN_1)_y (MN_2)_{1-y} = MN_y N_{2,1-y}$$

- **quaternary alloys**, they are obtained by either combining four different compound semiconductors sharing all metals and nonmetals:

$$\begin{aligned} (M_1N_1)_\alpha (M_1N_2)_\beta (M_2N_1)_\gamma (M_2N_2)_{1-\alpha-\beta-\gamma} &= M_{1,\alpha+\beta} M_{2,1-\alpha-\beta} N_{1,\alpha+\gamma} N_{2,1-\alpha-\gamma} \\ &= M_{1,x} M_{2,1-x} N_{1,y} N_{2,1-y} \end{aligned}$$

or by combining three different compound semiconductors which share the same non-metallic element:

$$(M_1N)_x (M_2N)_y (M_3N)_{1-x-y} = M_x M_{2,y} M_{3,1-x-y} N$$

(where M represent metals and N represent nonmetals, x represents the molar fraction of a metal and y represents the molar fraction of a non-metal)

It is important to remark that in heterostructures continuity of the crystalline structure must be guaranteed at the heterojunction to guarantee conduction through it in electronic applications. Epitaxial growth is typically the process of choice for creating heterostructures that satisfy this requirement.

9.1.1 Modeling of Heterojunctions

When devices with heterojunctions are considered, the potential energies E_c and E_v for electrons in the conduction band and for holes in the valence band typically exhibit spatial discontinuities.

This is expected and unavoidable with abrupt heterojunctions since as a result of abrupt spatial changes in bandgap energy and electron affinity the conduction band edge E_c , the valence band E_v and the bandgap energy E_g cannot all be continuous.

The discontinuities in the potential energies for the free particles however constitute a major issue when trying to extend Poisson's equation:

$$\nabla \cdot [\epsilon \nabla \phi] = -\nabla \cdot [\epsilon \varepsilon] = -\rho$$

to the case with heterojunctions.

While in treatments involving homojunctions only the electrostatic potential ϕ can be taken to be coincident with either the conduction band edge E_c , the valence band edge E_v , the vacuum level U_0 or the intrinsic Fermi energy E_{fi} , this is not possible anymore when heterojunctions are included. The main reason for this is that a discontinuity in the potential energy at the heterojunction would cause Dirac deltas in the electric field and therefore derivatives of Dirac deltas in the charge, which is obviously not a physical condition.

The best choice is then to take the electrostatic potential to be parallel to the energy band edges within every layer but at the same time imposing its continuity at the heterojunctions. This means that only a piecewise constant difference will exist between the energy band edges and the electrostatic potential, as is depicted in Figure 9.2 for the case of the conduction band.

In the case of Figure 9.2 the electrostatic potential is taken so that the conduction band edge can be written as:

$$E_c(z) = -q\phi(z) + \Delta E_c(z) \quad \text{with} \quad \Delta E_c(z=0) = 0 \quad (9.1)$$

with $\Delta E_c(z)$ a piecewise constant function of the spatial coordinate z . The constraint that has been added on the conduction band offset ΔE_c at the spatial coordinate $z = 0$ is meant to remove any possible ambiguity in the definition of the electrostatic potential which could otherwise still arise.

The definition of the electrostatic potential given in Equation 9.1 will be used all throughout this treatment.

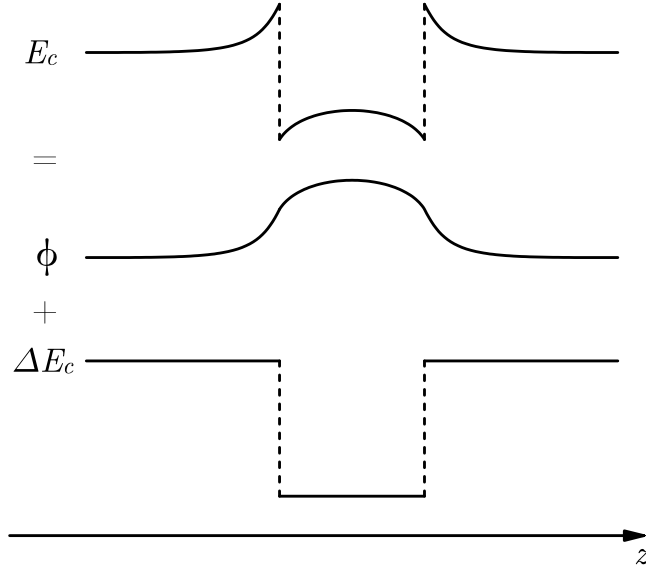


Figure 9.2: Continuous definition of the electrostatic potential with a heterojunction

Another useful quantity to be defined is the valence band offset $\Delta E_v(z)$, which is defined so that:

$$E_v(z) = -q\phi(z) + \Delta E_v(z) - E_g(0) \quad \text{with} \quad \Delta E_v(z=0) = 0 \quad (9.2)$$

with $\Delta E_v(z)$ a piecewise constant function of the spatial coordinate z . The constraint that has been added on the valence band offset ΔE_v at the spatial coordinate $z = 0$ is meant to remove any possible ambiguity in the definition of the electrostatic potential which could otherwise still arise.

It is important to notice that, adopting these definitions:

- all the information about the band discontinuities is encoded in the conduction and valence band offsets ΔE_c and ΔE_v
- all the information about the continuous variations of the energy bands is enclosed in the electrostatic potential ϕ
- the valence band offset E_v includes also the discontinuities related to the variations in the bandgap

Moreover, another important point to be remarked is that in the interior points of every layer of the structure the gradients of:

- the conduction band edge E_c
- the valence band edge E_v
- the opposite of the electrostatic potential energy $-q\phi$
- the vacuum energy U_0

exist and are identical:

$$\nabla E_c = \nabla E_v = \nabla U_0 = -q\nabla\phi$$

This is extremely practical since it allows to identify the electrostatic potential energy with a discontinuous energy band in each layer (therefore adopting a different reference for the electrostatic potential energy in each layer) and then simply apply boundary conditions at the interfaces between layers. In particular, these conditions will be shown to be extremely simple and leading to very compact results in the next section.

9.2 Boundary Conditions

9.2.1 Heterojunctions and Homojunctions

Since the final goal is to develop a simulator that solves numerically the system composed of 5 partial differential equations it is useful to consider them one at a time and to determine the best boundary conditions for each:

- Poisson's equation:

$$\nabla \cdot [\epsilon \nabla \phi] = -\rho \qquad \rho = q (N_D^+ - N_A^- + p - n) \qquad (9.3)$$

To derive a boundary condition for the electrostatic potential it is sufficient to enforce the previously mentioned definition for the electrostatic potential:

$$E_c = -q\phi + \Delta E_c$$

with ϕ a continuous function of the spatial coordinate \mathbf{r} and ΔE_c a piecewise constant function. The correct choice of boundary condition is then to impose the continuity of ϕ at the interface, as the effect of the interface on the conduction band edge E_c is already included within ΔE_c .

- electron continuity equation (static conditions):

$$\nabla_{\mathbf{r}} \cdot \{\mathbf{J}_{\mathbf{n}}(\mathbf{r})\} - q R_n = 0 \qquad \mathbf{J}_{\mathbf{n}}(\mathbf{r}) = \mu_n n(\mathbf{r}) \nabla E_{f,n}(\mathbf{r}) \qquad (9.4)$$

Since the derivatives of a discontinuous functions involve Dirac deltas and the recombination rates cannot physically be infinite, it is necessary to impose the continuity of the electron current density at the heterointerfaces.

- hole continuity equation (static conditions):

$$\nabla \cdot \{\mathbf{J}_{\mathbf{p}}(\mathbf{r})\} + q R_p = 0 \qquad \mathbf{J}_{\mathbf{p}}(\mathbf{r}) = \mu_p p(\mathbf{r}) \nabla E_{f,p}(\mathbf{r}) \qquad (9.5)$$

Similarly to the case of the electron continuity equation, also in this case the hole current density must be continuous at the heterointerfaces to avoid unphysical situations in which the recombination rates must be infinite.

- electron quantum potential definition:

$$\Lambda_n = \frac{\hbar^2}{6q} \frac{\nabla \cdot [(m_n^*)^{-1} \nabla \sqrt{n}]}{\sqrt{n}} \qquad (9.6)$$

Observing this equation shows that in order to avoid having derivatives (in the sense of distributions) of Dirac delta functions (which would arise from the double derivative of the square root of a discontinuous electron density \sqrt{n}), which are not physical, the electron density n must be continuous.

- hole quantum potential definition:

$$\Lambda_p = \frac{\hbar^2}{6q} \frac{\nabla \cdot [(m_p^*)^{-1} \nabla \sqrt{p}]}{\sqrt{p}} \qquad (9.7)$$

Similarly to the case of electrons, this equation shows that in order to avoid having derivatives of Dirac delta functions (which would arise from the double derivative of the square root of a discontinuous electron density \sqrt{p}), which are not physical, the hole density p must be continuous.

It is important to notice that, differently from the case of the semiclassical drift-diffusion model, in a density gradient (i.e. quantum drift-diffusion) model the electron and hole concentrations need to be continuous.

This is a clear sign that the solutions of the semiclassical drift-diffusion model in the presence of strong electron and hole density discontinuities are not efficient initial guesses for the solution of the corresponding density gradient problem.

All of these continuity conditions will allow for a very simple treatment in the discretization that will follow, since they usually imply that the internal boundaries corresponding to heterojunctions can simply be "forgotten" when assembling the discretized equation.

9.2.2 Ohmic Contact

An ohmic contact is a non-rectifying electrical junction between a semiconductor or metal and another semiconductor or metal.

In its ideal version it is perfectly absorbing, i.e. it is characterized by **infinitely large recombination rate**.

In order to model this phenomenon it is important to remember that recombination ultimately leads to charge neutrality, i.e. that recombination at the contact is proportional to the excess carrier concentration with respect to neutrality. In other words, the recombination rate is given at the contact for electrons and holes respectively by:

$$R_{n,\text{cont.}} = v_n (n - n_0) \qquad R_{p,\text{cont.}} = v_p (p - p_0)$$

where n_0 and p_0 are the neutrality carrier densities and v_n and v_p are constants (the recombination velocities at the contact). It is important to remark that the dimensions of the recombination rates must be $m^{-2}s^{-1}$ (since the contact is a 2-dimensional structure and the result must be a rate), hence the constants must have the dimensions of velocities.

The recombination currents can then be derived by multiplying these fluxes (the recombination rates have the dimensions of fluxes) by the elementary charge and adopting the appropriate signs for the current densities: [23]

$$\mathbf{J}_n \cdot \hat{\mathbf{n}} = q v_n (n - n_0) \qquad \mathbf{J}_p \cdot \hat{\mathbf{n}} = -q v_p (p - p_0)$$

where $\hat{\mathbf{n}}$ is the unit normal vector to the ohmic contact, oriented towards the interior of the device as shown in Figure 9.3 for the case of a 1-dimensional device.

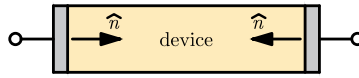


Figure 9.3: Reference frame definition for contacts (1D)

Assuming now an ideal ohmic contact to have infinite recombination velocities for electrons and holes, i.e. $v_n \rightarrow \infty$ and $v_p \rightarrow \infty$ and the current density to be finite leads to the condition:

$$n = n_0 \qquad p = p_0$$

which must hold true at an ideal ohmic contact.

Since the effect of an ohmic contact is to impose the neutrality condition to the material, it is also reasonable to assume the statistics to be the classical one at the ohmic contact, therefore considering the quantum potentials Λ_n and Λ_p to be approximately zero at ideal ohmic contacts.

This condition, supported by [23],[24] appears to be reasonable; other works by Ancona [25] suggest instead the usage of homogeneous Neumann boundary conditions, the results should however be similar as long as no heavy quantum effects are present near the contacts (which is the case for the high electron mobility transistors that are going to be treated, since both contacts are applied to layers far away from the quantum-confinement region).

Assuming then a quantum-corrected Boltzmann statistics, which reads:

$$n = N_c \exp \left\{ \frac{+q\phi - \Delta E_c + E_{f,n} + q \Lambda_n}{k_B T} \right\} \qquad p = N_v \exp \left\{ \frac{-q\phi - E_g(0) + \Delta E_v - E_{f,p} + q \Lambda_p}{k_B T} \right\} \quad (9.8)$$

the aforementioned conditions translate to:

$$\phi = \phi_0 - \frac{\Delta E_{f,n}}{q}$$

where:

- ϕ_0 is the electrostatic potential in equilibrium neutrality conditions and satisfies the condition:

$$n_0 = N_c \exp \left\{ \frac{+q\phi_0 - \Delta E_c + E_{f,n}^{eq}}{k_B T} \right\}$$

- $\Delta E_{f,n} = E_{f,n} - E_{f,n}^{eq}$ is the variation of the quasi-Fermi level from the equilibrium one

It is then clear that, since an applied voltage V at the contact has the effect of shifting the quasi-Fermi level by $-qV$, then the aforementioned variation in the quasi-Fermi level will be:

$$\Delta E_{f,n} = -qV$$

The neutrality electron and hole densities can be determined by imposing together:

- charge neutrality:

$$q(p_0 - n_0 + N_d^+ - N_a^-) = 0$$

- the mass-action law:

$$p_0 n_0 = n_i^2$$

Under a full ionization assumption the charge neutrality equation reduces to:

$$p_0 - n_0 + [N_d - N_a] = 0$$

Substituting the mass-action law into the charge neutrality condition to eliminate the hole density then leads to:

$$\frac{n_i^2}{n_0} - n_0 + [N_d - N_a] = 0$$

Multiplying by the neutrality electron density n_0 and solving the resulting 2nd degree equation gives:

$$\begin{aligned} n_i^2 - n_0^2 + [N_d - N_a] n_0 &= 0 \\ n_0 &= \frac{-[N_d - N_a] \pm \sqrt{[N_d - N_a]^2 + 4 n_i^2}}{-2} \end{aligned}$$

If $[N_d - N_a] > 0$ (net donor doping) then for the electron density to be positive the (which is the only physical situation) the correct root to be taken is:

$$n_0 = \frac{[N_d - N_a] + \sqrt{[N_d - N_a]^2 + 4 n_i^2}}{2} \quad p_0 = \frac{n_i^2}{n_0}$$

While this formula also works for $[N_d - N_a] < 0$, numerical cancellation between the terms $[N_d - N_a]$ and $\sqrt{[N_d - N_a]^2 + 4 n_i^2}$ of the sum leads to wrong results.

A better formula can be found instead by substituting the mass-action law into the charge neutrality condition to eliminate the electron density:

$$p_0 - \frac{n_i^2}{p_0} + [N_d - N_a] = 0$$

Multiplying by the neutrality hole density p_0 and solving the resulting 2nd degree equation gives:

$$\begin{aligned} p_0^2 - n_i^2 + [N_d - N_a] p_0 &= 0 \\ p_0 &= \frac{[N_d - N_a] \pm \sqrt{[N_d - N_a]^2 + 4 n_i^2}}{2} \end{aligned}$$

If $[N_d - N_a] < 0$ (net acceptor doping) then for the hole density to be positive (which is the only physical situation) the correct root to be taken is:

$$p_0 = \frac{[N_d - N_a] + \sqrt{[N_d - N_a]^2 + 4 n_i^2}}{2} \quad n_0 = \frac{n_i^2}{p_0}$$

Similarly to the previous case, this formula also works for $[N_d - N_a] > 0$; due to numerical cancellation between the terms $[N_d - N_a]$ and $\sqrt{[N_d - N_a]^2 + 4 n_i^2}$ the numerical implementation would however be problematic.

The best way of determining the neutrality carrier densities is then to adopt a piecewise model for the computation:

$$\left\{ \begin{array}{ll} n_0 = \frac{[N_d - N_a] + \sqrt{[N_d - N_a]^2 + 4 n_i^2}}{2} & p_0 = \frac{n_i^2}{n_0} \quad \text{if } [N_d - N_a] > 0 \\ p_0 = \frac{[N_d - N_a] + \sqrt{[N_d - N_a]^2 + 4 n_i^2}}{2} & n_0 = \frac{n_i^2}{p_0} \quad \text{if } [N_d - N_a] < 0 \end{array} \right. \quad (9.9)$$

9.2.3 Schottky Contact

Schottky contacts are rectifying contacts, i.e. contacts in which a potential barrier arises between the contact metal and the semiconductor.

In order to understand the physics of these contacts it is useful to first consider:

- a metal with workfunction $q\phi_m$
- a semiconductor with electron affinity $q\chi_s$

as the ones that are shown in the example of Figure 9.4.

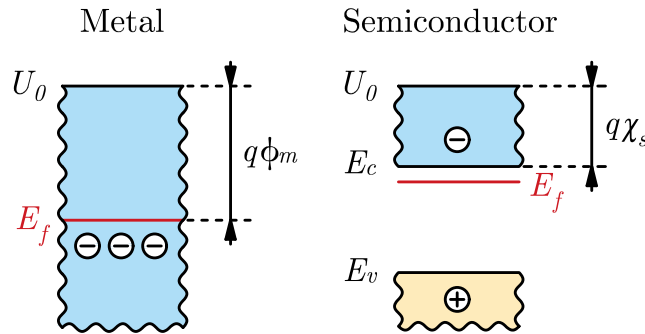


Figure 9.4: Isolated metal and semiconductor

When they are then put into contact at thermodynamic equilibrium, if the metal-semiconductor junction is assumed to be ideal and no dipole charge is created at the interface, the vacuum level must be continuous. This leads to the formation of a barrier of height:

$$q\phi_b = q\phi_m - q\chi_s \quad (9.10)$$

between the Fermi level $E_{f,m}$ in the metal and the conduction band edge E_c , as is represented in Figure 9.5.

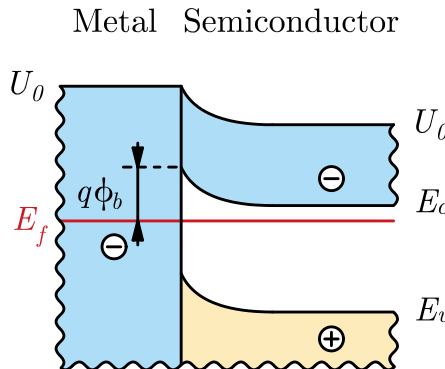


Figure 9.5: Schottky contact on n-type semiconductor band diagram

This situation can be further generalized by modeling the Schottky contact by means of a barrier $q\phi_b$ between the Fermi level in the metal and the conduction band edge in the semiconductor also in the case of discontinuous vacuum level (i.e. when dipole charge is present at the interface).

In such a case the value of the barrier $q\phi_b$ won't however be determined by Equation 9.10 but will be determined experimentally instead.

The boundary conditions for the continuity equations for electrons and holes are given by determining the recombination velocities at the contacts and imposing the current densities at the electrode to be recombination currents. According to the model derived for ohmic contacts in subsection 9.2.2 the current densities at the contact can be expressed as [23]:

$$\mathbf{J}_n \cdot \hat{\mathbf{n}} = q v_n (n - n_0) \qquad \mathbf{J}_p \cdot \hat{\mathbf{n}} = -q v_p (p - p_0) \qquad (9.11)$$

where:

- $\hat{\mathbf{n}}$ is the unit normal vector to the ohmic contact, oriented towards the interior of the device as shown in Figure 9.3 for the case of a 1-dimensional device.
- n_0, p_0 are the neutrality free carrier densities.
- v_n, v_p are the recombination velocities (constant properties of the contact).

These boundary conditions are of Neumann type for the electron and hole continuity equations.

In order to derive the boundary conditions on the quantum potentials for the case of a Schottky contact the gradient operator can be applied to Equation 9.11, obtaining:

$$\nabla [\mathbf{J}_n \cdot \hat{\mathbf{n}}] = q v_n \nabla n \qquad \nabla [\mathbf{J}_p \cdot \hat{\mathbf{n}}] = -q v_p \nabla p$$

Isolating then the gradient of the electron density leads to:

$$\frac{\nabla [\mathbf{J}_n \cdot \hat{\mathbf{n}}]}{q v_n} = \nabla n \qquad \frac{\nabla [\mathbf{J}_p \cdot \hat{\mathbf{n}}]}{-q v_p} = \nabla p \qquad (9.12)$$

Since the static continuity equations basically tell that spatial variations in the flux densities are only related to recombination phenomena, which are typically limited, it is then reasonable to assume that $\frac{1}{q} \nabla [\mathbf{J}_n \cdot \hat{\mathbf{n}}]$ and $\frac{1}{-q} \nabla [\mathbf{J}_p \cdot \hat{\mathbf{n}}]$ be negligible with respect to the recombination velocities v_n and v_p at the contact.

As a result, the following approximate boundary conditions can be used for the quantum potentials at a Schottky contact [23]:

$$\nabla n \approx 0 \qquad \nabla p \approx 0 \qquad (9.13)$$

These conditions, when plugged into the discretized definitions of the quantum potentials, will play the role of Neumann boundary conditions (naturally disappearing from the system).

Part III

Discretization and Implementation

Chapter 10

1D Discretization Scheme

10.1 Poisson Equation Discretization

Poisson's equation in one dimension reads:

$$\frac{\partial}{\partial z} \left\{ \epsilon \frac{\partial \phi}{\partial z} \right\} = -q (p - n + N_d^+ - N_a^-) \quad (10.1)$$

Under full ionization hypothesis $N_a^- = N_a$ and $N_d^+ = N_d$ and Poisson's equation in one dimension simplifies to:

$$\frac{\partial}{\partial z} \left\{ \epsilon \frac{\partial \phi}{\partial z} \right\} = -q (p - n + N_d - N_a) \quad (10.2)$$

The domain of the problem is split into N edges, corresponding to the definition of $N + 1$ nodes (including the nodes between two edges and two side nodes), as is shown in Figure 10.1.

Then, the discretizations of the unknown functions ϕ , n , p are defined on the nodes (their goal is therefore to interpolate the true solution at the nodes of the problem). The same is done for the doping profiles N_a and N_d

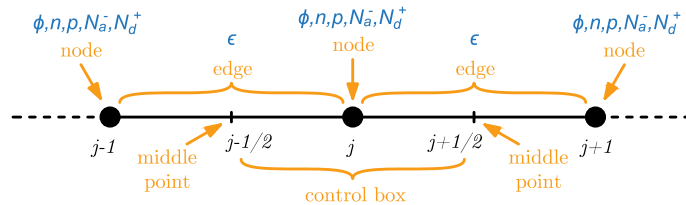


Figure 10.1: Poisson equation discretization

The notation which will be adopted in the following is to number the edges with the indexes j_1, j_2, \dots and to represent as:

- $j - \frac{1}{2}$ the center of the edge at the immediate left of the j^{th} node
- $j + \frac{1}{2}$ the center of the edge at the immediate right of the j^{th} node

The choice that is adopted is then to define the discretized permittivity ϵ at the center of each edge.

The positions at which each quantity appearing in Poisson's equation is discretized is shown in Figure 10.1.

The discretization is then carried out according to the **finite box** technique.

The first step is to integrate both sides of Poisson's equation over each control box. Control boxes are defined in one dimension as the segments connecting the middle points of two consecutive edges, as is shown in Figure 10.1.

Each control box can in principle be assigned to the interior node it includes; $N - 1$ control boxes can then be defined in the discretized space.

For each adjacent couple of edges with centers $j - \frac{1}{2}$ and $j + \frac{1}{2}$ such as the one shown in Figure 10.1 Poisson's equation is integrated as:

$$\int_{z_{j-\frac{1}{2}}}^{z_{j+\frac{1}{2}}} \frac{\partial}{\partial z} \left\{ \epsilon \frac{\partial \phi}{\partial z} \right\} dz = \int_{z_{j-\frac{1}{2}}}^{z_{j+\frac{1}{2}}} -q(p - n + N_d - N_a) dz$$

The left-hand side can be treated by applying the fundamental theorem of integral calculus, therefore obtaining:

$$\left[\epsilon \frac{\partial \phi}{\partial z} \right]_{z_{j-\frac{1}{2}}}^{z_{j+\frac{1}{2}}} = \int_{z_{j-\frac{1}{2}}}^{z_{j+\frac{1}{2}}} -q(p - n + N_d - N_a) dz$$

The next approximation that can be made is then to assume n , p , N_a and N_d to be approximately uniform over the control box; the integral then reduces to the integral of a rectangular function, giving:

$$\left[\epsilon \frac{\partial \phi}{\partial z} \right]_{z_{j-\frac{1}{2}}}^{z_{j+\frac{1}{2}}} = -q(p_j - n_j + N_{d,j} - N_{a,j}) L_{j-\frac{1}{2},j+\frac{1}{2}}$$

where $L_{z_{j-\frac{1}{2}},z_{j+\frac{1}{2}}} \triangleq z_{j-\frac{1}{2}} - z_{j+\frac{1}{2}}$ is the length of the control box that goes from the middle of the edge with center $j - \frac{1}{2}$ to the middle of edge with center $j + \frac{1}{2}$.

Expanding also the left-hand side leads to the result:

$$\epsilon \frac{1}{z_{j+\frac{1}{2}}} \frac{\partial \phi}{\partial z} \Big|_{z_{j+\frac{1}{2}}} - \epsilon_{j-\frac{1}{2}} \frac{\partial \phi}{\partial z} \Big|_{z_{j-\frac{1}{2}}} = -q(p_j - n_j + N_{d,j} - N_{a,j}) L_{j-\frac{1}{2},j+\frac{1}{2}}$$

The derivatives at the centers of the edges can then be approximated by means of a finite difference as:

$$\frac{\partial \phi}{\partial z} \Big|_{z_{j+\frac{1}{2}}} \approx \frac{\phi_{j+1} - \phi_j}{L_{j,j+1}} \qquad \frac{\partial \phi}{\partial z} \Big|_{z_{j-\frac{1}{2}}} \approx \frac{\phi_j - \phi_{j-1}}{L_{j-1,j}}$$

where $L_{j,j+1} \triangleq z_{j+1} - z_j$ and $L_{j-1,j} \triangleq z_j - z_{j-1}$ are the lengths of the edges whose centers are $j + \frac{1}{2}$ and $j - \frac{1}{2}$ respectively.

Substituting these finite difference approximations for the derivatives the following result is obtained:

$$\boxed{\epsilon_{j+\frac{1}{2}} \frac{\phi_{j+1} - \phi_j}{L_{j,j+1}} - \epsilon_{j-\frac{1}{2}} \frac{\phi_j - \phi_{j-1}}{L_{j-1,j}} + q(p_j - n_j + N_{d,j} - N_{a,j}) L_{j-\frac{1}{2},j+\frac{1}{2}} = 0} \quad (10.3)$$

Since one equation can be written for every couple of neighboring edges (i.e. for every inner node of the discretized domain) the total number of equations that can be written from Poisson's equation is $N - 1$; two additional equations can then be added by taking the boundary conditions into account.

10.1.1 Boundary Conditions

The first step is now to understand how to deal with **heterostructures** in Poisson's equation.

Since the potential has been shown to be continuous at a heterojunction, the discretization that has been derived above also holds when the two neighboring edges being considered are of different materials.

The presence of heterostructures therefore simply does not need to be taken into account when assembling the discretized problem.

For the outer contacts instead two main types of contact will be considered:

- **ideal ohmic contacts**

These contacts have been shown in subsection 9.2.2 to correspond to Dirichlet boundary conditions on the electrostatic potential ϕ . Specifically, they impose the neutrality potential shifted by the applied voltage:

$$\phi(z_{\text{cont}}) = \phi_0 + V$$

If an ideal ohmic contact is applied to the left boundary of the device then the corresponding equation is simply given by:

$$\phi_1 = \phi_{0,1} + V_{\text{left}}$$

where $\phi_{0,1}$ is the value of the electrostatic potential at the left boundary under neutrality conditions (which are denoted by the 0 subscript).

Similarly, if an ideal ohmic contact is applied to the right boundary of the device then the corresponding equation is simply given by:

$$\phi_{N+1} = \phi_{0,N+1} + V_{\text{right}}$$

where $\phi_{0,N+1}$ is the value of the electrostatic potential at the right boundary under neutrality conditions (which are denoted by the 0 subscript).

- **ideal schottky contacts**

Also these contacts have been shown in subsection 9.2.3 to impose Dirichlet boundary conditions on the electrostatic potential ϕ .

Since the electrostatic potential has been defined in such a way that:

$$E_c \triangleq -q\phi + \Delta E_c$$

and the boundary condition imposed by Schottky contacts has been shown in subsection 9.2.3 to be:

$$E_c = E_{f,m} + q\phi_b$$

where:

- $E_{f,m}$ is the Fermi level within the metal
- E_c is the conduction band edge within the semiconductor
- $q\phi_b$ is the barrier height between the Fermi level in the metal and the conduction band edge within the semiconductor

Considering then the quasi-Fermi level within the metal to be the equilibrium one shifted by the applied voltage V as $-qV$ leads to the final condition:

$$-q\phi + \Delta E_c = E_{f,\text{eq}} - qV + q\phi_b$$

Inverting this relationship for the electrostatic potential ϕ leads to the final result:

$$\phi = \frac{-E_{f,\text{eq}} + qV - q\phi_b + \Delta E_c}{q}$$

which is valid at a Schottky contact.

10.2 Electron Continuity Equation Discretization

Consider now the expression for the electron drift-diffusion current density that was presented in Equation 7.26:

$$\mathbf{J}_n(\mathbf{r}) = \mu_n n(\mathbf{r}) \nabla E_{f,n}(\mathbf{r}) \quad (10.4)$$

The quasi-Fermi level $E_{f,n}$ can be derived from the quantum-corrected Boltzmann statistics as:

$$n = N_c \exp \left\{ \frac{-E_c + E_{f,n} + q \Lambda_n}{k_B T} \right\} \quad \Rightarrow \quad E_{f,n} = k_B T \ln \left\{ \frac{n}{N_c} \right\} \underbrace{-q\phi + \Delta E_c}_{E_c} - q\Lambda_n$$

Plugging then this expression for the quasi-Fermi level into Equation 10.4 and exploiting the properties of the logarithms and the linearity of the differential operators leads to the following expression:

$$\begin{aligned} J_n &= n\mu_n \nabla \left(k_B T \ln \left\{ \frac{n}{N_c} \right\} - q\phi + \Delta E_c - q\Lambda_n \right) \\ &= n\mu_n \nabla (k_B T \ln \{n\} - k_B T \ln \{N_c\} - q\phi + \Delta E_c - q\Lambda_n) \\ &= n\mu_n \nabla (-k_B T \ln \{N_c\} - q\phi + \Delta E_c - q\Lambda_n) + n k_B T \mu_n \nabla (\ln \{n\}) \end{aligned}$$

Since the gradient of the logarithm of a function obeys the property (deriving from the chain rule):

$$\nabla \ln \{f(\mathbf{r})\} = \frac{1}{f(\mathbf{r})} \nabla \{f(\mathbf{r})\}$$

then the previous expression for the drift-diffusion current simplifies as:

$$J_n = n\mu_n \nabla (-k_B T \ln \{N_c\} - q\phi + \Delta E_c - q\Lambda_n) + k_B T \mu_n \nabla \{n\}$$

By Einstein's relationships the electron mobility is then related to the electron diffusivity as:

$$D_n = \frac{k_B T}{q} \mu_n$$

Further substitution of this expression in the previous one leads to the result:

$$J_n = n\mu_n \nabla (-k_B T \ln \{N_c\} - q\phi + \Delta E_c - q\Lambda_n) + qD_n \nabla n$$

Collecting the electron charge at the first term allows to cast this equation in the same form as the traditional drift-diffusion equation with Boltzmann statistics:

$$J_n = -q n \mu_n \nabla \left(\frac{k_B T}{q} \ln \{N_c\} + \phi - \frac{\Delta E_c}{q} + \Lambda_n \right) + qD_n \nabla n$$

The main difference with respect to the traditional drift-diffusion equation with Boltzmann statistics is that the drift term $-q n \mu_n \nabla \phi$ is replaced by a more complex equivalent drift term.

Defining the equivalent potential $\phi_n^{(eq)}$ for the electrons as:

$$\phi_n^{(eq)} \triangleq \frac{k_B T}{q} \ln \{N_c\} + \phi - \frac{\Delta E_c}{q} + \Lambda_n \quad (10.5)$$

then the final form for the continuity equation to be discretized is obtained:

$$J_n = -q n \mu_n \nabla \phi_n^{(eq)} + qD_n \nabla n \quad (10.6)$$

Drift-diffusion differential problems are notoriously unstable when discretized with a simple finite-box or finite-element discretization. In particular, it is possible to show that when the solution has exponential-like behavior (such as in presence of boundary layers of electrons and/or holes) the solution will be oscillating.

Even though different stabilization schemes have been proposed for the drift-diffusion equations, stabilization leads to worse interpolating behavior of the discretized solution when the solution behavior is exponential-like (i.e. it leads to a solution exhibiting quite a large error at the nodes when it should track a solution with exponential growth).

The main stability issue with drift-diffusion schemes is that a piecewise linear approximation for the solution is not able to properly reproduce an exponentially growing/decaying true solution to the problem.

The idea proposed by Scharfetter and Gummel (which will be adopted here) to improve the stability of the discretization of the continuity equations is then to adopt a **piecewise exponential approximate solution** [26].

The approximate solution in one dimension is then assumed to be piecewise exponential and therefore to behave as:

$$n_e(z) = A_e \exp \{ \alpha_e z \} + C_e \quad (10.7)$$

over each edge e of the mesh.

For the following derivations, the convention of Figure 10.2 is then adopted, with:

- e_L denoting the left node of edge e
- e_R denoting the right node of edge e

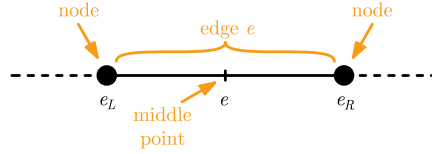


Figure 10.2: Edge and node notation (for the continuity equations)

This approximate piecewise exponential solution aims at interpolating the true solution.

For the case of the electron density n this can be written mathematically for each edge e as:

$$n_e(z_{eL}) \approx n(z_{eL}) \quad \text{and} \quad n_e(z_{eR}) \approx n(z_{eR})$$

In order to proceed with the discretization procedure it is useful to define the discretized electron density at the nodes of the mesh as:

$$n_{eL} \triangleq n(z_{eL}) \quad \text{and} \quad n_{eR} \triangleq n(z_{eR})$$

where according to the previously mentioned notation e_L and e_R are the nodes of the mesh corresponding to the extrema of the edge e .

According to the exponential ansatz for the solution over the whole edge e , the electron density can be written at the extrema of the edge as:

$$n_{eL} = A_e \exp \{ \alpha_e z_{eL} \} + C_e \quad \text{and} \quad n_{eR} = A_e \exp \{ \alpha_e z_{eR} \} + C_e \quad (10.8)$$

where A_e , α_e and C_e are coefficients characteristic of the edge e .

An expression for the coefficient A_e can be determined from the first of the two equations as:

$$A_e = \frac{n_{eL} - C_e}{\exp \{ \alpha_e z_{eL} \}}$$

Substituting this result into the second expression of Equation 10.8 yields the expression:

$$n_{eR} = \frac{n_{eL} - C_e}{\exp \{ \alpha_e z_{eL} \}} \exp \{ \alpha_e z_{eR} \} + C_e$$

Defining the edge length $L_{eL,eR} \triangleq z_{eR} - z_{eL}$ the equation simplifies to:

$$n_{eR} = (n_{eL} - C_e) \exp \{ \alpha_e L_{eL,eR} \} + C_e$$

Expanding the expression on the right and collecting the coefficient C_e leads to:

$$n_{eR} = n_{eL} \exp \{ \alpha_e L_{eL,eR} \} - C_e \exp \{ \alpha_e L_{eL,eR} \} + C_e$$

$$n_{eR} = n_{eL} \exp \{ \alpha_e L_{eL,eR} \} + C_e [1 - \exp \{ \alpha_e L_{eL,eR} \}]$$

This last expression can be used to derive an expression for the coefficient C_e as:

$$C_e = \frac{n_{eR} - n_{eL} \exp \{ \alpha_e L_{eL,eR} \}}{1 - \exp \{ \alpha_e L_{eL,eR} \}}$$

Splitting the two terms, the previous equation can be rewritten as:

$$C_e = n_{eR} \frac{1}{1 - \exp\{\alpha_e L_{eL,eR}\}} - n_{eL} \frac{-1}{1 - \exp\{-\alpha_e L_{eL,eR}\}}$$

Multiplying both sides of the equation by $\alpha_e L_{eL,eR}$ the following result is obtained:

$$C_e \alpha_e L_{eL,eR} = n_{eR} \frac{\alpha_e L_{eL,eR}}{1 - \exp\{\alpha_e L_{eL,eR}\}} - n_{eL} \frac{-\alpha_e L_{eL,eR}}{1 - \exp\{-\alpha_e L_{eL,eR}\}}$$

Introducing the Bernoulli function as the function \mathcal{B} defined by:

$$\mathcal{B}(x) \triangleq \frac{x}{\exp\{x\} - 1}$$

then the previous equation can be cast into the more compact expression:

$$C_e \alpha_e L_{eL,eR} = -n_{eR} \mathcal{B}(\alpha_e L_{eL,eR}) + n_{eL} \mathcal{B}(-\alpha_e L_{eL,eR}) \quad (10.9)$$

The next step is then to start from the definition of the drift-diffusion current of Equation 10.6 rewritten in one dimension and over the edge e :

$$J_{n,e}(z) = -q \mu_n(z) n_e(z) \frac{\partial \phi_{n,e}^{(eq)}(z)}{\partial z} + q D_n(z) \frac{\partial n_e(z)}{\partial z}$$

and approximating the spatial derivative of the equivalent electrostatic potential $\phi_n^{(eq)}$ for the electrons over each edge e with finite differences as:

$$\frac{\partial \phi_{n,e}^{(eq)}(z)}{\partial z} \approx \frac{\phi_{n,eR}^{(eq)} - \phi_{n,eL}^{(eq)}}{L_{eL,eR}}$$

The result that is obtained is then:

$$J_{n,e}(z) \approx -q \mu_n(z) n_e(z) \frac{\phi_{n,eR}^{(eq)} - \phi_{n,eL}^{(eq)}}{L_{eL,eR}} + q D_n(z) \frac{\partial n_e(z)}{\partial z} \quad (10.10)$$

According to the exponential ansatz of Equation 10.7 for the solution n_e over the edge e then the partial derivative $\frac{\partial n_e(z)}{\partial z}$ can be rewritten as:

$$\begin{aligned} \frac{\partial n_e(z)}{\partial z} &= \frac{\partial}{\partial z} \{A_e \exp\{\alpha_e z\} + C_e\} \\ &= A_e \alpha_e \exp\{\alpha_e z\} \\ &= A_e \alpha_e \exp\{\alpha_e z\} + \alpha_e C_e - \alpha_e C_e \\ &= \alpha_e n_e(z) - \alpha_e C_e \\ &= \alpha_e [n_e(z) - C_e] \end{aligned}$$

Substituting this last identity into Equation 10.10 allows to finally obtain an approximation of the continuity equation for the electrons without any explicit derivatives:

$$J_{n,e}(z) \approx -q \mu_n(z) n_e(z) \frac{\phi_{n,eR}^{(eq)} - \phi_{n,eL}^{(eq)}}{L_{eL,eR}} + q D_n(z) \alpha_e [n_e(z) - C_e] \quad (10.11)$$

The next reasonable assumption that can be made is that the current varies slow enough so that it is almost constant over each edge of the mesh; this is entirely reasonable since the only variations of the current are related to recombination phenomena, which are assumed not to be too heavy in reasonable devices.

The spatial dependency of the electron current density over the edge can then be dropped according to a piecewise constant approximation as:

$$J_{n,e} \approx -q \mu_n(z) n_e(z) \frac{\phi_{n,eR}^{(eq)} - \phi_{n,eL}^{(eq)}}{L_{eL,eR}} + q D_n(z) \alpha_e [n_e(z) - C_e] \quad (10.12)$$

In particular, the electron current density over the edge is approximated with its value at the **center** of the edge e .

Similarly, the mobility and the diffusivity can be considered to be approximately constant over each edge and approximated with their values at the center of the edge, therefore obtaining:

$$J_{n,e} \approx -q \mu_{n,e} n_e(z) \frac{\phi_{n,eR}^{(eq)} - \phi_{n,eL}^{(eq)}}{L_{eL,eR}} + q D_{n,e} \alpha_e [n_e(z) - C_e] \quad (10.13)$$

An alternative possible choice is to take as mobility and diffusivity values the averages between the values at the extrema of the edge. This might be a good choice for obtaining a slight smoothing of abrupt transitions (therefore obtaining an intermediate value at the transition point).

Since this equation is involving only constant terms and linear terms in $n_e(z)$ the solution can be carried out by simply comparing the coefficients of each of the two kinds of terms; the equation therefore translates into the following pair of equations:

$$q \mu_{n,e} \frac{\phi_{n,eR}^{(eq)} - \phi_{n,eL}^{(eq)}}{L_{eL,eR}} = q D_{n,e} \alpha_e \quad J_{n,e} = -q D_{n,e} \alpha_e C_e$$

where:

- the first equation arises from the comparison of the coefficients of the linear terms.
- the second equation arises from the comparison of the constant terms

The first condition (arising from the comparison of the coefficients of the exponential terms) simplifies to the condition:

$$\mu_{n,e} \frac{\phi_{n,eR}^{(eq)} - \phi_{n,eL}^{(eq)}}{L_{eL,eR}} = D_{n,e} \alpha_e$$

which, remembering Einstein's relationship $D_{n,e} = \frac{k_B T}{q} \mu_{n,e}$ can be further rewritten as:

$$\frac{\phi_{n,eR}^{(eq)} - \phi_{n,eL}^{(eq)}}{L_{eL,eR}} = \frac{k_B T}{q} \alpha_e$$

Recognizing the voltage equivalent of temperature (also known as thermal voltage) V_T the expression can then be cast into the final form:

$$\alpha_e = \frac{\phi_{n,eR}^{(eq)} - \phi_{n,eL}^{(eq)}}{V_T L_{eL,eR}} \quad (10.14)$$

The second condition (arising from the comparison of the constant terms) can instead be multiplied by the edge length $L_{eL,eR}$ to obtain:

$$J_{n,e} L_{eL,eR} = -q L_{eL,eR} D_{n,e} \alpha_e C_e$$

which can be rearranged as:

$$L_{eL,eR} \alpha_e C_e = -\frac{J_{n,e} L_{eL,eR}}{q D_{n,e}} \quad (10.15)$$

Substituting Equation 10.14 and 10.15 in Equation 10.9 leads to the following expression:

$$\frac{J_{n,e}}{q} = \frac{D_{n,e}}{L_{eL,eR}} \left[n_{eR} \mathcal{B} \left(\frac{\phi_{n,eR}^{(eq)} - \phi_{n,eL}^{(eq)}}{V_T L_{eL,eR}} L_{eL,eR} \right) - n_{eL} \mathcal{B} \left(-\frac{\phi_{n,eR}^{(eq)} - \phi_{n,eL}^{(eq)}}{V_T L_{eL,eR}} L_{eL,eR} \right) \right]$$

which simplifies to the final form of the discretized drift-diffusion current density:

$$\frac{J_{n,e}}{q} = \frac{D_{n,e}}{L_{eL,eR}} \left[n_{eR} \mathcal{B} \left(\frac{\phi_{n,eR}^{(eq)} - \phi_{n,eL}^{(eq)}}{V_T} \right) - n_{eL} \mathcal{B} \left(-\frac{\phi_{n,eR}^{(eq)} - \phi_{n,eL}^{(eq)}}{V_T} \right) \right] \quad (10.16)$$

It is important to remark that the drift-diffusion electron current is defined for the edge and, specifically, at its **middle point** e , as is shown in the diagram of Figure 10.2.

Now that the expression for the drift-diffusion current has been discretized the next step is to work on the continuity equation for the electrons and eventually insert the previous results into it.

The electron continuity equation, which was already introduced in Equation 7.24 in stationary conditions and in one dimension only reads:

$$\frac{1}{q} \frac{dJ_n(z)}{dz} - U_n = 0 \quad (10.17)$$

Consider now the same discretization as the one defined in section 10.1 for Poisson's equation.

Define then the **control boxes** again as the segments connecting the centers of two adjacent edges, as is shown in Figure 10.3.

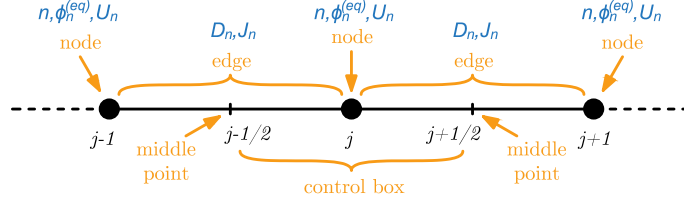


Figure 10.3: Electron continuity equation discretization

Then, following the method that is depicted in Figure 10.3, discretize:

- Electron current densities J_n and diffusivities D_n at the center of each edge
- Electron densities n , equivalent potentials for electrons $\phi_n^{(eq)}$ and net recombination rates U_n at the nodes of the mesh

The **finite box** method is then applied, as for Poisson's equation.

The first step is to integrate Equation 10.17 over the control box of node j (which ranges from $j - \frac{1}{2}$ to $j + \frac{1}{2}$, i.e. from the center of the previous edge to the center of the successive edge) as follows:

$$\frac{1}{q} \int_{z_{j-\frac{1}{2}}}^{z_{j+\frac{1}{2}}} \frac{dJ_n(z)}{dz} dz - \int_{z_{j-\frac{1}{2}}}^{z_{j+\frac{1}{2}}} U_n dz = 0$$

Applying the fundamental theorem of integral calculus to the first term gives:

$$\left[\frac{J_n}{q} \right]_{z_{j-\frac{1}{2}}}^{z_{j+\frac{1}{2}}} - \int_{z_{j-\frac{1}{2}}}^{z_{j+\frac{1}{2}}} U_n dz = 0$$

Assuming the variation of the recombination rate through the control box to be negligible the second term can be approximated with the rectangle rule as:

$$\left[\frac{J_n}{q} \right]_{z_{j-\frac{1}{2}}}^{z_{j+\frac{1}{2}}} - U_n L_{j-\frac{1}{2}, j+\frac{1}{2}} = 0 \quad (10.18)$$

where $L_{j-\frac{1}{2}, j+\frac{1}{2}} \triangleq z_{j+\frac{1}{2}} - z_{j-\frac{1}{2}}$ is the length of the control box.

The terms $\left. \frac{J_n}{q} \right|_{z_{j-\frac{1}{2}}}$ and $\left. \frac{J_n}{q} \right|_{z_{j+\frac{1}{2}}}$ can be substituted using with the expressions obtained from Equation 10.16:

$$\frac{J_{n, j-\frac{1}{2}}}{q} = \frac{D_{n, j-\frac{1}{2}}}{L_{j-1, j}} \left[n_j \mathcal{B} \left(\frac{\phi_{n, j}^{(eq)} - \phi_{n, j-1}^{(eq)}}{V_T} \right) - n_{j-1} \mathcal{B} \left(-\frac{\phi_{n, j}^{(eq)} - \phi_{n, j-1}^{(eq)}}{V_T} \right) \right] \quad (10.19)$$

$$\frac{J_{n, j+\frac{1}{2}}}{q} = \frac{D_{n, j+\frac{1}{2}}}{L_{j, j+1}} \left[n_{j+1} \mathcal{B} \left(\frac{\phi_{n, j+1}^{(eq)} - \phi_{n, j}^{(eq)}}{V_T} \right) - n_j \mathcal{B} \left(-\frac{\phi_{n, j+1}^{(eq)} - \phi_{n, j}^{(eq)}}{V_T} \right) \right] \quad (10.20)$$

Substituting Equation 10.19 and 10.20 into the discretized continuity equation Equation 10.18 yields the final expression:

$$\boxed{\frac{D_{n,j+\frac{1}{2}}}{L_{j,j+1}} \left[n_{j+1} \mathcal{B} \left(\frac{\phi_{n,j+1}^{(eq)} - \phi_{n,j}^{(eq)}}{V_T} \right) - n_j \mathcal{B} \left(-\frac{\phi_{n,j+1}^{(eq)} - \phi_{n,j}^{(eq)}}{V_T} \right) \right] + \frac{D_{n,j-\frac{1}{2}}}{L_{j-1,j}} \left[n_j \mathcal{B} \left(\frac{\phi_{n,j}^{(eq)} - \phi_{n,j-1}^{(eq)}}{V_T} \right) - n_{j-1} \mathcal{B} \left(-\frac{\phi_{n,j}^{(eq)} - \phi_{n,j-1}^{(eq)}}{V_T} \right) \right] - U_{n,j} L_{j-\frac{1}{2},j+\frac{1}{2}} = 0} \quad (10.21)$$

Also for the electron continuity equation a single equation can be written for every couple of adjacent edges, i.e. for every interior node of the mesh.

Therefore, only $N - 1$ equations can be written from the electron continuity equation. An additional two equations can be added by considering the boundary conditions for the electron continuity equation.

10.2.1 Boundary Conditions

Also in this case, the first step is to understand how to deal with **heterostructures** in the electron continuity equation.

Since the electron current density has been shown to be continuous at a heterojunction, the discretization that has been derived above also holds when the two neighboring edges being considered are of different materials.

The presence of heterostructures can therefore also in this case simply not be taken into account when assembling the discretized problem.

For the outer contacts instead two main types of contact will be considered:

- **ideal ohmic contacts**

Ideal ohmic contacts have been shown in subsection 9.2.2 to impose the neutrality electron concentration where they are applied:

$$n = n_0$$

where suitable models for the neutrality electron concentration have been presented in subsection 9.2.2.

These contacts therefore impose Dirichlet-type boundary conditions on the electron density n .

Therefore, for the case of an ideal ohmic contact at the left of the device the following equation can be added:

$$n_1 \approx n_0^{(left)}$$

where $n_0^{(left)}$ is the neutrality electron density for the first material layer on the left.

Similarly, for an ideal ohmic contact at the right of the device the equation that can be added is:

$$n_{N+1} \approx n_0^{(right)}$$

where $n_0^{(right)}$ is the neutrality electron density for the last material on the right.

- **ideal Schottky contacts**

To understand how to treat ideal Schottky contacts it is useful to consider the first and the last portions of the discretization (i.e. of the mesh) as they are shown in Figure 10.4.

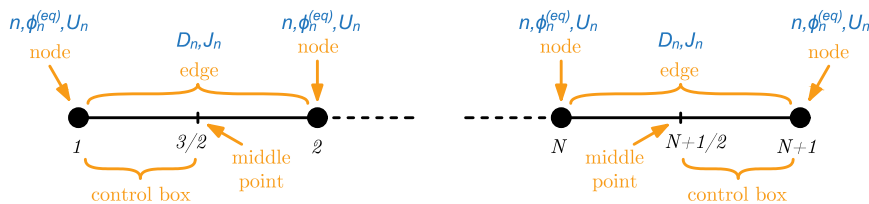


Figure 10.4: Discretization of the boundary conditions to the electron continuity equation

In order to treat a Schottky contact at the left side of the device it is useful to write the drift-diffusion electron current density at the center of the first edge:

$$\frac{J_{n,3/2}}{q} = \frac{D_{n,3/2}}{L_{1,2}} \left[n_2 \mathcal{B} \left(\frac{\phi_{n,2}^{(eq)} - \phi_{n,1}^{(eq)}}{V_T} \right) - n_1 \mathcal{B} \left(-\frac{\phi_{n,2}^{(eq)} - \phi_{n,1}^{(eq)}}{V_T} \right) \right] \quad (10.22)$$

Then, the electron continuity equation can be considered:

$$\frac{1}{q} \frac{dJ_n(z)}{dz} - U_n = 0 \quad (10.23)$$

and integrated over the “half control box” that goes from the first node 1 to the center 3/2 of the first edge of the mesh, obtaining:

$$\int_{z_1}^{z_{3/2}} \frac{1}{q} \frac{dJ_n(z)}{dz} dz - \int_{z_1}^{z_{3/2}} U_n dz = 0 \quad (10.24)$$

Applying the fundamental theorem of integral calculus allows to rewrite the first term as:

$$\left[\frac{J_n}{q} \right]_{z_1}^{z_{3/2}} - \int_{z_1}^{z_{3/2}} U_n dz = 0 \quad (10.25)$$

Then, assuming the recombination rate to be approximately constant over the first edge, the rectangle rule can be used to approximate the second term as:

$$\left[\frac{J_n}{q} \right]_{z_1}^{z_{3/2}} - U_{n,1} L_{1,3/2} = 0 \quad (10.26)$$

where $L_{1,3/2} \triangleq z_{3/2} - z_1$ is the length of the first “half control box”.

Replacing the drift-diffusion current (Equation 10.22) at the center of the edge within the finite box discretization (Equation 10.26) of the electron continuity equation yields:

$$\frac{D_{n,3/2}}{L_{1,2}} \left[n_2 \mathcal{B} \left(\frac{\phi_{n,2}^{(eq)} - \phi_{n,1}^{(eq)}}{V_T} \right) - n_1 \mathcal{B} \left(-\frac{\phi_{n,2}^{(eq)} - \phi_{n,1}^{(eq)}}{V_T} \right) \right] - \frac{J_n}{q} \Big|_{z_1} - U_{n,1} L_{1,3/2} = 0 \quad (10.27)$$

Finally, the Schottky contact is imposing a current at the leftmost node that is mainly a recombination current and is given by:

$$J_{n,1} = q v_n^{(left)} (n_1 - n_0^{(left)})$$

where $n_0^{(left)}$ is the equilibrium electron density at the left Schottky contact and $v_n^{(left)}$ is the recombination velocity of the same contact (as was shown in subsection 9.2.3).

Substituting this last constraint into Equation 10.27 leads to the result:

$$\boxed{\frac{D_{n,3/2}}{L_{1,2}} \left[n_2 \mathcal{B} \left(\frac{\phi_{n,2}^{(eq)} - \phi_{n,1}^{(eq)}}{V_T} \right) - n_1 \mathcal{B} \left(-\frac{\phi_{n,2}^{(eq)} - \phi_{n,1}^{(eq)}}{V_T} \right) \right] + v_n^{(left)} (n_1 - n_0^{(left)}) - U_{n,1} L_{1,3/2} = 0} \quad (10.28)$$

A similar procedure can be carried out for a Schottky contact at the right side, integrating the continuity equation over the last “half control box” yields:

$$\int_{z_{N+\frac{1}{2}}}^{z_{N+1}} \frac{1}{q} \frac{dJ_n(z)}{dz} dz - \int_{z_{N+\frac{1}{2}}}^{z_{N+1}} U_n dz = 0$$

Applying the fundamental theorem of integral calculus to the first term it simplifies as:

$$\left[\frac{J_n(z)}{q} \right]_{z_{N+\frac{1}{2}}}^{z_{N+1}} - \int_{z_{N+\frac{1}{2}}}^{z_{N+1}} U_n dz = 0$$

Assuming the net recombination rate to be approximately constant over the “half control box” and therefore approximating the second term with the rectangle rule yields:

$$\left[\frac{J_n(z)}{q} \right]_{z_{N+\frac{1}{2}}}^{z_{N+1}} - U_n L_{N+\frac{1}{2},N+1} = 0$$

where $L_{N+\frac{1}{2},N+1}$ is the length of the last (i.e. rightmost) “half control box”.

The approximated drift-diffusion electron current density at the center of the last edge (i.e. at the position denoted by $N + \frac{1}{2}$) can then be written according to the previously derived discretization as:

$$\frac{J_{n,N+\frac{1}{2}}}{q} = \frac{D_{n,N+\frac{1}{2}}}{L_{N,N+1}} \left[n_{N+1} \mathcal{B} \left(\frac{\phi_{n,N+1}^{(eq)} - \phi_{n,N}^{(eq)}}{V_T} \right) - n_N \mathcal{B} \left(-\frac{\phi_{n,N+1}^{(eq)} - \phi_{n,N}^{(eq)}}{V_T} \right) \right] \quad (10.29)$$

The last current density can instead be written from the boundary condition as:

$$J_{n,N+1} = -q v_n^{(right)} (n_{N+1} - n_0^{(right)})$$

Replacing them into the discretized electron continuity equation leads to the equation:

$$\boxed{\frac{D_{n,N+\frac{1}{2}}}{L_{N,N+1}} \left[n_N \mathcal{B} \left(-\frac{\phi_{n,N+1}^{(eq)} - \phi_{n,N}^{(eq)}}{V_T} \right) - n_{N+1} \mathcal{B} \left(\frac{\phi_{n,N+1}^{(eq)} - \phi_{n,N}^{(eq)}}{V_T} \right) \right] +} \quad (10.30)$$

$$- v_n^{(right)} (n_{N+1} - n_0^{(right)}) - U_{n,N+1} L_{N+\frac{1}{2},N+1} = 0$$

10.2.2 Generation and Recombination

In order to have a complete expression for the discretized electron continuity equation it is fundamental to now consider the discretization of the net recombination rate U_n .

If only SRH recombination is considered (i.e. neglecting radiative emission and Auger recombination, both reasonable assumptions when studying one cross-section of the channel of a HEMT since it is not an opto-electronic device) then the expression to be discretized is the one derived in Equation 8.11.

$$U^{SRH} \approx \frac{np - n_i^2}{\tau_p(n + n_t) + \tau_n(p + p_t)} \quad (10.31)$$

As was mentioned before and shown in Figure 10.3 the net recombination rate should be discretized at the nodes of the mesh; the expression that is then found for the electron recombination rate at node j is:

$$\boxed{U_{n,j}^{SRH} \approx \frac{n_j p_j - n_{i,j}^2}{\tau_{p,j}(n_j + n_{t,j}) + \tau_{n,j}(p_j + p_{t,j})}} \quad (10.32)$$

10.3 Hole Continuity Equation Discretization

Consider now the expression for the hole drift-diffusion current density that was presented in Equation 7.27:

$$\mathbf{J}_p(\mathbf{r}) = \mu_p p(\mathbf{r}) \nabla E_{f,p}(\mathbf{r}) \quad (10.33)$$

The quasi-Fermi level $E_{f,p}$ can be derived from the quantum-corrected Boltzmann statistics as:

$$p = N_v \exp \left\{ \frac{+E_v - E_{f,p} + q \Lambda_p}{k_B T} \right\} \quad \Rightarrow \quad E_{f,p} = -k_B T \ln \left\{ \frac{p}{N_v} \right\} \underbrace{-q\phi - E_g(0) + \Delta E_v + q\Lambda_p}_{E_v}$$

Plugging then this expression for the quasi-Fermi level into Equation 10.4 and exploiting the properties of the logarithms and the linearity of the differential operators leads to the following expression:

$$\begin{aligned} J_p &= p\mu_p \nabla \left(-k_B T \ln \left\{ \frac{p}{N_v} \right\} - q\phi - E_g(0) + \Delta E_v + q\Lambda_p \right) \\ &= p\mu_p \nabla (-k_B T \ln \{-\} - k_B T \ln \{N_v\} - q\phi + \Delta E_v - E_g(0) + q\Lambda_p) \\ &= p\mu_p \nabla (k_B T \ln \{N_v\} - q\phi + \Delta E_v - E_g(0) + q\Lambda_p) - p k_B T \mu_p \nabla (\ln \{p\}) \end{aligned}$$

Since the gradient of the logarithm of a function obeys the property (deriving from the chain rule):

$$\nabla \ln \{f(\mathbf{r})\} = \frac{1}{f(\mathbf{r})} \nabla \{f(\mathbf{r})\}$$

then the previous expression for the drift-diffusion current simplifies as:

$$J_p = p\mu_p \nabla (k_B T \ln \{N_v\} - q\phi + \Delta E_v - E_g(0) + q\Lambda_p) - k_B T \mu_p \nabla \{p\}$$

By Einstein's relationships the hole mobility is then related to the hole diffusivity as:

$$D_p = \frac{k_B T}{q} \mu_p$$

Further substitution of this expression in the previous one leads to the result:

$$J_p = p\mu_p \nabla (k_B T \ln \{N_v\} - q\phi + \Delta E_v - E_g(0) + q\Lambda_p) - qD_p \nabla p$$

Collecting the $-q$ at the first term allows to cast this equation in the same form as the traditional drift-diffusion equation with Boltzmann statistics:

$$J_p = -q p \mu_p \nabla \left(-\frac{k_B T}{q} \ln \{N_v\} + \phi - \frac{\Delta E_v}{q} + \frac{E_g(0)}{q} - \Lambda_p \right) - qD_p \nabla p$$

The main difference with respect to the traditional drift-diffusion equation with Boltzmann statistics is that the drift term $-q p \mu_p \nabla \phi$ is replaced by a more complex equivalent drift term.

Defining the equivalent potential $\phi_p^{(eq)}$ for the holes as:

$$\phi_p^{(eq)} \triangleq -\frac{k_B T}{q} \ln \{N_v\} + \phi - \frac{\Delta E_v}{q} + \frac{E_g(0)}{q} - \Lambda_p \quad (10.34)$$

then the final form for the continuity equation to be discretized is obtained:

$$J_p = -q p \mu_p \nabla \phi_p^{(eq)} - qD_p \nabla p \quad (10.35)$$

Also in the case of hole drift-diffusion problems instability is a fundamental issue when performing the discretization.

Scharfetter and Gummel's scheme is then again adopted to improve the stability of the discretization of the hole continuity equation. The main idea is then again to adopt a **piecewise exponential approximate solution**. [26]

The approximate solution in one dimension is then assumed to be piecewise exponential and therefore to behave as:

$$p_e(z) = A_e \exp \{\alpha_e z\} + C_e \quad (10.36)$$

over each edge e of the mesh.

For the following derivations, the convention of Figure 10.2 is then again adopted, with:

- e_L denoting the left node of edge e
- e_R denoting the right node of edge e

This approximate piecewise exponential solution aims at interpolating the true solution.

Imposing the solution over an edge e to be interpolating at the extrema e_L , e_R of the edge itself and manipulating the resulting equations as was done for electrons in section 10.2 the following expression is obtained:

$$C_e \alpha_e L_{e_L, e_R} = -p_{e_R} \mathcal{B}(\alpha_e L_{e_L, e_R}) + p_{e_L} \mathcal{B}(-\alpha_e L_{e_L, e_R}) \quad (10.37)$$

with $\mathcal{B}(x)$ the Bernoulli function as defined in section 10.2.

The next step is then to start from the definition of the drift-diffusion current of Equation 10.35 rewritten in one dimension and over the edge e :

$$J_{p,e}(z) = -q \mu_p(z) p_e(z) \frac{\partial \phi_{p,e}^{(eq)}(z)}{\partial z} - q D_p(z) \frac{\partial p_e(z)}{\partial z}$$

and approximating the spatial derivative of the equivalent electrostatic potential $\phi_n^{(eq)}$ for the electrons over each edge e with finite differences as:

$$\frac{\partial \phi_{p,e}^{(eq)}(z)}{\partial z} \approx \frac{\phi_{p,e_R}^{(eq)} - \phi_{p,e_L}^{(eq)}}{L_{e_L, e_R}}$$

The result that is obtained is then:

$$J_{p,e}(z) \approx -q \mu_p(z) p_e(z) \frac{\phi_{p,e_R}^{(eq)} - \phi_{p,e_L}^{(eq)}}{L_{e_L, e_R}} - q D_p(z) \frac{\partial p_e(z)}{\partial z} \quad (10.38)$$

According to the exponential ansatz of Equation 10.36 for the solution p_e over the edge e then the partial derivative $\frac{\partial p_e(z)}{\partial z}$ can be rewritten as:

$$\begin{aligned} \frac{\partial p_e(z)}{\partial z} &= \frac{\partial}{\partial z} \{A_e \exp\{\alpha_e z\} + C_e\} \\ &= A_e \alpha_e \exp\{\alpha_e z\} \\ &= A_e \alpha_e \exp\{\alpha_e z\} + \alpha_e C_e - \alpha_e C_e \\ &= \alpha_e p_e(z) - \alpha_e C_e \\ &= \alpha_e [p_e(z) - C_e] \end{aligned}$$

Substituting this last identity into Equation 10.38 allows to finally obtain an approximation of the continuity equation for the holes without any explicit derivatives:

$$J_{p,e}(z) \approx -q \mu_p(z) p_e(z) \frac{\phi_{p,e_R}^{(eq)} - \phi_{p,e_L}^{(eq)}}{L_{e_L, e_R}} - q D_p(z) \alpha_e [p_e(z) - C_e] \quad (10.39)$$

The next reasonable assumption that can be made is that the current varies slow enough so that it is almost constant over each edge of the mesh; this is entirely reasonable since the only variations of the current are related to recombination phenomena, which are assumed not to be too heavy in reasonable devices.

The spatial dependency of the hole current density over the edge can then be dropped according to a piecewise constant approximation as:

$$J_{p,e} \approx -q \mu_p(z) p_e(z) \frac{\phi_{p,e_R}^{(eq)} - \phi_{p,e_L}^{(eq)}}{L_{e_L, e_R}} - q D_p(z) \alpha_e [p_e(z) - C_e] \quad (10.40)$$

In particular, the hole current density over the edge is approximated with its value at the **center** of the edge e .

Similarly, the mobility and the diffusivity can be considered to be approximately constant over each edge and approximated with their values at the center of the edge, therefore obtaining:

$$J_{p,e} \approx -q \mu_{p,e} p_e(z) \frac{\phi_{p,eR}^{(eq)} - \phi_{p,eL}^{(eq)}}{L_{eL,eR}} - q D_{p,e} \alpha_e [p_e(z) - C_e] \quad (10.41)$$

An alternative possible choice is to take as constant mobility and diffusivity values the averages between the values at the extrema of the edge. This might be a good choice for obtaining a slight smoothing of abrupt transitions (therefore obtaining an intermediate value at the transition point).

Since this equation is involving only constant terms and linear terms in $p_e(z)$ the solution can be carried out by simply comparing the coefficients of each of the two kinds of terms; the equation therefore translates into the following pair of equations:

$$q \mu_{p,e} \frac{\phi_{p,eR}^{(eq)} - \phi_{p,eL}^{(eq)}}{L_{eL,eR}} = -q D_{p,e} \alpha_e \quad J_{p,e} = q D_{p,e} \alpha_e C_e$$

where:

- the first equation arises from the comparison of the coefficients of the linear terms in $p_e(z)$.
- the second equation arises from the comparison of the constant terms

The first condition (arising from the comparison of the coefficients of the exponential terms) simplifies to the condition:

$$\mu_{p,e} \frac{\phi_{n,eR}^{(eq)} - \phi_{n,eL}^{(eq)}}{L_{eL,eR}} = -D_{n,e} \alpha_e$$

which, remembering Einstein's relationship $D_{p,e} = \frac{k_B T}{q} \mu_{p,e}$ can be further rewritten as:

$$\frac{\phi_{p,eR}^{(eq)} - \phi_{p,eL}^{(eq)}}{L_{eL,eR}} = -\frac{k_B T}{q} \alpha_e$$

Recognizing the voltage equivalent of temperature (also known as thermal voltage) V_T the expression can then be cast into the final form:

$$\alpha_e = -\frac{\phi_{p,eR}^{(eq)} - \phi_{p,eL}^{(eq)}}{V_T L_{eL,eR}} \quad (10.42)$$

The second condition (arising from the comparison of the constant terms) can instead be multiplied by the edge length $L_{eL,eR}$ to obtain:

$$J_{p,e} L_{eL,eR} = q L_{eL,eR} D_{p,e} \alpha_e C_e$$

which can be rearranged as:

$$L_{eL,eR} \alpha_e C_e = \frac{J_{p,e} L_{eL,eR}}{q D_{p,e}} \quad (10.43)$$

Substituting Equation 10.42 and 10.43 in Equation 10.37 leads to the following expression:

$$\frac{J_{p,e}}{q} = \frac{D_{p,e}}{L_{eL,eR}} \left[p_{eL} \mathcal{B} \left(\frac{\phi_{p,eR}^{(eq)} - \phi_{p,eL}^{(eq)}}{V_T L_{eL,eR}} L_{eL,eR} \right) - p_{eR} \mathcal{B} \left(-\frac{\phi_{p,eR}^{(eq)} - \phi_{p,eL}^{(eq)}}{V_T L_{eL,eR}} L_{eL,eR} \right) \right]$$

which simplifies to the final form of the discretized drift-diffusion current density:

$$\frac{J_{p,e}}{q} = \frac{D_{p,e}}{L_{eL,eR}} \left[p_{eL} \mathcal{B} \left(\frac{\phi_{p,eR}^{(eq)} - \phi_{p,eL}^{(eq)}}{V_T} \right) - p_{eR} \mathcal{B} \left(-\frac{\phi_{p,eR}^{(eq)} - \phi_{p,eL}^{(eq)}}{V_T} \right) \right] \quad (10.44)$$

It is important to remark that the drift-diffusion hole current density is defined for the edge and, specifically, at its **middle point** e , as is shown in the diagram of Figure 10.2.

Now that the expression for the drift-diffusion current has been discretized the next step is to work on the continuity equation for the holes and eventually insert the previous results into it.

The hole continuity equation, which was already introduced in Equation 7.25 in stationary conditions and in one dimension only reads:

$$\frac{1}{q} \frac{dJ_p(z)}{dz} + U_p = 0 \quad (10.45)$$

Consider now the same kind of discretization already used for the electron continuity equation in section 10.2. Define then the **control boxes** again as the segments connecting the centers of two adjacent edges, as is shown in Figure 10.5.

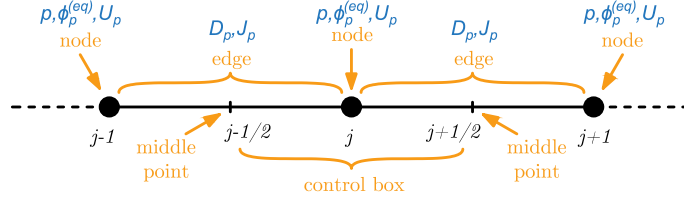


Figure 10.5: Hole continuity equation discretization

Then, following the method that is depicted in Figure 10.5, discretize:

- Hole current densities J_p , diffusivities D_p and net recombination rates U_p at the center of each edge
- Hole densities p and equivalent potentials for holes $\phi_p^{(eq)}$ at the nodes of the mesh

The **finite box** method is then applied, as was done for the electron continuity equation in section 10.2.

The first step is to integrate Equation 10.45 over the control box of node j (which ranges from $j - \frac{1}{2}$ to $j + \frac{1}{2}$, i.e. from the center of the previous edge to the center of the successive edge) as follows:

$$\frac{1}{q} \int_{z_{j-\frac{1}{2}}}^{z_{j+\frac{1}{2}}} \frac{dJ_p(z)}{dz} dz + \int_{z_{j-\frac{1}{2}}}^{z_{j+\frac{1}{2}}} U_p dz = 0$$

Applying the fundamental theorem of integral calculus to the first term gives:

$$\left[\frac{J_p}{q} \right]_{z_{j-\frac{1}{2}}}^{z_{j+\frac{1}{2}}} + \int_{z_{j-\frac{1}{2}}}^{z_{j+\frac{1}{2}}} U_p dz = 0$$

Assuming the variation of the recombination rate through the control box to be negligible the second term can be approximated with the rectangle rule as:

$$\left[\frac{J_p}{q} \right]_{z_{j-\frac{1}{2}}}^{z_{j+\frac{1}{2}}} + U_p L_{j-\frac{1}{2},j+\frac{1}{2}} = 0 \quad (10.46)$$

where $L_{j-\frac{1}{2},j+\frac{1}{2}} \triangleq z_{j+\frac{1}{2}} - z_{j-\frac{1}{2}}$ is the length of the control box.

The terms $\left. \frac{J_p}{q} \right|_{z_{j-\frac{1}{2}}}$ and $\left. \frac{J_p}{q} \right|_{z_{j+\frac{1}{2}}}$ can be substituted using with the expressions obtained from Equation 10.44:

$$\frac{J_{p,j-\frac{1}{2}}}{q} = \frac{D_{p,j-\frac{1}{2}}}{L_{j-1,j}} \left[p_{j-1} \mathcal{B} \left(\frac{\phi_{p,j}^{(eq)} - \phi_{p,j-1}^{(eq)}}{V_T} \right) - p_j \mathcal{B} \left(-\frac{\phi_{p,j}^{(eq)} - \phi_{p,j-1}^{(eq)}}{V_T} \right) \right] \quad (10.47)$$

$$\frac{J_{p,j+\frac{1}{2}}}{q} = \frac{D_{p,j+\frac{1}{2}}}{L_{j,j+1}} \left[p_j \mathcal{B} \left(\frac{\phi_{p,j+1}^{(eq)} - \phi_{p,j}^{(eq)}}{V_T} \right) - p_{j+1} \mathcal{B} \left(-\frac{\phi_{p,j+1}^{(eq)} - \phi_{p,j}^{(eq)}}{V_T} \right) \right] \quad (10.48)$$

Substituting Equation 10.19 and 10.20 into the discretized continuity equation Equation 10.46 yields the final expression:

$$\boxed{\frac{D_{p,j+\frac{1}{2}}}{L_{j,j+1}} \left[p_j \mathcal{B} \left(\frac{\phi_{p,j+1}^{(eq)} - \phi_{p,j}^{(eq)}}{V_T} \right) - p_{j+1} \mathcal{B} \left(-\frac{\phi_{p,j+1}^{(eq)} - \phi_{p,j}^{(eq)}}{V_T} \right) \right] + \frac{D_{p,j-\frac{1}{2}}}{L_{j-1,j}} \left[p_{j-1} \mathcal{B} \left(\frac{\phi_{p,j}^{(eq)} - \phi_{p,j-1}^{(eq)}}{V_T} \right) - p_j \mathcal{B} \left(-\frac{\phi_{p,j}^{(eq)} - \phi_{p,j-1}^{(eq)}}{V_T} \right) \right] + U_{p,j} L_{j-\frac{1}{2},j+\frac{1}{2}} = 0} \quad (10.49)$$

Also for the hole continuity equation a single equation can be written for every couple of adjacent edges, i.e. for every interior node of the mesh.

Therefore, only $N - 1$ equations can be written from the hole continuity equation. An additional two equations can be added by considering the boundary conditions for the hole continuity equation.

10.3.1 Boundary Conditions

Also in this case, the first step is to understand how to deal with **heterostructures** in the hole continuity equation.

Since the hole current density has been shown to be continuous at a heterojunction, the discretization that has been derived above also holds when the two neighboring edges being considered are of different materials. The presence of heterostructures can therefore also in this case simply not be taken into account when assembling the discretized problem.

For the outer contacts instead two main types of contact will be considered:

- **ideal ohmic contacts**

Ideal ohmic contacts have been shown in subsection 9.2.2 to impose the neutrality hole concentration where they are applied:

$$p = p_0$$

where suitable models for the neutrality hole concentration have been presented in subsection 9.2.2.

These contacts therefore impose Dirichlet-type boundary conditions on the hole density p .

Therefore, for the case of an ideal ohmic contact at the left of the device the following equation can be added:

$$p_1 \approx p_0^{(left)}$$

where $p_0^{(left)}$ is the neutrality hole density for the first material layer on the left.

Similarly, for an ideal ohmic contact at the right of the device the equation that can be added is:

$$p_{N+1} \approx p_0^{(right)}$$

where $p_0^{(right)}$ is the neutrality hole density for the last material on the right.

- **ideal Schottky contacts**

To understand how to treat ideal Schottky contacts it is useful to consider the first and the last portions of the discretization (i.e. of the mesh) as they are shown in Figure 10.4.

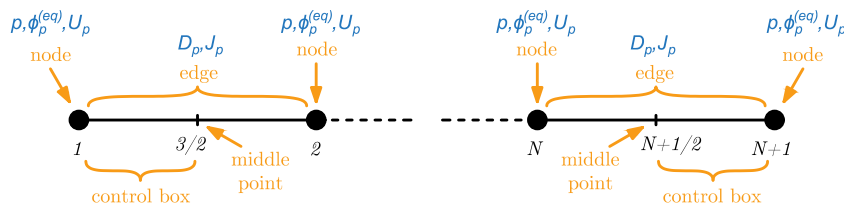


Figure 10.6: Discretization of the boundary conditions to the hole continuity equation

In order to treat a Schottky contact at the left side of the device it is useful to write the drift-diffusion hole current density at the center of the first edge:

$$\frac{J_{p,3/2}}{q} = \frac{D_{p,3/2}}{L_{1,2}} \left[p_1 \mathcal{B} \left(\frac{\phi_{p,2}^{(eq)} - \phi_{p,1}^{(eq)}}{V_T} \right) - p_2 \mathcal{B} \left(-\frac{\phi_{p,2}^{(eq)} - \phi_{p,1}^{(eq)}}{V_T} \right) \right] \quad (10.50)$$

Then, the hole continuity equation can be considered:

$$\frac{1}{q} \frac{dJ_p(z)}{dz} + U_p = 0 \quad (10.51)$$

and integrated over the “half control box” that goes from the first node 1 to the center 3/2 of the first edge of the mesh, obtaining:

$$\int_{z_1}^{z_{3/2}} \frac{1}{q} \frac{dJ_p(z)}{dz} dz + \int_{z_1}^{z_{3/2}} U_n dz = 0 \quad (10.52)$$

Applying the fundamental theorem of integral calculus allows to rewrite the first term as:

$$\left[\frac{J_p}{q} \right]_{z_1}^{z_{3/2}} + \int_{z_1}^{z_{3/2}} U_p dz = 0 \quad (10.53)$$

Then, assuming the recombination rate to be approximately constant over the first edge, the rectangle rule can be used to approximate the second term as:

$$\left[\frac{J_p}{q} \right]_{z_1}^{z_{3/2}} + U_{p,1} L_{1,3/2} = 0 \quad (10.54)$$

where $L_{1,3/2} \triangleq z_{3/2} - z_1$ is the length of the first “half control box”.

Replacing the drift-diffusion current (Equation 10.50) at the center of the edge within the finite box discretization (Equation 10.54) of the hole continuity equation yields:

$$\frac{D_{p,3/2}}{L_{1,2}} \left[p_1 \mathcal{B} \left(\frac{\phi_{p,2}^{(eq)} - \phi_{p,1}^{(eq)}}{V_T} \right) - p_2 \mathcal{B} \left(-\frac{\phi_{p,2}^{(eq)} - \phi_{p,1}^{(eq)}}{V_T} \right) \right] - \frac{J_p}{q} \Big|_{z_1} + U_{p,1} L_{1,3/2} = 0 \quad (10.55)$$

Finally, the Schottky contact is imposing a current at the leftmost node that is mainly a recombination current and is given by:

$$J_{p,1} = -q v_p^{(left)} (p_1 - p_0^{(left)})$$

where $p_0^{(left)}$ is the equilibrium hole density at the left Schottky contact and $v_p^{(left)}$ is the recombination velocity of the same contact (as was shown in subsection 9.2.3).

Substituting this last constraint into Equation 10.55 leads to the result:

$$\boxed{\frac{D_{p,3/2}}{L_{1,2}} \left[p_1 \mathcal{B} \left(\frac{\phi_{p,2}^{(eq)} - \phi_{p,1}^{(eq)}}{V_T} \right) - p_2 \mathcal{B} \left(-\frac{\phi_{p,2}^{(eq)} - \phi_{p,1}^{(eq)}}{V_T} \right) \right] + v_p^{(left)} (p_1 - p_0^{(left)}) + U_{p,1} L_{1,3/2} = 0} \quad (10.56)$$

A similar procedure can be carried out for a Schottky contact at the right side, integrating the hole continuity equation over the last “half control box” yields:

$$\int_{z_{N+\frac{1}{2}}}^{z_{N+1}} \frac{1}{q} \frac{dJ_p(z)}{dz} dz + \int_{z_{N+\frac{1}{2}}}^{z_{N+1}} U_p dz = 0$$

Applying the fundamental theorem of integral calculus to the first term it simplifies as:

$$\left[\frac{J_p(z)}{q} \right]_{z_{N+\frac{1}{2}}}^{z_{N+1}} + \int_{z_{N+\frac{1}{2}}}^{z_{N+1}} U_p dz = 0$$

Assuming the net recombination rate to be approximately constant over the “half control box” and therefore approximating the second term with the rectangle rule yields:

$$\left[\frac{J_p(z)}{q} \right]_{z_{N+\frac{1}{2}}}^{z_{N+1}} + U_p L_{N+\frac{1}{2},N+1} = 0$$

where $L_{N+\frac{1}{2},N+1}$ is the length of the last (i.e. rightmost) “half control box”.

The approximated drift-diffusion hole current density at the center of the last edge (i.e. at the position denoted by $N + \frac{1}{2}$) can then be written according to the previously derived discretization as:

$$\frac{J_{p,N+\frac{1}{2}}}{q} = \frac{D_{p,N+\frac{1}{2}}}{L_{N,N+1}} \left[p_N \mathcal{B} \left(\frac{\phi_{p,N+1}^{(eq)} - \phi_{p,N}^{(eq)}}{V_T} \right) - p_{N+1} \mathcal{B} \left(-\frac{\phi_{p,N+1}^{(eq)} - \phi_{p,N}^{(eq)}}{V_T} \right) \right] \quad (10.57)$$

Similarly, from the boundary conditions the last current density can be expressed as:

$$J_{p,1} = q v_p^{(right)} (p_1 - p_0^{(right)})$$

Replacing them into the discretized hole continuity equation leads to the equation:

$$\boxed{\frac{D_{p,N+\frac{1}{2}}}{L_{N,N+1}} \left[p_{N+1} \mathcal{B} \left(-\frac{\phi_{p,N+1}^{(eq)} - \phi_{p,N}^{(eq)}}{V_T} \right) - p_N \mathcal{B} \left(\frac{\phi_{p,N+1}^{(eq)} - \phi_{p,N}^{(eq)}}{V_T} \right) \right] + v_p^{(right)} (p_{N+1} - p_0^{(right)}) + U_{p,N+1} L_{N+\frac{1}{2},N+1} = 0} \quad (10.58)$$

10.3.2 Generation and Recombination

SRH generation/recombination rates have been already shown in chapter 8 to be the same for electrons and holes.

The discretized expression for the net recombination rate for holes is therefore the same as the one for electrons that was derived in subsection 10.2.2 and is given by:

$$\boxed{U_{p,j}^{SRH} \approx \frac{n_j p_j - n_{i,j}^2}{\tau_{p,j}(n_j + n_{t,j}) + \tau_{n,j}(p_j + p_{t,j})}} \quad (10.59)$$

10.4 Electron Density Gradient Equation Discretization

The density gradient equation for electrons that has to be discretized can be found by starting from the definition of the quantum potential Λ_n for electrons that was given in Equation 7.21:

$$\Lambda_n = \frac{\hbar^2}{6q} \frac{\nabla \cdot [(m_n^*)^{-1} \nabla \sqrt{n}]}{\sqrt{n}}$$

Multiplying both sides by the electron density n leads to the more convenient form:

$$\sqrt{n} \Lambda_n = \frac{\hbar^2}{6q} \nabla \cdot [(m_n^*)^{-1} \nabla \sqrt{n}]$$

which in one dimension reduces to the differential problem:

$$\sqrt{n} \Lambda_n = \frac{\hbar^2}{6q} \frac{\partial}{\partial z} \left[\frac{1}{m_n^*} \frac{\partial \sqrt{n}}{\partial z} \right] \quad (10.60)$$

Several implementation attempts have shown this form to yield best convergence results with initial guesses exhibiting discontinuities in the electron density n .

In order to simplify the discretization procedure, **control boxes** are defined, i.e. segments that connect the middle point of an edge with the middle point of the next edge.

Moreover, the discretization choices that are adopted are to discretize:

- electron densities n and quantum potentials Λ_n at the nodes of the mesh
- effective masses m_n^* at the centers of the edges

as is shown in Figure 10.7.

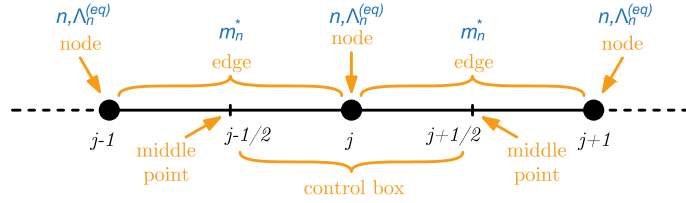


Figure 10.7: Electron density gradient equation discretization

The first step to determine a working discretization of the density gradient equation for electrons is to apply the **finite box** method.

Equation 10.60 must therefore be integrated over each control box, obtaining:

$$\int_{z_{j-\frac{1}{2}}}^{z_{j+\frac{1}{2}}} \sqrt{n} \Lambda_n dz = \frac{\hbar^2}{6q} \int_{z_{j-\frac{1}{2}}}^{z_{j+\frac{1}{2}}} \frac{\partial}{\partial z} \left[\frac{1}{m_n^*} \frac{\partial \sqrt{n}}{\partial z} \right] dz$$

Applying the fundamental theorem of integral calculus to the right-hand side of the equation reduces it to:

$$\int_{z_{j-\frac{1}{2}}}^{z_{j+\frac{1}{2}}} \sqrt{n} \Lambda_n dz = \frac{\hbar^2}{6q} \left[\frac{1}{m_n^*} \frac{\partial \sqrt{n}}{\partial z} \right]_{z_{j-\frac{1}{2}}}^{z_{j+\frac{1}{2}}}$$

The left-hand side can then be treated by assuming the product $\sqrt{n} \Lambda_n$ to be approximately constant over each edge, therefore applying the rectangle rule to obtain:

$$\sqrt{n_j} \Lambda_{n,j} L_{j-\frac{1}{2},j+\frac{1}{2}} = \frac{\hbar^2}{6q} \left[\frac{1}{m_n^*} \frac{\partial \sqrt{n}}{\partial z} \Big|_{z_{j+\frac{1}{2}}} - \frac{1}{m_n^*} \frac{\partial \sqrt{n}}{\partial z} \Big|_{z_{j-\frac{1}{2}}} \right]$$

where $L_{j-\frac{1}{2},j+\frac{1}{2}} \triangleq z_{j+\frac{1}{2}} - z_{j-\frac{1}{2}}$ is the length of the control box.

This last equation can be rearranged into the form:

$$\sqrt{n_j} \Lambda_{n,j} L_{j-\frac{1}{2},j+\frac{1}{2}} - \frac{\hbar^2}{6q} \left[\frac{1}{m_n^*} \frac{\partial \sqrt{n}}{\partial z} \Big|_{z_{j+\frac{1}{2}}} - \frac{1}{m_n^*} \frac{\partial \sqrt{n}}{\partial z} \Big|_{z_{j-\frac{1}{2}}} \right] = 0 \quad (10.61)$$

The derivatives can then be approximated by means of finite differences as follows:

$$\frac{\partial \sqrt{n}}{\partial z} \Big|_{z_{j+\frac{1}{2}}} \approx \frac{\sqrt{n_{j+1}} - \sqrt{n_j}}{L_{j,j+1}}$$

$$\left. \frac{\partial \sqrt{n}}{\partial z} \right|_{z_{j-\frac{1}{2}}} \approx \frac{\sqrt{n_j} - \sqrt{n_{j-1}}}{L_{j-1,j}}$$

which, substituted into Equation 10.61, yields the final result:

$$\boxed{\sqrt{n_j} \Lambda_{n,j} L_{j-\frac{1}{2},j+\frac{1}{2}} - \frac{\hbar^2}{6q} \left[\frac{1}{m_{n,j+\frac{1}{2}}^*} \frac{\sqrt{n_{j+1}} - \sqrt{n_j}}{L_{j,j+1}} - \frac{1}{m_{n,j-\frac{1}{2}}^*} \frac{\sqrt{n_j} - \sqrt{n_{j-1}}}{L_{j-1,j}} \right]} = 0 \quad (10.62)$$

Similarly to the previous cases, also the density gradient equation for electrons allows to write one equation for every couple of adjacent edges, i.e. one equation for every interior node of the mesh.

This equation therefore allows to write $N - 1$ equations in the unknowns; two additional equations can then be added by taking into account the boundary conditions at the contacts.

This kind of discretization is not the only possible one. Other discretization schemes have been proposed, such as the nonlinear discretization described in [26]. When tested on heterostructure devices these schemes are however numerically unstable and convergence resulted impossible to achieve, hence they won't be treated in this work.

10.4.1 Boundary Conditions

Also in this case, the first step is to understand how to deal with **heterostructures** in the electron density gradient equation.

Since the electron density and its derivative have been shown to be continuous at a heterojunction (since otherwise the quantum potential would exhibit Dirac δ 's or derivatives of Dirac δ 's), the discretization that has been derived above also holds when the two neighboring edges being considered are of different materials.

The presence of heterostructures can therefore also in this case simply not be taken into account when assembling the discretized problem.

For the outer contacts instead two main types of contact will be considered:

- **ideal ohmic contacts**

Ideal ohmic contacts have been shown in subsection 9.2.2 to impose a semiclassical distribution of electrons, hence:

$$\Lambda_n = 0$$

at an ideal ohmic contact.

These contacts therefore impose Dirichlet-type boundary conditions on the electron quantum potential Λ_n .

Therefore, for the case of an ideal ohmic contact at the left of the device the following equation can be added:

$$\boxed{\Lambda_{n,1} = 0}$$

Similarly, for an ideal ohmic contact at the right of the device the equation that can be added is:

$$\boxed{\Lambda_{n,N+1} = 0}$$

- **ideal Schottky contacts**

To understand how to treat ideal Schottky contacts it is useful to consider the first and the last portions of the discretization (i.e. of the mesh) as they are shown in Figure 10.8.

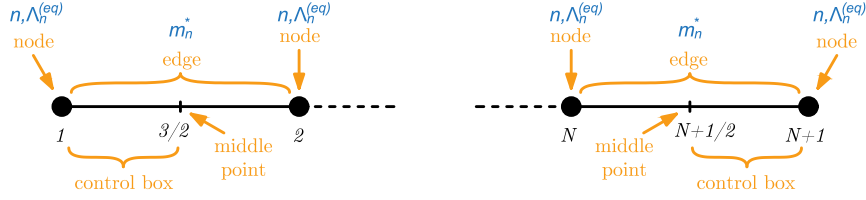


Figure 10.8: Discretization of the boundary conditions to the electron density gradient equation

In order to treat a Schottky contact at the left side of the device it is useful to integrate the electron density gradient equation over the first half of the first edge (i.e. over the “half control box” that goes from node 1 to the center $3/2$ of the first edge, as is shown in Figure 10.8):

$$\int_{z_1}^{z_{\frac{3}{2}}} \sqrt{n} \Lambda_n dz = \frac{\hbar^2}{6q} \int_{z_1}^{z_{\frac{3}{2}}} \frac{\partial}{\partial z} \left[\frac{1}{m_n^*} \frac{\partial \sqrt{n}}{\partial z} \right] dz$$

Applying the fundamental theorem of integral calculus to the first term and approximating the second term by means of the rectangle rule the equation becomes:

$$\sqrt{n_1} \Lambda_{n,1} L_{1,\frac{3}{2}} = \frac{\hbar^2}{6q} \left[\frac{1}{m_n^*} \frac{\partial \sqrt{n}}{\partial z} \right]_{z_1}^{z_{\frac{3}{2}}}$$

where $L_{1,\frac{3}{2}} \triangleq z_{\frac{3}{2}} - z_1$ is the length of the first (i.e. leftmost) “half control box”.

A Schottky contact was shown in subsection 9.2.3 to impose the condition:

$$\left. \frac{1}{m_n^*} \frac{\partial \sqrt{n}}{\partial z} \right|_{z_{\text{cont.}} \in \{z_1, z_{n+1}\}} \approx 0 \quad (10.63)$$

at the boundary (since $\nabla n \approx 0$ [23]). This condition can be substituted in the previous expression, obtaining:

$$\sqrt{n_1} \Lambda_{n,1} L_{1,\frac{3}{2}} = \frac{\hbar^2}{6q} \left. \frac{1}{m_n^*} \frac{\partial \sqrt{n}}{\partial z} \right|_{z_{\frac{3}{2}}}$$

Applying a finite-difference approximation for the derivative at the center of the edge:

$$\left. \frac{1}{m_n^*} \frac{\partial \sqrt{n}}{\partial z} \right|_{z_{\frac{3}{2}}} \approx \frac{1}{m_{n,\frac{3}{2}}^*} \frac{\sqrt{n_2} - \sqrt{n_1}}{L_{1,2}}$$

leads to the final result:

$$\boxed{\sqrt{n_1} \Lambda_{n,1} L_{1,\frac{3}{2}} - \frac{\hbar^2}{6q} \frac{1}{m_{n,\frac{3}{2}}^*} \frac{\sqrt{n_2} - \sqrt{n_1}}{L_{1,2}} = 0} \quad (10.64)$$

Similarly, to treat a Schottky contact at the right side of the device the electron density gradient equation can be integrated over the last half of the last edge (i.e. over the “half control box” that goes from the center $N + 1/2$ of the last edge to the last node $N + 1$ of the mesh) as:

$$\int_{z_{N+\frac{1}{2}}}^{z_{N+1}} \sqrt{n} \Lambda_n dz = \frac{\hbar^2}{6q} \int_{z_{N+\frac{1}{2}}}^{z_{N+1}} \frac{\partial}{\partial z} \left[\frac{1}{m_n^*} \frac{\partial \sqrt{n}}{\partial z} \right] dz$$

Applying the fundamental theorem of integral calculus to the first term and approximating the second term by means of the rectangle rule the equation becomes:

$$\sqrt{n_{N+1}} \Lambda_{n,N+1} L_{N+\frac{1}{2},N+1} = \frac{\hbar^2}{6q} \left[\frac{1}{m_n^*} \frac{\partial \sqrt{n}}{\partial z} \right]_{z_{N+\frac{1}{2}}}^{z_{N+1}}$$

where $L_{N+\frac{1}{2},N+1} \triangleq z_{N+1} - z_{N+\frac{1}{2}}$ is the length of the last (i.e. rightmost) “half control box”.

Imposing also in this case the Schottky boundary condition shown in Equation 10.63 the previous expression then becomes:

$$\sqrt{n_{N+1}} \Lambda_{n,N+1} L_{N+\frac{1}{2},N+1} = -\frac{\hbar^2}{6q} \frac{1}{m_n^*} \frac{\partial \sqrt{n}}{\partial z} \Big|_{z_{N+\frac{1}{2}}}$$

Applying a finite-difference approximation for the derivative at the center of the edge:

$$\frac{1}{m_n^*} \frac{\partial \sqrt{n}}{\partial z} \Big|_{z_{N+\frac{1}{2}}} \approx \frac{1}{m_{n,N+\frac{1}{2}}^*} \frac{\sqrt{n_{N+1}} - \sqrt{n_N}}{L_{N,N+1}}$$

leads to the final result:

$$\boxed{\sqrt{n_{N+1}} \Lambda_{n,N+1} L_{N+\frac{1}{2},N+1} + \frac{\hbar^2}{6q} \frac{1}{m_{n,N+\frac{1}{2}}^*} \frac{\sqrt{n_{N+1}} - \sqrt{n_N}}{L_{N,N+1}} = 0} \quad (10.65)$$

10.5 Hole Density Gradient Equation Discretization

The density gradient equation for holes that has to be discretized can be found by starting from the definition of the quantum potential Λ_p for electrons that was given in Equation 7.22:

$$\Lambda_p = \frac{\hbar^2}{6q} \frac{\nabla \cdot [(m_p^*)^{-1} \nabla \sqrt{p}]}{\sqrt{p}}$$

Multiplying both sides by the hole density p leads to the more convenient form:

$$\sqrt{p} \Lambda_p = \frac{\hbar^2}{6q} \nabla \cdot [(m_p^*)^{-1} \nabla \sqrt{p}]$$

which in one dimension reduces to the differential problem:

$$\sqrt{p} \Lambda_p = \frac{\hbar^2}{6q} \frac{\partial}{\partial z} \left[\frac{1}{m_p^*} \frac{\partial \sqrt{p}}{\partial z} \right] \quad (10.66)$$

Several implementation attempts have shown this form to yield best convergence results with initial guesses exhibiting discontinuities in the hole density p .

In order to simplify the discretization procedure, **control boxes** are again defined, i.e. segments that connect the middle point of an edge with the middle point of the next edge.

Moreover, the discretization choices that are adopted are to discretize:

- hole densities p and quantum potentials Λ_p at the nodes of the mesh
- effective masses m_p^* at the centers of the edges

as is shown in Figure 10.9.

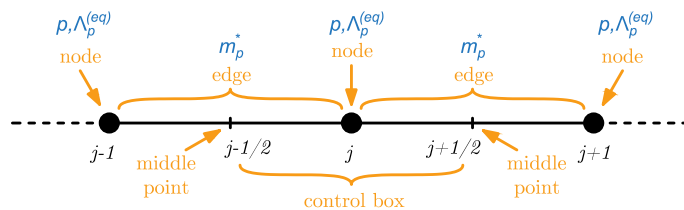


Figure 10.9: Hole density gradient equation discretization

The first step to determine a working discretization of the density gradient equation for holes is again to apply the **finite box** method.

Equation 10.66 must therefore be integrated over each control box, obtaining:

$$\int_{z_{j-\frac{1}{2}}}^{z_{j+\frac{1}{2}}} \sqrt{p} \Lambda_p dz = \frac{\hbar^2}{6q} \int_{z_{j-\frac{1}{2}}}^{z_{j+\frac{1}{2}}} \frac{\partial}{\partial z} \left[\frac{1}{m_p^*} \frac{\partial \sqrt{p}}{\partial z} \right] dz$$

Applying the fundamental theorem of integral calculus to the right-hand side of the equation reduces it to:

$$\int_{z_{j-\frac{1}{2}}}^{z_{j+\frac{1}{2}}} \sqrt{p} \Lambda_p dz = \frac{\hbar^2}{6q} \left[\frac{1}{m_p^*} \frac{\partial \sqrt{p}}{\partial z} \right]_{z_{j-\frac{1}{2}}}^{z_{j+\frac{1}{2}}}$$

The left-hand side can then be treated by assuming the product $\sqrt{p} \Lambda_p$ to be approximately constant over each edge, therefore applying the rectangle rule to obtain:

$$\sqrt{p_j} \Lambda_{p,j} L_{j-\frac{1}{2},j+\frac{1}{2}} = \frac{\hbar^2}{6q} \left[\frac{1}{m_p^*} \frac{\partial \sqrt{p}}{\partial z} \Big|_{z_{j+\frac{1}{2}}} - \frac{1}{m_p^*} \frac{\partial \sqrt{p}}{\partial z} \Big|_{z_{j-\frac{1}{2}}} \right]$$

where $L_{j-\frac{1}{2},j+\frac{1}{2}} \triangleq z_{j+\frac{1}{2}} - z_{j-\frac{1}{2}}$ is the length of the control box.

This last equation can be rearranged into the form:

$$\sqrt{p_j} \Lambda_{p,j} L_{j-\frac{1}{2},j+\frac{1}{2}} - \frac{\hbar^2}{6q} \left[\frac{1}{m_p^*} \frac{\partial \sqrt{p}}{\partial z} \Big|_{z_{j+\frac{1}{2}}} - \frac{1}{m_p^*} \frac{\partial \sqrt{p}}{\partial z} \Big|_{z_{j-\frac{1}{2}}} \right] = 0 \quad (10.67)$$

The derivatives can then be approximated by means of finite differences as follows:

$$\begin{aligned} \frac{\partial \sqrt{p}}{\partial z} \Big|_{z_{j+\frac{1}{2}}} &\approx \frac{\sqrt{p_{j+1}} - \sqrt{p_j}}{L_{j,j+1}} \\ \frac{\partial \sqrt{p}}{\partial z} \Big|_{z_{j-\frac{1}{2}}} &\approx \frac{\sqrt{p_j} - \sqrt{p_{j-1}}}{L_{j-1,j}} \end{aligned}$$

which, substituted into Equation 10.68, yields the final result:

$$\boxed{\sqrt{p_j} \Lambda_{p,j} L_{j-\frac{1}{2},j+\frac{1}{2}} - \frac{\hbar^2}{6q} \left[\frac{1}{m_{p,j+\frac{1}{2}}^*} \frac{\sqrt{p_{j+1}} - \sqrt{p_j}}{L_{j,j+1}} - \frac{1}{m_{p,j-\frac{1}{2}}^*} \frac{\sqrt{p_j} - \sqrt{p_{j-1}}}{L_{j-1,j}} \right]} = 0 \quad (10.68)$$

Similarly to the previous cases, also the density gradient equation for holes allows to write one equation for every couple of adjacent edges, i.e. one equation for every interior node of the mesh.

This equation therefore allows to write $N - 1$ equations in the unknowns; two additional equations can then be added by taking into account the boundary conditions at the contacts.

10.5.1 Boundary Conditions

Also in this case, the first step is to understand how to deal with **heterostructures** in the hole density gradient equation.

Since the hole density and its derivative have been shown to be continuous at a heterojunction (since otherwise the quantum potential would exhibit Dirac deltas or derivatives of Dirac deltas), the discretization that has been derived above also holds when the two neighboring edges being considered are of different materials.

The presence of heterostructures can therefore also in this case simply not be taken into account when assembling the discretized problem.

For the outer contacts instead two main types of contact will be considered:

- **ideal ohmic contacts**

Ideal ohmic contacts have been shown in subsection 9.2.2 to impose a semiclassical distribution of holes, hence:

$$\Lambda_p = 0$$

at an ideal ohmic contact.

These contacts therefore impose Dirichlet-type boundary conditions on the hole quantum potential Λ_p .

Therefore, for the case of an ideal ohmic contact at the left of the device the following equation can be added:

$$\Lambda_{p,1} = 0$$

Similarly, for an ideal ohmic contact at the right of the device the equation that can be added is:

$$\Lambda_{p,N+1} = 0$$

- **ideal Schottky contacts**

To understand how to treat ideal Schottky contacts it is useful to consider the first and the last portions of the discretization (i.e. of the mesh) as they are shown in Figure 10.10.



Figure 10.10: Discretization of the boundary conditions to the hole density gradient equation

In order to treat a Schottky contact at the left side of the device it is useful to integrate the hole density gradient equation over the first half of the first edge (i.e. over the “half control box” that goes from node 1 to the center 3/2 of the first edge, as is shown in Figure 10.10):

$$\int_{z_1}^{z_{\frac{3}{2}}} \sqrt{p} \Lambda_p dz = \frac{\hbar^2}{6q} \int_{z_1}^{z_{\frac{3}{2}}} \frac{\partial}{\partial z} \left[\frac{1}{m_p^*} \frac{\partial \sqrt{p}}{\partial z} \right] dz$$

Applying the fundamental theorem of integral calculus to the first term and approximating the second term by means of the rectangle rule the equation becomes:

$$\sqrt{p_1} \Lambda_{p,1} L_{1,\frac{3}{2}} = \frac{\hbar^2}{6q} \left[\frac{1}{m_p^*} \frac{\partial \sqrt{p}}{\partial z} \right]_{z_1}^{z_{\frac{3}{2}}}$$

where $L_{1,\frac{3}{2}} \triangleq z_{\frac{3}{2}} - z_1$ is the length of the first (i.e. leftmost) “half control box”.

A Schottky contact was shown in subsection 9.2.3 to impose the condition:

$$\left. \frac{1}{m_p^*} \frac{\partial \sqrt{p}}{\partial z} \right|_{z_{\text{cont.}} \in \{z_1, z_{n+1}\}} \approx 0 \quad (10.69)$$

at the boundary (since $\nabla p \approx 0$ [23]). This condition can be substituted in the previous expression, obtaining:

$$\sqrt{p_1} \Lambda_{p,1} L_{1,\frac{3}{2}} = \frac{\hbar^2}{6q} \left. \frac{1}{m_p^*} \frac{\partial \sqrt{p}}{\partial z} \right|_{z_{\frac{3}{2}}}$$

Applying a finite-difference approximation for the derivative at the center of the edge:

$$\left. \frac{1}{m_p^*} \frac{\partial \sqrt{p}}{\partial z} \right|_{z_{\frac{3}{2}}} \approx \frac{1}{m_{p,\frac{3}{2}}^*} \frac{\sqrt{p_2} - \sqrt{p_1}}{L_{1,2}}$$

leads to the final result:

$$\boxed{\sqrt{p_1} \Lambda_{p,1} L_{1,\frac{3}{2}} - \frac{\hbar^2}{6q} \frac{1}{m_{p,\frac{3}{2}}^*} \frac{\sqrt{p_2} - \sqrt{p_1}}{L_{1,2}} = 0} \quad (10.70)$$

Similarly, to treat a Schottky contact at the right side of the device the hole density gradient equation can be integrated over the last half of the last edge (i.e. over the “half control box” that goes from the center $N + 1/2$ of the last edge to the last node $N + 1$ of the mesh) as:

$$\int_{z_{N+\frac{1}{2}}}^{z_{N+1}} \sqrt{p} \Lambda_p dz = \frac{\hbar^2}{6q} \int_{z_{N+\frac{1}{2}}}^{z_{N+1}} \frac{\partial}{\partial z} \left[\frac{1}{m_p^*} \frac{\partial \sqrt{p}}{\partial z} \right] dz$$

Applying the fundamental theorem of integral calculus to the first term and approximating the second term by means of the rectangle rule the equation becomes:

$$\sqrt{p_{N+1}} \Lambda_{p,N+1} L_{N+\frac{1}{2},N+1} = \frac{\hbar^2}{6q} \left[\frac{1}{m_p^*} \frac{\partial \sqrt{p}}{\partial z} \right]_{z_{N+\frac{1}{2}}}^{z_{N+1}}$$

where $L_{N+\frac{1}{2},N+1} \triangleq z_{N+1} - z_{N+\frac{1}{2}}$ is the length of the last (i.e. rightmost) “half control box”.

Imposing also in this case the Schottky boundary condition shown in Equation 10.69 the previous expression then becomes:

$$\sqrt{p_{N+1}} \Lambda_{p,N+1} L_{N+\frac{1}{2},N+1} = - \frac{\hbar^2}{6q} \left. \frac{1}{m_p^*} \frac{\partial \sqrt{p}}{\partial z} \right|_{z_{N+\frac{1}{2}}}$$

Applying a finite-difference approximation for the derivative at the center of the edge:

$$\left. \frac{1}{m_p^*} \frac{\partial \sqrt{p}}{\partial z} \right|_{z_{N+\frac{1}{2}}} \approx \frac{1}{m_{p,N+\frac{1}{2}}^*} \frac{\sqrt{p_{N+1}} - \sqrt{p_N}}{L_{N,N+1}}$$

leads to the final result:

$$\boxed{\sqrt{p_{N+1}} \Lambda_{p,N+1} L_{N+\frac{1}{2},N+1} + \frac{\hbar^2}{6q} \frac{1}{m_{p,N+\frac{1}{2}}^*} \frac{\sqrt{p_{N+1}} - \sqrt{p_N}}{L_{N,N+1}} = 0} \quad (10.71)$$

Chapter 11

Numerical Techniques

The equations that have been derived in the previous chapter, though being discretized and not exhibiting any explicit differential operator, are for the most part **nonlinear** in the unknowns ϕ , n , p , λ_n and λ_p of the quantum drift-diffusion problem.

It is therefore useful to treat and apply here the most common method for the solution of nonlinear problems in one or more unknowns: **Newton's iterative method** [16][21].

11.1 Introduction to Newton's method

Let $f(x)$ be a (possibly) nonlinear function of the argument x for which one or more zeros exist.

The goal is to determine a zero of the function, i.e. a value x_0 of the unknown x that satisfies the constraint $f(x_0) = 0$.

An example of one such function is shown in Figure 11.1.

Newton's method is based on the idea of iteratively refining a guess of the solution (i.e. of the zero) by assuming the function to behave **approximately linearly** in the region of interest.

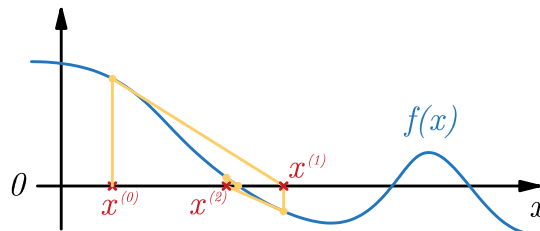


Figure 11.1: Newton's method (1 unknown)

Given a guess $x^{(k)}$ of the solution then each iteration refines this guess by:

1. linearizing the problem at the guess $x^{(k)}$ by means of a Taylor series:

$$f(x) \approx f(x^{(k)}) + \left. \frac{df}{dx} \right|_{x^{(k)}} [x - x^{(k)}]$$

2. solving the linearized problem for the new (ideally better) guess $x^{(k+1)}$ for the zero of the problem:

$$0 = f(x^{(k)}) + \left. \frac{df}{dx} \right|_{x^{(k)}} [x^{(k+1)} - x^{(k)}]$$

The correction $\Delta x^{(k)} = x^{(k+1)} - x^{(k)}$ to the guess for the zero at the k^{th} iteration of Newton's method is then given by:

$$\Delta x^{(k)} = -f(x^{(k)}) \left(\left. \frac{df}{dx} \right|_{x^{(k)}} \right)^{-1}$$

3. updating the guess as:

$$x^{(k+1)} = x^{(k)} + \Delta x^{(k)}$$

and reiterating the method to further refine the guess until it is accurate enough.

Since Newton's method is only good for refining a guess it is clear that a good enough initial guess for the method should be adopted.

It is also clear that both the properties of the curve whose zeros must be found and the choice of initial guess play a fundamental role in determining if and how the sequence of guesses converges to a zero and, if more than one zero is present, to which of them it converges.

Figure 11.1 shows graphically a few steps of Newton's method, starting from an arbitrary initial guess.

Since Newton's method is iterative in nature it is important to determine **stopping criteria** for it.

Possible ways to determine the convergence of Newton's method and therefore terminating the iterations are:

- Monitoring the residual $f(x^{(k)})$; if its value drops below a target value η_f the execution can be terminated successfully
- Monitoring the absolute value of the update to the guess $|\delta x|$; if its value drops below a target value η_x the execution can be terminated successfully

If more restrictive criteria are needed for determining the convergence of the method, both criteria can be enforced together.

11.2 Generalized Newton's method

Newton's method is an extremely useful tool, but it strictly applies to functions of one unknown only.

A generalization has been proposed (and will be adopted here) that exploits linearization in an N -dimensional space (where N is the number of unknowns) and matrix calculus to get an approximate solution to **systems of nonlinear equations**.

Consider a system of nonlinear equations:

$$\begin{cases} f_1(x_1, x_2, \dots, x_{N-1}, x_N) = 0 \\ f_2(x_1, x_2, \dots, x_{N-1}, x_N) = 0 \\ \dots \\ f_{N-1}(x_1, x_2, \dots, x_{N-1}, x_N) = 0 \\ f_N(x_1, x_2, \dots, x_{N-1}, x_N) = 0 \end{cases}$$

for which a numerical solution must be found.

Suppose now to know a good enough an initial guess $\mathbf{x}^{(0)} = [x_1^{(0)} \ x_2^{(0)} \ \dots \ x_{N-1}^{(0)} \ x_N^{(0)}]^T$ for the solution to the problem.

Similarly to the classical Newton's method, the idea is to linearize the problem around the solution guess $\mathbf{x}^{(k)} \triangleq [x_1^{(k)} \ x_2^{(k)} \ \dots \ x_{N-1}^{(k)} \ x_N^{(k)}]^T$ through the use of the multidimensional Taylor approximation:

$$f_m(x_1, x_2, \dots, x_{N-1}, x_N) \approx f_m(x_1^{(k)}, x_2^{(k)}, \dots, x_{N-1}^{(k)}, x_N^{(k)}) + \sum_{j=1}^N \left. \frac{\partial f_m}{\partial x_j} \right|_{\mathbf{x}=\mathbf{x}^{(k)}} (x_j - x_j^{(k)})$$

The next step is to try to refine the guess into a new one $\mathbf{x}^{(k+1)} \triangleq [x_1^{(k+1)} \ x_2^{(k+1)} \ \dots \ x_{N-1}^{(k+1)} \ x_N^{(k+1)}]^T$ by finding the zero of the linearized problem:

$$f_m(x_1^{(k)}, x_2^{(k)}, \dots, x_{N-1}^{(k)}, x_N^{(k)}) + \sum_{j=1}^N \left. \frac{\partial f_m}{\partial x_j} \right|_{\mathbf{x}=\mathbf{x}^{(k)}} (x_j^{(k+1)} - x_j^{(k)}) = 0$$

Defining the Jacobian matrix for the system of nonlinear equations as the matrix \mathbf{J} whose entries are:

$$[\mathbf{J}]_{m,j}^{(k)} \triangleq \left. \frac{\partial f_m}{\partial x_j} \right|_{\mathbf{x}=\mathbf{x}^{(k)}}$$

and defining also the “update” to the guess as the vector $\Delta \mathbf{x}^{(k)}$ whose entries are:

$$[\Delta \mathbf{x}^{(k)}]_j \triangleq x_j^{(k+1)} - x_j^{(k)}$$

the problem can be cast into matrix form as:

$$\mathbf{J} \Delta \mathbf{x}^{(k)} = -\mathbf{f}(\mathbf{x}^k) \quad (11.1)$$

where $\mathbf{f} \triangleq [f_1 \ f_2 \ \cdots \ f_{N-1} \ f_N]^T$ is the vector of all the functions within the nonlinear system.

The linear system of equations in Equation 11.1 can be solved for the unknown $\Delta \mathbf{x}^{(k)}$ and the result can be used to improve the guess $\mathbf{x}^{(k)}$ into the new guess $\mathbf{x}^{(k+1)}$ as:

$$\mathbf{x}^{(k+1)} = \mathbf{x}^{(k)} + \Delta \mathbf{x}^{(k)}$$

This procedure is then reiterated as many times as needed to refine the guess enough.

The stopping criteria can also in this case be defined in analogy to the case of the classical Newton’s method.

In particular, possible stopping criteria for the iterative method are:

- if the norm of the residual $\|\mathbf{f}(\mathbf{x}^k)\|$ drops below a target value η_f
- if the norm of the update $\|\Delta \mathbf{x}\|$ drops below a target value η_x

If more restrictive stopping criteria are needed the two conditions may be enforced together.

11.3 Quantum Drift-Diffusion problem

The goal of this section is now to first collect together the results of the discretization that was presented in chapter 10 and then to derive all the elements (in particular the entries of the Jacobian) that are necessary to perform a discretization according to the generalized Newton’s method.

The discretized equations that will have to be implemented are:

- **Poisson’s equation** (Equation 10.3)

$$\epsilon_{j+\frac{1}{2}} \frac{\phi_{j+1} - \phi_j}{L_{j,j+1}} - \epsilon_{j-\frac{1}{2}} \frac{\phi_j - \phi_{j-1}}{L_{j-1,j}} + q(p_j - n_j + N_{d,j} - N_{a,j}) L_{j-\frac{1}{2},j+\frac{1}{2}} = 0 \quad (11.2)$$

with boundary conditions for ohmic contacts:

$$\phi_1 - \phi_{0,1} - V_{\text{left}} = 0 \quad \phi_{N+1} - \phi_{0,N+1} - V_{\text{right}} = 0 \quad (11.3)$$

or with boundary conditions for Schottky contacts:

$$\phi_1 - \frac{-E_{f,\text{eq}}^{(\text{left})} + qV^{(\text{left})} - q\phi_b^{(\text{left})} + \Delta E_c^{(\text{left})}}{q} = 0 \quad (11.4)$$

$$\phi_{N+1} - \frac{-E_{f,\text{eq}}^{(\text{right})} + qV^{(\text{right})} - q\phi_b^{(\text{right})} + \Delta E_c^{(\text{right})}}{q} = 0 \quad (11.5)$$

• **Electron continuity equation** (Equation 10.21)

$$\begin{aligned} & \frac{D_{n,j+\frac{1}{2}}}{L_{j,j+1}} \left[n_{j+1} \mathcal{B} \left(\frac{\phi_{n,j+1}^{(eq)} - \phi_{n,j}^{(eq)}}{V_T} \right) - n_j \mathcal{B} \left(-\frac{\phi_{n,j+1}^{(eq)} - \phi_{n,j}^{(eq)}}{V_T} \right) \right] + \\ & - \frac{D_{n,j-\frac{1}{2}}}{L_{j-1,j}} \left[n_j \mathcal{B} \left(\frac{\phi_{n,j}^{(eq)} - \phi_{n,j-1}^{(eq)}}{V_T} \right) - n_{j-1} \mathcal{B} \left(-\frac{\phi_{n,j}^{(eq)} - \phi_{n,j-1}^{(eq)}}{V_T} \right) \right] - U_{n,j} L_{j-\frac{1}{2},j+\frac{1}{2}} = 0 \end{aligned} \quad (11.6)$$

with boundary conditions for ohmic contacts:

$$n_1 - n_0^{(left)} \approx 0 \quad n_{N+1} - n_0^{(right)} \approx 0 \quad (11.7)$$

or with boundary conditions for Schottky contacts:

$$\begin{aligned} & \frac{D_{n,3/2}}{L_{1,2}} \left[n_2 \mathcal{B} \left(\frac{\phi_{n,2}^{(eq)} - \phi_{n,1}^{(eq)}}{V_T} \right) - n_1 \mathcal{B} \left(-\frac{\phi_{n,2}^{(eq)} - \phi_{n,1}^{(eq)}}{V_T} \right) \right] + \\ & - v_n^{(left)} (n_1 - n_0^{(left)}) - U_{n,1} L_{1,3/2} = 0 \end{aligned} \quad (11.8)$$

$$\begin{aligned} & \frac{D_{n,N+\frac{1}{2}}}{L_{N,N+1}} \left[n_N \mathcal{B} \left(-\frac{\phi_{n,N+1}^{(eq)} - \phi_{n,N}^{(eq)}}{V_T} \right) - n_{N+1} \mathcal{B} \left(\frac{\phi_{n,N+1}^{(eq)} - \phi_{n,N}^{(eq)}}{V_T} \right) \right] + \\ & - v_n^{(right)} (n_{N+1} - n_0^{(right)}) - U_{n,N+1} L_{N+\frac{1}{2},N+1} = 0 \end{aligned} \quad (11.9)$$

The net SRH recombination rates for electrons are found as:

$$U_{n,j}^{SRH} \approx \frac{n_j p_j - n_{i,j}^2}{\tau_{p,j}(n_j + n_{t,j}) + \tau_{n,j}(p_j + p_{t,j})} \quad (11.10)$$

• **Hole continuity equation** (Equation 10.49)

$$\begin{aligned} & \frac{D_{p,j+\frac{1}{2}}}{L_{j,j+1}} \left[p_j \mathcal{B} \left(\frac{\phi_{p,j+1}^{(eq)} - \phi_{p,j}^{(eq)}}{V_T} \right) - p_{j+1} \mathcal{B} \left(-\frac{\phi_{p,j+1}^{(eq)} - \phi_{p,j}^{(eq)}}{V_T} \right) \right] + \\ & - \frac{D_{p,j-\frac{1}{2}}}{L_{j-1,j}} \left[p_{j-1} \mathcal{B} \left(\frac{\phi_{p,j}^{(eq)} - \phi_{p,j-1}^{(eq)}}{V_T} \right) - p_j \mathcal{B} \left(-\frac{\phi_{p,j}^{(eq)} - \phi_{p,j-1}^{(eq)}}{V_T} \right) \right] + U_{p,j} L_{j-\frac{1}{2},j+\frac{1}{2}} = 0 \end{aligned} \quad (11.11)$$

with boundary conditions for ohmic contacts:

$$p_1 - p_0^{(left)} \approx 0 \quad p_{N+1} - p_0^{(right)} \approx 0 \quad (11.12)$$

or with boundary conditions for Schottky contacts:

$$\begin{aligned} & \frac{D_{p,3/2}}{L_{1,2}} \left[p_1 \mathcal{B} \left(\frac{\phi_{p,2}^{(eq)} - \phi_{p,1}^{(eq)}}{V_T} \right) - p_2 \mathcal{B} \left(-\frac{\phi_{p,2}^{(eq)} - \phi_{p,1}^{(eq)}}{V_T} \right) \right] + \\ & + v_p^{(left)} (p_1 - p_0^{(left)}) + U_{p,1} L_{1,3/2} = 0 \end{aligned} \quad (11.13)$$

$$\begin{aligned} & \frac{D_{p,N+\frac{1}{2}}}{L_{N,N+1}} \left[p_{N+1} \mathcal{B} \left(-\frac{\phi_{p,N+1}^{(eq)} - \phi_{p,N}^{(eq)}}{V_T} \right) - p_N \mathcal{B} \left(\frac{\phi_{p,N+1}^{(eq)} - \phi_{p,N}^{(eq)}}{V_T} \right) \right] + \\ & + v_p^{(right)} (p_{N+1} - p_0^{(right)}) + U_{p,N+1} L_{N+\frac{1}{2},N+1} = 0 \end{aligned} \quad (11.14)$$

The net SRH recombination rates for holes are found as:

$$U_{p,j}^{SRH} \approx \frac{n_j p_j - n_{i,j}^2}{\tau_{p,j}(n_j + n_{t,j}) + \tau_{n,j}(p_j + p_{t,j})} \quad (11.15)$$

- **Electron density gradient equation** (Equation 10.61)

$$\sqrt{n_j} \Lambda_{n,j} L_{j-\frac{1}{2},j+\frac{1}{2}} - \frac{\hbar^2}{6q} \left[\frac{1}{m_{n,j+\frac{1}{2}}^*} \frac{\sqrt{n_{j+1}} - \sqrt{n_j}}{L_{j,j+1}} - \frac{1}{m_{n,j-\frac{1}{2}}^*} \frac{\sqrt{n_j} - \sqrt{n_{j-1}}}{L_{j-1,j}} \right] = 0 \quad (11.16)$$

with boundary conditions for ohmic contacts:

$$\Lambda_{n,1} = 0 \quad \Lambda_{n,N+1} = 0 \quad (11.17)$$

or with boundary conditions for Schottky contacts:

$$\sqrt{n_1} \Lambda_{n,1} L_{1,\frac{3}{2}} - \frac{\hbar^2}{6q} \frac{1}{m_{n,\frac{3}{2}}^*} \frac{\sqrt{n_2} - \sqrt{n_1}}{L_{1,2}} = 0 \quad (11.18)$$

$$\sqrt{n_{N+1}} \Lambda_{n,N+1} L_{N+\frac{1}{2},N+1} + \frac{\hbar^2}{6q} \frac{1}{m_{n,N+\frac{1}{2}}^*} \frac{\sqrt{n_{N+1}} - \sqrt{n_N}}{L_{N,N+1}} = 0 \quad (11.19)$$

- **Hole density gradient equation** (Equation 10.68)

$$\sqrt{p_j} \Lambda_{p,j} L_{j-\frac{1}{2},j+\frac{1}{2}} - \frac{\hbar^2}{6q} \left[\frac{1}{m_{p,j+\frac{1}{2}}^*} \frac{\sqrt{p_{j+1}} - \sqrt{p_j}}{L_{j,j+1}} - \frac{1}{m_{p,j-\frac{1}{2}}^*} \frac{\sqrt{p_j} - \sqrt{p_{j-1}}}{L_{j-1,j}} \right] = 0 \quad (11.20)$$

with boundary conditions for ohmic contacts:

$$\Lambda_{p,1} = 0 \quad \Lambda_{p,N+1} = 0 \quad (11.21)$$

or with boundary conditions for Schottky contacts:

$$\sqrt{p_1} \Lambda_{p,1} L_{1,\frac{3}{2}} - \frac{\hbar^2}{6q} \frac{1}{m_{p,\frac{3}{2}}^*} \frac{\sqrt{p_2} - \sqrt{p_1}}{L_{1,2}} = 0 \quad (11.22)$$

$$\sqrt{p_{N+1}} \Lambda_{p,N+1} L_{N+\frac{1}{2},N+1} + \frac{\hbar^2}{6q} \frac{1}{m_{p,N+\frac{1}{2}}^*} \frac{\sqrt{p_{N+1}} - \sqrt{p_N}}{L_{N,N+1}} = 0 \quad (11.23)$$

All these equations will have to be solved concurrently and form a system of equations of the kind of the one described in section 11.2.

11.3.1 Nonlinear Problem

The nonlinear problem obtained by assembling all the previously mentioned equations can be written in block matrix form as:

$$\begin{bmatrix} \mathbf{f}_{\mathbf{P}}(\phi, \mathbf{n}, \mathbf{p}) \\ \mathbf{f}_{\mathbf{C}_n}(\phi, \mathbf{n}, \Lambda_n) \\ \mathbf{f}_{\mathbf{C}_p}(\phi, \mathbf{p}, \Lambda_p) \\ \mathbf{f}_{\mathbf{D}_n}(\mathbf{n}, \Lambda_n) \\ \mathbf{f}_{\mathbf{D}_p}(\mathbf{p}, \Lambda_p) \end{bmatrix} = \begin{bmatrix} \mathbf{0} \\ \mathbf{0} \\ \mathbf{0} \\ \mathbf{0} \\ \mathbf{0} \end{bmatrix} \quad (11.24)$$

where:

- $\mathbf{f}_{\mathbf{P}}$ is the left-hand side of the discretized Poisson equation and of its boundary conditions
- $\mathbf{f}_{\mathbf{C}_n}$ is the left-hand side of the discretized electron continuity equation and of its boundary conditions
- $\mathbf{f}_{\mathbf{C}_p}$ is the left-hand side of the discretized hole continuity equation and of its boundary conditions
- $\mathbf{f}_{\mathbf{D}_n}$ is the left-hand side of the discretized electron density gradient equation and of its boundary conditions

- f_{D_p} is the left-hand side of the discretized hole density gradient equation and of its boundary conditions and ϕ , \mathbf{n} , \mathbf{p} , Λ_n , Λ_p are the discretized unknowns (i.e. are vectors that would ideally interpolate the true continuous solutions at the nodes of the mesh).

It is important to remark that each of these five equations when discretized over a mesh with N edges (and therefore $N + 1$ nodes) will introduce an equation for the left boundary condition, $N - 1$ equations for the inner nodes and an equation for the right boundary condition.

Together, the five equations will then introduce $5N + 5$ equations; since the number of unknown values is also $5N + 5$ (since there are $N + 1$ nodes and 5 unknowns defined on each node) the system is complete and solvable if no degeneracy arises that makes its determinant null.

11.3.2 Jacobian of the Nonlinear Problem

Since the goal is to solve the problem by means of Newton's method it is useful to first define the form that the Jacobian of the nonlinear problem will take and to then evaluate its components.

According to the form of the system that was defined in Equation 11.25 the Jacobian of the problem given by the left-hand side will take the form:

$$\mathbf{J}^{(k)}(\phi, \mathbf{n}, \mathbf{p}, \Lambda_n, \Lambda_p) = \begin{bmatrix} \mathbf{J}_{P,\phi}^{(k)} & \mathbf{J}_{P,n}^{(k)} & \mathbf{J}_{P,p}^{(k)} & \mathbf{0} & \mathbf{0} \\ \mathbf{J}_{C_n,\phi}^{(k)} & \mathbf{J}_{C_n,n}^{(k)} & \mathbf{J}_{C_n,p}^{(k)} & \mathbf{J}_{C_n,\Lambda_n}^{(k)} & \mathbf{0} \\ \mathbf{J}_{C_p,\phi}^{(k)} & \mathbf{J}_{C_p,n}^{(k)} & \mathbf{J}_{C_p,p}^{(k)} & \mathbf{0} & \mathbf{J}_{C_p,\Lambda_p}^{(k)} \\ \mathbf{0} & \mathbf{J}_{D_n,n}^{(k)} & \mathbf{0} & \mathbf{J}_{D_n,\Lambda_n}^{(k)} & \mathbf{0} \\ \mathbf{0} & \mathbf{0} & \mathbf{J}_{D_p,p}^{(k)} & \mathbf{0} & \mathbf{J}_{D_p,\Lambda_p}^{(k)} \end{bmatrix} (\phi, \mathbf{n}, \mathbf{p}, \Lambda_n, \Lambda_p) \quad (11.25)$$

where the notation $\mathbf{J}_{E,u}$ is adopted to denote the Jacobian of the discretized equation $E = 0$ with respect to the discretized unknown \mathbf{u} . In other words, it is the matrix whose entries are:

$$\left[\mathbf{J}_{E,u}^{(k)} \right]_{m,j} = \frac{\partial f_{E,m}}{\partial u_j} \Bigg|_{\substack{\phi=\phi^{(k)} \\ \mathbf{n}=\mathbf{n}^{(k)} \\ \mathbf{p}=\mathbf{p}^{(k)} \\ \Lambda_n=\Lambda_n^{(k)} \\ \Lambda_p=\Lambda_p^{(k)}}$$

being $f_{E,m}$ the residual of the m^{th} equation resulting from the discretization of equation E (as in the convention of Equation 11.25).

Notice that, in this convention, the index m denotes the equation number while the index j denotes the component of the unknown vector with respect to which differentiation is carried out.

In order to simplify the notation, the subscript $\phi = \phi^{(k)}$, $\mathbf{n} = \mathbf{n}^{(k)}$, $\mathbf{p} = \mathbf{p}^{(k)}$, $\Lambda_n = \Lambda_n^{(k)}$, $\Lambda_p = \Lambda_p^{(k)}$ will be replaced in the following by $\mathbf{x} = \mathbf{x}^{(k)}$ (where \mathbf{x} represents the vector of all the unknowns).

According to the method that was defined in section 11.2, the linearized problem that will have to be solved to determine the updates $\Delta\phi^{(k)}$, $\Delta\mathbf{n}^{(k)}$, $\Delta\mathbf{p}^{(k)}$, $\Delta\Lambda_n^{(k)}$, $\Delta\Lambda_p^{(k)}$ to the guesses is:

$$\mathbf{J}^{(k)} \begin{bmatrix} \Delta\phi^{(k)} \\ \Delta\mathbf{n}^{(k)} \\ \Delta\mathbf{p}^{(k)} \\ \Delta\Lambda_n^{(k)} \\ \Delta\Lambda_p^{(k)} \end{bmatrix} = \mathbf{0} \quad \Leftrightarrow \quad \begin{bmatrix} \mathbf{J}_{P,\phi}^{(k)} & \mathbf{J}_{P,n}^{(k)} & \mathbf{J}_{P,p}^{(k)} & \mathbf{0} & \mathbf{0} \\ \mathbf{J}_{C_n,\phi}^{(k)} & \mathbf{J}_{C_n,n}^{(k)} & \mathbf{J}_{C_n,p}^{(k)} & \mathbf{J}_{C_n,\Lambda_n}^{(k)} & \mathbf{0} \\ \mathbf{J}_{C_p,\phi}^{(k)} & \mathbf{J}_{C_p,n}^{(k)} & \mathbf{J}_{C_p,p}^{(k)} & \mathbf{0} & \mathbf{J}_{C_p,\Lambda_p}^{(k)} \\ \mathbf{0} & \mathbf{J}_{D_n,n}^{(k)} & \mathbf{0} & \mathbf{J}_{D_n,\Lambda_n}^{(k)} & \mathbf{0} \\ \mathbf{0} & \mathbf{0} & \mathbf{J}_{D_p,p}^{(k)} & \mathbf{0} & \mathbf{J}_{D_p,\Lambda_p}^{(k)} \end{bmatrix} \begin{bmatrix} \Delta\phi^{(k)} \\ \Delta\mathbf{n}^{(k)} \\ \Delta\mathbf{p}^{(k)} \\ \Delta\Lambda_n^{(k)} \\ \Delta\Lambda_p^{(k)} \end{bmatrix} = \mathbf{0} \quad (11.26)$$

The next step in the implementation of this model is then to determine analytical expressions for the components of each of the blocks appearing in the Jacobian for the problem.

Entries of $\mathbf{J}_{\mathbf{P},\phi}^{(k)}$

The matrix $\mathbf{J}_{\mathbf{P},\phi}^{(k)}$ is the block of the Jacobian containing the derivatives with respect to the potential at the nodes of the left-hand sides of the equations resulting from discretizing Poisson's equation.

The first line of this matrix is obtained from differentiating the boundary condition for Poisson's equation at the left contact with respect to the components of the discretized potential vector ϕ . It is then important to distinguish between the two types of contacts:

- if the left contact is of ohmic type then the only nonzero derivative with respect to the potentials at the nodes of Equation 11.3 is:

$$\left[\mathbf{J}_{\mathbf{P},\phi}^{(k)} \right]_{1,1} = \frac{\partial}{\partial \phi_1} \left\{ \phi_1 - \phi_{0,1} - V_{\text{left}} \right\} \Big|_{x=x^{(k)}} = 1$$

- if the left contact is of Schottky type then the only nonzero derivative with respect to the potentials at the nodes of Equation 11.4 is:

$$\left[\mathbf{J}_{\mathbf{P},\phi}^{(k)} \right]_{1,1} = \frac{\partial}{\partial \phi_1} \left\{ \phi_1 - \frac{-E_{f,\text{eq}}^{(\text{left})} + qV^{(\text{left})} - q\phi_b^{(\text{left})} + \Delta E_c^{(\text{left})}}{q} \right\} \Big|_{x=x^{(k)}} = 1$$

The inner lines of this matrix ($j = 2 \cdots N$) are obtained instead by differentiating the left-hand side of the j^{th} discretized Poisson's equation with respect to ϕ_{j-1} , ϕ_j and ϕ_{j+1} (which are the only non-null derivatives with respect to the potentials at the nodes):

$$\begin{aligned} \left[\mathbf{J}_{\mathbf{P},\phi}^{(k)} \right]_{j,j-1} &= \frac{\partial}{\partial \phi_{j-1}} \left\{ \epsilon_{j+\frac{1}{2}} \frac{\phi_{j+1} - \phi_j}{L_{j,j+1}} - \epsilon_{j-\frac{1}{2}} \frac{\phi_j - \phi_{j-1}}{L_{j-1,j}} + q(p_j - n_j + N_{d,j} - N_{a,j}) L_{j-\frac{1}{2},j+\frac{1}{2}} \right\} \Big|_{x=x^{(k)}} \\ &= + \frac{\epsilon_{j-\frac{1}{2}}}{L_{j-1,j}} \end{aligned}$$

$$\begin{aligned} \left[\mathbf{J}_{\mathbf{P},\phi}^{(k)} \right]_{j,j} &= \frac{\partial}{\partial \phi_j} \left\{ \epsilon_{j+\frac{1}{2}} \frac{\phi_{j+1} - \phi_j}{L_{j,j+1}} - \epsilon_{j-\frac{1}{2}} \frac{\phi_j - \phi_{j-1}}{L_{j-1,j}} + q(p_j - n_j + N_{d,j} - N_{a,j}) L_{j-\frac{1}{2},j+\frac{1}{2}} \right\} \Big|_{x=x^{(k)}} \\ &= - \frac{\epsilon_{j+\frac{1}{2}}}{L_{j,j+1}} - \frac{\epsilon_{j-\frac{1}{2}}}{L_{j-1,j}} \end{aligned}$$

$$\begin{aligned} \left[\mathbf{J}_{\mathbf{P},\phi}^{(k)} \right]_{j,j+1} &= \frac{\partial}{\partial \phi_{j+1}} \left\{ \epsilon_{j+\frac{1}{2}} \frac{\phi_{j+1} - \phi_j}{L_{j,j+1}} - \epsilon_{j-\frac{1}{2}} \frac{\phi_j - \phi_{j-1}}{L_{j-1,j}} + q(p_j - n_j + N_{d,j} - N_{a,j}) L_{j-\frac{1}{2},j+\frac{1}{2}} \right\} \Big|_{x=x^{(k)}} \\ &= + \frac{\epsilon_{j+\frac{1}{2}}}{L_{j,j+1}} \end{aligned}$$

The last line of this matrix is obtained from differentiating the boundary condition for Poisson's equation at the right contact with respect to the components of the discretized potential vector ϕ . It is then again necessary to distinguish between the two types of contacts:

- if the right contact is of ohmic type then the only nonzero derivative with respect to the potentials at the nodes of Equation 11.3 is:

$$\left[\mathbf{J}_{\mathbf{P},\phi}^{(k)} \right]_{N+1,N+1} = \frac{\partial}{\partial \phi_{N+1}} \left\{ \phi_{N+1} - \phi_{0,N+1} - V_{\text{right}} \right\} \Big|_{x=x^{(k)}} = 1$$

- if the right contact is of Schottky type then the only nonzero derivative with respect to the potentials at the nodes of Equation 11.5 is:

$$\left[\mathbf{J}_{\mathbf{P},\phi}^{(k)} \right]_{N+1,N+1} = \frac{\partial}{\partial \phi_{N+1}} \left\{ \phi_{N+1} - \frac{-E_{f,\text{eq}}^{(\text{right})} + qV^{(\text{right})} - q\phi_b^{(\text{right})} + \Delta E_c^{(\text{right})}}{q} \right\} \Big|_{x=x^{(k)}} = 1$$

Entries of $\mathbf{J}_{\mathbf{P},\mathbf{n}}^{(k)}$

The matrix $\mathbf{J}_{\mathbf{P},\mathbf{n}}^{(k)}$ is the block of the Jacobian containing the derivatives with respect to the electron densities at the nodes of the left-hand sides of the equations resulting from discretizing Poisson's equation.

Since the boundary conditions for Poisson's equation only involve the electrostatic potential as an unknown, the first and last rows of this matrix are identically zero.

The inner lines of this matrix ($j = 2 \cdots N$) are obtained instead by differentiating the left-hand side of the j^{th} discretized Poisson's equation with respect to n_j (which is the only non-null derivative with respect to the electron densities at the nodes):

$$\begin{aligned} \left[\mathbf{J}_{\mathbf{P},\mathbf{n}}^{(k)} \right]_{j,j} &= \frac{\partial}{\partial n_j} \left\{ \epsilon_{j+\frac{1}{2}} \frac{\phi_{j+1} - \phi_j}{L_{j,j+1}} - \epsilon_{j-\frac{1}{2}} \frac{\phi_j - \phi_{j-1}}{L_{j-1,j}} + q (p_j - n_j + N_{d,j} - N_{a,j}) L_{j-\frac{1}{2},j+\frac{1}{2}} \right\} \Big|_{x=x^{(k)}} \\ &= -q L_{j-\frac{1}{2},j+\frac{1}{2}} \end{aligned}$$

Entries of $\mathbf{J}_{\mathbf{P},\mathbf{p}}^{(k)}$

The matrix $\mathbf{J}_{\mathbf{P},\mathbf{p}}^{(k)}$ is the block of the Jacobian containing the derivatives with respect to the hole densities at the nodes of the left-hand sides of the equations resulting from discretizing Poisson's equation.

Since the boundary conditions for Poisson's equation only involve the electrostatic potential as an unknown, the first and last rows of this matrix are identically zero.

The inner lines of this matrix ($j = 2 \cdots N$) are obtained instead by differentiating the left-hand side of the j^{th} discretized Poisson's equation with respect to p_j (which is the only non-null derivative with respect to the hole densities at the nodes):

$$\begin{aligned} \left[\mathbf{J}_{\mathbf{P},\mathbf{p}}^{(k)} \right]_{j,j} &= \frac{\partial}{\partial p_j} \left\{ \epsilon_{j+\frac{1}{2}} \frac{\phi_{j+1} - \phi_j}{L_{j,j+1}} - \epsilon_{j-\frac{1}{2}} \frac{\phi_j - \phi_{j-1}}{L_{j-1,j}} + q (p_j - n_j + N_{d,j} - N_{a,j}) L_{j-\frac{1}{2},j+\frac{1}{2}} \right\} \Big|_{x=x^{(k)}} \\ &= +q L_{j-\frac{1}{2},j+\frac{1}{2}} \end{aligned}$$

Entries of $\mathbf{J}_{\mathbf{C}_n,\phi}^{(k)}$

The matrix $\mathbf{J}_{\mathbf{C}_n,\phi}^{(k)}$ is the block of the Jacobian containing the derivatives with respect to the potential at the nodes of the left-hand sides of the equations resulting from discretizing the continuity equation for electrons.

In order to make the derivatives more readable and to be able to apply the chain rule it is useful to define the derivative of Bernoulli's function as:

$$\mathcal{B}'(x) \triangleq \frac{\partial}{\partial x} \left\{ \frac{x}{\exp\{x\} - 1} \right\} = \frac{\exp\{x\} - 1 - x \exp\{x\}}{(\exp\{x\})^2}$$

Moreover, in order to develop the derivatives of the equivalent potential $\phi_n^{(eq)}$ with respect to ϕ it is useful to remember its definition that was provided in Equation 10.5.

The first line of this matrix is obtained from differentiating the boundary condition for the electron continuity equation at the left contact with respect to the components of the discretized potential vector ϕ . It is then important to distinguish between the two types of contacts:

- if the left contact is of ohmic type then all the derivatives with respect to the potentials at the nodes of Equation 11.7 are zero.
- if the left contact is of Schottky type then the only nonzero derivatives with respect to the potentials at the nodes of Equation 11.8 are:

$$\left[\mathbf{J}_{\mathbf{C}_n,\phi}^{(k)} \right]_{1,1} = \frac{\partial}{\partial \phi_1} \left\{ \frac{D_{n,3/2}}{L_{1,2}} \left[n_2 \mathcal{B} \left(\frac{\phi_{n,2}^{(eq)} - \phi_{n,1}^{(eq)}}{V_T} \right) - n_1 \mathcal{B} \left(-\frac{\phi_{n,2}^{(eq)} - \phi_{n,1}^{(eq)}}{V_T} \right) \right] \right\} +$$

$$\begin{aligned}
& \left. -v_n^{(left)} (n_1 - n_0^{(left)}) - U_{n,1} L_{1,3/2} \right\} \Big|_{x=x(\mathbf{k})} \\
& = \frac{1}{V_T} \frac{D_{n,3/2}}{L_{1,2}} \left[-n_2 \mathcal{B}' \left(\frac{\phi_{n,2}^{(eq)} - \phi_{n,1}^{(eq)}}{V_T} \right) \frac{\partial \phi_{n,1}^{(eq)}}{\partial \phi_1} - n_1 \mathcal{B}' \left(-\frac{\phi_{n,2}^{(eq)} - \phi_{n,1}^{(eq)}}{V_T} \right) \frac{\partial \phi_{n,1}^{(eq)}}{\partial \phi_1} \right] \\
& = \frac{1}{V_T} \frac{D_{n,3/2}}{L_{1,2}} \left[-n_2 \mathcal{B}' \left(\frac{\phi_{n,2}^{(eq)} - \phi_{n,1}^{(eq)}}{V_T} \right) - n_1 \mathcal{B}' \left(-\frac{\phi_{n,2}^{(eq)} - \phi_{n,1}^{(eq)}}{V_T} \right) \right] \\
\left[\mathbf{J}_{\mathbf{C}_n, \phi}^{(\mathbf{k})} \right]_{1,2} & = \frac{\partial}{\partial \phi_2} \left\{ \frac{D_{n,3/2}}{L_{1,2}} \left[n_2 \mathcal{B} \left(\frac{\phi_{n,2}^{(eq)} - \phi_{n,1}^{(eq)}}{V_T} \right) - n_1 \mathcal{B} \left(-\frac{\phi_{n,2}^{(eq)} - \phi_{n,1}^{(eq)}}{V_T} \right) \right] + \right. \\
& \quad \left. -v_n^{(left)} (n_1 - n_0^{(left)}) - U_{n,1} L_{1,3/2} \right\} \Big|_{x=x(\mathbf{k})} \\
& = \frac{1}{V_T} \frac{D_{n,3/2}}{L_{1,2}} \left[+n_2 \mathcal{B}' \left(\frac{\phi_{n,2}^{(eq)} - \phi_{n,1}^{(eq)}}{V_T} \right) \frac{\partial \phi_{n,2}^{(eq)}}{\partial \phi_2} + n_1 \mathcal{B}' \left(-\frac{\phi_{n,2}^{(eq)} - \phi_{n,1}^{(eq)}}{V_T} \right) \frac{\partial \phi_{n,2}^{(eq)}}{\partial \phi_2} \right] \\
& = \frac{1}{V_T} \frac{D_{n,3/2}}{L_{1,2}} \left[+n_2 \mathcal{B}' \left(\frac{\phi_{n,2}^{(eq)} - \phi_{n,2}^{(eq)}}{V_T} \right) + n_1 \mathcal{B}' \left(-\frac{\phi_{n,2}^{(eq)} - \phi_{n,2}^{(eq)}}{V_T} \right) \right]
\end{aligned}$$

The inner lines of this matrix ($j = 2 \cdots N$) are obtained instead by differentiating the left-hand side of the j^{th} discretized electron continuity equation with respect to ϕ_{j-1} , ϕ_j and ϕ_{j+1} (which are the only non-null derivatives with respect to the potentials at the nodes):

$$\begin{aligned}
\left[\mathbf{J}_{\mathbf{C}_n, \phi}^{(\mathbf{k})} \right]_{j,j} & = \frac{\partial}{\partial \phi_j} \left\{ \frac{D_{n,j+\frac{1}{2}}}{L_{j,j+1}} \left[n_{j+1} \mathcal{B} \left(\frac{\phi_{n,j+1}^{(eq)} - \phi_{n,j}^{(eq)}}{V_T} \right) - n_j \mathcal{B} \left(-\frac{\phi_{n,j+1}^{(eq)} - \phi_{n,j}^{(eq)}}{V_T} \right) \right] + \right. \\
& \quad \left. - \frac{D_{n,j-\frac{1}{2}}}{L_{j-1,j}} \left[n_j \mathcal{B} \left(\frac{\phi_{n,j}^{(eq)} - \phi_{n,j-1}^{(eq)}}{V_T} \right) - n_{j-1} \mathcal{B} \left(-\frac{\phi_{n,j}^{(eq)} - \phi_{n,j-1}^{(eq)}}{V_T} \right) \right] - U_{n,j} L_{j-\frac{1}{2},j+\frac{1}{2}} \right\} \Big|_{x=x(\mathbf{k})} \\
& = \frac{1}{V_T} \frac{D_{n,j+\frac{1}{2}}}{L_{j,j+1}} \left[-n_{j+1} \mathcal{B}' \left(\frac{\phi_{n,j+1}^{(eq)} - \phi_{n,j}^{(eq)}}{V_T} \right) \frac{\partial \phi_{n,j}^{(eq)}}{\partial \phi_j} - n_j \mathcal{B}' \left(-\frac{\phi_{n,j+1}^{(eq)} - \phi_{n,j}^{(eq)}}{V_T} \right) \frac{\partial \phi_{n,j}^{(eq)}}{\partial \phi_j} \right] + \\
& \quad + \frac{1}{V_T} \frac{D_{n,j-\frac{1}{2}}}{L_{j-1,j}} \left[-n_j \mathcal{B}' \left(\frac{\phi_{n,j}^{(eq)} - \phi_{n,j-1}^{(eq)}}{V_T} \right) \frac{\partial \phi_{n,j}^{(eq)}}{\partial \phi_j} - n_{j-1} \mathcal{B}' \left(-\frac{\phi_{n,j}^{(eq)} - \phi_{n,j-1}^{(eq)}}{V_T} \right) \frac{\partial \phi_{n,j}^{(eq)}}{\partial \phi_j} \right] \\
& = \frac{1}{V_T} \frac{D_{n,j+\frac{1}{2}}}{L_{j,j+1}} \left[-n_{j+1} \mathcal{B}' \left(\frac{\phi_{n,j+1}^{(eq)} - \phi_{n,j}^{(eq)}}{V_T} \right) - n_j \mathcal{B}' \left(-\frac{\phi_{n,j+1}^{(eq)} - \phi_{n,j}^{(eq)}}{V_T} \right) \right] + \\
& \quad + \frac{1}{V_T} \frac{D_{n,j-\frac{1}{2}}}{L_{j-1,j}} \left[-n_j \mathcal{B}' \left(\frac{\phi_{n,j}^{(eq)} - \phi_{n,j-1}^{(eq)}}{V_T} \right) - n_{j-1} \mathcal{B}' \left(-\frac{\phi_{n,j}^{(eq)} - \phi_{n,j-1}^{(eq)}}{V_T} \right) \right] \\
\left[\mathbf{J}_{\mathbf{C}_n, \phi}^{(\mathbf{k})} \right]_{j,j-1} & = \frac{\partial}{\partial \phi_{j-1}} \left\{ \frac{D_{n,j+\frac{1}{2}}}{L_{j,j+1}} \left[n_{j+1} \mathcal{B} \left(\frac{\phi_{n,j+1}^{(eq)} - \phi_{n,j}^{(eq)}}{V_T} \right) - n_j \mathcal{B} \left(-\frac{\phi_{n,j+1}^{(eq)} - \phi_{n,j}^{(eq)}}{V_T} \right) \right] + \right. \\
& \quad \left. - \frac{D_{n,j-\frac{1}{2}}}{L_{j-1,j}} \left[n_j \mathcal{B} \left(\frac{\phi_{n,j}^{(eq)} - \phi_{n,j-1}^{(eq)}}{V_T} \right) - n_{j-1} \mathcal{B} \left(-\frac{\phi_{n,j}^{(eq)} - \phi_{n,j-1}^{(eq)}}{V_T} \right) \right] - U_{n,j} L_{j-\frac{1}{2},j+\frac{1}{2}} \right\} \Big|_{x=x(\mathbf{k})} \\
& = \frac{1}{V_T} \frac{D_{n,j-\frac{1}{2}}}{L_{j-1,j}} \left[n_j \mathcal{B}' \left(\frac{\phi_{n,j}^{(eq)} - \phi_{n,j-1}^{(eq)}}{V_T} \right) \frac{\partial \phi_{n,j-1}^{(eq)}}{\partial \phi_{j-1}} + n_{j-1} \mathcal{B}' \left(-\frac{\phi_{n,j}^{(eq)} - \phi_{n,j-1}^{(eq)}}{V_T} \right) \frac{\partial \phi_{n,j-1}^{(eq)}}{\partial \phi_{j-1}} \right] \\
& = \frac{1}{V_T} \frac{D_{n,j-\frac{1}{2}}}{L_{j-1,j}} \left[n_j \mathcal{B}' \left(\frac{\phi_{n,j}^{(eq)} - \phi_{n,j-1}^{(eq)}}{V_T} \right) + n_{j-1} \mathcal{B}' \left(-\frac{\phi_{n,j}^{(eq)} - \phi_{n,j-1}^{(eq)}}{V_T} \right) \right]
\end{aligned}$$

$$\begin{aligned}
\left[\mathbf{J}_{\mathbf{C}_n, \phi}^{(k)} \right]_{j,j+1} &= \frac{\partial}{\partial \phi_{j+1}} \left\{ \frac{D_{n,j+\frac{1}{2}}}{L_{j,j+1}} \left[n_{j+1} \mathcal{B} \left(\frac{\phi_{n,j+1}^{(eq)} - \phi_{n,j}^{(eq)}}{V_T} \right) - n_j \mathcal{B} \left(-\frac{\phi_{n,j+1}^{(eq)} - \phi_{n,j}^{(eq)}}{V_T} \right) \right] + \right. \\
&\quad \left. - \frac{D_{n,j-\frac{1}{2}}}{L_{j-1,j}} \left[n_j \mathcal{B} \left(\frac{\phi_{n,j}^{(eq)} - \phi_{n,j-1}^{(eq)}}{V_T} \right) - n_{j-1} \mathcal{B} \left(-\frac{\phi_{n,j}^{(eq)} - \phi_{n,j-1}^{(eq)}}{V_T} \right) \right] - U_{n,j} L_{j-\frac{1}{2},j+\frac{1}{2}} \right\} \Big|_{x=x^{(k)}} \\
&= \frac{1}{V_T} \frac{D_{n,j+\frac{1}{2}}}{L_{j,j+1}} \left[n_{j+1} \mathcal{B}' \left(\frac{\phi_{n,j+1}^{(eq)} - \phi_{n,j}^{(eq)}}{V_T} \right) \frac{\partial \phi_{n,j+1}^{(eq)}}{\partial \phi_{j+1}} + n_j \mathcal{B}' \left(-\frac{\phi_{n,j+1}^{(eq)} - \phi_{n,j}^{(eq)}}{V_T} \right) \frac{\partial \phi_{n,j+1}^{(eq)}}{\partial \phi_{j+1}} \right] \\
&= \frac{1}{V_T} \frac{D_{n,j+\frac{1}{2}}}{L_{j,j+1}} \left[n_{j+1} \mathcal{B}' \left(\frac{\phi_{n,j+1}^{(eq)} - \phi_{n,j}^{(eq)}}{V_T} \right) + n_j \mathcal{B}' \left(-\frac{\phi_{n,j+1}^{(eq)} - \phi_{n,j}^{(eq)}}{V_T} \right) \right]
\end{aligned}$$

The last line of the matrix is obtained from differentiating the boundary condition for the electron continuity equation at the right contact with respect to the components of the discretized potential vector ϕ . It is then important to distinguish between the two types of contacts:

- if the right contact is of ohmic type then all the derivatives with respect to the potentials at the nodes of Equation 11.7 are zero.
- if the right contact is of Schottky type then the only nonzero derivatives with respect to the potentials at the nodes of Equation 11.9 are:

$$\begin{aligned}
\left[\mathbf{J}_{\mathbf{C}_n, \phi}^{(k)} \right]_{N+1,N+1} &= \frac{\partial}{\partial \phi_{N+1}} \left\{ \frac{D_{n,N+\frac{1}{2}}}{L_{N,N+1}} \left[n_N \mathcal{B} \left(-\frac{\phi_{n,N+1}^{(eq)} - \phi_{n,N}^{(eq)}}{V_T} \right) - n_{N+1} \mathcal{B} \left(\frac{\phi_{n,N+1}^{(eq)} - \phi_{n,N}^{(eq)}}{V_T} \right) \right] + \right. \\
&\quad \left. - v_n^{(right)} (n_{N+1} - n_0^{(right)}) - U_{n,N+1} L_{N+\frac{1}{2},N+1} \right\} \Big|_{x=x^{(k)}} \\
&= \frac{1}{V_T} \frac{D_{n,N+\frac{1}{2}}}{L_{N,N+1}} \left[-n_N \mathcal{B}' \left(-\frac{\phi_{n,N+1}^{(eq)} - \phi_{n,N}^{(eq)}}{V_T} \right) \frac{\partial \phi_{n,N+1}^{(eq)}}{\partial \phi_{N+1}} - n_{N+1} \mathcal{B}' \left(\frac{\phi_{n,N+1}^{(eq)} - \phi_{n,N}^{(eq)}}{V_T} \right) \frac{\partial \phi_{n,N+1}^{(eq)}}{\partial \phi_{N+1}} \right] \\
&= \frac{1}{V_T} \frac{D_{n,N+\frac{1}{2}}}{L_{N,N+1}} \left[-n_N \mathcal{B}' \left(-\frac{\phi_{n,N+1}^{(eq)} - \phi_{n,N}^{(eq)}}{V_T} \right) - n_{N+1} \mathcal{B}' \left(\frac{\phi_{n,N+1}^{(eq)} - \phi_{n,N}^{(eq)}}{V_T} \right) \right]
\end{aligned}$$

$$\begin{aligned}
\left[\mathbf{J}_{\mathbf{C}_n, \phi}^{(k)} \right]_{N+1,N} &= \frac{\partial}{\partial \phi_N} \left\{ \frac{D_{n,N+\frac{1}{2}}}{L_{N,N+1}} \left[n_N \mathcal{B} \left(-\frac{\phi_{n,N+1}^{(eq)} - \phi_{n,N}^{(eq)}}{V_T} \right) - n_{N+1} \mathcal{B} \left(\frac{\phi_{n,N+1}^{(eq)} - \phi_{n,N}^{(eq)}}{V_T} \right) \right] + \right. \\
&\quad \left. - v_n^{(right)} (n_{N+1} - n_0^{(right)}) - U_{n,N+1} L_{N+\frac{1}{2},N+1} \right\} \Big|_{x=x^{(k)}} \\
&= \frac{1}{V_T} \frac{D_{n,N+\frac{1}{2}}}{L_{N,N+1}} \left[n_N \mathcal{B}' \left(-\frac{\phi_{n,N+1}^{(eq)} - \phi_{n,N}^{(eq)}}{V_T} \right) \frac{\partial \phi_{n,N}^{(eq)}}{\partial \phi_N} + n_{N+1} \mathcal{B}' \left(\frac{\phi_{n,N+1}^{(eq)} - \phi_{n,N}^{(eq)}}{V_T} \right) \frac{\partial \phi_{n,N}^{(eq)}}{\partial \phi_N} \right] \\
&= \frac{1}{V_T} \frac{D_{n,N+\frac{1}{2}}}{L_{N,N+1}} \left[n_N \mathcal{B}' \left(-\frac{\phi_{n,N+1}^{(eq)} - \phi_{n,N}^{(eq)}}{V_T} \right) + n_{N+1} \mathcal{B}' \left(\frac{\phi_{n,N+1}^{(eq)} - \phi_{n,N}^{(eq)}}{V_T} \right) \right]
\end{aligned}$$

Entries of $\mathbf{J}_{\mathbf{C}_n, \mathbf{n}}^{(k)}$

The matrix $\mathbf{J}_{\mathbf{C}_n, \mathbf{n}}^{(k)}$ is the block of the Jacobian containing the derivatives with respect to the electron density at the nodes of the left-hand sides of the equations resulting from discretizing the continuity equation for electrons.

In order to develop the derivatives of the equivalent potential $\phi_n^{(eq)}$ with respect to n it is useful to remember its definition that was provided in Equation 10.5.

The first line of this matrix is obtained from differentiating the boundary condition for the electron continuity equation at the left contact with respect to the components of the discretized electron density vector \mathbf{n} . It is then important to distinguish between the two types of contacts:

- if the left contact is of ohmic type then the only nonzero derivative with respect to the electron density at the nodes of Equation 11.7 is:

$$\left[\mathbf{J}_{\mathbf{C}_{\mathbf{n},\mathbf{n}}}^{(\mathbf{k})} \right]_{1,1} = \frac{\partial}{\partial n_1} \left\{ n_1 - n_0^{(left)} \right\} \Big|_{\mathbf{x}=\mathbf{x}^{(\mathbf{k})}} = 1$$

- if the left contact is of Schottky type then the only nonzero derivatives with respect to the electron densities at the nodes of Equation 11.8 are:

$$\begin{aligned} \left[\mathbf{J}_{\mathbf{C}_{\mathbf{n},\mathbf{n}}}^{(\mathbf{k})} \right]_{1,1} &= \frac{\partial}{\partial n_1} \left\{ \frac{D_{n,3/2}}{L_{1,2}} \left[n_2 \mathcal{B} \left(\frac{\phi_{n,2}^{(eq)} - \phi_{n,1}^{(eq)}}{V_T} \right) - n_1 \mathcal{B} \left(-\frac{\phi_{n,2}^{(eq)} - \phi_{n,1}^{(eq)}}{V_T} \right) \right] + \right. \\ &\quad \left. - v_n^{(left)} (n_1 - n_0^{(left)}) - U_{n,1} L_{1,3/2} \right\} \Big|_{\mathbf{x}=\mathbf{x}^{(\mathbf{k})}} \\ &= -\frac{D_{n,3/2}}{L_{1,2}} \mathcal{B} \left(-\frac{\phi_{n,2}^{(eq)} - \phi_{n,1}^{(eq)}}{V_T} \right) - v_n^{(left)} - \frac{\partial U_{n,1}}{\partial n_1} L_{1,3/2} \end{aligned}$$

$$\begin{aligned} \left[\mathbf{J}_{\mathbf{C}_{\mathbf{n},\mathbf{n}}}^{(\mathbf{k})} \right]_{1,2} &= \frac{\partial}{\partial n_2} \left\{ \frac{D_{n,3/2}}{L_{1,2}} \left[n_2 \mathcal{B} \left(\frac{\phi_{n,2}^{(eq)} - \phi_{n,1}^{(eq)}}{V_T} \right) - n_1 \mathcal{B} \left(-\frac{\phi_{n,2}^{(eq)} - \phi_{n,1}^{(eq)}}{V_T} \right) \right] + \right. \\ &\quad \left. - v_n^{(left)} (n_1 - n_0^{(left)}) - U_{n,1} L_{1,3/2} \right\} \Big|_{\mathbf{x}=\mathbf{x}^{(\mathbf{k})}} \\ &= \frac{D_{n,3/2}}{L_{1,2}} \mathcal{B} \left(\frac{\phi_{n,2}^{(eq)} - \phi_{n,1}^{(eq)}}{V_T} \right) \end{aligned}$$

The inner lines of this matrix ($j = 2 \dots N$) are obtained instead by differentiating the left-hand side of the j^{th} discretized electron continuity equation with respect to n_{j-1} , n_j and n_{j+1} (which are the only non-null derivatives with respect to the electron densities at the nodes):

$$\begin{aligned} \left[\mathbf{J}_{\mathbf{C}_{\mathbf{n},\mathbf{n}}}^{(\mathbf{k})} \right]_{j,j} &= \frac{\partial}{\partial n_j} \left\{ \frac{D_{n,j+\frac{1}{2}}}{L_{j,j+1}} \left[n_{j+1} \mathcal{B} \left(\frac{\phi_{n,j+1}^{(eq)} - \phi_{n,j}^{(eq)}}{V_T} \right) - n_j \mathcal{B} \left(-\frac{\phi_{n,j+1}^{(eq)} - \phi_{n,j}^{(eq)}}{V_T} \right) \right] + \right. \\ &\quad \left. - \frac{D_{n,j-\frac{1}{2}}}{L_{j-1,j}} \left[n_j \mathcal{B} \left(\frac{\phi_{n,j}^{(eq)} - \phi_{n,j-1}^{(eq)}}{V_T} \right) - n_{j-1} \mathcal{B} \left(-\frac{\phi_{n,j}^{(eq)} - \phi_{n,j-1}^{(eq)}}{V_T} \right) \right] - U_{n,j} L_{j-\frac{1}{2},j+\frac{1}{2}} \right\} \Big|_{\mathbf{x}=\mathbf{x}^{(\mathbf{k})}} \\ &= -\frac{D_{n,j+\frac{1}{2}}}{L_{j,j+1}} \mathcal{B} \left(-\frac{\phi_{n,j+1}^{(eq)} - \phi_{n,j}^{(eq)}}{V_T} \right) - \frac{D_{n,j-\frac{1}{2}}}{L_{j-1,j}} \mathcal{B} \left(\frac{\phi_{n,j}^{(eq)} - \phi_{n,j-1}^{(eq)}}{V_T} \right) - \frac{\partial U_{n,j}}{\partial n_j} L_{j-\frac{1}{2},j+\frac{1}{2}} \end{aligned}$$

$$\begin{aligned} \left[\mathbf{J}_{\mathbf{C}_{\mathbf{n},\mathbf{n}}}^{(\mathbf{k})} \right]_{j,j-1} &= \frac{\partial}{\partial n_{j-1}} \left\{ \frac{D_{n,j+\frac{1}{2}}}{L_{j,j+1}} \left[n_{j+1} \mathcal{B} \left(\frac{\phi_{n,j+1}^{(eq)} - \phi_{n,j}^{(eq)}}{V_T} \right) - n_j \mathcal{B} \left(-\frac{\phi_{n,j+1}^{(eq)} - \phi_{n,j}^{(eq)}}{V_T} \right) \right] + \right. \\ &\quad \left. - \frac{D_{n,j-\frac{1}{2}}}{L_{j-1,j}} \left[n_j \mathcal{B} \left(\frac{\phi_{n,j}^{(eq)} - \phi_{n,j-1}^{(eq)}}{V_T} \right) - n_{j-1} \mathcal{B} \left(-\frac{\phi_{n,j}^{(eq)} - \phi_{n,j-1}^{(eq)}}{V_T} \right) \right] - U_{n,j} L_{j-\frac{1}{2},j+\frac{1}{2}} \right\} \Big|_{\mathbf{x}=\mathbf{x}^{(\mathbf{k})}} \\ &= \frac{D_{n,j-\frac{1}{2}}}{L_{j-1,j}} \mathcal{B} \left(\frac{\phi_{n,j}^{(eq)} - \phi_{n,j-1}^{(eq)}}{V_T} \right) \end{aligned}$$

$$\left[\mathbf{J}_{\mathbf{C}_{\mathbf{n},\mathbf{n}}}^{(\mathbf{k})} \right]_{j,j+1} = \frac{\partial}{\partial n_{j+1}} \left\{ \frac{D_{n,j+\frac{1}{2}}}{L_{j,j+1}} \left[n_{j+1} \mathcal{B} \left(\frac{\phi_{n,j+1}^{(eq)} - \phi_{n,j}^{(eq)}}{V_T} \right) - n_j \mathcal{B} \left(-\frac{\phi_{n,j+1}^{(eq)} - \phi_{n,j}^{(eq)}}{V_T} \right) \right] + \right.$$

$$\begin{aligned}
& -\frac{D_{n,j-\frac{1}{2}}}{L_{j-1,j}} \left[n_j \mathcal{B} \left(\frac{\phi_{n,j}^{(eq)} - \phi_{n,j-1}^{(eq)}}{V_T} \right) - n_{j-1} \mathcal{B} \left(-\frac{\phi_{n,j}^{(eq)} - \phi_{n,j-1}^{(eq)}}{V_T} \right) \right] - U_{n,j} L_{j-\frac{1}{2},j+\frac{1}{2}} \Bigg|_{x=x^{(k)}} \\
& = \frac{D_{n,j+\frac{1}{2}}}{L_{j,j+1}} \mathcal{B} \left(\frac{\phi_{n,j+1}^{(eq)} - \phi_{n,j}^{(eq)}}{V_T} \right)
\end{aligned}$$

The last line of this matrix is obtained from differentiating the boundary condition for the electron continuity equation at the right contact with respect to the components of the discretized electron density vector \mathbf{n} . It is then important to distinguish between the two types of contacts:

- if the right contact is of ohmic type then the only nonzero derivative with respect to the electron density at the nodes of Equation 11.7 is:

$$\left[\mathbf{J}_{\mathbf{C}_{n,\mathbf{n}}}^{(k)} \right]_{N+1,N+1} = \frac{\partial}{\partial n_{N+1}} \left\{ n_{N+1} - n_0^{(right)} \right\} \Bigg|_{x=x^{(k)}} = 1$$

- if the right contact is of Schottky type then the only nonzero derivatives with respect to the electron densities at the nodes of Equation 11.9 are:

$$\begin{aligned}
\left[\mathbf{J}_{\mathbf{C}_{n,\mathbf{n}}}^{(k)} \right]_{N+1,N+1} & = \frac{\partial}{\partial n_{N+1}} \left\{ \frac{D_{n,N+\frac{1}{2}}}{L_{N,N+1}} \left[n_N \mathcal{B} \left(-\frac{\phi_{n,N+1}^{(eq)} - \phi_{n,N}^{(eq)}}{V_T} \right) - n_{N+1} \mathcal{B} \left(\frac{\phi_{n,N+1}^{(eq)} - \phi_{n,N}^{(eq)}}{V_T} \right) \right] + \right. \\
& \quad \left. - v_n^{(right)} (n_{N+1} - n_0^{(right)}) - U_{n,N+1} L_{N+\frac{1}{2},N+1} \right\} \Bigg|_{x=x^{(k)}} \\
& = -\frac{D_{n,N+\frac{1}{2}}}{L_{N,N+1}} \mathcal{B} \left(\frac{\phi_{n,N+1}^{(eq)} - \phi_{n,N}^{(eq)}}{V_T} \right) - v_n^{(right)} - \frac{\partial U_{n,N+1}}{\partial n_{N+1}} L_{N+\frac{1}{2},N+1}
\end{aligned}$$

$$\begin{aligned}
\left[\mathbf{J}_{\mathbf{C}_{n,\mathbf{n}}}^{(k)} \right]_{N+1,N} & = \frac{\partial}{\partial n_N} \left\{ \frac{D_{n,N+\frac{1}{2}}}{L_{N,N+1}} \left[n_N \mathcal{B} \left(-\frac{\phi_{n,N+1}^{(eq)} - \phi_{n,N}^{(eq)}}{V_T} \right) - n_{N+1} \mathcal{B} \left(\frac{\phi_{n,N+1}^{(eq)} - \phi_{n,N}^{(eq)}}{V_T} \right) \right] + \right. \\
& \quad \left. - v_n^{(right)} (n_{N+1} - n_0^{(right)}) - U_{n,N+1} L_{N+\frac{1}{2},N+1} \right\} \Bigg|_{x=x^{(k)}} \\
& = \frac{D_{n,N+\frac{1}{2}}}{L_{N,N+1}} \mathcal{B} \left(-\frac{\phi_{n,N+1}^{(eq)} - \phi_{n,N}^{(eq)}}{V_T} \right)
\end{aligned}$$

In order to obtain the complete formulations it is then necessary to compute the derivative $\frac{\partial U_{n,j}}{\partial n_j}$. For SRH generation/recombination it is evaluated as:

$$\begin{aligned}
\frac{\partial U_{n,j}^{(SRH)}}{\partial n_j} & = \frac{\partial}{\partial n_j} \left\{ \frac{n_j p_j - n_{i,j}^2}{\tau_{p,j}(n_j + n_{t,j}) + \tau_{n,j}(p_j + p_{t,j})} \right\} \Bigg|_{x=x^{(k)}} \\
& = \frac{n_j [\tau_{p,j}(n_j + n_{t,j}) + \tau_{n,j}(p_j + p_{t,j})] - [n_j p_j - n_{i,j}^2] \tau_{p,j}}{[\tau_{p,j}(n_j + n_{t,j}) + \tau_{n,j}(p_j + p_{t,j})]^2}
\end{aligned}$$

Entries of $\mathbf{J}_{\mathbf{C}_{n,\mathbf{p}}}^{(k)}$

The matrix $\mathbf{J}_{\mathbf{C}_{n,\mathbf{p}}}^{(k)}$ is the block of the Jacobian containing the derivatives with respect to the hole density at the nodes of the left-hand sides of the equations resulting from discretizing the continuity equation for electrons.

In order to develop the derivatives of the equivalent potential $\phi_n^{(eq)}$ with respect to p it is useful to remember its definition that was provided in Equation 10.5.

The first line of this matrix is obtained from differentiating the boundary condition for the electron continuity equation at the left contact with respect to the components of the discretized hole density vector \mathbf{p} . It is then important to distinguish between the two types of contacts:

- if the left contact is of ohmic type then Equation 11.7 does not include any dependency on the hole density and, therefore, all the derivatives are zero;
- if the left contact is of Schottky type then the only nonzero derivative with respect to the hole densities at the nodes of Equation 11.8 is:

$$\begin{aligned} \left[\mathbf{J}_{\mathbf{C}_{n,\mathbf{p}}}^{(\mathbf{k})} \right]_{1,1} &= \frac{\partial}{\partial p_1} \left\{ \frac{D_{n,3/2}}{L_{1,2}} \left[n_2 \mathcal{B} \left(\frac{\phi_{n,2}^{(eq)} - \phi_{n,1}^{(eq)}}{V_T} \right) - n_1 \mathcal{B} \left(-\frac{\phi_{n,2}^{(eq)} - \phi_{n,1}^{(eq)}}{V_T} \right) \right] + \right. \\ &\quad \left. - v_n^{(left)} (n_1 - n_0^{(left)}) - U_{n,1} L_{1,3/2} \right\} \Big|_{x=x^{(\mathbf{k})}} \\ &= -\frac{\partial U_{n,1}}{\partial p_1} L_{1,3/2} \end{aligned}$$

The inner lines of this matrix ($j = 2 \cdots N$) are obtained instead by differentiating the left-hand side of the j^{th} discretized electron continuity equation with respect to p_j (which is the only non-null derivative with respect to the hole densities at the nodes):

$$\begin{aligned} \left[\mathbf{J}_{\mathbf{C}_{n,\mathbf{p}}}^{(\mathbf{k})} \right]_{j,j} &= \frac{\partial}{\partial p_j} \left\{ \frac{D_{n,j+1/2}}{L_{j,j+1}} \left[n_{j+1} \mathcal{B} \left(\frac{\phi_{n,j+1}^{(eq)} - \phi_{n,j}^{(eq)}}{V_T} \right) - n_j \mathcal{B} \left(-\frac{\phi_{n,j+1}^{(eq)} - \phi_{n,j}^{(eq)}}{V_T} \right) \right] + \right. \\ &\quad \left. - \frac{D_{n,j-1/2}}{L_{j-1,j}} \left[n_j \mathcal{B} \left(\frac{\phi_{n,j}^{(eq)} - \phi_{n,j-1}^{(eq)}}{V_T} \right) - n_{j-1} \mathcal{B} \left(-\frac{\phi_{n,j}^{(eq)} - \phi_{n,j-1}^{(eq)}}{V_T} \right) \right] - U_{n,j} L_{j-1/2,j+1/2} \right\} \Big|_{x=x^{(\mathbf{k})}} \\ &= -\frac{\partial U_{n,j}}{\partial p_j} L_{j-1/2,j+1/2} \end{aligned}$$

The last line of this matrix is obtained from differentiating the boundary condition for the electron continuity equation at the right contact with respect to the components of the discretized hole density vector \mathbf{p} . It is then important to distinguish between the two types of contacts:

- if the right contact is of ohmic type then Equation 11.7 does not include any dependency on the hole density and, therefore, all the derivatives are zero;
- if the right contact is of Schottky type then the only nonzero derivative with respect to the hole densities at the nodes of Equation 11.9 is:

$$\begin{aligned} \left[\mathbf{J}_{\mathbf{C}_{n,\mathbf{p}}}^{(\mathbf{k})} \right]_{N+1,N+1} &= \frac{\partial}{\partial n_{N+1}} \left\{ \frac{D_{n,N+1/2}}{L_{N,N+1}} \left[n_N \mathcal{B} \left(-\frac{\phi_{n,N+1}^{(eq)} - \phi_{n,N}^{(eq)}}{V_T} \right) - n_{N+1} \mathcal{B} \left(\frac{\phi_{n,N+1}^{(eq)} - \phi_{n,N}^{(eq)}}{V_T} \right) \right] + \right. \\ &\quad \left. - v_n^{(right)} (n_{N+1} - n_0^{(right)}) - U_{n,N+1} L_{N+1/2,N+1} \right\} \Big|_{x=x^{(\mathbf{k})}} \\ &= -\frac{\partial U_{n,N+1}}{\partial p_{N+1}} L_{N+1/2,N+1} \end{aligned}$$

In order to obtain the complete formulations it is then necessary to compute the derivative $\frac{\partial U_{n,j}}{\partial p_j}$. For SRH generation/recombination it is evaluated as:

$$\begin{aligned} \frac{\partial U_{n,j}^{(SRH)}}{\partial p_j} &= \frac{\partial}{\partial p_j} \left\{ \frac{n_j p_j - n_{i,j}^2}{\tau_{p,j}(n_j + n_{t,j}) + \tau_{n,j}(p_j + p_{t,j})} \right\} \Big|_{x=x^{(\mathbf{k})}} \\ &= \frac{p_j [\tau_{p,j}(n_j + n_{t,j}) + \tau_{n,j}(p_j + p_{t,j})] - [n_j p_j - n_{i,j}^2] \tau_{n,j}}{[\tau_{p,j}(n_j + n_{t,j}) + \tau_{n,j}(p_j + p_{t,j})]^2} \end{aligned}$$

Entries of $\mathbf{J}_{\mathbf{C}_n, \Lambda_n}^{(k)}$

The matrix $\mathbf{J}_{\mathbf{C}_n, \Lambda_n}^{(k)}$ is the block of the Jacobian containing the derivatives with respect to the electron quantum potentials at the nodes of the left-hand sides of the equations resulting from discretizing the continuity equation for electrons.

In order to develop the derivatives of the equivalent potential $\phi_n^{(eq)}$ with respect to Λ_n it is useful to remember its definition that was provided in Equation 10.5.

The first line of this matrix is obtained from differentiating the boundary condition for the electron continuity equation at the left contact with respect to the components of the discretized electron quantum potential vector $\mathbf{\Lambda}_n$. It is then important to distinguish between the two types of contacts:

- if the left contact is of ohmic type then all the derivatives with respect to the electron quantum potentials at the nodes of Equation 11.7 are zero.
- if the left contact is of Schottky type then the only nonzero derivatives with respect to the electron quantum potentials at the nodes of Equation 11.8 are:

$$\begin{aligned}
\left[\mathbf{J}_{\mathbf{C}_n, \Lambda_n}^{(k)} \right]_{1,1} &= \frac{\partial}{\partial \Lambda_{n,1}} \left\{ \frac{D_{n,3/2}}{L_{1,2}} \left[n_2 \mathcal{B} \left(\frac{\phi_{n,2}^{(eq)} - \phi_{n,1}^{(eq)}}{V_T} \right) - n_1 \mathcal{B} \left(-\frac{\phi_{n,2}^{(eq)} - \phi_{n,1}^{(eq)}}{V_T} \right) \right] + \right. \\
&\quad \left. - v_n^{(left)} (n_1 - n_0^{(left)}) - U_{n,1} L_{1,3/2} \right\} \Big|_{\mathbf{x}=\mathbf{x}^{(k)}} \\
&= \frac{1}{V_T} \frac{D_{n,3/2}}{L_{1,2}} \left[-n_2 \mathcal{B}' \left(\frac{\phi_{n,2}^{(eq)} - \phi_{n,1}^{(eq)}}{V_T} \right) \frac{\partial \phi_{n,1}^{(eq)}}{\partial \Lambda_{n,1}} - n_1 \mathcal{B}' \left(-\frac{\phi_{n,2}^{(eq)} - \phi_{n,1}^{(eq)}}{V_T} \right) \frac{\partial \phi_{n,1}^{(eq)}}{\partial \Lambda_{n,1}} \right] \\
&= \frac{1}{V_T} \frac{D_{n,3/2}}{L_{1,2}} \left[-n_2 \mathcal{B}' \left(\frac{\phi_{n,2}^{(eq)} - \phi_{n,1}^{(eq)}}{V_T} \right) - n_1 \mathcal{B}' \left(-\frac{\phi_{n,2}^{(eq)} - \phi_{n,1}^{(eq)}}{V_T} \right) \right] \\
\left[\mathbf{J}_{\mathbf{C}_n, \Lambda_n}^{(k)} \right]_{1,2} &= \frac{\partial}{\partial \Lambda_{n,2}} \left\{ \frac{D_{n,3/2}}{L_{1,2}} \left[n_2 \mathcal{B} \left(\frac{\phi_{n,2}^{(eq)} - \phi_{n,1}^{(eq)}}{V_T} \right) - n_1 \mathcal{B} \left(-\frac{\phi_{n,2}^{(eq)} - \phi_{n,1}^{(eq)}}{V_T} \right) \right] + \right. \\
&\quad \left. - v_n^{(left)} (n_1 - n_0^{(left)}) - U_{n,1} L_{1,3/2} \right\} \Big|_{\mathbf{x}=\mathbf{x}^{(k)}} \\
&= \frac{1}{V_T} \frac{D_{n,3/2}}{L_{1,2}} \left[n_2 \mathcal{B}' \left(\frac{\phi_{n,2}^{(eq)} - \phi_{n,1}^{(eq)}}{V_T} \right) \frac{\partial \phi_{n,2}^{(eq)}}{\partial \Lambda_{n,2}} + n_1 \mathcal{B}' \left(-\frac{\phi_{n,2}^{(eq)} - \phi_{n,1}^{(eq)}}{V_T} \right) \frac{\partial \phi_{n,2}^{(eq)}}{\partial \Lambda_{n,2}} \right] \\
&= \frac{1}{V_T} \frac{D_{n,3/2}}{L_{1,2}} \left[n_2 \mathcal{B}' \left(\frac{\phi_{n,2}^{(eq)} - \phi_{n,2}^{(eq)}}{V_T} \right) + n_1 \mathcal{B}' \left(-\frac{\phi_{n,2}^{(eq)} - \phi_{n,2}^{(eq)}}{V_T} \right) \right]
\end{aligned}$$

The inner lines of this matrix ($j = 2 \cdots N$) are obtained instead by differentiating the left-hand side of the j^{th} discretized electron continuity equation with respect to $\Lambda_{n,j-1}$, $\Lambda_{n,j}$ and $\Lambda_{n,j+1}$ (which are the only non-null derivatives with respect to the electron quantum potentials at the nodes):

$$\begin{aligned}
\left[\mathbf{J}_{\mathbf{C}_n, \Lambda_n}^{(k)} \right]_{j,j} &= \frac{\partial}{\partial \Lambda_{n,j}} \left\{ \frac{D_{n,j+\frac{1}{2}}}{L_{j,j+1}} \left[n_{j+1} \mathcal{B} \left(\frac{\phi_{n,j+1}^{(eq)} - \phi_{n,j}^{(eq)}}{V_T} \right) - n_j \mathcal{B} \left(-\frac{\phi_{n,j+1}^{(eq)} - \phi_{n,j}^{(eq)}}{V_T} \right) \right] + \right. \\
&\quad \left. - \frac{D_{n,j-\frac{1}{2}}}{L_{j-1,j}} \left[n_j \mathcal{B} \left(\frac{\phi_{n,j}^{(eq)} - \phi_{n,j-1}^{(eq)}}{V_T} \right) - n_{j-1} \mathcal{B} \left(-\frac{\phi_{n,j}^{(eq)} - \phi_{n,j-1}^{(eq)}}{V_T} \right) \right] - U_{n,j} L_{j-\frac{1}{2},j+\frac{1}{2}} \right\} \Big|_{\mathbf{x}=\mathbf{x}^{(k)}} \\
&= \frac{1}{V_T} \frac{D_{n,j+\frac{1}{2}}}{L_{j,j+1}} \left[-n_{j+1} \mathcal{B}' \left(\frac{\phi_{n,j+1}^{(eq)} - \phi_{n,j}^{(eq)}}{V_T} \right) \frac{\partial \phi_{n,j}^{(eq)}}{\partial \Lambda_{n,j}} - n_j \mathcal{B}' \left(-\frac{\phi_{n,j+1}^{(eq)} - \phi_{n,j}^{(eq)}}{V_T} \right) \frac{\partial \phi_{n,j}^{(eq)}}{\partial \Lambda_{n,j}} \right] + \\
&\quad + \frac{1}{V_T} \frac{D_{n,j-\frac{1}{2}}}{L_{j-1,j}} \left[-n_j \mathcal{B}' \left(\frac{\phi_{n,j}^{(eq)} - \phi_{n,j-1}^{(eq)}}{V_T} \right) \frac{\partial \phi_{n,j}^{(eq)}}{\partial \Lambda_{n,j}} - n_{j-1} \mathcal{B}' \left(-\frac{\phi_{n,j}^{(eq)} - \phi_{n,j-1}^{(eq)}}{V_T} \right) \frac{\partial \phi_{n,j}^{(eq)}}{\partial \Lambda_{n,j}} \right]
\end{aligned}$$

$$= \frac{1}{V_T} \frac{D_{n,j+\frac{1}{2}}}{L_{j,j+1}} \left[-n_{j+1} \mathcal{B}' \left(\frac{\phi_{n,j+1}^{(eq)} - \phi_{n,j}^{(eq)}}{V_T} \right) - n_j \mathcal{B}' \left(-\frac{\phi_{n,j+1}^{(eq)} - \phi_{n,j}^{(eq)}}{V_T} \right) \right] +$$

$$+ \frac{1}{V_T} \frac{D_{n,j-\frac{1}{2}}}{L_{j-1,j}} \left[-n_j \mathcal{B}' \left(\frac{\phi_{n,j}^{(eq)} - \phi_{n,j-1}^{(eq)}}{V_T} \right) - n_{j-1} \mathcal{B}' \left(-\frac{\phi_{n,j}^{(eq)} - \phi_{n,j-1}^{(eq)}}{V_T} \right) \right]$$

$$\left[\mathbf{J}_{\mathbf{C}_n, \Lambda_n}^{(k)} \right]_{j,j-1} = \frac{\partial}{\partial \Lambda_{n,j-1}} \left\{ \frac{D_{n,j+\frac{1}{2}}}{L_{j,j+1}} \left[n_{j+1} \mathcal{B} \left(\frac{\phi_{n,j+1}^{(eq)} - \phi_{n,j}^{(eq)}}{V_T} \right) - n_j \mathcal{B} \left(-\frac{\phi_{n,j+1}^{(eq)} - \phi_{n,j}^{(eq)}}{V_T} \right) \right] + \right.$$

$$\left. - \frac{D_{n,j-\frac{1}{2}}}{L_{j-1,j}} \left[n_j \mathcal{B} \left(\frac{\phi_{n,j}^{(eq)} - \phi_{n,j-1}^{(eq)}}{V_T} \right) - n_{j-1} \mathcal{B} \left(-\frac{\phi_{n,j}^{(eq)} - \phi_{n,j-1}^{(eq)}}{V_T} \right) \right] - U_{n,j} L_{j-\frac{1}{2},j+\frac{1}{2}} \right\} \Big|_{x=x^{(k)}}$$

$$= \frac{1}{V_T} \frac{D_{n,j-\frac{1}{2}}}{L_{j-1,j}} \left[n_j \mathcal{B}' \left(\frac{\phi_{n,j}^{(eq)} - \phi_{n,j-1}^{(eq)}}{V_T} \right) \frac{\partial \phi_{n,j-1}^{(eq)}}{\partial \Lambda_{n,j-1}} + n_{j-1} \mathcal{B}' \left(-\frac{\phi_{n,j}^{(eq)} - \phi_{n,j-1}^{(eq)}}{V_T} \right) \frac{\partial \phi_{n,j-1}^{(eq)}}{\partial \Lambda_{n,j-1}} \right]$$

$$= \frac{1}{V_T} \frac{D_{n,j-\frac{1}{2}}}{L_{j-1,j}} \left[n_j \mathcal{B}' \left(\frac{\phi_{n,j}^{(eq)} - \phi_{n,j-1}^{(eq)}}{V_T} \right) + n_{j-1} \mathcal{B}' \left(-\frac{\phi_{n,j}^{(eq)} - \phi_{n,j-1}^{(eq)}}{V_T} \right) \right]$$

$$\left[\mathbf{J}_{\mathbf{C}_n, \Lambda_n}^{(k)} \right]_{j,j+1} = \frac{\partial}{\partial \Lambda_{n,j+1}} \left\{ \frac{D_{n,j+\frac{1}{2}}}{L_{j,j+1}} \left[n_{j+1} \mathcal{B} \left(\frac{\phi_{n,j+1}^{(eq)} - \phi_{n,j}^{(eq)}}{V_T} \right) - n_j \mathcal{B} \left(-\frac{\phi_{n,j+1}^{(eq)} - \phi_{n,j}^{(eq)}}{V_T} \right) \right] + \right.$$

$$\left. - \frac{D_{n,j-\frac{1}{2}}}{L_{j-1,j}} \left[n_j \mathcal{B} \left(\frac{\phi_{n,j}^{(eq)} - \phi_{n,j-1}^{(eq)}}{V_T} \right) - n_{j-1} \mathcal{B} \left(-\frac{\phi_{n,j}^{(eq)} - \phi_{n,j-1}^{(eq)}}{V_T} \right) \right] - U_{n,j} L_{j-\frac{1}{2},j+\frac{1}{2}} \right\} \Big|_{x=x^{(k)}}$$

$$= \frac{1}{V_T} \frac{D_{n,j+\frac{1}{2}}}{L_{j,j+1}} \left[n_{j+1} \mathcal{B}' \left(\frac{\phi_{n,j+1}^{(eq)} - \phi_{n,j}^{(eq)}}{V_T} \right) \frac{\partial \phi_{n,j+1}^{(eq)}}{\partial \Lambda_{n,j+1}} + n_j \mathcal{B}' \left(-\frac{\phi_{n,j+1}^{(eq)} - \phi_{n,j}^{(eq)}}{V_T} \right) \frac{\partial \phi_{n,j+1}^{(eq)}}{\partial \Lambda_{n,j+1}} \right]$$

$$= \frac{1}{V_T} \frac{D_{n,j+\frac{1}{2}}}{L_{j,j+1}} \left[n_{j+1} \mathcal{B}' \left(\frac{\phi_{n,j+1}^{(eq)} - \phi_{n,j}^{(eq)}}{V_T} \right) + n_j \mathcal{B}' \left(-\frac{\phi_{n,j+1}^{(eq)} - \phi_{n,j}^{(eq)}}{V_T} \right) \right]$$

The last line of this matrix is obtained from differentiating the boundary condition for the electron continuity equation at the right contact with respect to the components of the discretized electron quantum potential vector Λ_n . It is then important to distinguish between the two types of contacts:

- if the right contact is of ohmic type then all the derivatives with respect to the electron quantum potentials at the nodes of Equation 11.7 are zero.
- if the right contact is of Schottky type then the only nonzero derivatives with respect to the electron quantum potentials at the nodes of Equation 11.9 are:

$$\left[\mathbf{J}_{\mathbf{C}_n, \Lambda_n}^{(k)} \right]_{N+1,N+1} = \frac{\partial}{\partial \Lambda_{n,N+1}} \left\{ \frac{D_{n,N+\frac{1}{2}}}{L_{N,N+1}} \left[n_N \mathcal{B} \left(-\frac{\phi_{n,N+1}^{(eq)} - \phi_{n,N}^{(eq)}}{V_T} \right) - n_{N+1} \mathcal{B} \left(\frac{\phi_{n,N+1}^{(eq)} - \phi_{n,N}^{(eq)}}{V_T} \right) \right] + \right.$$

$$\left. - v_n^{(right)} (n_{N+1} - n_0^{(right)}) - U_{n,N+1} L_{N+\frac{1}{2},N+1} \right\} \Big|_{x=x^{(k)}}$$

$$= \frac{1}{V_T} \frac{D_{n,N+\frac{1}{2}}}{L_{N,N+1}} \left[-n_N \mathcal{B}' \left(-\frac{\phi_{n,N+1}^{(eq)} - \phi_{n,N}^{(eq)}}{V_T} \right) \frac{\partial \phi_{n,N+1}^{(eq)}}{\partial \Lambda_{n,N+1}} - n_{N+1} \mathcal{B}' \left(\frac{\phi_{n,N+1}^{(eq)} - \phi_{n,N}^{(eq)}}{V_T} \right) \frac{\partial \phi_{n,N+1}^{(eq)}}{\partial \Lambda_{n,N+1}} \right]$$

$$= \frac{1}{V_T} \frac{D_{n,N+\frac{1}{2}}}{L_{N,N+1}} \left[-n_N \mathcal{B}' \left(-\frac{\phi_{n,N+1}^{(eq)} - \phi_{n,N}^{(eq)}}{V_T} \right) - n_{N+1} \mathcal{B}' \left(\frac{\phi_{n,N+1}^{(eq)} - \phi_{n,N}^{(eq)}}{V_T} \right) \right]$$

$$\left[\mathbf{J}_{\mathbf{C}_n, \Lambda_n}^{(k)} \right]_{N+1,N} = \frac{\partial}{\partial \Lambda_{n,N}} \left\{ \frac{D_{n,N+\frac{1}{2}}}{L_{N,N+1}} \left[n_N \mathcal{B} \left(-\frac{\phi_{n,N+1}^{(eq)} - \phi_{n,N}^{(eq)}}{V_T} \right) - n_{N+1} \mathcal{B} \left(\frac{\phi_{n,N+1}^{(eq)} - \phi_{n,N}^{(eq)}}{V_T} \right) \right] + \right.$$

$$\begin{aligned}
& \left. \left. + v_n^{(right)} (n_{N+1} - n_0^{(right)}) - U_{n,N+1} L_{N+\frac{1}{2},N+1} \right\} \Big|_{x=x^{(k)}} \\
& = \frac{1}{V_T} \frac{D_{n,N+\frac{1}{2}}}{L_{N,N+1}} \left[n_N \mathcal{B}' \left(-\frac{\phi_{n,N+1}^{(eq)} - \phi_{n,N}^{(eq)}}{V_T} \right) \frac{\partial \phi_{n,N}^{(eq)}}{\partial \Lambda_{n,N}} + n_{N+1} \mathcal{B}' \left(\frac{\phi_{n,N+1}^{(eq)} - \phi_{n,N}^{(eq)}}{V_T} \right) \frac{\partial \phi_{n,N}^{(eq)}}{\partial \Lambda_{n,N}} \right] \\
& = \frac{1}{V_T} \frac{D_{n,N+\frac{1}{2}}}{L_{N,N+1}} \left[n_N \mathcal{B}' \left(-\frac{\phi_{n,N+1}^{(eq)} - \phi_{n,N}^{(eq)}}{V_T} \right) + n_{N+1} \mathcal{B}' \left(\frac{\phi_{n,N+1}^{(eq)} - \phi_{n,N}^{(eq)}}{V_T} \right) \right]
\end{aligned}$$

Entries of $\mathbf{J}_{\mathbf{C}_p, \phi}^{(k)}$

The matrix $\mathbf{J}_{\mathbf{C}_p, \phi}^{(k)}$ is the block of the Jacobian containing the derivatives with respect to the potential at the nodes of the left-hand sides of the equations resulting from discretizing the continuity equation for holes.

In order to develop the derivatives of the equivalent potential $\phi_p^{(eq)}$ with respect to ϕ it is useful to remember its definition that was provided in Equation 10.34.

The first line of this matrix is obtained from differentiating the boundary condition for the hole continuity equation at the left contact with respect to the components of the discretized potential vector ϕ . It is then important to distinguish between the two types of contacts:

- if the left contact is of ohmic type then all the derivatives with respect to the potentials at the nodes of Equation 11.12 are zero.
- if the left contact is of Schottky type then the only nonzero derivatives with respect to the potentials at the nodes of Equation 11.13 are:

$$\begin{aligned}
\left[\mathbf{J}_{\mathbf{C}_p, \phi}^{(k)} \right]_{1,1} & = \frac{\partial}{\partial \phi_1} \left\{ \frac{D_{p,3/2}}{L_{1,2}} \left[p_1 \mathcal{B} \left(\frac{\phi_{p,2}^{(eq)} - \phi_{p,1}^{(eq)}}{V_T} \right) - p_2 \mathcal{B} \left(-\frac{\phi_{p,2}^{(eq)} - \phi_{p,1}^{(eq)}}{V_T} \right) \right] + \right. \\
& \quad \left. + v_p^{(left)} (p_1 - p_0^{(left)}) + U_{p,1} L_{1,3/2} \right\} \Big|_{x=x^{(k)}} \\
& = \frac{1}{V_T} \frac{D_{p,3/2}}{L_{1,2}} \left[-p_1 \mathcal{B}' \left(\frac{\phi_{p,2}^{(eq)} - \phi_{p,1}^{(eq)}}{V_T} \right) \frac{\partial \phi_{p,1}^{(eq)}}{\partial \phi_1} - p_2 \mathcal{B}' \left(-\frac{\phi_{p,2}^{(eq)} - \phi_{p,1}^{(eq)}}{V_T} \right) \frac{\partial \phi_{p,1}^{(eq)}}{\partial \phi_1} \right] \\
& = \frac{1}{V_T} \frac{D_{p,3/2}}{L_{1,2}} \left[-p_1 \mathcal{B}' \left(\frac{\phi_{p,2}^{(eq)} - \phi_{p,1}^{(eq)}}{V_T} \right) - p_2 \mathcal{B}' \left(-\frac{\phi_{p,2}^{(eq)} - \phi_{p,1}^{(eq)}}{V_T} \right) \right] \\
\left[\mathbf{J}_{\mathbf{C}_p, \phi}^{(k)} \right]_{1,2} & = \frac{\partial}{\partial \phi_2} \left\{ \frac{D_{p,3/2}}{L_{1,2}} \left[p_1 \mathcal{B} \left(\frac{\phi_{p,2}^{(eq)} - \phi_{p,1}^{(eq)}}{V_T} \right) - p_2 \mathcal{B} \left(-\frac{\phi_{p,2}^{(eq)} - \phi_{p,1}^{(eq)}}{V_T} \right) \right] + \right. \\
& \quad \left. + v_p^{(left)} (p_1 - p_0^{(left)}) + U_{p,1} L_{1,3/2} \right\} \Big|_{x=x^{(k)}} \\
& = \frac{1}{V_T} \frac{D_{p,3/2}}{L_{1,2}} \left[p_1 \mathcal{B}' \left(\frac{\phi_{p,2}^{(eq)} - \phi_{p,1}^{(eq)}}{V_T} \right) \frac{\partial \phi_{p,2}^{(eq)}}{\partial \phi_2} + p_2 \mathcal{B}' \left(-\frac{\phi_{p,2}^{(eq)} - \phi_{p,1}^{(eq)}}{V_T} \right) \frac{\partial \phi_{p,2}^{(eq)}}{\partial \phi_2} \right] \\
& = \frac{1}{V_T} \frac{D_{p,3/2}}{L_{1,2}} \left[p_1 \mathcal{B}' \left(\frac{\phi_{p,2}^{(eq)} - \phi_{p,1}^{(eq)}}{V_T} \right) + p_2 \mathcal{B}' \left(-\frac{\phi_{p,2}^{(eq)} - \phi_{p,1}^{(eq)}}{V_T} \right) \right]
\end{aligned}$$

The inner lines of this matrix ($j = 2 \dots N$) are obtained instead by differentiating the left-hand side of the j^{th} discretized hole continuity equation with respect to ϕ_{j-1} , ϕ_j and ϕ_{j+1} (which are the only non-null derivatives with respect to the potentials at the nodes):

$$\left[\mathbf{J}_{\mathbf{C}_p, \phi}^{(k)} \right]_{j,j} = \frac{\partial}{\partial \phi_j} \left\{ \frac{D_{p,j+\frac{1}{2}}}{L_{j,j+1}} \left[p_j \mathcal{B} \left(\frac{\phi_{p,j+1}^{(eq)} - \phi_{p,j}^{(eq)}}{V_T} \right) - p_{j+1} \mathcal{B} \left(-\frac{\phi_{p,j+1}^{(eq)} - \phi_{p,j}^{(eq)}}{V_T} \right) \right] + \right.$$

$$\begin{aligned}
& -\frac{D_{p,j-\frac{1}{2}}}{L_{j-1,j}} \left[p_{j-1} \mathcal{B} \left(\frac{\phi_{p,j}^{(eq)} - \phi_{p,j-1}^{(eq)}}{V_T} \right) - p_j \mathcal{B} \left(-\frac{\phi_{p,j}^{(eq)} - \phi_{p,j-1}^{(eq)}}{V_T} \right) \right] + U_{p,j} L_{j-\frac{1}{2},j+\frac{1}{2}} \Bigg|_{x=x(\mathbf{k})} \\
& = \frac{1}{V_T} \frac{D_{p,j+\frac{1}{2}}}{L_{j,j+1}} \left[-p_j \mathcal{B}' \left(\frac{\phi_{p,j+1}^{(eq)} - \phi_{p,j}^{(eq)}}{V_T} \right) \frac{\partial \phi_{p,j}^{(eq)}}{\partial \phi_j} - p_{j+1} \mathcal{B}' \left(-\frac{\phi_{p,j+1}^{(eq)} - \phi_{p,j}^{(eq)}}{V_T} \right) \frac{\partial \phi_{p,j}^{(eq)}}{\partial \phi_j} \right] \\
& + \frac{1}{V_T} \frac{D_{p,j-\frac{1}{2}}}{L_{j-1,j}} \left[-p_{j-1} \mathcal{B}' \left(\frac{\phi_{p,j}^{(eq)} - \phi_{p,j-1}^{(eq)}}{V_T} \right) \frac{\partial \phi_{p,j}^{(eq)}}{\partial \phi_j} - p_j \mathcal{B}' \left(-\frac{\phi_{p,j}^{(eq)} - \phi_{p,j-1}^{(eq)}}{V_T} \right) \frac{\partial \phi_{p,j}^{(eq)}}{\partial \phi_j} \right] \\
& = \frac{1}{V_T} \frac{D_{p,j+\frac{1}{2}}}{L_{j,j+1}} \left[-p_j \mathcal{B}' \left(\frac{\phi_{p,j+1}^{(eq)} - \phi_{p,j}^{(eq)}}{V_T} \right) - p_{j+1} \mathcal{B}' \left(-\frac{\phi_{p,j+1}^{(eq)} - \phi_{p,j}^{(eq)}}{V_T} \right) \right] \\
& + \frac{1}{V_T} \frac{D_{p,j-\frac{1}{2}}}{L_{j-1,j}} \left[-p_{j-1} \mathcal{B}' \left(\frac{\phi_{p,j}^{(eq)} - \phi_{p,j-1}^{(eq)}}{V_T} \right) - p_j \mathcal{B}' \left(-\frac{\phi_{p,j}^{(eq)} - \phi_{p,j-1}^{(eq)}}{V_T} \right) \right] \\
\left[\mathbf{J}_{\mathbf{C}_p, \phi}^{(\mathbf{k})} \right]_{j,j-1} & = \frac{\partial}{\partial \phi_{j-1}} \left\{ \frac{D_{p,j+\frac{1}{2}}}{L_{j,j+1}} \left[p_j \mathcal{B} \left(\frac{\phi_{p,j+1}^{(eq)} - \phi_{p,j}^{(eq)}}{V_T} \right) - p_{j+1} \mathcal{B} \left(-\frac{\phi_{p,j+1}^{(eq)} - \phi_{p,j}^{(eq)}}{V_T} \right) \right] + \right. \\
& \left. -\frac{D_{p,j-\frac{1}{2}}}{L_{j-1,j}} \left[p_{j-1} \mathcal{B} \left(\frac{\phi_{p,j}^{(eq)} - \phi_{p,j-1}^{(eq)}}{V_T} \right) - p_j \mathcal{B} \left(-\frac{\phi_{p,j}^{(eq)} - \phi_{p,j-1}^{(eq)}}{V_T} \right) \right] + U_{p,j} L_{j-\frac{1}{2},j+\frac{1}{2}} \right\} \Bigg|_{x=x(\mathbf{k})} \\
& = \frac{1}{V_T} \frac{D_{p,j-\frac{1}{2}}}{L_{j-1,j}} \left[p_{j-1} \mathcal{B}' \left(\frac{\phi_{p,j}^{(eq)} - \phi_{p,j-1}^{(eq)}}{V_T} \right) \frac{\partial \phi_{p,j-1}^{(eq)}}{\partial \phi_{j-1}} + p_j \mathcal{B}' \left(-\frac{\phi_{p,j}^{(eq)} - \phi_{p,j-1}^{(eq)}}{V_T} \right) \frac{\partial \phi_{p,j-1}^{(eq)}}{\partial \phi_{j-1}} \right] \\
& = \frac{1}{V_T} \frac{D_{p,j-\frac{1}{2}}}{L_{j-1,j}} \left[p_{j-1} \mathcal{B}' \left(\frac{\phi_{p,j}^{(eq)} - \phi_{p,j-1}^{(eq)}}{V_T} \right) + p_j \mathcal{B}' \left(-\frac{\phi_{p,j}^{(eq)} - \phi_{p,j-1}^{(eq)}}{V_T} \right) \right] \\
\left[\mathbf{J}_{\mathbf{C}_p, \phi}^{(\mathbf{k})} \right]_{j,j+1} & = \frac{\partial}{\partial \phi_{j+1}} \left\{ \frac{D_{p,j+\frac{1}{2}}}{L_{j,j+1}} \left[p_j \mathcal{B} \left(\frac{\phi_{p,j+1}^{(eq)} - \phi_{p,j}^{(eq)}}{V_T} \right) - p_{j+1} \mathcal{B} \left(-\frac{\phi_{p,j+1}^{(eq)} - \phi_{p,j}^{(eq)}}{V_T} \right) \right] + \right. \\
& \left. -\frac{D_{p,j-\frac{1}{2}}}{L_{j-1,j}} \left[p_{j-1} \mathcal{B} \left(\frac{\phi_{p,j}^{(eq)} - \phi_{p,j-1}^{(eq)}}{V_T} \right) - p_j \mathcal{B} \left(-\frac{\phi_{p,j}^{(eq)} - \phi_{p,j-1}^{(eq)}}{V_T} \right) \right] + U_{p,j} L_{j-\frac{1}{2},j+\frac{1}{2}} \right\} \Bigg|_{x=x(\mathbf{k})} \\
& = \frac{1}{V_T} \frac{D_{p,j+\frac{1}{2}}}{L_{j,j+1}} \left[p_j \mathcal{B}' \left(\frac{\phi_{p,j+1}^{(eq)} - \phi_{p,j}^{(eq)}}{V_T} \right) \frac{\partial \phi_{p,j+1}^{(eq)}}{\partial \phi_{j+1}} + p_{j+1} \mathcal{B}' \left(-\frac{\phi_{p,j+1}^{(eq)} - \phi_{p,j}^{(eq)}}{V_T} \right) \frac{\partial \phi_{p,j+1}^{(eq)}}{\partial \phi_{j+1}} \right] \\
& = \frac{1}{V_T} \frac{D_{p,j+\frac{1}{2}}}{L_{j,j+1}} \left[p_j \mathcal{B}' \left(\frac{\phi_{p,j+1}^{(eq)} - \phi_{p,j}^{(eq)}}{V_T} \right) + p_{j+1} \mathcal{B}' \left(-\frac{\phi_{p,j+1}^{(eq)} - \phi_{p,j}^{(eq)}}{V_T} \right) \right]
\end{aligned}$$

The last line of this matrix is obtained from differentiating the boundary condition for the hole continuity equation at the right contact with respect to the components of the discretized potential vector ϕ . It is then important to distinguish between the two types of contacts:

- if the right contact is of ohmic type then all the derivatives with respect to the potentials at the nodes of Equation 11.12 are zero.
- if the right contact is of Schottky type then the only nonzero derivatives with respect to the potentials at the nodes of Equation 11.14 are:

$$\begin{aligned}
\left[\mathbf{J}_{\mathbf{C}_p, \phi}^{(\mathbf{k})} \right]_{N+1,N+1} & = \frac{\partial}{\partial \phi_{N+1}} \left\{ \frac{D_{p,N+\frac{1}{2}}}{L_{N,N+1}} \left[p_{N+1} \mathcal{B} \left(-\frac{\phi_{p,N+1}^{(eq)} - \phi_{p,N}^{(eq)}}{V_T} \right) - p_N \mathcal{B} \left(\frac{\phi_{p,N+1}^{(eq)} - \phi_{p,N}^{(eq)}}{V_T} \right) \right] + \right. \\
& \left. + v_p^{(right)} (p_{N+1} - p_0^{(right)}) + U_{p,N+1} L_{N+\frac{1}{2},N+1} \right\} \Bigg|_{x=x(\mathbf{k})}
\end{aligned}$$

$$\begin{aligned}
&= \frac{1}{V_T} \frac{D_{p,N+\frac{1}{2}}}{L_{N,N+1}} \left[-p_{N+1} \mathcal{B}' \left(-\frac{\phi_{p,N+1}^{(eq)} - \phi_{p,N}^{(eq)}}{V_T} \right) \frac{\partial \phi_{p,N+1}^{(eq)}}{\partial \phi_{N+1}} - p_N \mathcal{B}' \left(\frac{\phi_{p,N+1}^{(eq)} - \phi_{p,N}^{(eq)}}{V_T} \right) \frac{\partial \phi_{p,N+1}^{(eq)}}{\partial \phi_{N+1}} \right] \\
&= \frac{1}{V_T} \frac{D_{p,N+\frac{1}{2}}}{L_{N,N+1}} \left[-p_{N+1} \mathcal{B}' \left(-\frac{\phi_{p,N+1}^{(eq)} - \phi_{p,N}^{(eq)}}{V_T} \right) - p_N \mathcal{B}' \left(\frac{\phi_{p,N+1}^{(eq)} - \phi_{p,N}^{(eq)}}{V_T} \right) \right] \\
\left[\mathbf{J}_{\mathbf{C}_{p,\phi}}^{(k)} \right]_{N+1,N} &= \frac{\partial}{\partial \phi_N} \left\{ \frac{D_{p,N+\frac{1}{2}}}{L_{N,N+1}} \left[p_{N+1} \mathcal{B} \left(-\frac{\phi_{p,N+1}^{(eq)} - \phi_{p,N}^{(eq)}}{V_T} \right) - p_N \mathcal{B} \left(\frac{\phi_{p,N+1}^{(eq)} - \phi_{p,N}^{(eq)}}{V_T} \right) \right] + \right. \\
&\quad \left. + v_p^{(right)} (p_{N+1} - p_0^{(right)}) + U_{p,N+1} L_{N+\frac{1}{2},N+1} \right\} \Big|_{x=x^{(k)}} \\
&= \frac{1}{V_T} \frac{D_{p,N+\frac{1}{2}}}{L_{N,N+1}} \left[p_{N+1} \mathcal{B}' \left(-\frac{\phi_{p,N+1}^{(eq)} - \phi_{p,N}^{(eq)}}{V_T} \right) \frac{\partial \phi_{p,N}^{(eq)}}{\partial \phi_N} + p_N \mathcal{B}' \left(\frac{\phi_{p,N+1}^{(eq)} - \phi_{p,N}^{(eq)}}{V_T} \right) \frac{\partial \phi_{p,N}^{(eq)}}{\partial \phi_N} \right] \\
&= \frac{1}{V_T} \frac{D_{p,N+\frac{1}{2}}}{L_{N,N+1}} \left[p_{N+1} \mathcal{B}' \left(-\frac{\phi_{p,N+1}^{(eq)} - \phi_{p,N}^{(eq)}}{V_T} \right) + p_N \mathcal{B}' \left(\frac{\phi_{p,N+1}^{(eq)} - \phi_{p,N}^{(eq)}}{V_T} \right) \right]
\end{aligned}$$

Entries of $\mathbf{J}_{\mathbf{C}_{p,\mathbf{p}}}^{(k)}$

The matrix $\mathbf{J}_{\mathbf{C}_{p,\mathbf{p}}}^{(k)}$ is the block of the Jacobian containing the derivatives with respect to the hole density at the nodes of the left-hand sides of the equations resulting from discretizing the continuity equation for holes.

In order to develop the derivatives of the equivalent potential $\phi_p^{(eq)}$ with respect to p it is useful to remember its definition that was provided in Equation 10.34.

The first line of this matrix is obtained from differentiating the boundary condition for the hole continuity equation at the left contact with respect to the components of the discretized hole density vector \mathbf{p} . It is then important to distinguish between the two types of contacts:

- if the left contact is of ohmic type then the only nonzero derivative with respect to the hole density at the nodes of Equation 11.12 is:

$$\left[\mathbf{J}_{\mathbf{C}_{p,\mathbf{p}}}^{(k)} \right]_{1,1} = \frac{\partial}{\partial p_1} \left\{ p_1 - p_0^{(left)} \right\} \Big|_{x=x^{(k)}} = 1$$

- if the left contact is of Schottky type then the only nonzero derivatives with respect to the holes densities at the nodes of Equation 11.8 are:

$$\begin{aligned}
\left[\mathbf{J}_{\mathbf{C}_{p,\mathbf{p}}}^{(k)} \right]_{1,1} &= \frac{\partial}{\partial p_1} \left\{ \frac{D_{p,3/2}}{L_{1,2}} \left[p_1 \mathcal{B} \left(\frac{\phi_{p,2}^{(eq)} - \phi_{p,1}^{(eq)}}{V_T} \right) - p_2 \mathcal{B} \left(-\frac{\phi_{p,2}^{(eq)} - \phi_{p,1}^{(eq)}}{V_T} \right) \right] + \right. \\
&\quad \left. + v_p^{(left)} (p_1 - p_0^{(left)}) + U_{p,1} L_{1,3/2} \right\} \Big|_{x=x^{(k)}} \\
&= \frac{D_{p,3/2}}{L_{1,2}} \mathcal{B} \left(\frac{\phi_{p,2}^{(eq)} - \phi_{p,1}^{(eq)}}{V_T} \right) + v_p^{(left)} + \frac{\partial U_{p,1}}{\partial p_1} L_{1,3/2}
\end{aligned}$$

$$\begin{aligned}
\left[\mathbf{J}_{\mathbf{C}_{p,\mathbf{p}}}^{(k)} \right]_{1,2} &= \frac{\partial}{\partial p_2} \left\{ \frac{D_{p,3/2}}{L_{1,2}} \left[p_1 \mathcal{B} \left(\frac{\phi_{p,2}^{(eq)} - \phi_{p,1}^{(eq)}}{V_T} \right) - p_2 \mathcal{B} \left(-\frac{\phi_{p,2}^{(eq)} - \phi_{p,1}^{(eq)}}{V_T} \right) \right] + \right. \\
&\quad \left. + v_p^{(left)} (p_1 - p_0^{(left)}) + U_{p,1} L_{1,3/2} \right\} \Big|_{x=x^{(k)}}
\end{aligned}$$

$$= -\frac{D_{p,3/2}}{L_{1,2}} \mathcal{B} \left(-\frac{\phi_{p,2}^{(eq)} - \phi_{p,1}^{(eq)}}{V_T} \right)$$

The inner lines of this matrix ($j = 2 \dots N$) are obtained instead by differentiating the left-hand side of the j^{th} discretized hole continuity equation with respect to p_{j-1} , p_j and p_{j+1} (which are the only non-null derivatives with respect to the hole densities at the nodes):

$$\begin{aligned} [\mathbf{J}_{\mathbf{C}_{\mathbf{p},\mathbf{p}}}^{(k)}]_{j,j} &= \frac{\partial}{\partial p_j} \left\{ \frac{D_{p,j+\frac{1}{2}}}{L_{j,j+1}} \left[p_j \mathcal{B} \left(\frac{\phi_{p,j+1}^{(eq)} - \phi_{p,j}^{(eq)}}{V_T} \right) - p_{j+1} \mathcal{B} \left(-\frac{\phi_{p,j+1}^{(eq)} - \phi_{p,j}^{(eq)}}{V_T} \right) \right] + \right. \\ &\quad \left. - \frac{D_{p,j-\frac{1}{2}}}{L_{j-1,j}} \left[p_{j-1} \mathcal{B} \left(\frac{\phi_{p,j}^{(eq)} - \phi_{p,j-1}^{(eq)}}{V_T} \right) - p_j \mathcal{B} \left(-\frac{\phi_{p,j}^{(eq)} - \phi_{p,j-1}^{(eq)}}{V_T} \right) \right] + U_{p,j} L_{j-\frac{1}{2},j+\frac{1}{2}} \right\} \Big|_{x=x^{(k)}} \\ &= \frac{D_{p,j+\frac{1}{2}}}{L_{j,j+1}} \mathcal{B} \left(\frac{\phi_{p,j+1}^{(eq)} - \phi_{p,j}^{(eq)}}{V_T} \right) + \frac{D_{p,j-\frac{1}{2}}}{L_{j-1,j}} \mathcal{B} \left(-\frac{\phi_{p,j}^{(eq)} - \phi_{p,j-1}^{(eq)}}{V_T} \right) + \frac{\partial U_{p,j}}{\partial p_j} L_{j-\frac{1}{2},j+\frac{1}{2}} \end{aligned}$$

$$\begin{aligned} [\mathbf{J}_{\mathbf{C}_{\mathbf{p},\mathbf{p}}}^{(k)}]_{j,j-1} &= \frac{\partial}{\partial p_{j-1}} \left\{ \frac{D_{p,j+\frac{1}{2}}}{L_{j,j+1}} \left[p_j \mathcal{B} \left(\frac{\phi_{p,j+1}^{(eq)} - \phi_{p,j}^{(eq)}}{V_T} \right) - p_{j+1} \mathcal{B} \left(-\frac{\phi_{p,j+1}^{(eq)} - \phi_{p,j}^{(eq)}}{V_T} \right) \right] + \right. \\ &\quad \left. - \frac{D_{p,j-\frac{1}{2}}}{L_{j-1,j}} \left[p_{j-1} \mathcal{B} \left(\frac{\phi_{p,j}^{(eq)} - \phi_{p,j-1}^{(eq)}}{V_T} \right) - p_j \mathcal{B} \left(-\frac{\phi_{p,j}^{(eq)} - \phi_{p,j-1}^{(eq)}}{V_T} \right) \right] + U_{p,j} L_{j-\frac{1}{2},j+\frac{1}{2}} \right\} \Big|_{x=x^{(k)}} \\ &= -\frac{D_{p,j-\frac{1}{2}}}{L_{j-1,j}} \mathcal{B} \left(\frac{\phi_{p,j}^{(eq)} - \phi_{p,j-1}^{(eq)}}{V_T} \right) \end{aligned}$$

$$\begin{aligned} [\mathbf{J}_{\mathbf{C}_{\mathbf{p},\mathbf{p}}}^{(k)}]_{j,j+1} &= \frac{\partial}{\partial p_{j+1}} \left\{ \frac{D_{p,j+\frac{1}{2}}}{L_{j,j+1}} \left[p_j \mathcal{B} \left(\frac{\phi_{p,j+1}^{(eq)} - \phi_{p,j}^{(eq)}}{V_T} \right) - p_{j+1} \mathcal{B} \left(-\frac{\phi_{p,j+1}^{(eq)} - \phi_{p,j}^{(eq)}}{V_T} \right) \right] + \right. \\ &\quad \left. - \frac{D_{p,j-\frac{1}{2}}}{L_{j-1,j}} \left[p_{j-1} \mathcal{B} \left(\frac{\phi_{p,j}^{(eq)} - \phi_{p,j-1}^{(eq)}}{V_T} \right) - p_j \mathcal{B} \left(-\frac{\phi_{p,j}^{(eq)} - \phi_{p,j-1}^{(eq)}}{V_T} \right) \right] + U_{p,j} L_{j-\frac{1}{2},j+\frac{1}{2}} \right\} \Big|_{x=x^{(k)}} \\ &= -\frac{D_{p,j+\frac{1}{2}}}{L_{j,j+1}} p_{j+1} \mathcal{B} \left(-\frac{\phi_{p,j+1}^{(eq)} - \phi_{p,j}^{(eq)}}{V_T} \right) \end{aligned}$$

The last line of this matrix is obtained from differentiating the boundary condition for the hole continuity equation at the right contact with respect to the components of the discretized hole density vector \mathbf{p} . It is then important to distinguish between the two types of contacts:

- if the right contact is of ohmic type then the only nonzero derivative with respect to the hole density at the nodes of Equation 11.12 is:

$$[\mathbf{J}_{\mathbf{C}_{\mathbf{p},\mathbf{p}}}^{(k)}]_{N+1,N+1} = \frac{\partial}{\partial p_{N+1}} \left\{ p_{N+1} - p_0^{(right)} \right\} \Big|_{x=x^{(k)}} = 1$$

- if the right contact is of Schottky type then the only nonzero derivatives with respect to the hole densities at the nodes of Equation 11.14 are:

$$\begin{aligned} [\mathbf{J}_{\mathbf{C}_{\mathbf{p},\mathbf{p}}}^{(k)}]_{N+1,N+1} &= \frac{\partial}{\partial p_{N+1}} \left\{ \frac{D_{p,N+\frac{1}{2}}}{L_{N,N+1}} \left[p_{N+1} \mathcal{B} \left(-\frac{\phi_{p,N+1}^{(eq)} - \phi_{p,N}^{(eq)}}{V_T} \right) - p_N \mathcal{B} \left(\frac{\phi_{p,N+1}^{(eq)} - \phi_{p,N}^{(eq)}}{V_T} \right) \right] + \right. \\ &\quad \left. + v_p^{(right)} (p_{N+1} - p_0^{(right)}) + U_{p,N+1} L_{N+\frac{1}{2},N+1} \right\} \Big|_{x=x^{(k)}} \\ &= \frac{D_{p,N+\frac{1}{2}}}{L_{N,N+1}} \mathcal{B} \left(-\frac{\phi_{p,N+1}^{(eq)} - \phi_{p,N}^{(eq)}}{V_T} \right) + v_p^{(right)} + \frac{\partial U_{p,N+1}}{\partial p_{N+1}} L_{N+\frac{1}{2},N+1} \end{aligned}$$

$$\begin{aligned}
\left[\mathbf{J}_{\mathbf{C}_{\mathbf{p},\mathbf{p}}}^{(\mathbf{k})} \right]_{N+1,N} &= \frac{\partial}{\partial p_N} \left\{ \frac{D_{\mathbf{p},N+\frac{1}{2}}}{L_{N,N+1}} \left[p_{N+1} \mathcal{B} \left(-\frac{\phi_{\mathbf{p},N+1}^{(eq)} - \phi_{\mathbf{p},N}^{(eq)}}{V_T} \right) - p_N \mathcal{B} \left(\frac{\phi_{\mathbf{p},N+1}^{(eq)} - \phi_{\mathbf{p},N}^{(eq)}}{V_T} \right) \right] + \right. \\
&\quad \left. + v_p^{(right)} (p_{N+1} - p_0^{(right)}) + U_{\mathbf{p},N+1} L_{N+\frac{1}{2},N+1} \right\} \Big|_{\mathbf{x}=\mathbf{x}^{(\mathbf{k})}} \\
&= -\frac{D_{\mathbf{p},N+\frac{1}{2}}}{L_{N,N+1}} \mathcal{B} \left(\frac{\phi_{\mathbf{p},N+1}^{(eq)} - \phi_{\mathbf{p},N}^{(eq)}}{V_T} \right)
\end{aligned}$$

In order to obtain the complete formulations it is then necessary to compute the derivative $\frac{\partial U_{\mathbf{p},j}}{\partial p_j}$. For SRH generation/recombination it is evaluated as:

$$\begin{aligned}
\frac{\partial U_{\mathbf{p},j}^{(SRH)}}{\partial p_j} &= \frac{\partial}{\partial p_j} \left\{ \frac{n_j p_j - n_{i,j}^2}{\tau_{\mathbf{p},j}(n_j + n_{t,j}) + \tau_{\mathbf{n},j}(p_j + p_{t,j})} \right\} \Big|_{\mathbf{x}=\mathbf{x}^{(\mathbf{k})}} \\
&= \frac{p_j [\tau_{\mathbf{p},j}(n_j + n_{t,j}) + \tau_{\mathbf{n},j}(p_j + p_{t,j})] - [n_j p_j - n_{i,j}^2] \tau_{\mathbf{n},j}}{[\tau_{\mathbf{p},j}(n_j + n_{t,j}) + \tau_{\mathbf{n},j}(p_j + p_{t,j})]^2}
\end{aligned}$$

Entries of $\mathbf{J}_{\mathbf{C}_{\mathbf{p},\mathbf{n}}}^{(\mathbf{k})}$

The matrix $\mathbf{J}_{\mathbf{C}_{\mathbf{p},\mathbf{n}}}^{(\mathbf{k})}$ is the block of the Jacobian containing the derivatives with respect to the electron density at the nodes of the left-hand sides of the equations resulting from discretizing the continuity equation for holes.

Moreover, in order to develop the derivatives of the equivalent potential $\phi_p^{(eq)}$ with respect to n it is useful to remember its definition that was provided in Equation 10.5.

The first line of this matrix is obtained from differentiating the boundary condition for the hole continuity equation at the left contact with respect to the components of the discretized electron density vector \mathbf{n} . It is then important to distinguish between the two types of contacts:

- if the left contact is of ohmic type then Equation 11.12 does not include any dependency on the electron density and, therefore, all the derivatives are zero;
- if the left contact is of Schottky type then the only nonzero derivative with respect to the electron densities at the nodes of Equation 11.8 is:

$$\begin{aligned}
\left[\mathbf{J}_{\mathbf{C}_{\mathbf{p},\mathbf{n}}}^{(\mathbf{k})} \right]_{1,1} &= \frac{\partial}{\partial p_1} \left\{ \frac{D_{\mathbf{p},3/2}}{L_{1,2}} \left[p_1 \mathcal{B} \left(\frac{\phi_{\mathbf{p},2}^{(eq)} - \phi_{\mathbf{p},1}^{(eq)}}{V_T} \right) - p_2 \mathcal{B} \left(-\frac{\phi_{\mathbf{p},2}^{(eq)} - \phi_{\mathbf{p},1}^{(eq)}}{V_T} \right) \right] + \right. \\
&\quad \left. + v_p^{(left)} (p_1 - p_0^{(left)}) + U_{\mathbf{p},1} L_{1,3/2} \right\} \Big|_{\mathbf{x}=\mathbf{x}^{(\mathbf{k})}} \\
&= \frac{\partial U_{\mathbf{p},1}}{\partial p_1} L_{1,3/2}
\end{aligned}$$

The inner lines of this matrix ($j = 2 \dots N$) are obtained instead by differentiating the left-hand side of the j^{th} discretized hole continuity equation with respect to p_j (which is the only non-null derivative with respect to the electron densities at the nodes):

$$\begin{aligned}
\left[\mathbf{J}_{\mathbf{C}_{\mathbf{p},\mathbf{n}}}^{(\mathbf{k})} \right]_{j,j} &= \frac{\partial}{\partial p_j} \left\{ \frac{D_{\mathbf{p},j+\frac{1}{2}}}{L_{j,j+1}} \left[p_j \mathcal{B} \left(\frac{\phi_{\mathbf{p},j+1}^{(eq)} - \phi_{\mathbf{p},j}^{(eq)}}{V_T} \right) - p_{j+1} \mathcal{B} \left(-\frac{\phi_{\mathbf{p},j+1}^{(eq)} - \phi_{\mathbf{p},j}^{(eq)}}{V_T} \right) \right] + \right. \\
&\quad \left. - \frac{D_{\mathbf{p},j-\frac{1}{2}}}{L_{j-1,j}} \left[p_{j-1} \mathcal{B} \left(\frac{\phi_{\mathbf{p},j}^{(eq)} - \phi_{\mathbf{p},j-1}^{(eq)}}{V_T} \right) - p_j \mathcal{B} \left(-\frac{\phi_{\mathbf{p},j}^{(eq)} - \phi_{\mathbf{p},j-1}^{(eq)}}{V_T} \right) \right] + U_{\mathbf{p},j} L_{j-\frac{1}{2},j+\frac{1}{2}} \right\} \Big|_{\mathbf{x}=\mathbf{x}^{(\mathbf{k})}}
\end{aligned}$$

$$= \frac{\partial U_{p,j}}{\partial p_j} L_{j-\frac{1}{2},j+\frac{1}{2}}$$

The last line of this matrix is obtained from differentiating the boundary condition for the hole continuity equation at the right contact with respect to the components of the discretized electron density vector \mathbf{n} . It is then important to distinguish between the two types of contacts:

- if the right contact is of ohmic type then Equation 11.12 does not include any dependency on the electron density and, therefore, all the derivatives are zero;
- if the right contact is of Schottky type then the only nonzero derivative with respect to the electron densities at the nodes of Equation 11.9 is:

$$\begin{aligned} \left[\mathbf{J}_{\mathbf{C}_{n,p}}^{(k)} \right]_{N+1,N+1} &= \frac{\partial}{\partial n_{N+1}} \left\{ \frac{D_{p,N+\frac{1}{2}}}{L_{N,N+1}} \left[p_{N+1} \mathcal{B} \left(-\frac{\phi_{p,N+1}^{(eq)} - \phi_{p,N}^{(eq)}}{V_T} \right) - p_N \mathcal{B} \left(\frac{\phi_{p,N+1}^{(eq)} - \phi_{p,N}^{(eq)}}{V_T} \right) \right] + \right. \\ &\quad \left. + v_p^{(right)} (p_{N+1} - p_0^{(right)}) + U_{p,N+1} L_{N+\frac{1}{2},N+1} \right\} \Big|_{x=x^{(k)}} \\ &= \frac{\partial U_{p,N+1}}{\partial p_{N+1}} L_{N+\frac{1}{2},N+1} \end{aligned}$$

In order to obtain the complete formulations it is then necessary to compute the derivative $\frac{\partial U_{p,j}}{\partial n_j}$. For SRH generation/recombination it is evaluated as:

$$\begin{aligned} \frac{\partial U_{p,j}^{(SRH)}}{\partial n_j} &= \frac{\partial}{\partial n_j} \left\{ \frac{n_j p_j - n_{i,j}^2}{\tau_{p,j}(n_j + n_{t,j}) + \tau_{n,j}(p_j + p_{t,j})} \right\} \Big|_{x=x^{(k)}} \\ &= \frac{n_j [\tau_{p,j}(n_j + n_{t,j}) + \tau_{n,j}(p_j + p_{t,j})] - [n_j p_j - n_{i,j}^2] \tau_{p,j}}{[\tau_{p,j}(n_j + n_{t,j}) + \tau_{n,j}(p_j + p_{t,j})]^2} \end{aligned}$$

Entries of $\mathbf{J}_{\mathbf{C}_p, \Lambda_p}^{(k)}$

The matrix $\mathbf{J}_{\mathbf{C}_p, \Lambda_p}^{(k)}$ is the block of the Jacobian containing the derivatives with respect to the hole quantum potential at the nodes of the left-hand sides of the equations resulting from discretizing the continuity equation for holes.

Moreover, in order to develop the derivatives of the equivalent potential $\phi_p^{(eq)}$ with respect to Λ_p it is useful to remember its definition that was provided in Equation 10.5.

The first line of this matrix is obtained from differentiating the boundary condition for the hole continuity equation at the left contact with respect to the components of the discretized hole quantum potential vector Λ_p . It is then important to distinguish between the two types of contacts:

- if the left contact is of ohmic type then all the derivatives with respect to the hole quantum potentials at the nodes of Equation 11.12 are zero.
- if the left contact is of Schottky type then the only nonzero derivatives with respect to the hole quantum potentials at the nodes of Equation 11.13 are:

$$\begin{aligned} \left[\mathbf{J}_{\mathbf{C}_p, \Lambda_p}^{(k)} \right]_{1,1} &= \frac{\partial}{\partial \Lambda_{p,1}} \left\{ \frac{D_{p,3/2}}{L_{1,2}} \left[p_1 \mathcal{B} \left(\frac{\phi_{p,2}^{(eq)} - \phi_{p,1}^{(eq)}}{V_T} \right) - p_2 \mathcal{B} \left(-\frac{\phi_{p,2}^{(eq)} - \phi_{p,1}^{(eq)}}{V_T} \right) \right] + \right. \\ &\quad \left. + v_p^{(left)} (p_1 - p_0^{(left)}) + U_{p,1} L_{1,3/2} \right\} \Big|_{x=x^{(k)}} \\ &= \frac{1}{V_T} \frac{D_{p,3/2}}{L_{1,2}} \left[-p_1 \mathcal{B}' \left(\frac{\phi_{p,2}^{(eq)} - \phi_{p,1}^{(eq)}}{V_T} \right) \frac{\partial \phi_{p,1}^{(eq)}}{\partial \Lambda_{p,1}} - p_2 \mathcal{B}' \left(-\frac{\phi_{p,2}^{(eq)} - \phi_{p,1}^{(eq)}}{V_T} \right) \frac{\partial \phi_{p,1}^{(eq)}}{\partial \Lambda_{p,1}} \right] \end{aligned}$$

$$\begin{aligned}
&= \frac{1}{V_T} \frac{D_{p,3/2}}{L_{1,2}} \left[p_1 \mathcal{B}' \left(\frac{\phi_{p,2}^{(eq)} - \phi_{p,1}^{(eq)}}{V_T} \right) + p_2 \mathcal{B}' \left(-\frac{\phi_{p,2}^{(eq)} - \phi_{p,1}^{(eq)}}{V_T} \right) \right] \\
\left[\mathbf{J}_{\mathbf{C}_p, \Lambda_p}^{(k)} \right]_{1,2} &= \frac{\partial}{\partial \Lambda_{p,2}} \left\{ \frac{D_{p,3/2}}{L_{1,2}} \left[p_1 \mathcal{B} \left(\frac{\phi_{p,2}^{(eq)} - \phi_{p,1}^{(eq)}}{V_T} \right) - p_2 \mathcal{B} \left(-\frac{\phi_{p,2}^{(eq)} - \phi_{p,1}^{(eq)}}{V_T} \right) \right] + \right. \\
&\quad \left. + v_p^{(left)} (p_1 - p_0^{(left)}) + U_{p,1} L_{1,3/2} \right\} \Big|_{x=x^{(k)}} \\
&= \frac{1}{V_T} \frac{D_{p,3/2}}{L_{1,2}} \left[p_1 \mathcal{B}' \left(\frac{\phi_{p,2}^{(eq)} - \phi_{p,1}^{(eq)}}{V_T} \right) \frac{\partial \phi_{p,2}^{(eq)}}{\partial \Lambda_{p,2}} + p_2 \mathcal{B}' \left(-\frac{\phi_{p,2}^{(eq)} - \phi_{p,1}^{(eq)}}{V_T} \right) \frac{\partial \phi_{p,2}^{(eq)}}{\partial \Lambda_{p,2}} \right] \\
&= \frac{1}{V_T} \frac{D_{p,3/2}}{L_{1,2}} \left[-p_1 \mathcal{B}' \left(\frac{\phi_{p,2}^{(eq)} - \phi_{p,1}^{(eq)}}{V_T} \right) - p_2 \mathcal{B}' \left(-\frac{\phi_{p,2}^{(eq)} - \phi_{p,1}^{(eq)}}{V_T} \right) \right]
\end{aligned}$$

The inner lines of this matrix ($j = 2 \cdots N$) are obtained instead by differentiating the left-hand side of the j^{th} discretized hole continuity equation with respect to $\Lambda_{p,j-1}$, $\Lambda_{p,j}$ and $\Lambda_{p,j+1}$ (which are the only non-null derivatives with respect to the potentials at the nodes):

$$\begin{aligned}
\left[\mathbf{J}_{\mathbf{C}_p, \Lambda_p}^{(k)} \right]_{j,j} &= \frac{\partial}{\partial \Lambda_{p,j}} \left\{ \frac{D_{p,j+\frac{1}{2}}}{L_{j,j+1}} \left[p_j \mathcal{B} \left(\frac{\phi_{p,j+1}^{(eq)} - \phi_{p,j}^{(eq)}}{V_T} \right) - p_{j+1} \mathcal{B} \left(-\frac{\phi_{p,j+1}^{(eq)} - \phi_{p,j}^{(eq)}}{V_T} \right) \right] + \right. \\
&\quad \left. - \frac{D_{p,j-\frac{1}{2}}}{L_{j-1,j}} \left[p_{j-1} \mathcal{B} \left(\frac{\phi_{p,j}^{(eq)} - \phi_{p,j-1}^{(eq)}}{V_T} \right) - p_j \mathcal{B} \left(-\frac{\phi_{p,j}^{(eq)} - \phi_{p,j-1}^{(eq)}}{V_T} \right) \right] + U_{p,j} L_{j-\frac{1}{2},j+\frac{1}{2}} \right\} \Big|_{x=x^{(k)}} \\
&= \frac{1}{V_T} \frac{D_{p,j+\frac{1}{2}}}{L_{j,j+1}} \left[-p_j \mathcal{B}' \left(\frac{\phi_{p,j+1}^{(eq)} - \phi_{p,j}^{(eq)}}{V_T} \right) \frac{\partial \phi_{p,j}^{(eq)}}{\partial \Lambda_{p,j}} - p_{j+1} \mathcal{B}' \left(-\frac{\phi_{p,j+1}^{(eq)} - \phi_{p,j}^{(eq)}}{V_T} \right) \frac{\partial \phi_{p,j}^{(eq)}}{\partial \Lambda_{p,j}} \right] \\
&\quad + \frac{1}{V_T} \frac{D_{p,j-\frac{1}{2}}}{L_{j-1,j}} \left[-p_{j-1} \mathcal{B}' \left(\frac{\phi_{p,j}^{(eq)} - \phi_{p,j-1}^{(eq)}}{V_T} \right) \frac{\partial \phi_{p,j}^{(eq)}}{\partial \Lambda_{p,j}} - p_j \mathcal{B}' \left(-\frac{\phi_{p,j}^{(eq)} - \phi_{p,j-1}^{(eq)}}{V_T} \right) \frac{\partial \phi_{p,j}^{(eq)}}{\partial \Lambda_{p,j}} \right] \\
&= \frac{1}{V_T} \frac{D_{p,j+\frac{1}{2}}}{L_{j,j+1}} \left[p_j \mathcal{B}' \left(\frac{\phi_{p,j+1}^{(eq)} - \phi_{p,j}^{(eq)}}{V_T} \right) + p_{j+1} \mathcal{B}' \left(-\frac{\phi_{p,j+1}^{(eq)} - \phi_{p,j}^{(eq)}}{V_T} \right) \right] \\
&\quad + \frac{1}{V_T} \frac{D_{p,j-\frac{1}{2}}}{L_{j-1,j}} \left[p_{j-1} \mathcal{B}' \left(\frac{\phi_{p,j}^{(eq)} - \phi_{p,j-1}^{(eq)}}{V_T} \right) + p_j \mathcal{B}' \left(-\frac{\phi_{p,j}^{(eq)} - \phi_{p,j-1}^{(eq)}}{V_T} \right) \right]
\end{aligned}$$

$$\begin{aligned}
\left[\mathbf{J}_{\mathbf{C}_p, \Lambda_p}^{(k)} \right]_{j,j-1} &= \frac{\partial}{\partial \Lambda_{p,j-1}} \left\{ \frac{D_{p,j+\frac{1}{2}}}{L_{j,j+1}} \left[p_j \mathcal{B} \left(\frac{\phi_{p,j+1}^{(eq)} - \phi_{p,j}^{(eq)}}{V_T} \right) - p_{j+1} \mathcal{B} \left(-\frac{\phi_{p,j+1}^{(eq)} - \phi_{p,j}^{(eq)}}{V_T} \right) \right] + \right. \\
&\quad \left. - \frac{D_{p,j-\frac{1}{2}}}{L_{j-1,j}} \left[p_{j-1} \mathcal{B} \left(\frac{\phi_{p,j}^{(eq)} - \phi_{p,j-1}^{(eq)}}{V_T} \right) - p_j \mathcal{B} \left(-\frac{\phi_{p,j}^{(eq)} - \phi_{p,j-1}^{(eq)}}{V_T} \right) \right] + U_{p,j} L_{j-\frac{1}{2},j+\frac{1}{2}} \right\} \Big|_{x=x^{(k)}} \\
&= \frac{1}{V_T} \frac{D_{p,j-\frac{1}{2}}}{L_{j-1,j}} \left[p_{j-1} \mathcal{B}' \left(\frac{\phi_{p,j}^{(eq)} - \phi_{p,j-1}^{(eq)}}{V_T} \right) \frac{\partial \phi_{p,j-1}^{(eq)}}{\partial \Lambda_{p,j-1}} + p_j \mathcal{B}' \left(-\frac{\phi_{p,j}^{(eq)} - \phi_{p,j-1}^{(eq)}}{V_T} \right) \frac{\partial \phi_{p,j-1}^{(eq)}}{\partial \Lambda_{p,j-1}} \right] \\
&= \frac{1}{V_T} \frac{D_{p,j-\frac{1}{2}}}{L_{j-1,j}} \left[-p_{j-1} \mathcal{B}' \left(\frac{\phi_{p,j}^{(eq)} - \phi_{p,j-1}^{(eq)}}{V_T} \right) - p_j \mathcal{B}' \left(-\frac{\phi_{p,j}^{(eq)} - \phi_{p,j-1}^{(eq)}}{V_T} \right) \right]
\end{aligned}$$

$$\begin{aligned}
\left[\mathbf{J}_{\mathbf{C}_p, \Lambda_p}^{(k)} \right]_{j,j+1} &= \frac{\partial}{\partial \Lambda_{p,j+1}} \left\{ \frac{D_{p,j+\frac{1}{2}}}{L_{j,j+1}} \left[p_j \mathcal{B} \left(\frac{\phi_{p,j+1}^{(eq)} - \phi_{p,j}^{(eq)}}{V_T} \right) - p_{j+1} \mathcal{B} \left(-\frac{\phi_{p,j+1}^{(eq)} - \phi_{p,j}^{(eq)}}{V_T} \right) \right] + \right. \\
&\quad \left. - \frac{D_{p,j-\frac{1}{2}}}{L_{j-1,j}} \left[p_{j-1} \mathcal{B} \left(\frac{\phi_{p,j}^{(eq)} - \phi_{p,j-1}^{(eq)}}{V_T} \right) - p_j \mathcal{B} \left(-\frac{\phi_{p,j}^{(eq)} - \phi_{p,j-1}^{(eq)}}{V_T} \right) \right] + U_{p,j} L_{j-\frac{1}{2},j+\frac{1}{2}} \right\} \Big|_{x=x^{(k)}}
\end{aligned}$$

$$\begin{aligned}
&= \frac{1}{V_T} \frac{D_{p,j+\frac{1}{2}}}{L_{j,j+1}} \left[p_j \mathcal{B}' \left(\frac{\phi_{p,j+1}^{(eq)} - \phi_{p,j}^{(eq)}}{V_T} \right) \frac{\partial \phi_{p,j+1}^{(eq)}}{\partial \Lambda_{p,j+1}} + p_{j+1} \mathcal{B}' \left(-\frac{\phi_{p,j+1}^{(eq)} - \phi_{p,j}^{(eq)}}{V_T} \right) \frac{\partial \phi_{p,j+1}^{(eq)}}{\partial \Lambda_{p,j+1}} \right] \\
&= \frac{1}{V_T} \frac{D_{p,j+\frac{1}{2}}}{L_{j,j+1}} \left[-p_j \mathcal{B}' \left(\frac{\phi_{p,j+1}^{(eq)} - \phi_{p,j}^{(eq)}}{V_T} \right) - p_{j+1} \mathcal{B}' \left(-\frac{\phi_{p,j+1}^{(eq)} - \phi_{p,j}^{(eq)}}{V_T} \right) \right]
\end{aligned}$$

The last line of this matrix is obtained from differentiating the boundary condition for the hole continuity equation at the right contact with respect to the components of the discretized hole quantum potential vector Λ_p . It is then important to distinguish between the two types of contacts:

- if the right contact is of ohmic type then all the derivatives with respect to the potentials at the nodes of Equation 11.12 are zero.
- if the right contact is of Schottky type then the only nonzero derivatives with respect to the hole quantum potentials at the nodes of Equation 11.14 are:

$$\begin{aligned}
[\mathbf{J}_{\mathbf{C}_n, \Lambda_p}^{(k)}]_{N+1, N+1} &= \frac{\partial}{\partial \Lambda_{p, N+1}} \left\{ \frac{D_{p, N+\frac{1}{2}}}{L_{N, N+1}} \left[p_{N+1} \mathcal{B} \left(-\frac{\phi_{p, N+1}^{(eq)} - \phi_{p, N}^{(eq)}}{V_T} \right) - p_N \mathcal{B} \left(\frac{\phi_{p, N+1}^{(eq)} - \phi_{p, N}^{(eq)}}{V_T} \right) \right] + \right. \\
&\quad \left. + v_p^{(right)} (p_{N+1} - p_0^{(right)}) + U_{p, N+1} L_{N+\frac{1}{2}, N+1} \right\} \Big|_{x=x^{(k)}} \\
&= \frac{1}{V_T} \frac{D_{p, N+\frac{1}{2}}}{L_{N, N+1}} \left[-p_{N+1} \mathcal{B} \left(-\frac{\phi_{p, N+1}^{(eq)} - \phi_{p, N}^{(eq)}}{V_T} \right) \frac{\partial \phi_{p, N+1}^{(eq)}}{\partial \Lambda_{p, N+1}} - p_N \mathcal{B} \left(\frac{\phi_{p, N+1}^{(eq)} - \phi_{p, N}^{(eq)}}{V_T} \right) \frac{\partial \phi_{p, N+1}^{(eq)}}{\partial \Lambda_{p, N+1}} \right] \\
&= \frac{1}{V_T} \frac{D_{p, N+\frac{1}{2}}}{L_{N, N+1}} \left[p_{N+1} \mathcal{B} \left(-\frac{\phi_{p, N+1}^{(eq)} - \phi_{p, N}^{(eq)}}{V_T} \right) + p_N \mathcal{B} \left(\frac{\phi_{p, N+1}^{(eq)} - \phi_{p, N}^{(eq)}}{V_T} \right) \right]
\end{aligned}$$

$$\begin{aligned}
[\mathbf{J}_{\mathbf{C}_p, \Lambda_p}^{(k)}]_{N+1, N} &= \frac{\partial}{\partial \Lambda_{p, N}} \left\{ \frac{D_{p, N+\frac{1}{2}}}{L_{N, N+1}} \left[p_{N+1} \mathcal{B} \left(-\frac{\phi_{p, N+1}^{(eq)} - \phi_{p, N}^{(eq)}}{V_T} \right) - p_N \mathcal{B} \left(\frac{\phi_{p, N+1}^{(eq)} - \phi_{p, N}^{(eq)}}{V_T} \right) \right] + \right. \\
&\quad \left. + v_p^{(right)} (p_{N+1} - p_0^{(right)}) + U_{p, N+1} L_{N+\frac{1}{2}, N+1} \right\} \Big|_{x=x^{(k)}} \\
&= \frac{1}{V_T} \frac{D_{p, N+\frac{1}{2}}}{L_{N, N+1}} \left[p_{N+1} \mathcal{B} \left(-\frac{\phi_{p, N+1}^{(eq)} - \phi_{p, N}^{(eq)}}{V_T} \right) \frac{\partial \phi_{p, N}^{(eq)}}{\partial \Lambda_{p, N}} + p_N \mathcal{B} \left(\frac{\phi_{p, N+1}^{(eq)} - \phi_{p, N}^{(eq)}}{V_T} \right) \frac{\partial \phi_{p, N}^{(eq)}}{\partial \Lambda_{p, N}} \right] \\
&= \frac{1}{V_T} \frac{D_{p, N+\frac{1}{2}}}{L_{N, N+1}} \left[-p_{N+1} \mathcal{B} \left(-\frac{\phi_{p, N+1}^{(eq)} - \phi_{p, N}^{(eq)}}{V_T} \right) - p_N \mathcal{B} \left(\frac{\phi_{p, N+1}^{(eq)} - \phi_{p, N}^{(eq)}}{V_T} \right) \right]
\end{aligned}$$

Entries of $\mathbf{J}_{\mathbf{D}_n, \mathbf{n}}^{(k)}$

The matrix $\mathbf{J}_{\mathbf{D}_n, \mathbf{n}}^{(k)}$ is the block of the Jacobian containing the derivatives with respect to the electron density at the nodes of the left-hand sides of the equations resulting from discretizing the electron density gradient equation.

The first line of this matrix is obtained from differentiating the boundary condition for the electron density gradient equation at the left contact with respect to the components of the discretized electron density vector \mathbf{n} . It is then important to distinguish between the two types of contacts:

- if the left contact is of ohmic type then all the derivatives with respect to the electron densities at the nodes of Equation 11.17 are zero;

- if the left contact is of Schottky type then the only nonzero derivatives with respect to the electron densities at the nodes of Equation 11.18 are:

$$\begin{aligned} \left[\mathbf{J}_{\mathbf{D}_{\mathbf{n}}, \mathbf{n}}^{(\mathbf{k})} \right]_{1,1} &= \frac{\partial}{\partial n_1} \left\{ \sqrt{n_1} \Lambda_{n,1} L_{1,\frac{3}{2}} - \frac{\hbar^2}{6q} \frac{1}{m_{n,\frac{3}{2}}^*} \frac{\sqrt{n_2} - \sqrt{n_1}}{L_{1,2}} \right\} \Bigg|_{\mathbf{x}=\mathbf{x}(\mathbf{k})} \\ &= \Lambda_{n,1} L_{1,\frac{3}{2}} \frac{1}{2\sqrt{n_1}} + \frac{\hbar^2}{6q} \frac{1}{m_{n,\frac{3}{2}}^*} \frac{1}{2\sqrt{n_1} L_{1,2}} \\ \left[\mathbf{J}_{\mathbf{D}_{\mathbf{n}}, \mathbf{n}}^{(\mathbf{k})} \right]_{1,2} &= \frac{\partial}{\partial n_2} \left\{ \sqrt{n_1} \Lambda_{n,1} L_{1,\frac{3}{2}} - \frac{\hbar^2}{6q} \frac{1}{m_{n,\frac{3}{2}}^*} \frac{\sqrt{n_2} - \sqrt{n_1}}{L_{1,2}} \right\} \Bigg|_{\mathbf{x}=\mathbf{x}(\mathbf{k})} \\ &= -\frac{\hbar^2}{6q} \frac{1}{m_{n,\frac{3}{2}}^*} \frac{1}{2\sqrt{n_2} L_{1,2}} \end{aligned}$$

The inner lines of this matrix ($j = 2 \cdots N$) are obtained instead by differentiating the left-hand side of the j^{th} discretized electron density gradient equation with respect to n_{j-1} , n_j and n_{j+1} (which are the only non-null derivatives with respect to the electron densities at the nodes):

$$\begin{aligned} \left[\mathbf{J}_{\mathbf{D}_{\mathbf{n}}, \mathbf{n}}^{(\mathbf{k})} \right]_{j,j} &= \frac{\partial}{\partial n_j} \left\{ \sqrt{n_j} \Lambda_{n,j} L_{j-\frac{1}{2},j+\frac{1}{2}} - \frac{\hbar^2}{6q} \left[\frac{1}{m_{n,j+\frac{1}{2}}^*} \frac{\sqrt{n_{j+1}} - \sqrt{n_j}}{L_{j,j+1}} - \frac{1}{m_{n,j-\frac{1}{2}}^*} \frac{\sqrt{n_j} - \sqrt{n_{j-1}}}{L_{j-1,j}} \right] \right\} \Bigg|_{\mathbf{x}=\mathbf{x}(\mathbf{k})} \\ &= \frac{1}{2\sqrt{n_j}} \Lambda_{n,j} L_{j-\frac{1}{2},j+\frac{1}{2}} + \frac{\hbar^2}{6q} \left[\frac{1}{m_{n,j+\frac{1}{2}}^*} \frac{1}{2\sqrt{n_j} L_{j,j+1}} + \frac{1}{m_{n,j-\frac{1}{2}}^*} \frac{1}{2\sqrt{n_j} L_{j-1,j}} \right] \\ \left[\mathbf{J}_{\mathbf{D}_{\mathbf{n}}, \mathbf{n}}^{(\mathbf{k})} \right]_{j,j-1} &= \frac{\partial}{\partial n_{j-1}} \left\{ \sqrt{n_j} \Lambda_{n,j} L_{j-\frac{1}{2},j+\frac{1}{2}} - \frac{\hbar^2}{6q} \left[\frac{1}{m_{n,j+\frac{1}{2}}^*} \frac{\sqrt{n_{j+1}} - \sqrt{n_j}}{L_{j,j+1}} - \frac{1}{m_{n,j-\frac{1}{2}}^*} \frac{\sqrt{n_j} - \sqrt{n_{j-1}}}{L_{j-1,j}} \right] \right\} \Bigg|_{\mathbf{x}=\mathbf{x}(\mathbf{k})} \\ &= -\frac{\hbar^2}{6q} \frac{1}{m_{n,j-\frac{1}{2}}^*} \frac{1}{2\sqrt{n_{j-1}} L_{j-1,j}} \\ \left[\mathbf{J}_{\mathbf{D}_{\mathbf{n}}, \mathbf{n}}^{(\mathbf{k})} \right]_{j,j+1} &= \frac{\partial}{\partial n_{j+1}} \left\{ \sqrt{n_j} \Lambda_{n,j} L_{j-\frac{1}{2},j+\frac{1}{2}} - \frac{\hbar^2}{6q} \left[\frac{1}{m_{n,j+\frac{1}{2}}^*} \frac{\sqrt{n_{j+1}} - \sqrt{n_j}}{L_{j,j+1}} - \frac{1}{m_{n,j-\frac{1}{2}}^*} \frac{\sqrt{n_j} - \sqrt{n_{j-1}}}{L_{j-1,j}} \right] \right\} \Bigg|_{\mathbf{x}=\mathbf{x}(\mathbf{k})} \\ &= -\frac{\hbar^2}{6q} \left[\frac{1}{m_{n,j+\frac{1}{2}}^*} \frac{1}{2\sqrt{n_{j+1}} L_{j,j+1}} \right] \end{aligned}$$

The last line of this matrix is obtained from differentiating the boundary condition for the electron density gradient equation at the right contact with respect to the components of the discretized electron density vector $\Lambda_{\mathbf{p}}$. It is then important to distinguish between the two types of contacts:

- if the right contact is of ohmic type then all the derivatives with respect to the electron densities at the nodes of Equation 11.17 are zero.
- if the right contact is of Schottky type then the only nonzero derivatives with respect to the electron densities at the nodes of Equation 11.19 are:

$$\begin{aligned} \left[\mathbf{J}_{\mathbf{D}_{\mathbf{n}}, \mathbf{n}}^{(\mathbf{k})} \right]_{N+1,N+1} &= \frac{\partial}{\partial n_{N+1}} \left\{ \sqrt{n_{N+1}} \Lambda_{n,N+1} L_{N+\frac{1}{2},N+1} + \frac{\hbar^2}{6q} \frac{1}{m_{n,N+\frac{1}{2}}^*} \frac{\sqrt{n_{N+1}} - \sqrt{n_N}}{L_{N,N+1}} \right\} \Bigg|_{\mathbf{x}=\mathbf{x}(\mathbf{k})} \\ &= \frac{1}{2\sqrt{n_{N+1}}} \Lambda_{n,N+1} L_{N+\frac{1}{2},N+1} + \frac{\hbar^2}{6q} \frac{1}{m_{n,N+\frac{1}{2}}^*} \frac{1}{2\sqrt{n_{N+1}} L_{N,N+1}} \end{aligned}$$

$$\begin{aligned} \left[\mathbf{J}_{\mathbf{D}_n, \mathbf{n}}^{(k)} \right]_{N+1, N} &= \frac{\partial}{\partial n_{N+1}} \left\{ \sqrt{n_{N+1}} \Lambda_{n, N+1} L_{N+\frac{1}{2}, N+1} + \frac{\hbar^2}{6 q m_{n, N+\frac{1}{2}}^*} \frac{1}{L_{N, N+1}} \frac{\sqrt{n_{N+1}} - \sqrt{n_N}}{L_{N, N+1}} \right\} \Bigg|_{x=x^{(k)}} \\ &= -\frac{\hbar^2}{6 q m_{n, N+\frac{1}{2}}^*} \frac{1}{2 \sqrt{n_N} L_{N, N+1}} \end{aligned}$$

Entries of $\mathbf{J}_{\mathbf{D}_n, \mathbf{n}}^{(k)}$

The matrix $\mathbf{J}_{\mathbf{D}_n, \mathbf{n}}^{(k)}$ is the block of the Jacobian containing the derivatives with respect to the electron quantum potential at the nodes of the left-hand sides of the equations resulting from discretizing the electron density gradient equation.

The first line of this matrix is obtained from differentiating the boundary condition for the electron density gradient equation at the left contact with respect to the components of the discretized electron quantum potential vector $\mathbf{\Lambda}_n$. It is then important to distinguish between the two types of contacts:

- if the left contact is of ohmic type then the only nonzero derivative with respect to the electron quantum potentials at the nodes of Equation 11.17 is:

$$\left[\mathbf{J}_{\mathbf{D}_n, \mathbf{n}}^{(k)} \right]_{1,1} = \frac{\partial}{\partial \Lambda_{n,1}} \{ \Lambda_{n,1} \} \Bigg|_{x=x^{(k)}} = 1$$

- if the left contact is of Schottky type then the only nonzero derivative with respect to the electron quantum potentials at the nodes of Equation 11.18 is:

$$\begin{aligned} \left[\mathbf{J}_{\mathbf{D}_n, \mathbf{n}}^{(k)} \right]_{1,1} &= \frac{\partial}{\partial \Lambda_{n,1}} \left\{ \sqrt{n_1} \Lambda_{n,1} L_{1, \frac{3}{2}} - \frac{\hbar^2}{6 q m_{n, \frac{3}{2}}^*} \frac{1}{L_{1,2}} \frac{\sqrt{n_2} - \sqrt{n_1}}{L_{1,2}} \right\} \Bigg|_{x=x^{(k)}} \\ &= \sqrt{n_1} L_{1, \frac{3}{2}} \end{aligned}$$

The inner lines of this matrix ($j = 2 \dots N$) are obtained instead by differentiating the left-hand side of the j^{th} discretized electron density gradient equation with respect to $\Lambda_{n,j}$ (which is the only non-null derivative with respect to the electron quantum potentials at the nodes):

$$\begin{aligned} \left[\mathbf{J}_{\mathbf{D}_n, \mathbf{n}}^{(k)} \right]_{j,j} &= \frac{\partial}{\partial \Lambda_{n,j}} \left\{ \sqrt{n_j} \Lambda_{n,j} L_{j-\frac{1}{2}, j+\frac{1}{2}} - \frac{\hbar^2}{6 q} \left[\frac{1}{m_{n, j+\frac{1}{2}}^*} \frac{\sqrt{n_{j+1}} - \sqrt{n_j}}{L_{j, j+1}} - \frac{1}{m_{n, j-\frac{1}{2}}^*} \frac{\sqrt{n_j} - \sqrt{n_{j-1}}}{L_{j-1, j}} \right] \right\} \Bigg|_{x=x^{(k)}} \\ &= \sqrt{n_j} L_{j-\frac{1}{2}, j+\frac{1}{2}} \end{aligned}$$

The last line of this matrix is obtained from differentiating the boundary condition for the electron density gradient equation at the right contact with respect to the components of the discretized electron quantum potential vector $\mathbf{\Lambda}_n$. It is then important to distinguish between the two types of contacts:

- if the right contact is of ohmic type then the only nonzero derivative with respect to the electron quantum potentials at the nodes of Equation 11.17 is:

$$\left[\mathbf{J}_{\mathbf{D}_n, \mathbf{n}}^{(k)} \right]_{N+1, N+1} = \frac{\partial}{\partial \Lambda_{n, N+1}} \{ \Lambda_{n, N+1} \} \Bigg|_{x=x^{(k)}} = 1$$

- if the right contact is of Schottky type then the only nonzero derivative with respect to the electron quantum potentials at the nodes of Equation 11.19 is:

$$\begin{aligned} \left[\mathbf{J}_{\mathbf{D}_n, \mathbf{n}}^{(k)} \right]_{N+1, N+1} &= \frac{\partial}{\partial \Lambda_{n, N+1}} \left\{ \sqrt{n_{N+1}} \Lambda_{n, N+1} L_{N+\frac{1}{2}, N+1} + \frac{\hbar^2}{6 q m_{n, N+\frac{1}{2}}^*} \frac{1}{L_{N, N+1}} \frac{\sqrt{n_{N+1}} - \sqrt{n_N}}{L_{N, N+1}} \right\} \Bigg|_{x=x^{(k)}} \\ &= \sqrt{n_{N+1}} L_{N+\frac{1}{2}, N+1} \end{aligned}$$

Entries of $\mathbf{J}_{\mathbf{D}_{\mathbf{p}},\mathbf{p}}^{(k)}$

The matrix $\mathbf{J}_{\mathbf{D}_{\mathbf{p}},\mathbf{p}}^{(k)}$ is the block of the Jacobian containing the derivatives with respect to the hole density at the nodes of the left-hand sides of the equations resulting from discretizing the hole density gradient equation.

The first line of this matrix is obtained from differentiating the boundary condition for the hole density gradient equation at the left contact with respect to the components of the discretized hole density vector \mathbf{p} . It is then important to distinguish between the two types of contacts:

- if the left contact is of ohmic type then all the derivatives with respect to the hole densities at the nodes of Equation 11.21 are zero;
- if the left contact is of Schottky type then the only nonzero derivatives with respect to the hole densities at the nodes of Equation 11.22 are:

$$\begin{aligned} \left[\mathbf{J}_{\mathbf{D}_{\mathbf{p}},\mathbf{p}}^{(k)} \right]_{1,1} &= \frac{\partial}{\partial p_1} \left\{ \sqrt{p_1} \Lambda_{p,1} L_{1,\frac{3}{2}} - \frac{\hbar^2}{6 q m_{p,\frac{3}{2}}^*} \frac{1}{L_{1,2}} \frac{\sqrt{p_2} - \sqrt{p_1}}{L_{1,2}} \right\} \Bigg|_{x=x^{(k)}} \\ &= \frac{1}{2 \sqrt{p_1}} \Lambda_{p,1} L_{1,\frac{3}{2}} + \frac{\hbar^2}{6 q m_{p,\frac{3}{2}}^*} \frac{1}{2 \sqrt{p_1} L_{1,2}} \\ \left[\mathbf{J}_{\mathbf{D}_{\mathbf{p}},\mathbf{p}}^{(k)} \right]_{1,2} &= \frac{\partial}{\partial p_2} \left\{ \sqrt{p_1} \Lambda_{p,1} L_{1,\frac{3}{2}} - \frac{\hbar^2}{6 q m_{p,\frac{3}{2}}^*} \frac{1}{L_{1,2}} \frac{\sqrt{p_2} - \sqrt{p_1}}{L_{1,2}} \right\} \Bigg|_{x=x^{(k)}} \\ &= -\frac{\hbar^2}{6 q m_{p,\frac{3}{2}}^*} \frac{1}{2 \sqrt{p_2} L_{1,2}} \end{aligned}$$

The inner lines of this matrix ($j = 2 \cdots N$) are obtained instead by differentiating the left-hand side of the j^{th} discretized hole density gradient equation with respect to p_{j-1} , p_j and p_{j+1} (which are the only non-null derivatives with respect to the hole densities at the nodes):

$$\begin{aligned} \left[\mathbf{J}_{\mathbf{D}_{\mathbf{p}},\mathbf{p}}^{(k)} \right]_{j,j} &= \frac{\partial}{\partial p_j} \left\{ \sqrt{p_j} \Lambda_{p,j} L_{j-\frac{1}{2},j+\frac{1}{2}} - \frac{\hbar^2}{6 q} \left[\frac{1}{m_{p,j+\frac{1}{2}}^*} \frac{\sqrt{p_{j+1}} - \sqrt{p_j}}{L_{j,j+1}} - \frac{1}{m_{p,j-\frac{1}{2}}^*} \frac{\sqrt{p_j} - \sqrt{p_{j-1}}}{L_{j-1,j}} \right] \right\} \Bigg|_{x=x^{(k)}} \\ &= \frac{1}{2 \sqrt{p_j}} \Lambda_{p,j} L_{j-\frac{1}{2},j+\frac{1}{2}} + \frac{\hbar^2}{6 q} \left[\frac{1}{m_{p,j+\frac{1}{2}}^*} \frac{1}{2 \sqrt{p_j} L_{j,j+1}} + \frac{1}{m_{p,j-\frac{1}{2}}^*} \frac{1}{2 \sqrt{p_j} L_{j-1,j}} \right] \\ \left[\mathbf{J}_{\mathbf{D}_{\mathbf{p}},\mathbf{p}}^{(k)} \right]_{j,j-1} &= \frac{\partial}{\partial p_{j-1}} \left\{ \sqrt{p_j} \Lambda_{p,j} L_{j-\frac{1}{2},j+\frac{1}{2}} - \frac{\hbar^2}{6 q} \left[\frac{1}{m_{p,j+\frac{1}{2}}^*} \frac{\sqrt{p_{j+1}} - \sqrt{p_j}}{L_{j,j+1}} - \frac{1}{m_{p,j-\frac{1}{2}}^*} \frac{\sqrt{p_j} - \sqrt{p_{j-1}}}{L_{j-1,j}} \right] \right\} \Bigg|_{x=x^{(k)}} \\ &= -\frac{\hbar^2}{6 q} \frac{1}{m_{p,j-\frac{1}{2}}^*} \frac{1}{2 \sqrt{p_{j-1}} L_{j-1,j}} \\ \left[\mathbf{J}_{\mathbf{D}_{\mathbf{p}},\mathbf{p}}^{(k)} \right]_{j,j+1} &= \frac{\partial}{\partial p_{j+1}} \left\{ \sqrt{p_j} \Lambda_{p,j} L_{j-\frac{1}{2},j+\frac{1}{2}} - \frac{\hbar^2}{6 q} \left[\frac{1}{m_{p,j+\frac{1}{2}}^*} \frac{\sqrt{p_{j+1}} - \sqrt{p_j}}{L_{j,j+1}} - \frac{1}{m_{p,j-\frac{1}{2}}^*} \frac{\sqrt{p_j} - \sqrt{p_{j-1}}}{L_{j-1,j}} \right] \right\} \Bigg|_{x=x^{(k)}} \\ &= -\frac{\hbar^2}{6 q} \frac{1}{m_{p,j+\frac{1}{2}}^*} \frac{1}{2 \sqrt{p_{j+1}} L_{j,j+1}} \end{aligned}$$

The last line of this matrix is obtained from differentiating the boundary condition for the hole density gradient equation at the right contact with respect to the components of the discretized hole density vector $\Lambda_{\mathbf{p}}$. It is then important to distinguish between the two types of contacts:

- if the right contact is of ohmic type then all the derivatives with respect to the hole densities at the nodes of Equation 11.21 are zero.
- if the right contact is of Schottky type then the only nonzero derivatives with respect to the hole densities at the nodes of Equation 11.23 are:

$$\begin{aligned}
\left[\mathbf{J}_{\mathbf{D}_p, \mathbf{p}}^{(k)} \right]_{N+1, N+1} &= \frac{\partial}{\partial p_{N+1}} \left\{ \sqrt{p_{N+1}} \Lambda_{p, N+1} L_{N+\frac{1}{2}, N+1} + \frac{\hbar^2}{6 q m_{p, N+\frac{1}{2}}^*} \frac{1}{L_{N, N+1}} \frac{\sqrt{p_{N+1}} - \sqrt{p_N}}{L_{N, N+1}} \right\} \Bigg|_{x=x^{(k)}} \\
&= \frac{1}{2 \sqrt{p_{N+1}}} \Lambda_{p, N+1} L_{N+\frac{1}{2}, N+1} + \frac{\hbar^2}{6 q m_{p, N+\frac{1}{2}}^*} \frac{1}{2 \sqrt{p_{N+1}} L_{N, N+1}} \\
\left[\mathbf{J}_{\mathbf{D}_p, \mathbf{p}}^{(k)} \right]_{N+1, N} &= \frac{\partial}{\partial p_{N+1}} \left\{ \sqrt{p_{N+1}} \Lambda_{p, N+1} L_{N+\frac{1}{2}, N+1} + \frac{\hbar^2}{6 q m_{p, N+\frac{1}{2}}^*} \frac{1}{L_{N, N+1}} \frac{\sqrt{p_{N+1}} - \sqrt{p_N}}{L_{N, N+1}} \right\} \Bigg|_{x=x^{(k)}} \\
&= -\frac{\hbar^2}{6 q m_{p, N+\frac{1}{2}}^*} \frac{1}{2 \sqrt{p_N} L_{N, N+1}}
\end{aligned}$$

Entries of $\mathbf{J}_{\mathbf{D}_p, \Lambda_p}^{(k)}$

The matrix $\mathbf{J}_{\mathbf{D}_p, \Lambda_p}^{(k)}$ is the block of the Jacobian containing the derivatives with respect to the hole quantum potential at the nodes of the left-hand sides of the equations resulting from discretizing the hole density gradient equation.

The first line of this matrix is obtained from differentiating the boundary condition for the hole density gradient equation at the left contact with respect to the components of the discretized hole quantum potential vector Λ_p . It is then important to distinguish between the two types of contacts:

- if the left contact is of ohmic type then the only nonzero derivative with respect to the hole quantum potentials at the nodes of Equation 11.21 is:

$$\left[\mathbf{J}_{\mathbf{D}_p, \Lambda_p}^{(k)} \right]_{1,1} = \frac{\partial}{\partial \Lambda_{p,1}} \{ \Lambda_{p,1} \} \Bigg|_{x=x^{(k)}} = 1$$

- if the left contact is of Schottky type then the only nonzero derivative with respect to the hole quantum potentials at the nodes of Equation 11.22 is:

$$\begin{aligned}
\left[\mathbf{J}_{\mathbf{D}_p, \Lambda_p}^{(k)} \right]_{1,1} &= \frac{\partial}{\partial \Lambda_{p,1}} \left\{ \sqrt{p_1} \Lambda_{p,1} L_{1, \frac{3}{2}} - \frac{\hbar^2}{6 q m_{p, \frac{3}{2}}^*} \frac{1}{L_{1,2}} \frac{\sqrt{p_2} - \sqrt{p_1}}{L_{1,2}} \right\} \Bigg|_{x=x^{(k)}} \\
&= \sqrt{p_1} L_{1, \frac{3}{2}}
\end{aligned}$$

The inner lines of this matrix ($j = 2 \cdots N$) are obtained instead by differentiating the left-hand side of the j^{th} discretized hole density gradient equation with respect to $\Lambda_{p,j}$ (which is the only non-null derivative with respect to the hole quantum potentials at the nodes):

$$\begin{aligned}
\left[\mathbf{J}_{\mathbf{D}_p, \Lambda_p}^{(k)} \right]_{j,j} &= \frac{\partial}{\partial \Lambda_{p,j}} \left\{ \sqrt{p_j} \Lambda_{p,j} L_{j-\frac{1}{2}, j+\frac{1}{2}} - \frac{\hbar^2}{6 q} \left[\frac{1}{m_{p, j+\frac{1}{2}}^*} \frac{\sqrt{p_{j+1}} - \sqrt{p_j}}{L_{j, j+1}} - \frac{1}{m_{p, j-\frac{1}{2}}^*} \frac{\sqrt{p_j} - \sqrt{p_{j-1}}}{L_{j-1, j}} \right] \right\} \Bigg|_{x=x^{(k)}} \\
&= \sqrt{p_j} L_{j-\frac{1}{2}, j+\frac{1}{2}}
\end{aligned}$$

The last line of this matrix is obtained from differentiating the boundary condition for the hole density gradient equation at the right contact with respect to the components of the discretized hole quantum potential vector Λ_p . It is then important to distinguish between the two types of contacts:

- if the right contact is of ohmic type then the only nonzero derivative with respect to the hole quantum potentials at the nodes of Equation 11.21 is:

$$\left[\mathbf{J}_{\mathbf{D}_p, \Lambda_p}^{(k)} \right]_{N+1, N+1} = \frac{\partial}{\partial \Lambda_{p, N+1}} \{ \Lambda_{p, N+1} \} \Big|_{x=x^{(k)}} = 1$$

- if the right contact is of Schottky type then the only nonzero derivative with respect to the hole quantum potentials at the nodes of Equation 11.23 is:

$$\begin{aligned} \left[\mathbf{J}_{\mathbf{D}_p, \Lambda_p}^{(k)} \right]_{N+1, N+1} &= \frac{\partial}{\partial p_{N+1}} \left\{ \sqrt{p_{N+1}} \Lambda_{p, N+1} L_{N+\frac{1}{2}, N+1} + \frac{\hbar^2}{6 q m_{p, N+\frac{1}{2}}^*} \frac{\sqrt{p_{N+1}} - \sqrt{p_N}}{L_{N, N+1}} \right\} \Big|_{x=x^{(k)}} \\ &= \sqrt{p_{N+1}} L_{N+\frac{1}{2}, N+1} \end{aligned}$$

11.4 Initial guess

In order to be able to solve the density gradient problem for a given device, a reasonable initial equilibrium guess needs to be found for the solution.

The problem of determining a good initial equilibrium guess for this model is however extremely complex, as ideally such an initial guess should include also some quantum effects already in order to have continuous electron and hole densities in space.

Therefore, in the following work the **semiclassical Boltzmann distribution** will be considered together with **Poisson's equation** to determine as an initial guess for the solution of the problem. This initial guess isn't the most efficient one in the presence of heterostructures (which in a Poisson-Boltzmann model make the electron and hole density discontinuous) but convergence can still be achieved by damping the Newton solver.

The main differential equation to be solved is Poisson's equation at equilibrium (under the assumption of full ionization of the dopant atoms):

$$\frac{\partial}{\partial z} \left\{ \epsilon \frac{\partial \phi}{\partial z} \right\} = -q (p - n + N_d - N_a) \quad (11.27)$$

This equation can be discretized exactly as was done in section 10.1, obtaining the algebraic equation:

$$\epsilon_{j+\frac{1}{2}} \frac{\phi_{j+1} - \phi_j}{L_{j, j+1}} - \epsilon_{j-\frac{1}{2}} \frac{\phi_j - \phi_{j-1}}{L_{j-1, j}} + q (p_j - n_j + N_{d, j} - N_{a, j}) L_{j-\frac{1}{2}, j+\frac{1}{2}} = 0 \quad (11.28)$$

with boundary conditions for ohmic contacts:

$$\phi_1 - \phi_{0,1} - V_{\text{left}} = 0 \quad \phi_{N+1} - \phi_{0, N+1} - V_{\text{right}} = 0 \quad (11.29)$$

or with boundary conditions for Schottky contacts:

$$\phi_1 - \frac{-E_{f, \text{eq}}^{(\text{left})} + qV^{(\text{left})} - q\phi_b^{(\text{left})} + \Delta E_c^{(\text{left})}}{q} = 0 \quad (11.30)$$

$$\phi_{N+1} - \frac{-E_{f, \text{eq}}^{(\text{right})} + qV^{(\text{right})} - q\phi_b^{(\text{right})} + \Delta E_c^{(\text{right})}}{q} = 0 \quad (11.31)$$

The electron and hole densities are instead found now by imposing the classical equilibrium Boltzmann distributions evaluated at the nodes of the mesh:

$$n_j = N_{c, j} \exp \left\{ \frac{q\phi_j - \Delta E_{c, j} + E_f}{k_B T} \right\} \quad p_j = N_{v, j} \exp \left\{ \frac{-q\phi_j - E_{g, j}(0) + \Delta E_{v, j} - E_f}{k_B T} \right\}$$

Substituting the electron and hole densities into the discretized Poisson's equation the following result is found:

$$\epsilon_{j+\frac{1}{2}} \frac{\phi_{j+1} - \phi_j}{L_{j, j+1}} - \epsilon_{j-\frac{1}{2}} \frac{\phi_j - \phi_{j-1}}{L_{j-1, j}} + q \left(N_{v, j} \exp \left\{ \frac{-q\phi_j - E_{g, j}(0) + \Delta E_{v, j} - E_f}{k_B T} \right\} - \right.$$

$$N_{c,j} \exp \left\{ \frac{q\phi_j - \Delta E_{c,j} + E_f}{k_B T} \right\} + N_{d,j} - N_{a,j} \Big) L_{j-\frac{1}{2},j+\frac{1}{2}} = 0$$

Taking the Fermi level as a reference value for defining the energies, the problem can then be solved by applying the generalized Newton's method.

Since the only unknown is the electrostatic potential ϕ , the only jacobian of the previous expression that needs to be computed is the one with respect to it.

When computing the inner lines of the jacobian of the problem, the only nonzero partial derivatives are those taken with respect to ϕ_j , ϕ_{j-1} and ϕ_{j+1} , which can be evaluated as:

$$\begin{aligned} [\mathbf{J}_{\mathbf{P},\phi}^{(k)}]_{j,j-1} &= \frac{\partial}{\partial \phi_{j-1}} \left\{ \epsilon_{j+\frac{1}{2}} \frac{\phi_{j+1} - \phi_j}{L_{j,j+1}} - \epsilon_{j-\frac{1}{2}} \frac{\phi_j - \phi_{j-1}}{L_{j-1,j}} + q \left(N_{v,j} \exp \left\{ \frac{-q\phi_j - E_{g,j}(0) + \Delta E_{v,j} - E_f}{k_B T} \right\} \right. \right. \\ &\quad \left. \left. - N_{c,j} \exp \left\{ \frac{q\phi_j - \Delta E_{c,j} + E_f}{k_B T} \right\} + N_{d,j} - N_{a,j} \right) L_{j-\frac{1}{2},j+\frac{1}{2}} \right\} \Big|_{\mathbf{x}=\mathbf{x}^{(k)}} \\ &= + \frac{\epsilon_{j-\frac{1}{2}}}{L_{j-1,j}} \end{aligned}$$

$$\begin{aligned} [\mathbf{J}_{\mathbf{P},\phi}^{(k)}]_{j,j} &= \frac{\partial}{\partial \phi_j} \left\{ \epsilon_{j+\frac{1}{2}} \frac{\phi_{j+1} - \phi_j}{L_{j,j+1}} - \epsilon_{j-\frac{1}{2}} \frac{\phi_j - \phi_{j-1}}{L_{j-1,j}} + q \left(N_{v,j} \exp \left\{ \frac{-q\phi_j - E_{g,j}(0) + \Delta E_{v,j} - E_f}{k_B T} \right\} \right. \right. \\ &\quad \left. \left. - N_{c,j} \exp \left\{ \frac{q\phi_j - \Delta E_{c,j} + E_f}{k_B T} \right\} + N_{d,j} - N_{a,j} \right) L_{j-\frac{1}{2},j+\frac{1}{2}} \right\} \Big|_{\mathbf{x}=\mathbf{x}^{(k)}} \\ &= - \frac{\epsilon_{j+\frac{1}{2}}}{L_{j,j+1}} - \frac{\epsilon_{j-\frac{1}{2}}}{L_{j-1,j}} + \frac{q}{k_B T} \left(-N_{v,j} \exp \left\{ \frac{-q\phi_j - E_{g,j}(0) + \Delta E_{v,j} - E_f}{k_B T} \right\} + \right. \\ &\quad \left. - N_{c,j} \exp \left\{ \frac{q\phi_j - \Delta E_{c,j} + E_f}{k_B T} \right\} \right) L_{j-\frac{1}{2},j+\frac{1}{2}} \end{aligned}$$

$$\begin{aligned} [\mathbf{J}_{\mathbf{P},\phi}^{(k)}]_{j,j+1} &= \frac{\partial}{\partial \phi_{j+1}} \left\{ \epsilon_{j+\frac{1}{2}} \frac{\phi_{j+1} - \phi_j}{L_{j,j+1}} - \epsilon_{j-\frac{1}{2}} \frac{\phi_j - \phi_{j-1}}{L_{j-1,j}} + q \left(N_{v,j} \exp \left\{ \frac{-q\phi_j - E_{g,j}(0) + \Delta E_{v,j} - E_f}{k_B T} \right\} \right. \right. \\ &\quad \left. \left. - N_{c,j} \exp \left\{ \frac{q\phi_j - \Delta E_{c,j} + E_f}{k_B T} \right\} + N_{d,j} - N_{a,j} \right) L_{j-\frac{1}{2},j+\frac{1}{2}} \right\} \Big|_{\mathbf{x}=\mathbf{x}^{(k)}} \\ &= + \frac{\epsilon_{j+\frac{1}{2}}}{L_{j,j+1}} \end{aligned}$$

The first and the last line of the jacobian matrix for the problem instead only have nonzero terms:

$$[\mathbf{J}_{\mathbf{P},\phi}^{(k)}]_{1,1} = 1 \qquad [\mathbf{J}_{\mathbf{P},\phi}^{(k)}]_{N+1,N+1} = 1$$

independently of whether the boundaries are ohmic or of Schottky type.

A good enough initial guess for applying the generalized Newton's method is the **neutrality condition** applied to the semiconductor together with the hypothesis of **classical Boltzmann statistics**.

A numerically stable way of determining the neutrality electron and hole densities is to apply the piecewise model that was already derived in subsection 9.2.2:

$$\begin{cases} n_0 = \frac{[N_d - N_a] + \sqrt{[N_d - N_a]^2 + 4 n_i^2}}{2} & p_0 = \frac{n_i^2}{n_0} & \text{if } [N_d - N_a] > 0 \\ p_0 = \frac{[N_d - N_a] + \sqrt{[N_d - N_a]^2 + 4 n_i^2}}{2} & n_0 = \frac{n_i^2}{p_0} & \text{if } [N_d - N_a] < 0 \end{cases} \quad (11.32)$$

The electrostatic potential is then determined by inverting the classical Boltzmann statistics:

$$n_j = N_{c,j} \exp \left\{ \frac{q\phi_j - \Delta E_{c,j} + E_f}{k_B T} \right\} \quad \Rightarrow \quad \phi_j = \frac{1}{q} \left(k_B T \ln \left\{ \frac{n_j}{N_{c,j}} \right\} + \Delta E_{c,j} - E_f \right)$$

The solution is therefore refined according to the following order:

1. Neutrality condition + semiclassical Boltzmann distribution at equilibrium
 2. Poisson equation + semiclassical Boltzmann distribution at equilibrium
 3. Poisson equation + continuity equations + density gradient equations at equilibrium
- in order to ensure good convergence of the method.

11.5 MATLAB[®] Implementation

The previously described algorithm was implemented and tested on MATLAB[®] R2018a.



The implementation of the solution algorithm described in this chapter can be found in the MATLAB[®] LiveScript **QDD_Opt.mlx** for the cases of HEMT and PHEMT structures (which will be defined in the next chapters).

Chapter 12

Materials and Parameters

In order to be able to simulate HEMT and PHEMT structures realized with III-V semiconductors it is first necessary to summarize their main physical properties and parameters.

12.1 Materials

For the sake of simplicity, only **AlGaAs** (aluminum gallium arsenide) ternary alloys will be considered in this document and for the examples of device structures that will be proposed later on.

This alloy is obtained by combining together AlAs (aluminum arsenide) and GaAs (gallium arsenide) with arbitrary proportions. The choice of the molar fraction of each of these compound semiconductors within the alloy determines the properties of the material that is obtained.

It is convenient to first define the molar fraction x as the fraction of aluminum in the alloy, therefore considering a chemical formula of the kind: $\text{Al}_x\text{Ga}_{1-x}\text{As}$.

AlGaAs alloys are characterized by a **zinc blende crystal structure**.

Zinc blende crystals are the result of interpenetrating two face-centered-cubic lattices:

- one that consists of only atoms belonging to group III of the periodic table (Ga, Al)
- one that consists of only atoms belonging to group V of the periodic table (As)

with a shift $\Delta\mathbf{r}$ between the two, as is shown in Figure 12.1.

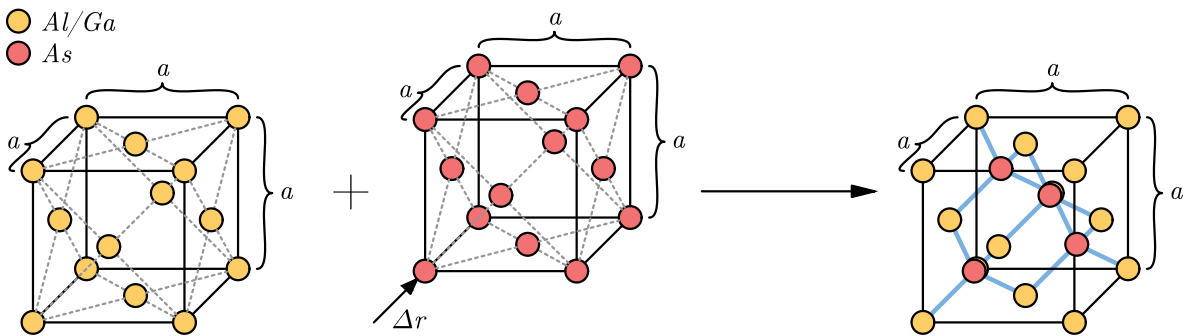


Figure 12.1: Zinc blende crystal structure for AlGaAs.

In particular, the two face-centered cubic lattices that are interpenetrated have the same lattice constant a so the resulting zinc blende crystal has periodic structure with periodicity a and unit cell of size $a \times a \times a$. Moreover, the offset between the two compenetrated face-centered cubic lattices is typically in the direction of the diagonal and has modulus equal to $1/4$ of the diagonal lengths, i.e.:

$$\Delta\mathbf{r} = \frac{a}{4} (\hat{\mathbf{x}} + \hat{\mathbf{y}} + \hat{\mathbf{z}})$$

where $\hat{\mathbf{x}}$, $\hat{\mathbf{y}}$, $\hat{\mathbf{z}}$ are the (unit) versors identifying the three cartesian axes.

Observing the energy-gap diagram that is reported in Figure 12.2 it is possible to notice that AlGaAs is extremely well suited for creating heterostructures, since the lattice constants of all the possible alloys in this family are extremely similar (hence allowing for the creation of interfaces with a limited number of defects).

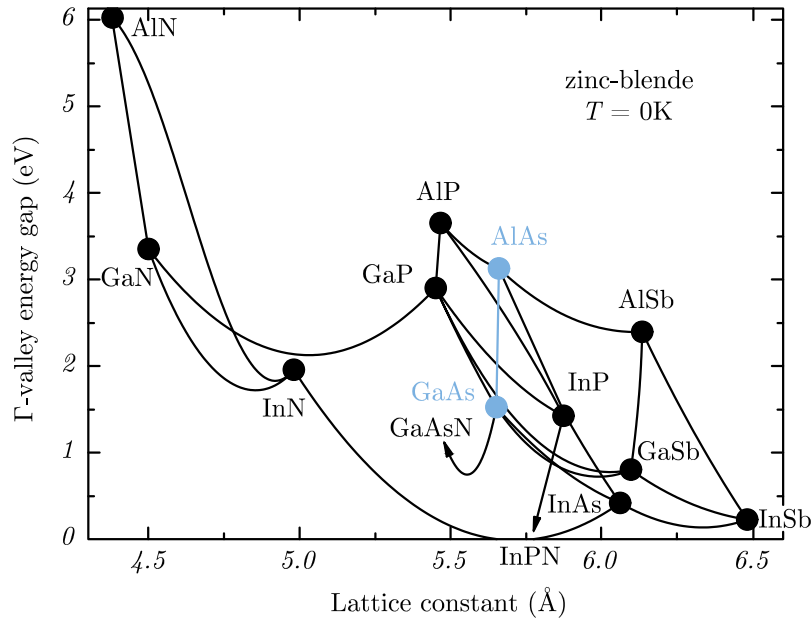


Figure 12.2: Semiconductor alloys (AlGaAs is reported in cyan).

One last important property of $\text{Al}_x\text{Ga}_{1-x}\text{As}$ alloys is that there is a critical molar fraction x_c of aluminum such that:

- the alloy is direct bandgap for $x < x_c$
- the alloy is indirect bandgap for $x > x_c$

The value of this critical molar fraction is $x_c \approx 0.45$.

Because of this important change in the material properties of the alloy around $x_c \approx 0.45$ the models for most of the material parameters will be defined in a piecewise manner, separating the intervals $x \in [0, 0.45)$ and $x \in (0.45, 1]$.

Most of the models for the material parameters that will be reported next are resulting from multiband $k \cdot p$ analyses. [27]. Some are instead the results of experimental measurements on the materials.

12.2 Material Parameters

In this section the main approximate models for the material parameters that are needed to implement a density gradient solver for AlGaAs devices will be introduced.

12.2.1 Electromagnetic Parameters

The main electromagnetic parameter is the relative dielectric constant ϵ_r .

In this treatment, a Vegard law (i.e. a linear interpolation between the components of the alloy) will be assumed to be valid for the relative dielectric constant of $\text{Al}_x\text{Ga}_{1-x}\text{As}$, hence:

$$\epsilon_r \approx \epsilon_r^{\text{AlAs}} x + \epsilon_r^{\text{GaAs}} (1 - x)$$

where:

- $\epsilon_r^{\text{AlAs}} \approx 10.06$ is the relative dielectric constant of AlAs [28]
- $\epsilon_r^{\text{GaAs}} \approx 12.90$ is the relative dielectric constant of GaAs [28]

12.2.2 Band Structure Parameters

In order to express the model for the bandgap of AlGaAs in a simpler form it is useful to first define:

- the bandgap E_g^{GaAs} of gallium arsenide as: [27]

$$E_g^{\text{GaAs}} = E_{g0}^{\text{GaAs}} - \alpha^{\text{GaAs}} \frac{T^2}{T + \beta^{\text{GaAs}}}$$

where T is the temperature and E_{g0}^{GaAs} , α^{GaAs} , β^{GaAs} are constants for gallium arsenide with values:

$$\begin{aligned} E_{g0}^{\text{GaAs}} &\approx 1.519 \text{ eV} \\ \alpha^{\text{GaAs}} &\approx 0.5405 \times 10^{-3} \text{ K}^{-1} \\ \beta^{\text{GaAs}} &\approx 204 \text{ K} \end{aligned}$$

- the bandgap E_g^{AlAs} of aluminum arsenide as: [27]

$$E_g^{\text{AlAs}} = E_{g0}^{\text{AlAs}} - \alpha^{\text{AlAs}} \frac{T^2}{T + \beta^{\text{AlAs}}}$$

where T is the temperature and E_{g0}^{AlAs} , α^{AlAs} , β^{AlAs} are constants for aluminum arsenide with values:

$$\begin{aligned} E_{g0}^{\text{AlAs}} &\approx 3.099 \text{ eV} \\ \alpha^{\text{AlAs}} &\approx 0.885 \times 10^{-3} \text{ K}^{-1} \\ \beta^{\text{AlAs}} &\approx 530 \text{ K} \end{aligned}$$

The **bandgap** of an $\text{Al}_x\text{Ga}_{1-x}\text{As}$ alloy can then be determined as: [27]

$$E_g \approx E_g^{\text{GaAs}} + (E_g^{\text{AlAs}} - E_g^{\text{GaAs}}) x - (\gamma_1^{\text{AlGaAs}} + \gamma_2^{\text{AlGaAs}} x) x (1 - x)$$

where γ_1^{AlGaAs} and γ_2^{AlGaAs} are constants with values:

$$\begin{aligned} \gamma_1^{\text{AlGaAs}} &\approx -0.127 \text{ eV} \\ \gamma_2^{\text{AlGaAs}} &\approx 1.310 \text{ eV} \end{aligned}$$

The **valence band offset** for the material is assumed to satisfy the Vegard law: [27]

$$\Delta E_v \approx \Delta E_v^{\text{GaAs}} + \left(\Delta E_v^{\text{AlAs}} - \Delta E_v^{\text{GaAs}} \right) x$$

where:

- $\Delta E_v^{\text{GaAs}} \approx -0.80 \text{ eV}$ is the valence band offset for gallium arsenide
- $\Delta E_v^{\text{AlAs}} \approx -1.33 \text{ eV}$ is the valence band offset for aluminum arsenide

The **conduction band offset** is then found from the valence band offset through the relationship:

$$\Delta E_c = \Delta E_v + E_g$$

It is to be noticed that these band offsets are still to be shifted so as to make them zero at the reference electrode (as only their variations actually matter), which will be taken to be the left electrode.

The **electron affinity** for AlGaAs is instead found from the one of GaSb (gallium antimonide, which is adopted as a reference material in [27]) by making use of the conduction band offset information as:

$$q\chi^{\text{AlGaAs}} = q\chi^{\text{GaSb}} - \Delta E_c^{\text{AlGaAs}} + \Delta E_c^{\text{GaSb}}$$

where:

- $q\chi^{\text{GaSb}} \approx 4.06 \text{ eV}$ is the electron affinity of gallium antimonide; [27]

- $\Delta E_c^{\text{GaSb}} = \Delta E_v^{\text{GaSb}} + E_g^{\text{GaSb}}$ is the conduction band offset of gallium antimonide; [27]

To determine the bandgap E_g^{GaSb} of gallium antimonide the following approximate model can be used: [27]

$$E_g^{\text{GaSb}} = E_{g0}^{\text{GaSb}} - \alpha^{\text{GaSb}} \frac{T^2}{T + \beta^{\text{GaSb}}}$$

where T is the temperature and E_{g0}^{GaSb} , α^{GaSb} , β^{GaSb} are constants for gallium antimonide with values: [27]

$$\begin{aligned} E_{g0}^{\text{GaSb}} &\approx 0.812 \text{ eV} \\ \alpha^{\text{GaSb}} &\approx 0.417 \times 10^{-3} \text{ K}^{-1} \\ \beta^{\text{GaSb}} &\approx 140 \text{ K} \end{aligned}$$

The valence band offset ΔE_v^{GaSb} of gallium antimonide is instead given by $\Delta E_v^{\text{GaSb}} \approx -0.03 \text{ eV}$ [27]

The normalized **effective mass for the density of states in conduction band** can be modeled instead as: [27]

$$\frac{m_n^*}{m_0} \approx \frac{1}{x \frac{m_0}{m_n^{\text{AlAs}}} + (1-x) \frac{m_0}{m_n^{\text{GaAs}}}}$$

where:

- $\frac{m_n^{\text{AlAs}}}{m_0} \approx 0.15$ is the normalized effective mass for the density of states in conduction band for aluminum arsenide
- $\frac{m_n^{\text{GaAs}}}{m_0} \approx 0.067$ is the normalized effective mass for the density of states in conduction band for gallium arsenide

The normalized **effective mass for the density of states in the light hole band** can instead be expressed as: [27]

$$\frac{m_{p,\text{LH}}^*}{m_0} \approx \frac{1}{\frac{m_0}{m_{p,\text{LH}}^{\text{GaAs}}} + \left(\frac{m_0}{m_{p,\text{LH}}^{\text{AlAs}}} - \frac{m_0}{m_{p,\text{LH}}^{\text{GaAs}}} \right) x}$$

where:

- $\frac{m_{p,\text{LH}}^{\text{AlAs}}}{m_0} \approx \frac{1}{\gamma_1^{\text{AlAs}} + 2\gamma_2^{\text{AlAs}}}$ is the normalized effective mass for the density of states in the light hole band for aluminum arsenide
- $\frac{m_{p,\text{LH}}^{\text{GaAs}}}{m_0} \approx \frac{1}{\gamma_1^{\text{GaAs}} + 2\gamma_2^{\text{GaAs}}}$ is the normalized effective mass for the density of states in the light hole band for gallium arsenide

with $\gamma_1^{\text{AlAs}} \approx 3.76$ and $\gamma_2^{\text{AlAs}} \approx 0.82$ constant parameters for aluminum arsenide and $\gamma_1^{\text{GaAs}} \approx 6.98$ and $\gamma_2^{\text{GaAs}} \approx 2.06$ constant parameters for gallium arsenide.

Similarly, the normalized **effective mass for the density of states in the heavy hole band** can be expressed as: [27]

$$\frac{m_{p,\text{HH}}^*}{m_0} \approx \frac{1}{\frac{m_0}{m_{p,\text{HH}}^{\text{GaAs}}} + \left(\frac{m_0}{m_{p,\text{HH}}^{\text{AlAs}}} - \frac{m_0}{m_{p,\text{HH}}^{\text{GaAs}}} \right) x}$$

where:

- $\frac{m_{p,\text{HH}}^{\text{AlAs}}}{m_0} \approx \frac{1}{\gamma_1^{\text{AlAs}} - 2\gamma_2^{\text{AlAs}}}$ is the normalized effective mass for the density of states in the heavy hole band for aluminum arsenide

- $\frac{m_{p,HH}^{*GaAs}}{m_0} \approx \frac{1}{\gamma_1^{GaAs} - 2\gamma_2^{GaAs}}$ is the normalized effective mass for the density of states in the heavy hole band for gallium arsenide

with γ_1^{AlAs} , γ_2^{AlAs} , γ_1^{GaAs} and γ_2^{GaAs} are constant parameters with the same values as those reported above.

The normalized **effective mass for the density of states in valence band** can finally be found as an average of those for light and heavy holes: [27]

$$\frac{m_p^*}{m_0} \approx \left(\left[\frac{m_{p,LH}^*}{m_0} \right]^{3/2} + \left[\frac{m_{p,HH}^*}{m_0} \right]^{3/2} \right)^{2/3}$$

12.2.3 Transport Parameters

Mobility in a semiconductor is quite strongly dependent on its doping level, as a too high dopant concentration tends to degrade the transport properties of the semiconductor.

The models and values that follow have been obtained from the Ioffe website [28] and are the results of **Hall measurements** for the mobility on samples with relatively **low dopant concentrations** (of the order of $1 \times 10^{15} \div 1 \times 10^{16} \text{ cm}^{-3}$).

The **electron mobility** is defined in a piecewise Taylor series way over the molar fraction intervals $[0, 0.45)$ and $(0.45, 1]$ since AlGaAs is direct bandgap for $x < 0.45$ and is indirect bandgap for $x > 0.45$:

$$\mu_n \approx \begin{cases} \eta_1 + \eta_2 x + \eta_3 x^2 & \text{if } x < 0.45 \\ \eta_4 + \eta_5 x + \eta_6 x^2 & \text{if } x > 0.45 \end{cases}$$

where $\eta_1, \eta_2, \eta_3, \eta_4, \eta_5, \eta_6$ are material parameters for $\text{Al}_x\text{Ga}_{1-x}\text{As}$ and have values: [28]

$$\begin{aligned} \eta_1 &\approx 0.8 \text{ m}^2\text{V}^{-1}\text{s}^{-1} & \eta_2 &\approx -2.2 \text{ m}^2\text{V}^{-1}\text{s}^{-1} & \eta_3 &\approx 1 \text{ m}^2\text{V}^{-1}\text{s}^{-1} \\ \eta_4 &\approx -0.0225 \text{ m}^2\text{V}^{-1}\text{s}^{-1} & \eta_5 &\approx 0.116 \text{ m}^2\text{V}^{-1}\text{s}^{-1} & \eta_6 &\approx 0.072 \text{ m}^2\text{V}^{-1}\text{s}^{-1} \end{aligned}$$

The **hole mobility** is instead defined in a Taylor series way as:

$$\mu_p \approx \eta_7 + \eta_8 x + \eta_9 x^2$$

where η_7, η_8 and η_9 are material parameters for $\text{Al}_x\text{Ga}_{1-x}\text{As}$ and have values: [28]

$$\eta_7 \approx 0.04 \text{ m}^2\text{V}^{-1}\text{s}^{-1} \quad \eta_8 \approx -0.07 \text{ m}^2\text{V}^{-1}\text{s}^{-1} \quad \eta_9 \approx 0.045 \text{ m}^2\text{V}^{-1}\text{s}^{-1}$$

12.2.4 SRH Recombination Parameters

Finally, in order to be able to simulate SRH generation/recombination processes (i.e. thermal trap-assisted generation/recombination processes) it is useful to also define the position of the trap level within the semiconductor and the carrier lifetimes due to SRH generation/recombination.

The **trap level** is assumed to coincide with the intrinsic Fermi level (therefore being approximately in the middle of the gap), hence setting:

$$E_t - E_{fi} \approx 0$$

The **lifetime for electrons in SRH generation/recombination processes** for AlGaAs is assumed to be:

$$\tau_n^{SRH} \approx 250 \text{ ns}$$

while the **lifetime for holes in SRH generation/recombination processes** is instead assumed to be:

$$\tau_p^{SRH} \approx 5 \text{ ns}$$

The values of these parameters are extremely dependent on the defects and/or impurities that act as traps and have been therefore selected arbitrarily (even though their order of magnitude is selected to be of the correct time scale, i.e. of the order of ns).

Part IV

HEMT and QW-HEMT Simulations

Chapter 13

Single Heterostructure HEMT

Single-heterostructure **High electron mobility transistors** (commonly called high electron mobility transistors only) are heterostructure-based field effect transistors (FET) that are widely used for high-speed electronics.

These devices used in cellphones, satellite receivers, radar equipment and, more in general, in most communication-oriented circuits for which operation within the microwave and/or millimeter wave frequency range is required.

Among the multiple technologies that can be used to realize HEMTs, some of the most widely known ones are:

- GaAs: the most widely used one technology for HEMTs with average performance and with reasonable cost
- GaN: the best technology for obtaining high powers at relatively good frequency performance
- InP: the best technology for reaching extremely high frequencies of operation (demonstrations have been presented that have cutoff frequencies beyond 1 THz)

In the following work, the GaAs technology will be considered as it is the most common and widely used in the field of high-speed electronics. In particular, the technology that will be considered is that of AlGaAs on GaAs (in which AlGaAs is used for the supply layer).

13.1 Device Structure

The structure of a high electron mobility transistor (HEMT) is shown in Figure 13.1.

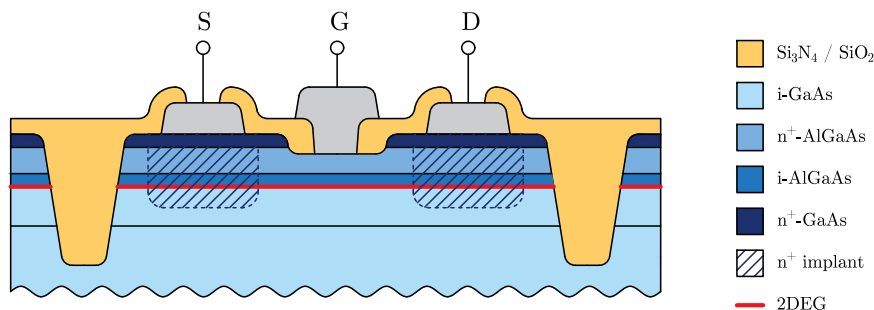


Figure 13.1: AlGaAs HEMT structure.

These devices are grown on top of a **semi-insulating** (i.e. intrinsic) **gallium arsenide substrate**. This substrate only acts as mechanical support for the device and plays no role in its operation.

Then, an **intrinsic** (semi-insulating) **gallium arsenide** layer is grown by means of epitaxy on top of the substrate. This allows to obtain an extremely high-quality layer in which the carrier motion will take place. This layer is often known as **well layer**.

An **intrinsic aluminum gallium arsenide** layer is then epitaxially grown on top of the previous structure so as to introduce a discontinuity in the conduction band between AlGaAs and GaAs. This allows the creation of a quantum well (which will be more evident when observing the band diagram of this structure) in which the carriers self-confine. The resulting quantum well will be positioned approximately at the interface with the previous layer.

An **n-doped aluminum gallium arsenide** layer is then grown through epitaxy. This layer, which is known as **supply layer**, acts as an electron donor; in a correctly working device this layer is fully depleted and its carriers are transferred into the quantum well at the interface between intrinsic GaAs and intrinsic AlGaAs.

Finally, a **metal gate** is added on top of the stack of layers. The main function of the metallic gate is to act as Schottky contact, therefore fixing the electrostatic potential at the top of the supply layer while maintaining the supply layer depleted.

The **drain and source regions** are instead realized to behave as ohmic contact. They are therefore strongly doped so as to minimize resistance and obtain strong enough tunnelling to guarantee the correct ohmic behavior that is wanted. An **n-doped gallium arsenide** layer is added at the source and drain regions before creating the metal contacts in order to better tailor the band diagram in those regions and ensure that these regions conduct properly.

13.2 Operating Principle

Since the transistor effect takes place below the gate it is useful to analyze a vertical cross-section below it to understand how the device works. The 1-dimensional structure to be considered is therefore the one that is shown in Figure 13.2.

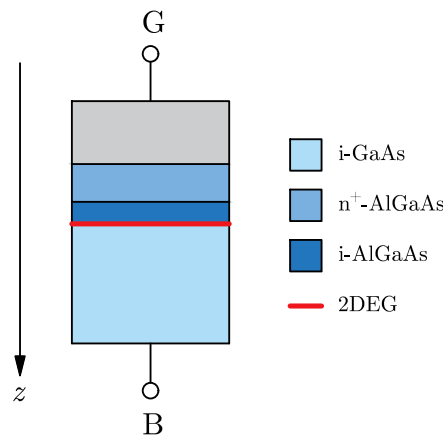


Figure 13.2: 1-dimensional AlGaAs HEMT structure.

Since the bulk of the device can be assumed to be at equilibrium and in neutrality conditions, it is possible to treat the bottom of the device by means of an ohmic contact boundary condition.

The upper contact will instead in general be a reverse-biased Schottky (i.e. rectifying) contact. This is extremely important to guarantee that little to no vertical current flow can take place within the layered structure.

The band diagram of a structure similar to the one represented in Figure 13.2 behaves similarly to the one that is shown in Figure 13.3.

The bias applied between the gate (G) and the bulk (B) of the device is affecting the relative positions of the Fermi level E_{fm} within the metal and of the Fermi level E_{fs} within the bulk of the substrate, according to the relationship:

$$E_{fm} - E_{fs} = -qV_{GB}$$

The presence of an heterojunction between the supply and the well layer allows to obtain a quasi-triangular quantum well at the interface between AlGaAs and GaAs (it is shown in red in Figure 13.3); the barrier introduced by the Schottky contact allows instead to “lift” the left part of the band diagram, therefore

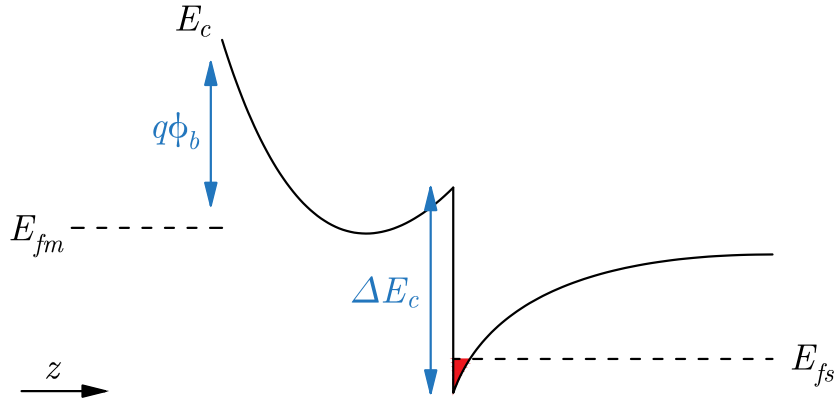


Figure 13.3: 1-dimensional AlGaAs HEMT band diagram.

allowing for most of the electron charge that originated within the supply layer to “slide” within the quantum well, where it is confined.

By controlling the applied voltage V_{GB} between the gate (G) and the bulk (B) of the device it is then also possible to control the depth of penetration $E_{fs} - E_c$ of the conduction band E_c below the Fermi level E_{fs} at the quantum well. Since the electron charge within the quantum well is related to the energy difference $E_{fs} - E_c$ by the classical Fermi or Boltzmann distributions, this means that the applied voltage V_{GB} is able to **modulate the channel charge** (i.e. the charge within the quantum well).

More precisely:

- increasing the voltage V_{GB} causes the depth of penetration $E_{fs} - E_c$ of the conduction band below the Fermi level of the semiconductor to increase, therefore leading to a larger channel charge
- decreasing the voltage V_{GB} causes the depth of penetration $E_{fs} - E_c$ of the conduction band below the Fermi level of the semiconductor to decrease, therefore leading to a smaller channel charge

It is then clear that this structure can be effectively used to create a field-effect transistor, as it is able to provide the required charge modulation capabilities.

In order for this structure to be used to obtain an FET it is however fundamental to ensure that the quantum well be the only possible conductive channel. Since the supply layer has been doped (as is shown in Figure 13.2) then only possible way to block conduction in that layer is to ensure that it is fully depleted in all possible bias conditions in which the device might have to operate.

If this were not the case, a second conductive channel would form within the supply layer. This phenomenon is known as the formation of a **parasitic MESFET**, since this channel would be modulated by the applied voltage through the modulation of the depletion region width exactly as happens in MESFET devices. This condition is represented in the band diagram of Figure 13.4.

This condition has to be avoided as MESFET have performance that is much worse than the one of high electron mobility transistors.

The condition that must be satisfied by the band diagram to avoid the formation of a parasitic MESFET is that the distance between the conduction band and the Fermi level within the semiconductor be large enough within the supply layer, i.e. that:

$$E_c \gg E_{fs}$$

within the supply layer.

This condition gives rise to a limitation to the maximum voltage V_{GB} that can be applied to this device. There is therefore a limit voltage $V_{GB,lim}$ beyond which the parasitic MESFET is formed. Correct operation of the device can then be ensured by operating with gate voltages below such limit (i.e. with $V_{GB} < V_{GB,lim}$).

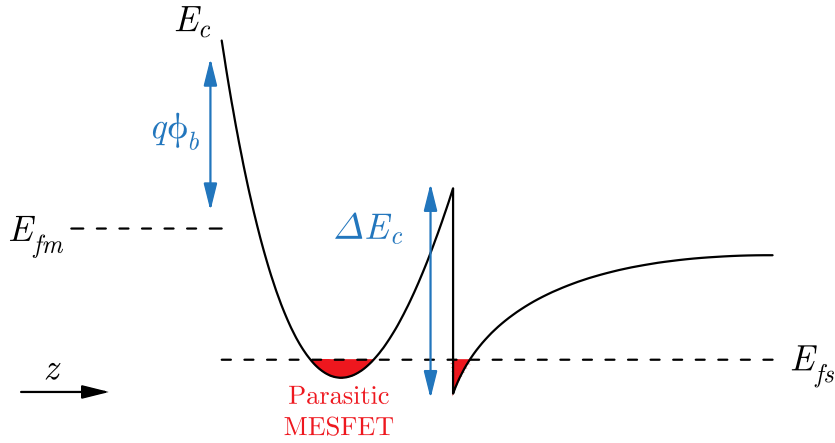


Figure 13.4: Parasitic MESFET formation in a HEMT.

The main advantage of high electron mobility transistors is that the channel charge is localized within an intrinsic semiconductor layer. Because this layer is not doped or extremely weakly doped the electron mobility in such layer is extremely good (it is not degraded by doping), hence allowing for better transport properties within the channel when compared with MESFET or MOSFET. For this reason these devices are named high electron mobility transistors.

Moreover, high electron mobility transistors exhibit better equivalent gate capacitance and charge control properties than common MOSFET or MESFET devices.

13.3 Density Gradient Simulation

The main focus when studying this kind of devices is in determining the relationship between the applied gate voltage and the electron charge density that is localized within the quantum well region.

Different models can be used to estimate the dependency of the charge density within the quantum well on the applied gate voltage V_{GB} . The main goal of this treatment is to apply the **1-dimensional density gradient** (i.e. quantum drift-diffusion) solver that has been developed in the previous chapters to the **vertical cross-section of a HEMT** such as the one shown in Figure 13.2.

The reference structure that will be considered for the simulations and the comparisons across different models is the one shown in Figure 13.5.

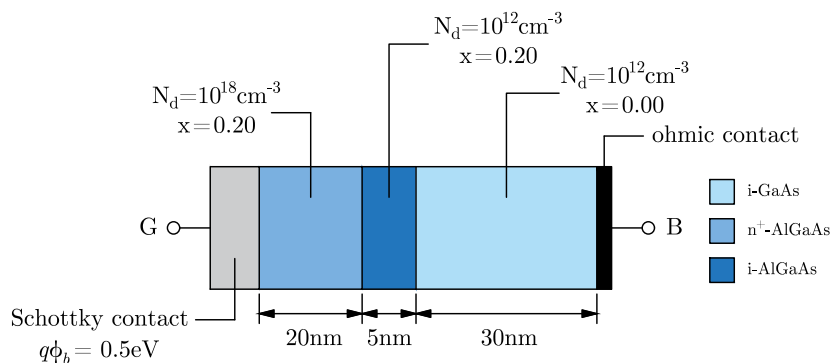


Figure 13.5: HEMT cross-section to be simulated.

The structure that is being considered is quite small with respect to typical HEMTs used for high-frequency analog applications.

Since the confinement in high electron mobility transistors is mostly electrical and not geometrical, the quantum confinement will be just weakly affected by the size of the device (the only influence of the geometry comes from the increase of the vertical electric fields when the device is scaled but since the confinement is mostly arising from the heterostructure this should only be a secondary effect).

The size of the structure is however kept limited to reduce the computational resources needed to treat the same structure within a Poisson-Schrödinger solver and therefore allow for the validation of the results.

Figure 13.6 shows the results of applying the density gradient model to the cross-section of a HEMT in **reverse bias**.

As expected from the considerations of section 11.4, the resulting electron density that is shown in Figure 13.6a is continuous and smooth (with continuous first derivative). Moreover, from the same figure it can be noticed that the parasitic MESFET is well suppressed in this kind of structure, as the electron density is much lower within the position interval $[0, 25]$ nm, i.e. within the supply layer and the 5 nm AlGaAs spacer. The results of the simulations in reverse bias presented in Figure 13.6 also clearly show that the electron density within the channel is strongly reduced as the reverse bias of the structure increases. This is consistent with the expected behavior for a threshold system to be employed within a field effect transistor, in which the drain-source current flow must be blocked when the gate-bulk voltage is below the threshold for the operation of the device.

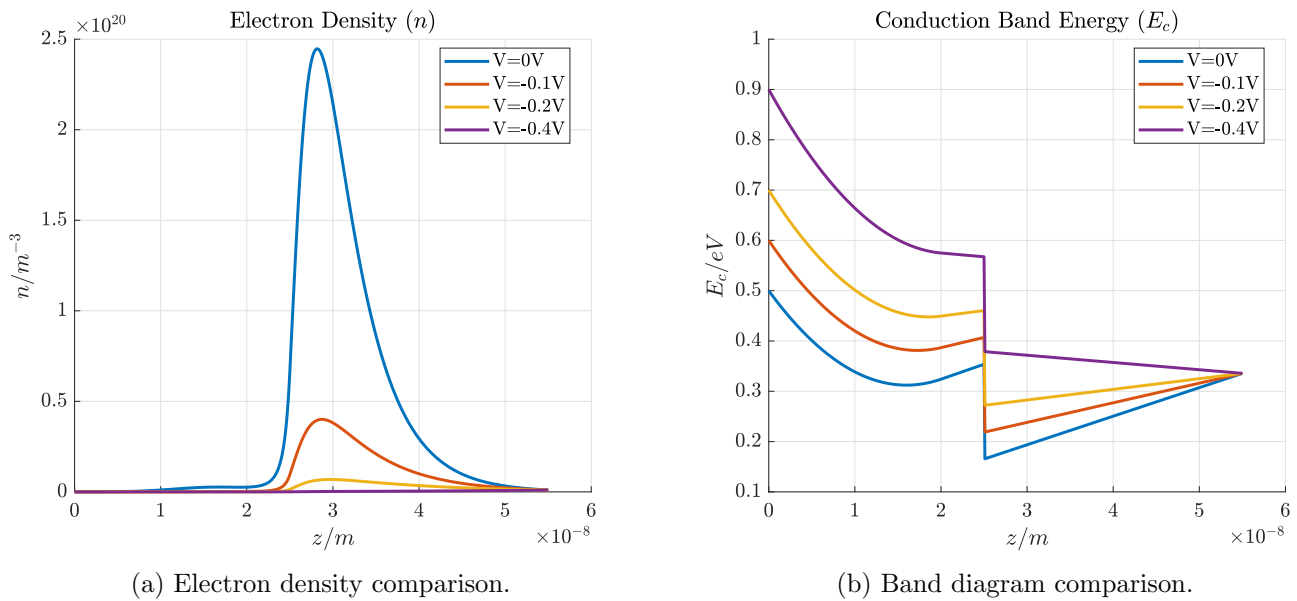


Figure 13.6: HEMT - Density Gradient simulations in reverse bias.

The results of applying the density gradient model to the cross-section of a HEMT in **forward bias** are instead reported in Figure 13.7.

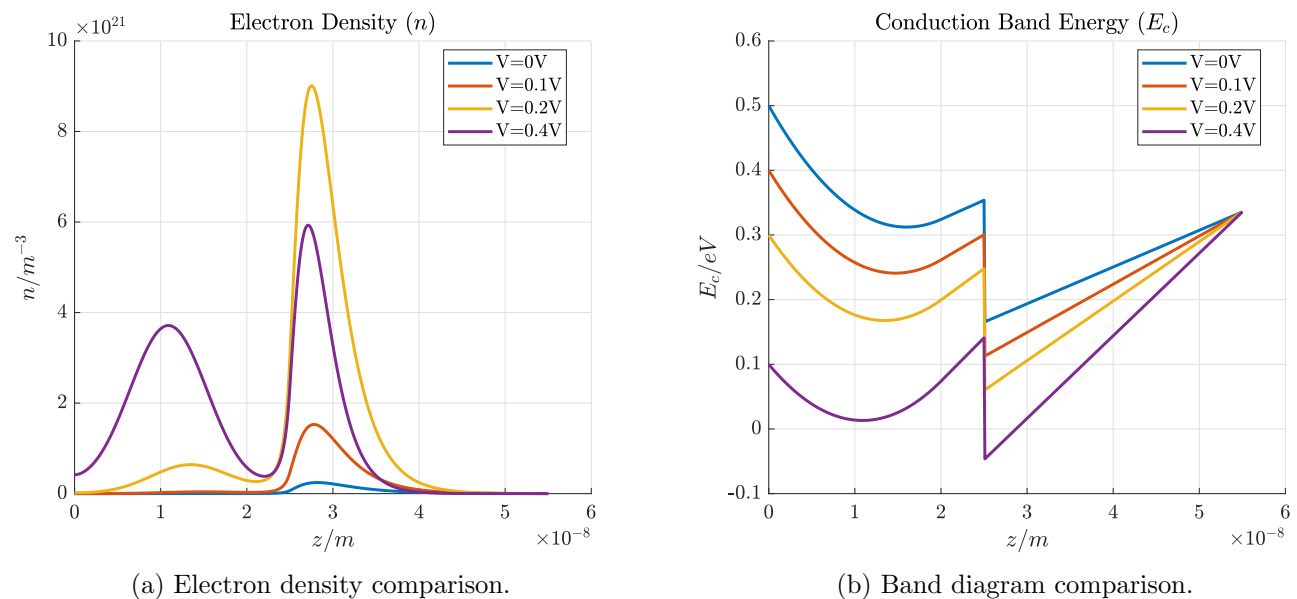


Figure 13.7: HEMT - Density Gradient simulations in forward bias.

From the plots of the electron density within the one-dimensional structure that are shown in Figure 13.7a two phenomena can be observed:

- for small forward bias of the structure, the channel of the device is enhanced, therefore leading to better conduction within the FET structure in which this gate stack is employed
- for excessive forward bias of the structure (this is clearly evident for a forward bias $V = 0.4$ V) however the electron density within the channel region (i.e. near $z = 25$ nm) actually decreases for increasing bias; this is related to the formation of a **parasitic MESFET** channel within the supply layer (i.e. in the $[0, 20]$ nm position interval) which subtracts electrons from the channel region

The total channel electron density (including both the electrons within the channel of the HEMT and the ones within the channel of the parasitic MESFET) can then be computed for both cases by simply integrating the electron density over the whole cross-section of the device:

$$N = \int_0^{\infty} n(z) dz$$

The total channel electron density for the device can then be plotted against the bias voltage V for the gate stack, obtaining the results of Figure 13.8.

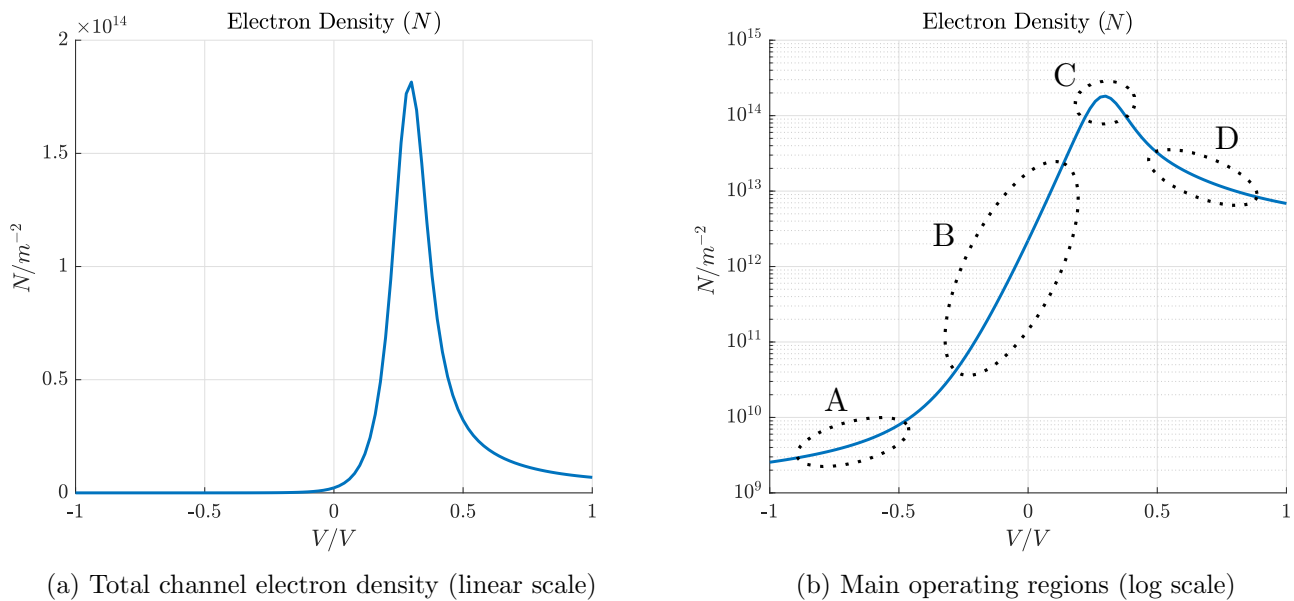


Figure 13.8: HEMT - Density Gradient simulations for the total channel electron density.

From the plot of Figure 13.8b four main conditions of operation can be identified for the structure of Figure 13.5:

- full depletion: since the substrate that is being considered in the simulations has comparatively small size (only 30 nm) for excessive reverse bias voltage a condition is reached in which not just the channel and the supply layer but also the substrate (i.e. the well layer) are **fully depleted**; the depletion of the structure then slows down
- channel modulation**: in this region changes in the bias voltage for the device strongly affect the total amount of charge that is available for conduction in the cross-section of the device
- parasitic MESFET formation: in this region the growth of the charge in the structure slows down because the **parasitic MESFET** starts forming and the channel stops growing; the charge is simply transferred from the HEMT channel to the parasitic MESFET channel but no new charge is being added

D. MS junction operation: in this region the Schottky junction stops being rectifying and a **gate current** flow forms within the structure (perpendicularly to the channel of the HEMT); the transition from C to D therefore corresponds to the structure switching from being a quantum well to being a conducting junction. A drop in the channel charge corresponds to this transition.

Operating condition A should not be observed then in real devices as the substrate is to a first approximation semi-infinite, while conditions C and D should be avoided when operating these devices.

A threshold for the channel formation can be determined by identifying the gate voltage V_{th} for which the channel charge is 1% of its peak value, obtaining as a result:

$$V_{th} \approx -0.0131 \text{ V}$$

In order to determine the onset of the parasitic MESFET it is useful to define the total electron density within the parasitic MESFET:

$$N_{MESFET} = \int_M n(z) dz$$

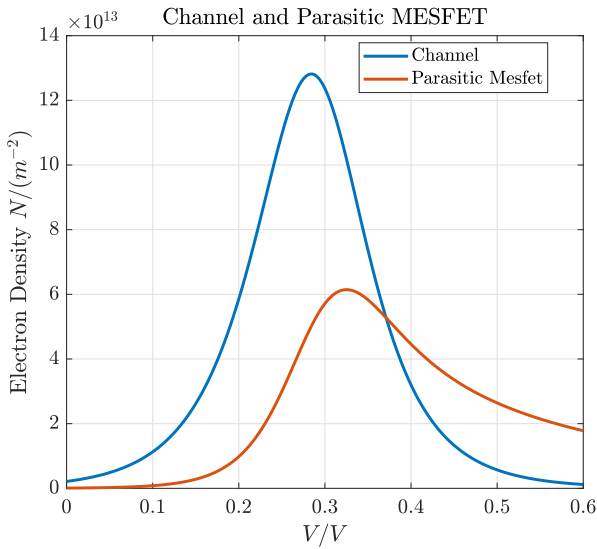
where M represents the supply and spacer layers.

It is also useful to define the total electron density within the actual channel of the HEMT as:

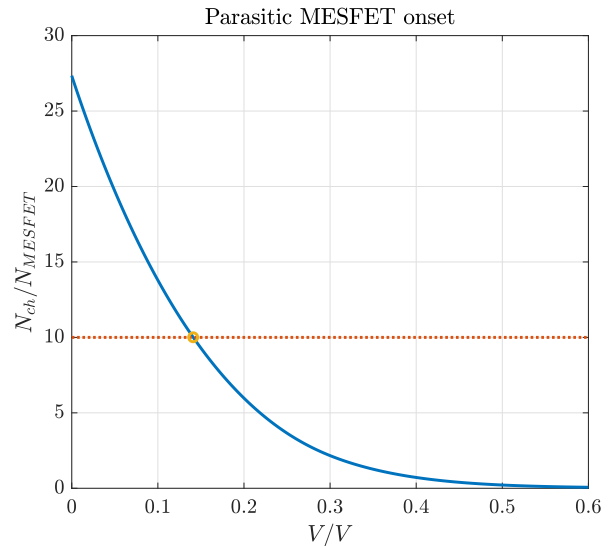
$$N_{ch} = \int_C n(z) dz$$

where C represents the channel region and the substrate region.

The comparison between the channel charge density $N_{ch}(V)$ and the parasitic MESFET charge density $N_{MESFET}(V)$ as functions of the gate voltage (which is shown in Figure 13.9a) shows that the channel is the first to form, as expected from a working device.



(a) Channel and parasitic MESFET electron densities (linear scale)



(b) Extraction of the parasitic MESFET onset voltage

Figure 13.9: HEMT - Parasitic MESFET onset.

To understand from which gate voltage the parasitic MESFET starts to form it is useful to define the **limit voltage** beyond which the device operates as a MESFET as the voltage beyond which the charge in the MESFET N_{MESFET} is more than 10% of the channel charge N_{ch} . This limit voltage can then be estimated for the current device to be:

$$V_{lim} \approx 0.141 \text{ V}$$

The extraction procedure for this limit voltage is shown in Figure 13.9b.

In order to verify assumption D. (the structure operating as a metal-semiconductor junction beyond a certain voltage, therefore causing part of the overall charge stored in both the channel and the parasitic MESFET to be "flushed" out of the device) it is useful to look at the current through the metal-semiconductor junction, which is shown in Figure 13.10a.

From the gate current plot it is immediate to notice that the structure starts to conduct heavily for gate voltages beyond 0.2 V, which justifies the decrease in the charge which is observed at high gate voltages.

Another figure of merit which is worth observing is the channel capacitance, which is defined as:

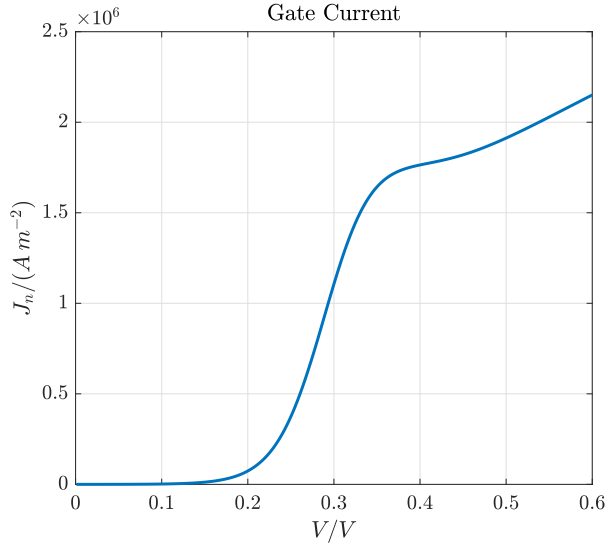
$$C_{ch} = \frac{d N_{ch}}{d V}$$

and whose plot is reported in Figure 13.10b.

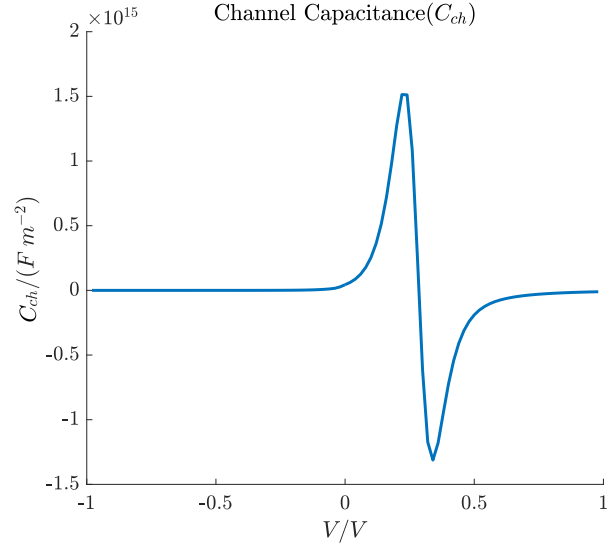
This parameter represents the effectiveness of the voltage variations for building up channel charge at different bias points.

From its plot it is clearly evident how:

- Below threshold ($V_{th} \approx -0.0131$ V) the channel is almost not sensitive on the gate voltage
- Above threshold the channel is initially extremely sensitive on the gate voltage
- Beyond a limit voltage ($V_{lim} \approx 0.141$ V) the gate control over the channel charge starts being reduced because of the formation of the parasitic MESFET
- For high gate bias the device becomes a conducting junction and the charge is actually drained from the channel instead of building up



(a) HEMT - Gate current through the structure



(b) HEMT - Channel capacitance

Figure 13.10: HEMT - Gate capacitance and current

While the structure seems to behave as expected from the cross-section of a HEMT, it is useful to validate the results against a Poisson-Schrödinger-Boltzmann solver to try and understand which are the main limitations of the density gradient model when applied to high electron mobility transistors or, more in general, to heterostructure-based devices.

It is then also interesting to try and observe the improvement in the results that is obtained by considering a density-gradient model instead of a drift-diffusion model (with Boltzmann statistics). This comparison also allows to effectively observe the issues of using semiclassical models when investigating the behavior of devices in which quantum confinement is an essential effect (such as MOS systems and HEMT).

13.3.1 Comparison with Poisson-Boltzmann

For the sake of simplicity, the comparison between the density gradient model and the drift-diffusion model is performed at **equilibrium**. The comparison is then effectively between the density gradient model and the Poisson Boltzmann model.

The results of the comparison between the two models are shown in Figure 13.11.

The first evident difference is that, while a semiclassical Poisson-Boltzmann model allows for a discontinuous electron density, a density gradient model requires the electron density to be continuous and smooth (i.e. with continuous first derivative).

Another important difference is that, while a Poisson-Boltzmann model predicts the electron density to have a peak in correspondence to the interface between GaAs and AlGaAs, this is not actually the case when quantum effects are taken into account to a first order (which is the case of the density gradient model).

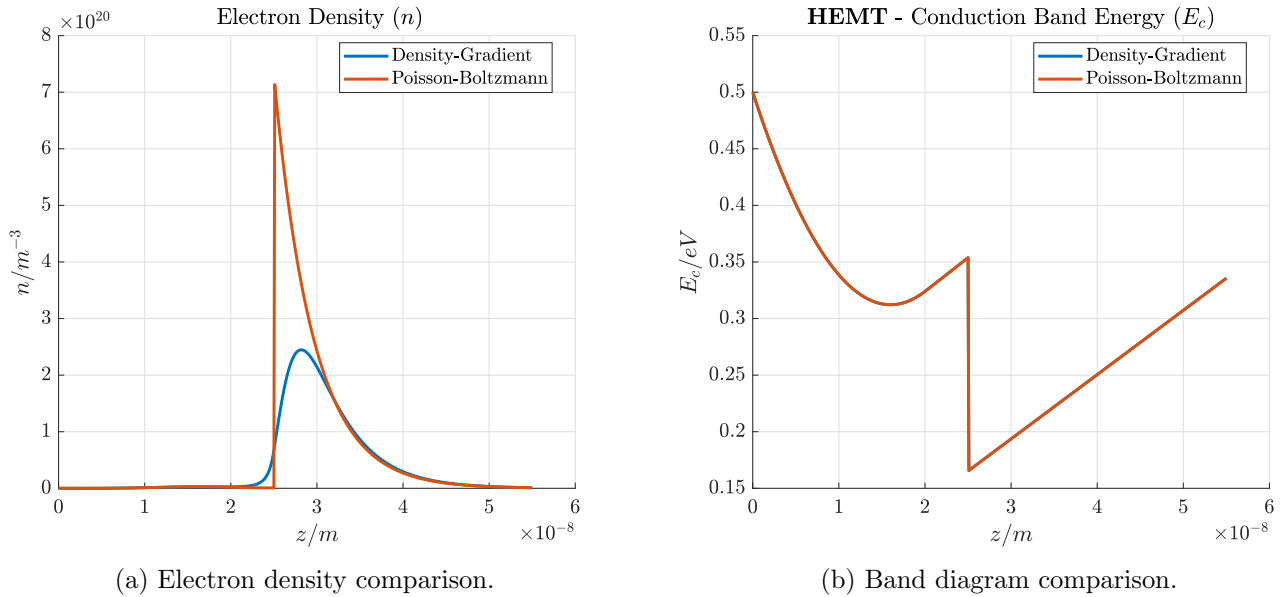


Figure 13.11: HEMT simulation comparison at equilibrium (Density-Gradient vs Poisson-Boltzmann solver).

When a density gradient model is adopted, an offset Δz is found between the GaAs-AlGaAs interface and the peak electron density.

From this comparison it is also possible to notice that a Poisson-Boltzmann model (or, more in general, a drift-diffusion model) is quite severely overestimating the electron density within the channel. The reason behind this is that within the quantum well near the GaAs-AlGaAs interface the allowed energy bands are altered by the level discretization due to quantum confinement, as is shown in Figure 13.12. As a result of this discretization phenomenon, less electrons can be hosted and confined within the well (this is mostly because the fundamental state in the quantum well always has energy larger than E_c).

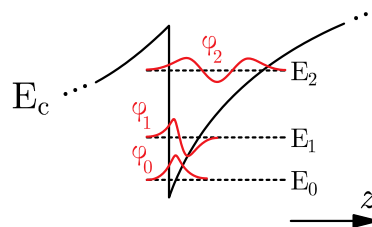


Figure 13.12: Quantum confinement in the well of a HEMT.

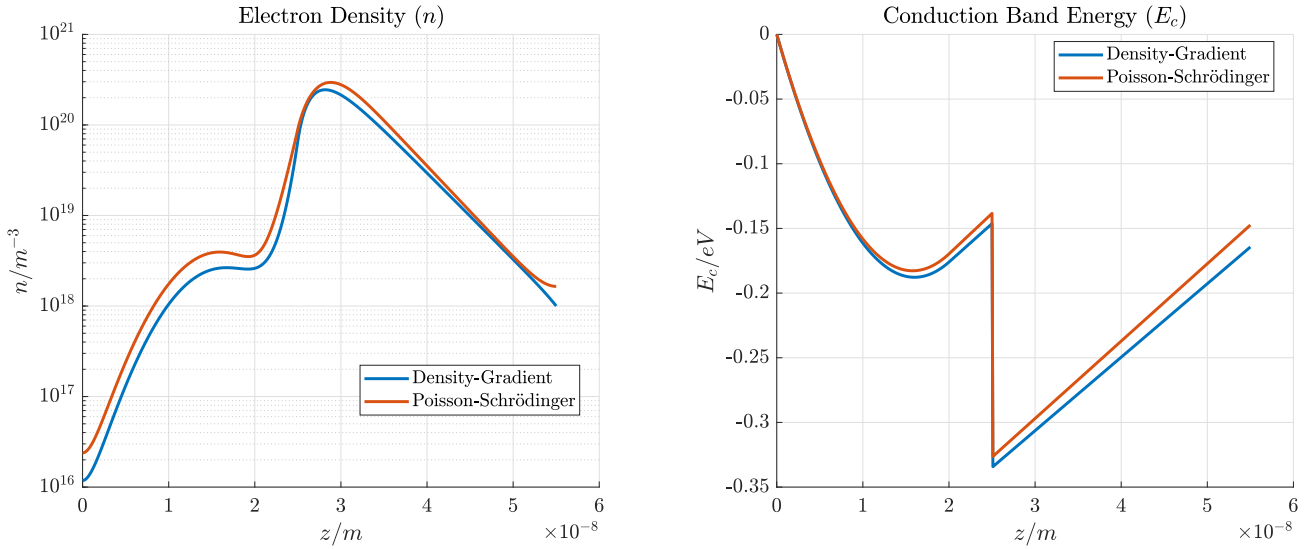
It is interesting to notice that, despite the electron density being quite different in the two cases (the peak concentration estimated by the Poisson-Boltzmann solver is approximately 3 times the one estimated by the density gradient solver) the band diagrams obtained with the two solvers are extremely similar. This is related to the exponential nature of the Boltzmann distribution, which allows to obtain large variations of the carrier density with small variations of the conduction band energy.

13.3.2 Comparison with Poisson-Schrödinger

In order to understand the validity and limitations of the density gradient model when applied to heterostructures made of III-V semiconductors it is useful to compare the equilibrium solution found with the density gradient model with the one obtained with a Poisson-Schrödinger solver.

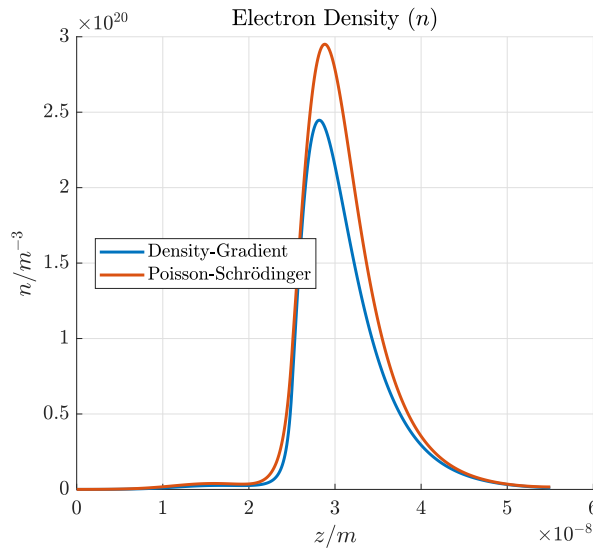
In particular, the Poisson-Schrödinger solver described and developed in [29] will be considered for the comparisons. The solution obtained from this solver will be considered here to be exact and therefore to include all the quantum effects that are taking place in the device under study.

The results of the comparison described above are reported in Figure 13.13.



(a) Electron density comparison (log scale).

(b) Band diagram comparison.



(c) Electron density comparison (linear scale).

Figure 13.13: HEMT simulation comparison (Density-Gradient vs Poisson-Schrödinger solver at equilibrium).

The comparison of the electron densities obtained with the two models, whose results are reported in Figure 13.13c, immediately shows that the general trend of the solution that is found is quite similar to the exact solution given by the Poisson-Schrödinger solver (with Boltzmann statistics). The results are much better than the ones that have been previously obtained with a semiclassical Poisson-Boltzmann approach. The density gradient model however still presents an error of approximately 30% when compared to the reference Poisson-Schrödinger solver. While this result is quite encouraging, it however underlines how also the terms of the Wigner function having order higher than \hbar^2 can play quite an important role, especially when considering strongly discontinuous potential profiles.

When very accurate estimates of the charge are needed a Poisson-Schrödinger or Poisson-NEGF solver therefore remains the best solution. The density gradient model however allows to easily obtain reasonably good estimates of the charge density that are significantly more reliable than the ones obtained from a semiclassical drift-diffusion model.

The most difference appears to arise from the different boundary conditions used by these models. The Poisson-Schrödinger solver which has been considered (which is described in [29]) assumes semi-infinite contacts which are perfectly absorbing. This assumption is instead relaxed in the quantum drift-diffusion solver, which is the most likely reason behind the differences that are observed between the two models.

Following the approach adopted by [24],[23] an attempt at improving the model was performed by introducing a numeric fitting factor Γ in the definition of the quantum potential:

$$\Lambda_n = \frac{\hbar^2 \Gamma_n}{6 m_n^* q} \frac{\nabla^2 \sqrt{n}}{\sqrt{n}} \quad \Lambda_p = \frac{\hbar^2 \Gamma_p}{6 m_p^* q} \frac{\nabla^2 \sqrt{p}}{\sqrt{p}}$$

For a n-type high electron mobility transistor cross-section like the one of Figure 13.5 holes give negligible contribution to the behavior of the device. The only carriers for which the fitting factor Γ needs to be determined are the electrons.

A trial and error procedure shows that the value of Γ_n that leads to the correct result in terms of height of the electron density peak within the channel is:

$$\Gamma_n \approx 0.58$$

Introducing this fitting factor into the density gradient model and comparing the results against the reference Poisson-Schrödinger solver leads to the results which are shown in Figure 13.14.

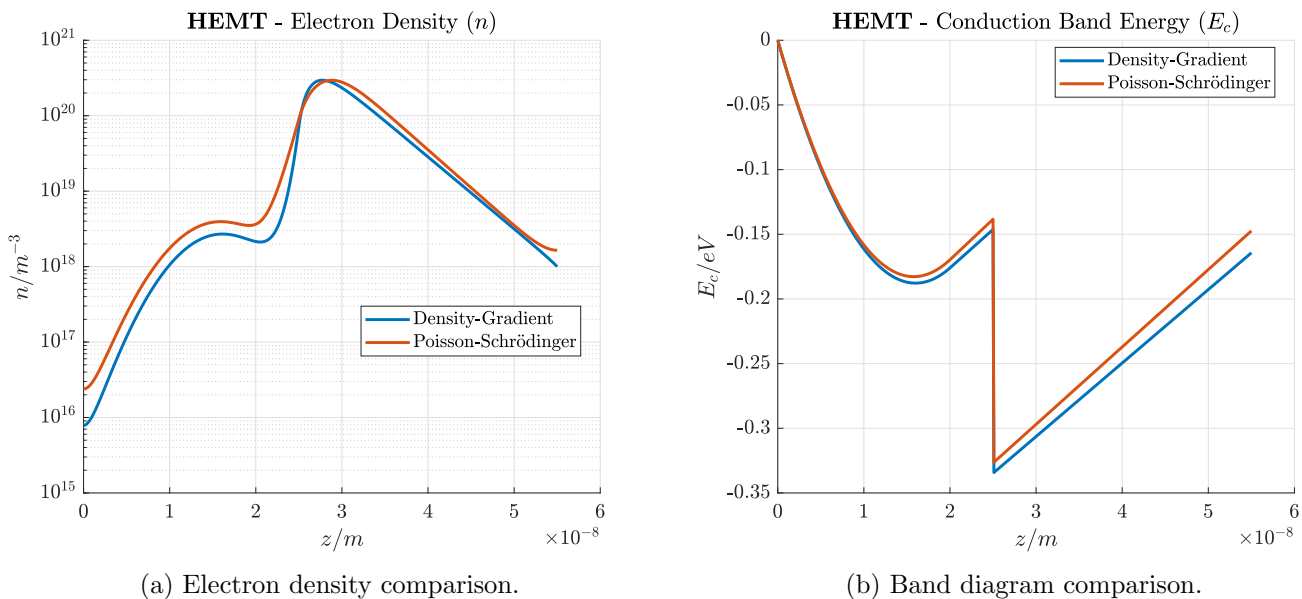


Figure 13.14: HEMT simulation comparison (fitted Density-Gradient vs Poisson-Schrödinger solver).

The comparison clearly shows that while introducing the fitting factor allows to correct the height of the peak in the electron density, the quality of the approximation is worsened everywhere else and even the position of the peak is significantly shifted. This is a clear symptom of the limitation due to adopting an approximation of order \hbar^2 of the Wigner function in the presence of jumps in the potential energy for the electrons (a fitting factor cannot therefore give any significant improvement in this situation).

13.3.3 Modeling Issues: Classical vs Quantum

From the analysis presented above it is immediate to understand that semiclassical modeling is not enough for HEMT devices and, more in general, when quantum confinement strongly affects the operation of the device (which is often the case in high electron mobility transistors).

The density gradient model could be adopted to overcome some of these limitations of drift-diffusion models with little increase in the computational cost and simulation time. The results are quite good approximations of the true solution (which would be obtained with a Poisson-Schrödinger solver) but the price to be paid for keeping the computational cost limited is an error in the estimate of the charge density that for the cases that have been considered reached 30%.

The accuracy of the solutions that have been obtained on the reference structure is comparable to the one obtained by [30] when working on silicon MOSFETs, showing that this model approximately works equally well for silicon and for III-V semiconductors.

Chapter 14

Double Heterostructure HEMT

The high electron mobility transistor, which was presented in chapter 13, is a device whose operation is based on quantum confinement. This is because the charge provided by the supply layer is transferred and confined within a quantum well.

Increasing the level of confinement of the structure would be beneficial for the performance of the device, reducing the gate current (because it would confine the charge in it, therefore stopping it from drifting and diffusing transversally to the channel), increasing the electron density within the channel and improving the frequency performance of the resulting FET.

This can be achieved by using a double heterostructure instead of a single heterostructure, obtaining confinement from two sides of the channel charge. The resulting conduction band profile is then close to a rectangular well; this device is therefore often referred to as double heterostructure high electron mobility transistor (double heterostructure-HEMT).

14.1 Device Structure

The HEMT structure that was presented in Figure 13.1 can be improved by adding a second heterojunction to the stack, therefore obtaining a double heterojunction of the kind AlGaAs-GaAs-AlGaAs, as is shown in Figure 14.1.

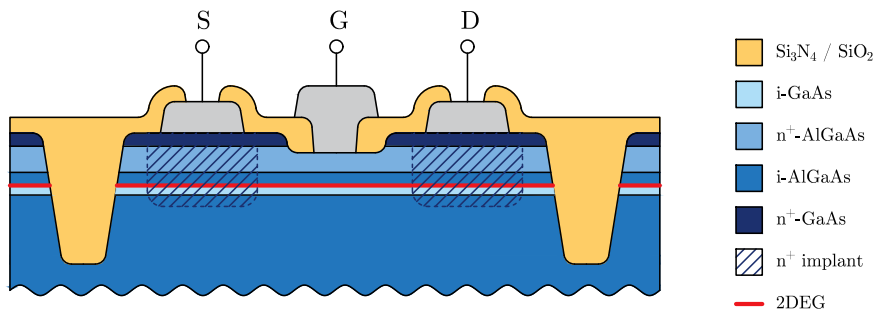


Figure 14.1: AlGaAs double heterostructure HEMT structure.

The two-dimensional electron gas (2DEG) in this device is then confined in a quantum well with almost rectangular shape, as is shown in Figure 14.2. The interior of the quantum well corresponds to the thin GaAs layer that is placed in between the AlGaAs layers.

The confinement in this device is then mostly geometrical and is not self-induced (i.e. electrical), hence the dimensions of these devices will play an important role in their performance.

The bottom of the well exhibits a curvature which is related to the non-uniform concentration of the electrons within the well. In particular, in the band diagram shown in Figure 14.2 charge is self-confining mostly at the two sides of the quantum well, which results in a deeper drop in the conduction band near the well walls.

Also for this device, as was already described in chapter 13 for simple high electron mobility transistors, varying the bias voltage allows to vary the depth of penetration $E_{fs} - E_c$ of the conduction band below the Fermi level of the semiconductor within the well region. This therefore allows, by the classical Fermi or

Boltzmann distributions, to modulate the channel charge (i.e. the charge stored within the quantum well) by means of the applied electrostatic potential between the gate and the bulk.

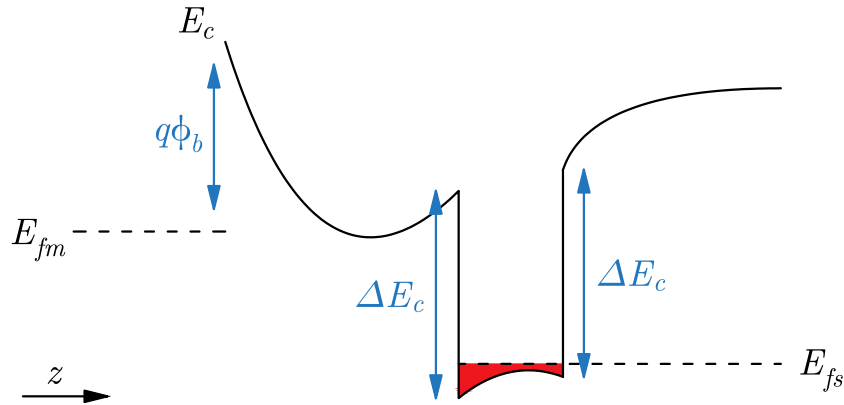


Figure 14.2: AlGaAs double heterostructure HEMT operation.

All the considerations that have been made in the previous chapter about high electron mobility transistors still apply also to the double-heterostructure well variant, making also these devices extremely well-suited for high-frequency analog and digital applications.

14.2 Density Gradient Simulation

Similarly to what was done in the previous chapter for simple HEMT devices, also for double heterostructure HEMTs the main goal is to determine the relationship between the applied gate voltage and the electron charge density that is confined within the GaAs well layer.

Also in this case, the choice is to apply the **1-dimensional density gradient** (i.e. quantum drift-diffusion) solver that has been developed in the previous chapters to the vertical cross-section of the double heterostructure HEMT that is shown in Figure 14.1.

The reference structure that will be considered for the simulations and the comparisons across different models is then the one shown in Figure 14.3.

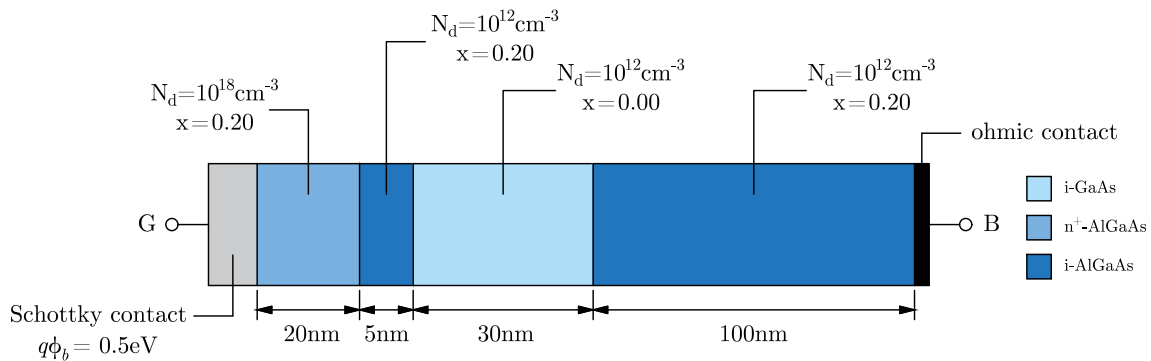


Figure 14.3: Double heterostructure HEMT cross-section to be simulated.

The structure that is being considered is again quite small with respect to typical double heterostructure HEMTs used for high-frequency analog applications. Also in this case, the device size choice is aimed at keeping the number of nodes within the discretized device limited to allow for its simulation also with a Poisson-Schrödinger simulator, hence allowing for validation of the results at equilibrium. Moreover, since in this kind of device geometrical confinement is also important, reducing the device size will make the quantum confinement effects more relevant.

Figure 14.4 shows the results of applying the density gradient model to the cross-section of a double heterostructure HEMT in **reverse bias**.

Also in this case (as for the HEMT structure that was treated in the previous chapter) the electron density is continuous and smooth (with continuous first derivative), as expected from the considerations of section 11.4. Moreover, from the same figure it can be noticed that the parasitic MESFET is well suppressed in this structure when it operates in reverse bias, as the electron density is much lower within the position range [0, 25] nm, i.e. within the supply layer and the 5 nm AlGaAs spacer.

The results of the simulations in reverse bias presented in Figure 14.4a clearly show that, due to the effect of the Schottky barrier and of the supply layer the two sides of the well are not equally populated; the side that is closer to the supply layer presents a higher electron concentration. The well is therefore not rectangular but exhibits instead a quasi-triangular behavior at its sides.

The behavior that is observed for the structure is consistent with what is expected from the qualitative treatment of the physics of high electron mobility transistors that has been presented in chapter 13: as the reverse bias of the gate stack is increased the electron density within the channel is reduced, until the channel is (almost) completely suppressed.

This behavior is typical of threshold structures in which the applied bias can be used to populate a channel when operating above threshold (therefore allowing for a drain-source current flow) or to deplete it (therefore blocking the drain-source current flow) when operating below threshold.

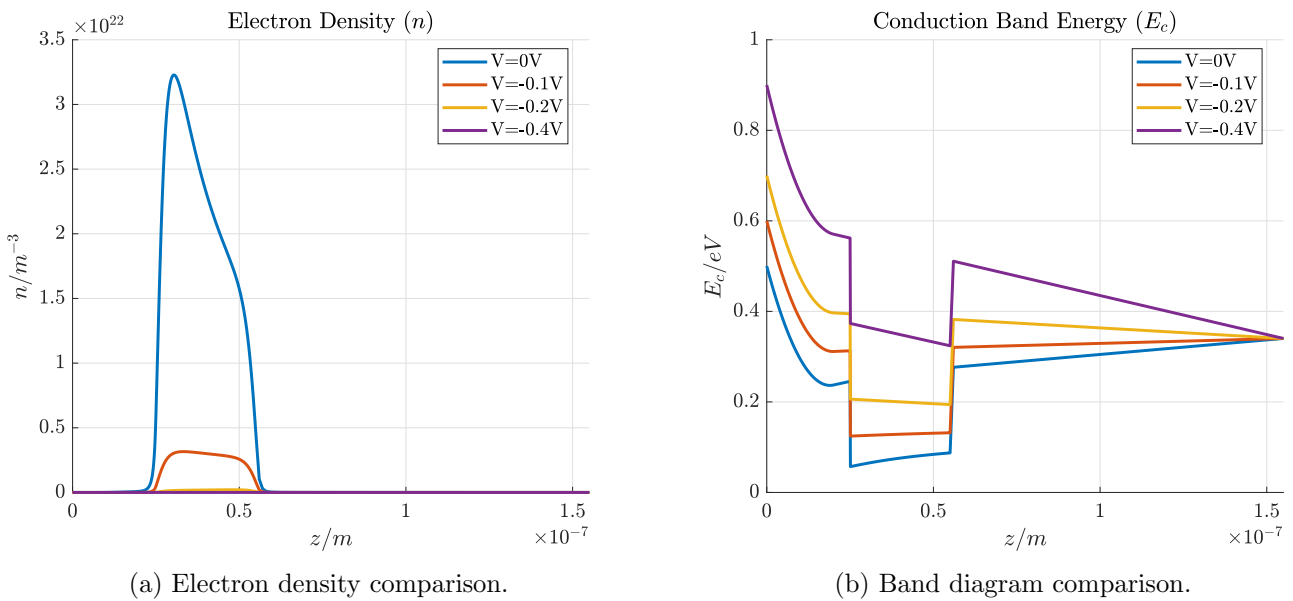


Figure 14.4: Double heterostructure HEMT - Density Gradient simulations in reverse bias.

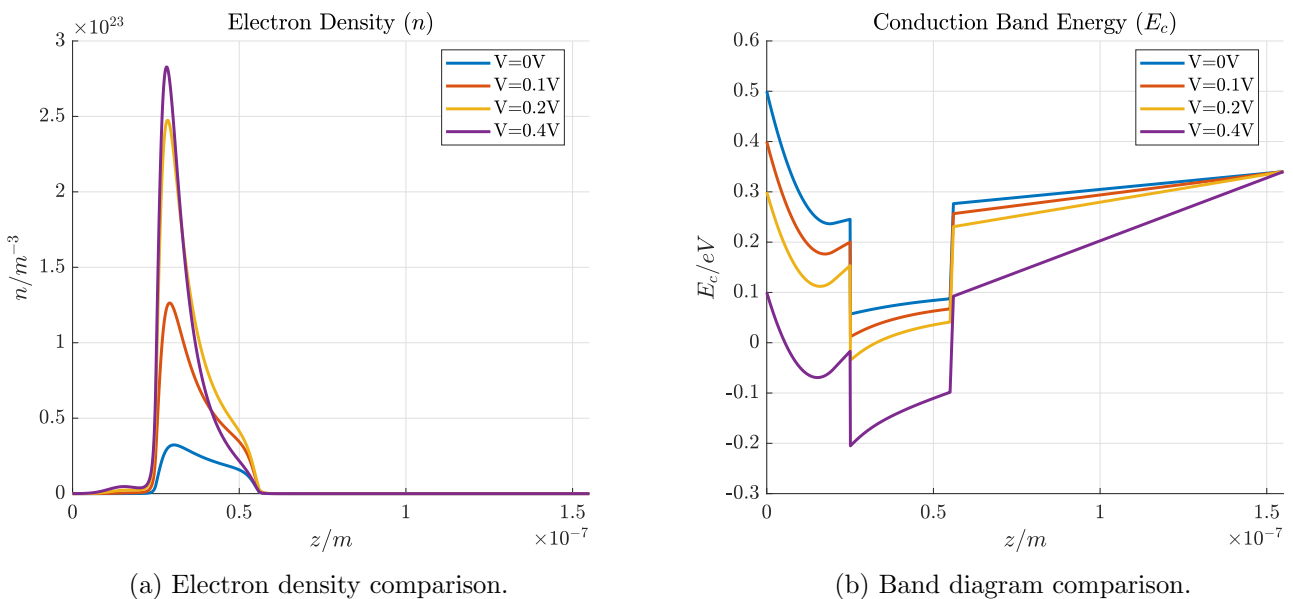


Figure 14.5: Double heterostructure HEMT - Density Gradient simulations in forward bias.

The results of applying the density gradient model to the cross-section of a double-heterostructure HEMT in **forward bias** are instead reported in Figure 14.5.

From these plots it is evident how increasing the forward bias voltage applied to the structure causes the channel charge to increase. Moreover, it is possible to notice that:

- for small applied voltages the quantum well is quasi-rectangular, hence the concentration of electrons is more uniform along the quantum well
- for higher applied voltages the quantum well is being tilted, hence the electrons tend to shift towards the region with lower conduction-band energy E_c , therefore making the well a quasi-triangular one

This structure appears to be better at suppressing the parasitic MESFET than the one of a simple HEMT (such as the one presented in chapter 13); this is an interesting advantage of employing a confinement approach based on a double heterojunction.

Integrating the electron density (including both the channel electrons and the parasitic channel electrons) as:

$$N = \int_0^{+\infty} n(z) dz$$

the total electron density N within the channel that is shown in Figure 14.6 is obtained.

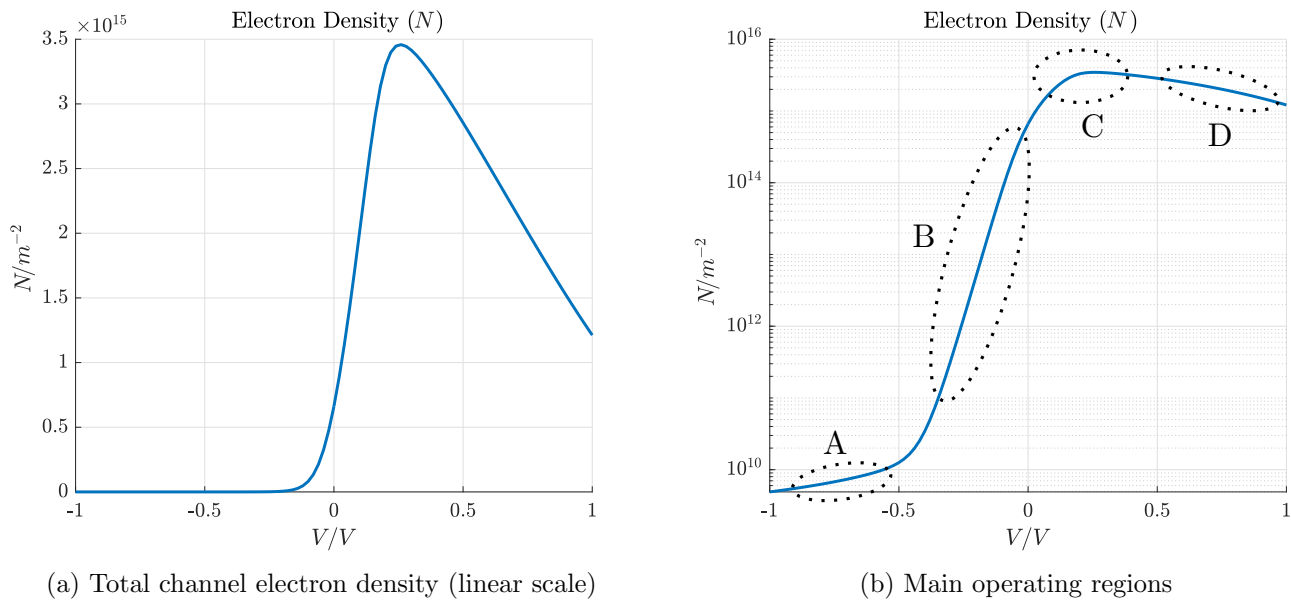


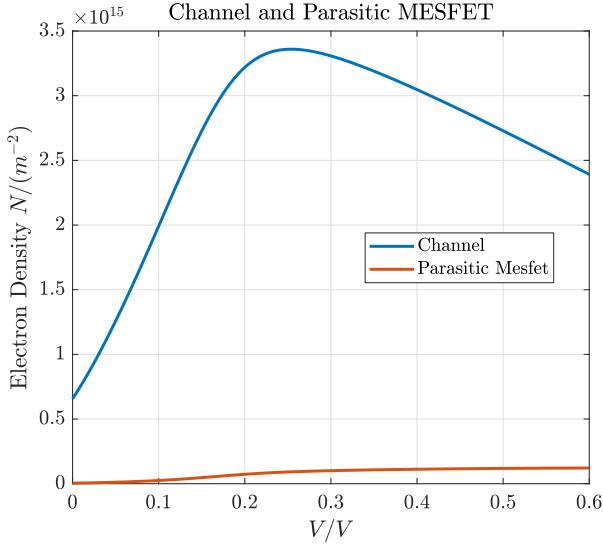
Figure 14.6: Double heterostructure HEMT - Density Gradient simulations for the total channel electron density (log scale).

From the plot of Figure 14.6b four main conditions of operation can be identified for the structure of Figure 14.3:

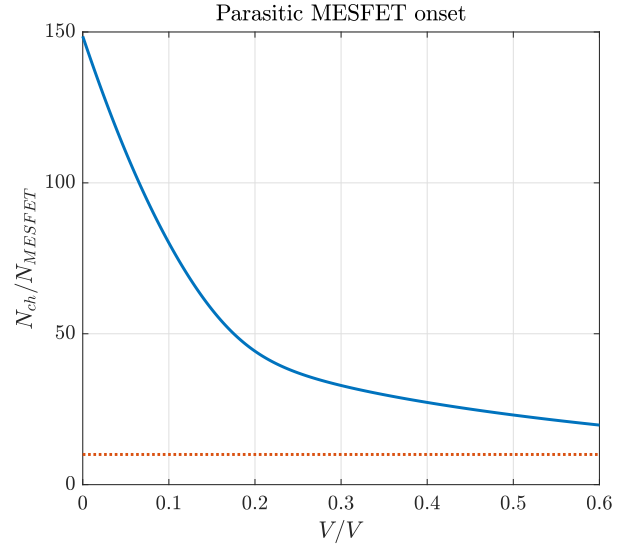
- full depletion: being the substrate that is considered in the simulations quite short, for strong reverse bias voltage a condition is reached in which the substrate is fully depleted; the depletion of the structure then slows down
- channel modulation: in this region changes in the bias voltage for the device strongly affect the total amount of charge that is available for conduction in the cross-section of the device
- parasitic MESFET formation and well triangularization: in this region two effects start to emerge:
 - a parasitic MESFET starts to form in the supply layer, therefore subtracting electron charge from the actual channel of the device
 - the well changes from being quasi-rectangular to being quasi-triangular as the applied bias is increased; to this phenomenon corresponds a partial reduction of the channel charge for the device for high bias voltages

D. MS junction operation: in this region the Schottky junction stops being rectifying and a current flow forms within the gate structure; this corresponds to the system changing from being a charge accumulator to being a conducting junction. A drop in the channel charge corresponds to this transition

Operating condition A should also in this case (as for the HEMT treated in chapter 13) not be observed in real devices as the substrate is to a first approximation semi-infinite, while conditions C and D should be avoided when operating these devices.

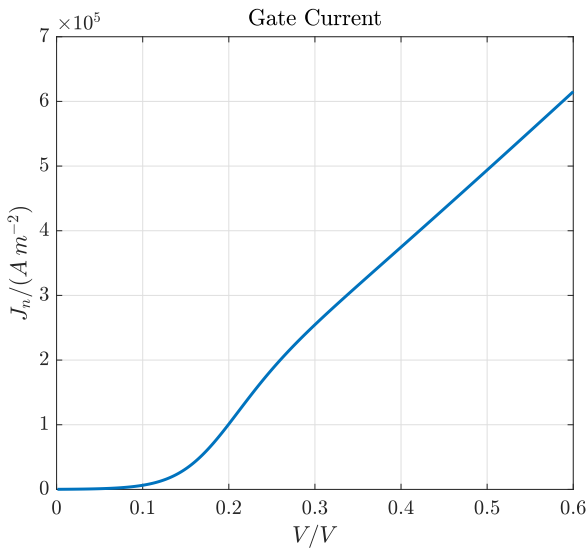


(a) Channel and parasitic MESFET electron densities (linear scale)

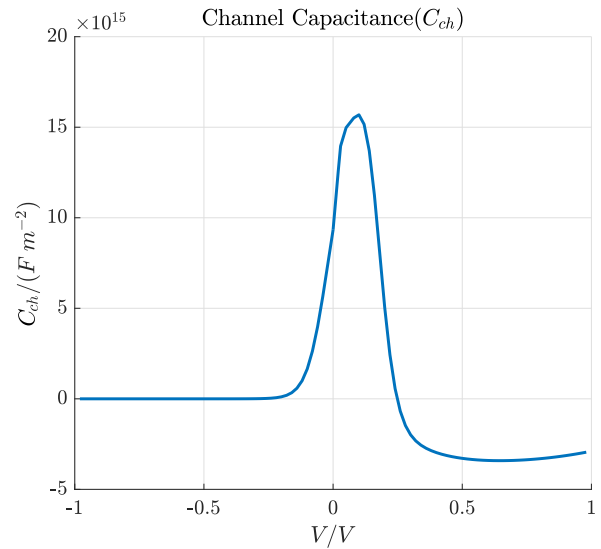


(b) Extraction of the parasitic MESFET onset voltage

Figure 14.7: Double heterostructure HEMT - Parasitic MESFET onset.



(a) Double heterostructure HEMT - Gate current through the structure



(b) Double heterostructure HEMT - Channel capacitance

Figure 14.8: Double heterostructure HEMT - Gate capacitance and current

Also in this case as was done in section 13.3 for single heterostructure HEMTs, it is useful to define:

- the total electron density within the parasitic MESFET:

$$N_{\text{MESFET}} = \int_M n(z) dz$$

where M represents the supply and spacer layers.

- the total electron density within the actual channel of the HEMT as:

$$N_{\text{ch}} = \int_C n(z) dz$$

where C represents the channel region and the substrate region.

When observing the relative behavior of the channel charge and of the parasitic MESFET charge, as is shown in Figure 14.7a, it is then immediate to notice that the charge in the parasitic MESFET channel is always much smaller than the one in the main channel of the HEMT.

This is even more evident when noticing that the ratio $N_{\text{ch}}/N_{\text{MESFET}}$ is always larger than 10 on the whole interval that is considered for Figure 14.7. This means that the limit voltage (defined as the voltage beyond which the parasitic MESFET channel is more than 10% of the main channel of the HEMT in terms of electron density) will be beyond 0.6 V of gate bias. This confirms that double heterostructure HEMT always perform much better than single-heterostructure HEMT from the parasitics point of view.

The threshold for this gate structure can then be evaluated as described in section 13.3 (by defining it as the gate voltage for which the channel charge is 1% of its maximum) to be:

$$V_{\text{th}} \approx -0.133 \text{ V}$$

The plot of the gate current, which is shown in Figure 14.8a clearly shows that the gate current in a double heterostructure HEMT is quite lower than the one in a single heterostructure HEMT (such as the one in Figure 13.10a). This is due to the quantum well blocking conduction in the direction transverse to the channel. From this plot it can also be seen that the decay in the total electron density for high gate bias is tightly related to the metal-semiconductor junction starting to conduct and "flushing" out the charge from the channel region (confirming hypothesis D.).

Finally, looking at the channel capacitance reported in Figure 14.8b (the operative definition of the channel capacitance was given in section 13.3) shows that:

- For gate voltages below the structure threshold the control of the gate over the channel charge is close to none
- For gate voltages immediately above the threshold voltage the gate can control the channel charge extremely effectively, hence the capacitance is large and positive
- For excessive gate voltages the parasitic MESFET starts to form and the junction starts to conduct, reducing the channel charge with the applied voltage, hence draining the charge stored within the channel region

Also for this reference structure it is useful to observe then two interesting comparisons at equilibrium:

- the results of applying a semiclassical Poisson-Boltzmann solver against those of employing a density gradient solver in order to observe how relevant quantum effects can be in the operation of a device
- the results of applying a Poisson-Schrödinger solver against those of employing a density gradient solver in order to determine whether the density gradient method is a viable option for accurate simulation of these devices

14.2.1 Comparison with Drift-Diffusion

For the sake of simplicity, the comparison between the density gradient model and the drift-diffusion model is performed at equilibrium. The comparison is then effectively between the density gradient model and the Poisson Boltzmann model.

The results of the comparison between the two models are shown in Figure 14.9.

From the comparison it is immediately seen that a Poisson-Boltzmann model is giving a shape of the electron density that is quite different from the actual one.

In particular, while the Poisson-Boltzmann model predicts the formation of a boundary layer of electrons at the first interface between AlGaAs and GaAs, the density gradient model predicts the presence of an offset between the interface and the peak electron density. This is a well-known phenomenon that stems from quantization effects.

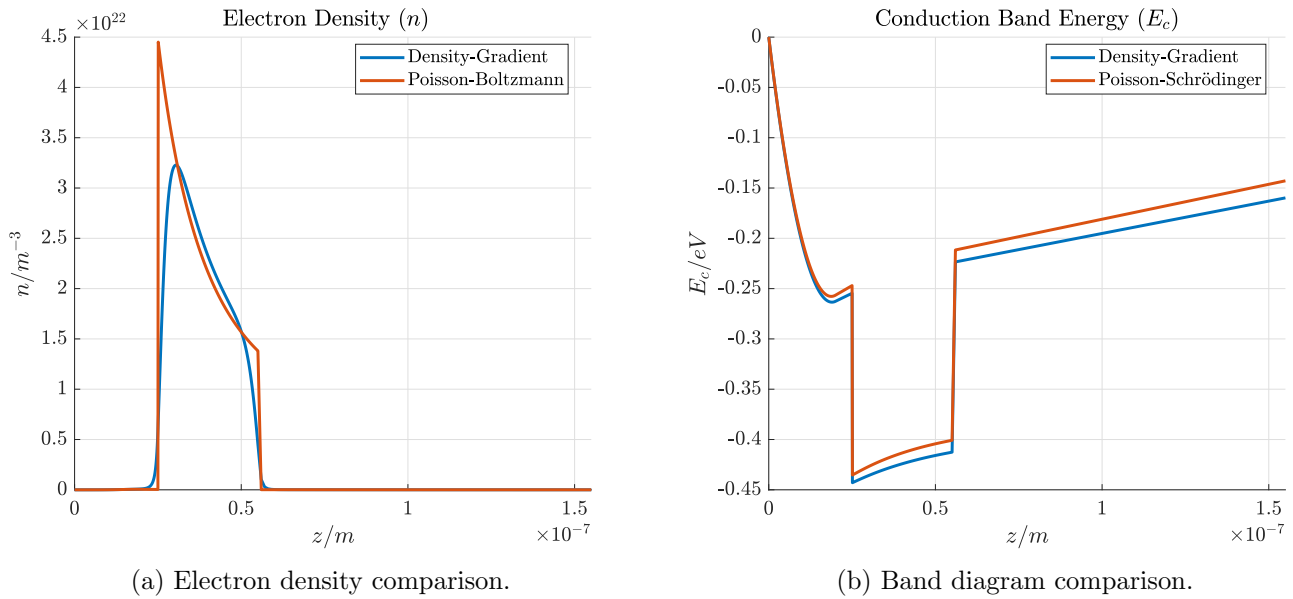


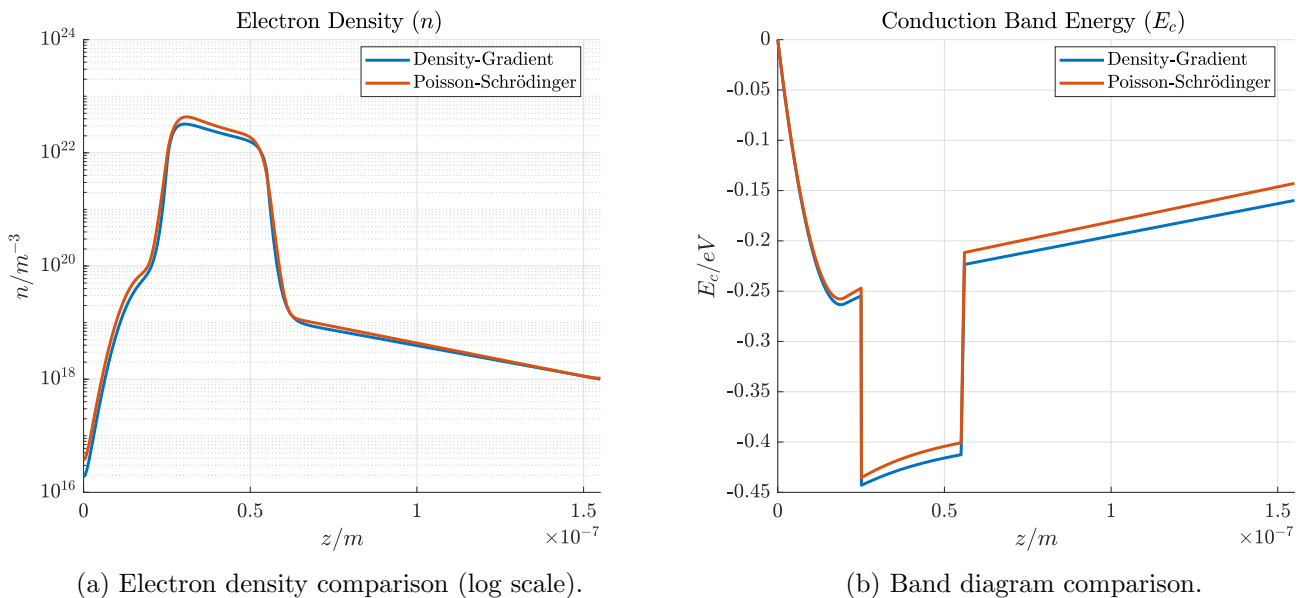
Figure 14.9: Double heterostructure HEMT simulation comparison (Density-Gradient vs Poisson-Boltzmann solver).

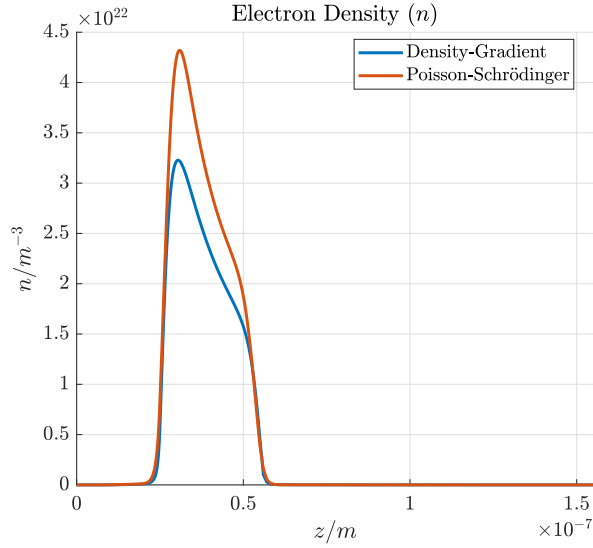
14.2.2 Comparison with Poisson-Schrödinger

Also in this case, as was done for the HEMT structure proposed in chapter 13 the density gradient model is validated against the Poisson-Schrödinger solver (with Boltzmann statistics) that is described in [29]. The purpose of this comparison is to determine whether the density gradient model can be a viable option for the simulation of heterostructure device and, specifically, of quantum-well high electron mobility transistors.

The results of the comparison are shown in Figure 14.10.

From the comparison of Figure 14.10 it can be noticed that the density gradient model can predict extremely well the trend for the electron density and quite accurately, with a relative error of approximately 30%, also its absolute values.





(c) Electron density comparison (linear scale).

Figure 14.10: Double heterostructure HEMT simulation comparison (Density-Gradient vs Poisson-Schrödinger solver).

The band diagram is instead slightly different from the one expected from a Poisson-Schrödinger approach; the error between the conduction band curves arises from the double integration of the error in the electron density (according to Poisson's equation: $\frac{\partial}{\partial z} \left\{ \epsilon \frac{\partial \phi}{\partial z} \right\} = -q(p - n + N_d - N_a)$).

Relative errors of this entity are comparable with the ones that can be observed for silicon MOSFET devices in works such as [30]. The density gradient therefore appears to be quite an appealing approach for including quantum corrections in simulations of III-V semiconductor-based heterostructure devices, allowing to obtain quite accurate results with a computational time that is only slightly higher than that for a semiclassical drift-diffusion approach and much lower than that required by a Poisson-Schrödinger approach.

This analysis therefore confirms the results that have been summarized in subsection 13.3.3 for a single heterostructure HEMT structure also for the case of a double heterostructure HEMT.

Chapter 15

Conclusions

The quantum drift-diffusion model is very simple in nature and can be seen as a straightforward quantum extension of the traditional drift-diffusion model.

Because of these similarities it can be implemented with the same techniques already known for drift-diffusion problems (i.e. a finite-box discretization for Poisson's equation and Scharfetter-Gummel schema for the electron and hole continuity equations), which makes it extremely suitable for implementation in pre-existing drift-diffusion solvers.

The only additional complexity that is introduced are the two additional density gradient equations (which relate the quantum potentials to the gradients of the electron and hole densities), which must be solved self-consistently with the drift-diffusion equations.

Over the years, multiple schema have been proposed for discretizing the density gradient equations [26] when treating homostructures, but the only implementation that has been found to be stable for heterostructures in this work is a simple **finite-box discretization**.

The main criticality that was observed for this model lies in the choice of the **initial guess** for the solution of the problem. This is because, while a Poisson-Boltzmann solution at equilibrium is simple to obtain (semiclassical equilibrium problems tend to be much better conditioned than quantum-corrected problems), the guesses for the carrier densities are typically discontinuous at heterointerfaces. This constitutes a fundamental issue when iteratively correcting the guess by means of a quantum drift-diffusion model since this model always attempts at driving the carrier densities towards a continuous solution, which gives rise to delta corrections at the beginning of the iterative correction process.

The result is that if the equilibrium quantum drift-diffusion solver is not damped at equilibrium the solver may result to be unstable. This issue doesn't however arise when ramping up the voltage from the equilibrium solution, hence damping is only needed when correcting the initial equilibrium guess.

Further research on numerical implementation of this model could be focused on determining a "numerically inexpensive" initial equilibrium guess with continuous carrier densities that might resolve the convergence issues without requiring damping (which worsens the computational time for this method during the solution at equilibrium) or on determining adaptive damping methods (such as variants of the Bank and Rose method for dynamic damping) that call allow to minimize the amount of damping needed to ensure convergence of the solution at equilibrium.

The treatment that was given in Part I highlights how pretty severe approximations and assumptions are applied in order to get to the quantum drift-diffusion model (among which the truncation of the wigner function to order \hbar^2 and various assumptions of the quantum correction being small and localized in a small region of space). This doesn't however appear to limit the applicability of the quantum drift-diffusion model to the most common cases of quantum confinement (electrical and geometrical confinement in most MOS and HEMT devices), which all appear to be phenomena well described by a wigner function of order \hbar^2 .

Moreover, while the usage of this model has been historically mostly limited to silicon devices, the results of Part IV of this work show that it is applicable with similar accuracy also to **III-V semiconductors**. This should lead the way to this model being applied also for first-order studying of optoelectronic devices which are currently studied with extremely computationally intensive NEGF techniques.

| # nodes | Quantum Drift Diffusion (damping) | Poisson Schrödinger |
|---------|-----------------------------------|---------------------|
| 551 | 2.52 s (0.45) | 33.07 s |
| 1101 | 4.14 s (0.2) | 44.37 s |
| 5501 | 25.84 s (0.15) | 250.47 s |

Table 15.1: Computational time comparison between the quantum drift-diffusion model and the reference Poisson-Schrödinger solver at equilibrium

While the quantum drift-diffusion model is more approximate than a self-consistent Poisson-Schrödinger model, it compensates with much lower **computational time**. Table 15.1 shows how the computational time required to treat the HEMT problem of chapter 13 with a quantum drift-diffusion model is approximately an order of magnitude lower than the time required to treat it using a self-consistent Poisson-Schrödinger solver.

This analysis also shows how refining the mesh (i.e. increasing the size of the numerical problem to be solved) requires to also reduce the damping that is used in the Newton’s method. It appears however that the reduction in the damping saturates for large number of nodes (a damping of 0.1 fits most devices and reasonable discretizations).

Reducing the amount of damping needed (i.e. increasing the damping factor) would surely further reduce the computational time needed for the quantum drift-diffusion solver, therefore further improving its performance with respect to the reference Schrödinger solver.

The other advantage that quantum drift-diffusion approaches offer is that they can be implemented in **2D and 3D simulators** with techniques very similar to those used for conventional drift-diffusion models. Self-consistent Poisson-Schrödinger and Poisson-NEGF solvers cannot instead be implemented in 2D and 3D, which is quite a strong limitation when dealing with most electronic devices (especially with FETs, which require at least two dimensions to be simulated).

The results obtained in this work for one dimension would then suggest to discretize the additional density gradient equations using a conventional finite-box discretization technique in order to be able to effectively treat heterostructures in **III-V semiconductors**.

The main standing limitation of this model (besides the 30% accuracy) is that, being a corrected drift-diffusion model, it still relies on the **effective mass approximation**. The quantum drift-diffusion model cannot therefore treat devices which rely on quantum phenomena that involve multiple bands (such as interband tunnelling phenomena, which are extremely important for the operation of TFET devices), for which self-consistent Poisson-Schrödinger and Poisson-NEGF solvers are still the best choices.

A final summary of the main pros and cons of each of the above mentioned models is presented in Table 15.2.

| Metric | Poisson Schrödinger | Quantum Drift Diffusion |
|----------------|---------------------|---|
| Runtime | Longer runtime | Shorter runtime |
| Dimensionality | Only 1D | 1D, 2D and 3D |
| Approximations | None | Effective mass, Wigner function with order lower than \hbar^2 |

Table 15.2: Pros and cons of the quantum drift-diffusion model with respect to the self-consistent Poisson-Schrödinger model

Bibliography

- [1] E. G. Barbagiovanni, D. J. Lockwood, P. J. Simpson, and L. V. Goncharova, “Quantum confinement in si and ge nanostructures: Theory and experiment,” *Applied Physics Reviews*, vol. 1, no. 1, 2014.
- [2] F. Bertazzi, M. Goano, G. Ghione, A. Tibaldi, P. Debernardi, and E. Bellotti, “Electron transport,” *Handbook of Optoelectronic Device Modeling and Simulation*, vol. 1, 2017.
- [3] A. Jünger, *Transport Equations for Semiconductors*. Austria: Springer, 1 ed., 2009.
- [4] M. G. Ancona, “Density-gradient theory: a macroscopic approach to quantum confinement and tunneling in semiconductor devices,” *Journal of Computational Electronics*, vol. 10, pp. 65–97, 2011.
- [5] C. D. Sherrill, *A Brief Review of Elementary Quantum Chemistry*. Georgia, USA: Georgia Institute of Technology, 1 ed., 2001.
- [6] R. Shankar, *Principles of Quantum Mechanics*. Connecticut, USA: Kluwer Academic/Plenum Publishers, 2 ed., 2008.
- [7] R. A. Bertlmann, *Theoretical Physics T2, Quantum Mechanics*. Vienna: University of Vienna, 1 ed., 2008.
- [8] Wikipedia, “Liouville’s theorem (hamiltonian).” [https://en.wikipedia.org/wiki/Liouville%27s_theorem_\(Hamiltonian\)](https://en.wikipedia.org/wiki/Liouville%27s_theorem_(Hamiltonian)), 2022. Accessed: 2022-05-15.
- [9] B. C. Hall, *Quantum Theory for Mathematicians*. Indiana, USA: Springer, 1 ed., 2013.
- [10] T. Tao, “Some notes on weyl quantization.” <https://terrytao.wordpress.com/2012/10/07/some-notes-on-weyl-quantisation/>, 2012. Accessed: 2022-05-15.
- [11] Wikipedia, “Baker-campbell-hausdorff formula.” https://en.wikipedia.org/wiki/Baker%E2%80%9393Campbell%E2%80%9393Hausdorff_formula, 2022. Accessed: 2022-05-15.
- [12] Wikipedia, “Canonical commutation relation.” https://en.wikipedia.org/wiki/Canonical_commutation_relation, 2022. Accessed: 2022-05-15.
- [13] W. B. Case, “Wigner functions and weyl transforms for pedestrians,” *American Journal of Physics*, vol. 76, no. 10, pp. 937–946, 2008.
- [14] D. Chafaï, “Determinant of block matrices.” <https://djalil.chafai.net/blog/2012/10/14/determinant-of-block-matrices/>, 2012. Accessed: 2022-05-15.
- [15] E. Wigner, “On the quantum corrections for thermodynamic equilibrium,” *Physical Review*, vol. 40, pp. 749–759, 1932.
- [16] S. Selberherr, *Analysis and Simulation of Semiconductor Devices*. Vienna, Austria: Springer, 1 ed., 1984.
- [17] M. G. Ancona and G. J. Iafrate, “Quantum correction to the equation of state of an electron gas in a semiconductor,” *Physical Review B*, vol. 39, p. 9536–9540, 1989.
- [18] Colby College, “Some handy integrals.” <https://www.colby.edu/chemistry/PChem/notes/Integral.pdf>, 2022. Accessed: 2022-05-15.

- [19] Wikipedia, “Vector calculus identities.” https://en.wikipedia.org/wiki/Vector_calculus_identities, 2022. Accessed: 2022-05-15.
- [20] C. Liu, “Intro to density-gradient theory for semiconductor device simulation.” <https://www.comsol.com/blogs/intro-to-density-gradient-theory-for-semiconductor-device-simulation/>, 2019. Accessed: 2022-05-15.
- [21] A. Tibaldi, F. Bertazzi, and M. Goano, “Simulation of electronic devices at thermodynamic equilibrium (CAD of semiconductor devices).” 2021.
- [22] COMSOL Multiphysics, Stockholm, Sweden, *Semiconductor Module User’s Guide (5.5)*, 2019.
- [23] Synopsys, California, USA, *Sentaurus Device User Guide (N-2017-09)*, 2017.
- [24] A. Wettstein, *Quantum Effects in MOS Devices*. PhD thesis, ETH Zürich, Zurich, Switzerland, Apr. 2020.
- [25] M. G. Ancona, “On ohmic boundary conditions for density-gradient theory,” *Journal of Computational Electronics*, vol. 1, no. 2, pp. 103–107, 2002.
- [26] M. G. Ancona, “Finite-difference schemes for the density-gradient equations,” *Journal of Computational Electronics*, vol. 1, no. 3, pp. 435–443, 2002.
- [27] I. Vurgaftman, J. R. Meyer, and L. R. Ram-Mohan, “Band parameters for iii-v semiconductors and their alloys,” *Journal of Applied Physics*, vol. 89, no. 5815, 2001.
- [28] IOFFE, “Semiconductors on NSM.” <http://www.ioffe.ru/SVA/NSM/Semicond/>, 2022. Accessed: 2022-05-15.
- [29] A. Tibaldi, F. Bertazzi, and M. Goano, “Modeling carrier transport in nanoscale devices.” 2022.
- [30] S. Odanaka, “Multidimensional discretization of the stationary quantum drift-diffusion model for ultrasmall mosfet structures,” *IEEE Transactions on Computer-Aided Design of Integrated Circuits and Systems*, vol. 23, no. 6, pp. 837–842, 2004.
- [31] A. Tibaldi and F. Bertazzi, “Physics-based modeling of semiconductor devices.” 2022.